The University Of Sheffield.

Functional characterisation of (p)ppGpp synthetases in *Staphylococcus aureus*

Sophie Irving

A thesis submitted in partial fulfilment of the requirements for the degree of Doctor of Philosophy

The University of Sheffield
Faculty of Science
Department of Molecular Biology and Biotechnology

April 2019

Abstract

Staphylococcus aureus is a Gram positive bacterium that can colonise the nose and skin asymptomatically but can also invade the host as a pathogen. In the host, bacteria encounter various nutrient stresses which trigger the activation of the stringent response. This conserved mechanism allows bacteria adapt to environmental changes such as amino acid starvation and cell wall stress. It is mediated by two nucleotides, ppGpp and pppGpp, collectively known as (p)ppGpp. These small alarmones have many binding targets and cause the cells to enter a slow growing state through altering the transcriptional profile and inhibiting ribosome formation. In *S. aureus,* (p)ppGpp is synthesised by three members of the RSH superfamily: Rel_{Sa}, RelP and RelQ.

In this study we investigate how these synthetases are regulated transcriptionally and post-translationally, as well as the role of the stringent response in stress survival and growth in *S. aureus*. Promoter-*lacZ* reporter fusions were used to show that the synthetase genes are negatively regulated by several transcription factors, highlighting the intricacies of their regulation. We have also identified several binding partners of the Rel_{Sa} and RelP that may play a role in post-translational regulation of the proteins. In particular, we examine the effects of the interaction between Rel_{Sa} and the arginase, RocF which appears to be augmented by ppGpp. The arginase activity of RocF and the hydrolase activity of Rel_{Sa} are not affected by the interaction. Rel_{Sa} was also shown to bind to L-arg, suggesting that non-protein ligands may also regulate Rel_{Sa} activity. Finally, as arginine metabolism and urease production in *S. aureus* are regulated by the carbon catabolite repressor CcpA, we investigate the importance of the stringent response in certain aspects of CcpA-regulated metabolism, including long term survival, arginase activity and urease activity using a panel of synthetase mutants. A double mutant without functional Rel_{Sa} or RelP proteins showed reduced long term survival, reduced arginase activity in the absence of glucose and increased urease activity in the absence of glucose.

Publications

Irving, S.E. and Corrigan, R.M., 2018. Triggering the stringent response: signals responsible for activating (p)ppGpp synthesis in bacteria. Microbiology, 164: 268-276

Wood, A., Irving, S.E., Bennison, D.J., Corrigan, R.M., 2018. Stringent response-mediated control of rRNA processing via the ribosomal assembly GTPase Era. BioRχiv, doi:10.1101/477745

Acknowledgements

Firstly, I would like to thank my supervisor Rebecca for her continued support throughout my time as a PhD student. Her approach as a PI and mentor ensured I made the most out of my time as a PhD student. I would also like to thank the Florey Institute that funded my PhD. Organising symposia and outreach events with the other Florey students certainly enriched my PhD experience. I would also like to thank the other members of the Corrigan group, Alison, Dan and several excellent undergraduate students, for their help in the lab.

Thanks as well to all the F25 and F10 lab members for their day-to-day advice and support in group meetings and in the lab. Thanks especially to Luz, Shauna, Rob, Nadia, Greg, Laurence, Bartek and Joe. Always up for a coffee or a pint when needed – which was pretty often. The last few years would have been rather miserable without your weird sense of humour. In particular, Joe has been a massive influence on the way I've approached my PhD; offering invaluable advice since he first supervised me as an undergraduate student.

Finally, I would like to thank my friends and family for providing a healthy dose of perspective. Ruby has kept me smiling through the highs and lows of my project and I probably would have burnt-out long ago without her. Mum, Dad, Nana and Sam, you have helped me in so many ways over the years and I am forever grateful for all your love and support.

Table of Contents

List of Figures

List of Tables

List of Abbreviations

°C	degrees Celsius
A	amps
ACP	acyl carrier protein
ACT	aspartate kinase, chorismate and TyrA
AIP	autoinducing peptide
aMG	a-methyl-D-glucoside
ATP	adenosine triphosphate
BACTH	bacterial adenylate cyclase two-hybrid
BCAAs	branched chain amino acids (leucine, isoleucine, valine)
BHI	Brain Heart Infusion
BSA	bovine serum albumin
CA-MRSA	community acquired methicillin resistant *Staphylococcus aureus*
CAP	catabolite activator protein
CC	conserved cysteine
CDM	chemically defined media without glucose
CDMG	chemically defined media with glucose
CDM-P	chemically defined media without glucose or L-pro
CDM-R	chemically defined media without glucose or L-arg
CTD	C terminal domain
Da	Dalton
dansyl-arg	dansyl-arginine
ddH_2O	double distilled water
DNA	deoxyribonucleic acid
DRaCALA	Differential Radial Capillary Action of Ligand Assay

g	gram
gDNA	genomic DNA
GSH	glutathione
GST	glutathione S-transferase
h	hour
HA-MRSA	hospital acquired methicillin resistant *Staphylococcus aureus*
HD	hydrolase domain
HRP	horseradish peroxidase
IgG	immunoglobulin G
IPTG	isopropyl β-D-thiogalactosidase
IP	Imaging Plate
kb	kilo base pair
kDa	kilodalton
L	Litre
LB	lysogeny broth
L-arg	L-arginine
L-ile	L-isoleucine
L-leu	L-leucine
L-ser	L-serine
L-val	L-valine
long –RSH	long RelA SpoT homologues
LU	luciferase activity (units)
M	molar
MIC	minimum inhibitory concentration
Min	minute

ml	milliletre
mm	millimetre
mRNA	messenger RNA
MRSA	methicillin resistant *Staphylococcus aureus*
MSSA	methicillin sensitive *Staphylococcus aureus*
MU	4-methylumbilliferone
MUG	4-methylumbilliferone-β-D-galactopyranoside
nm	nanometre
NTML	Nebraska Transposon Mutant Library
NTD	N-terminal domain
OD	optical density
p	probability
PBS	phosphate buffered saline
PCR	polymerase chain reaction
PCR-SOE	polymerase chain reaction splicing by overlap extension
PM	phenotype microarray
PMSF	phenylmethanesulfonyl fluoride
Pi	phosphate
PG	peptidoglycan
PPi	pyrophosphate
ppGpp	guanosine tetraphosphate
pppGpp	guanosine pentaphosphate
(p)ppGpp	guanosine pentaphosphate and/or tetraphosphate
PVDF	polyvinylidene difluoride
RAC	ribosome activation complex

RNA	ribonucleic acid
RNAP	RNA polymerase
RRM	RNA recognition motif
rRNA	ribosomal RNA
SAH	small alarmone hydrolase
SAS	small alarmone synthetase
SCV	small colony variant
SDS	sodium dodecyl sulfate
SDS-PAGE	sodium dodecyl sulfate-polyacrylamide gel electrophoresis
sec	second
SHU	synthetic human urine
ss-DNA	single stranded DNA
ss-RNA	single stranded RNA
SYNTH	synthetase domain
TF	transcription factor
Tfb	Transformation buffer
TGS	ThrRS, GTPase and SpoT
TLC	thin layer chromatography
Tn	transposon
TSA	tryptic soy agar
TSB	tryptic soy broth
U	unit
VISA	vancomycin intermediate-resistant *Staphylococcus aureus*
VRSA	vancomycin resistant *Staphylococcus aureus*
WT	wild type

X-gal	5-bromo-4-chloro-3-indolyl-β-D-galactopyranoside
Xg	times gravity
ZFD	zinc finger domain

Chapter 1 – Introduction

1.1 *Staphylococcus aureus*

1.1.1 Epidemiology of *S. aureus* infection

Staphylococcus aureus is a non-motile, Gram positive bacteria, so-called due to its round, grape-like cell shape and its golden colour (staphyl = grape bunch; coccus = round; aureus = golden). This golden colour is due to the production of staphyloxanthin which also protects against reactive oxygen species (Marshall and Wilmoth, 1981; Clauditz *et al.*, 2006). *S. aureus* belongs to the Firmicutes phylum due to its low GC content DNA and is a member of the *Staphylococcacae*. There are at least 38 species in the *Staphylococcus* genus (Takahashi *et al.*, 1999) and these can be sorted into three groups based on genetic orthologues: Group A - including *S. aureus* and *S. epidermidis*; Group B - including *S. xylosus* and *S. equorum* and Group C - including *S. delphini* and *S. intermedius* (Coates-Brown *et al.*, 2018). *S. aureus* can be distinguished from other staphylococci by its ability to produce coagulases. Coagulases are a virulence factors produced by most *S. aureus* strains that results in blood coagulation in the host (Loeb, 1903). Whilst most *S. aureus* strains produce coagulase, during species identification tests it is important to remember that some atypical strains do not (Matthews *et al.*, 1997).

The genome of *S. aureus* is roughly 3 Mb and encodes over 2,600 genes (Baba *et al.*, 2008). There are several mobile genetic elements encoded by the *S. aureus* genome, including large pathogenicity islands, prophages and transposons (Baba *et al.,* 2008). Bacterial strains within the *S. aureus* species can be grouped, based on their sequence type, into clonal complexes. Seven genes are analysed when assigning clonal complexes and these are *arcC*, *aroE*, *glpF*, *gmk*, *pta*, *tpi*, and *yqiL*.

S. aureus can cause a variety of infections, ranging from subclinical inflammation or skin infections to severe infections such as pneumonia, septicaemia and endocarditis (van Wamel, 2017). Whilst *S. aureus* is a disease causing bacterium in humans, it is also a natural commensal amongst humans and is considered an opportunistic pathogen. Around one in three humans carry *S. aureus* asymptomatically in the nasal cavity (Graham *et al.*, 2006) and it also forms part of the skin flora (Grice and Segre, 2011). Around 5% of humans are colonised by *S. aureus* on the skin, whist more than 90% of atopic dermatitis sufferers carry *S. aureus* on their skin (Leyden *et al.*, 1974; Hanifin and Rogge, 1977). The presence of Esp-producing *S. epidermidis* in the nares inhibits colonisation by *S. aureus* (Iwase *et al.*, 2010). Esp is a serine protease that can inhibit *S. aureus* biofilm formation and disrupt mature biofilms (Iwase *et al.,* 2010). Although humans can carry *S. aureus* asymptomatically, it is important to note that colonisation is a risk factor for *S. aureus* infection (von Eiff *et al.*, 2001). As such,

it has become common practice to screen for, and treat, *S. aureus* colonisation before surgery in order to avoid infection (Perl *et al.*, 2002).

1.1.2 Treatment of *S. aureus* infections

Current treatment of *S. aureus* infections relies on use of antibiotics, including methicillin (and related antibiotics), vancomycin, linezolid, daptomycin, mupirocin and trimethoprim. As is the case with most bacterial pathogens, the prevalence of antibiotic resistance in *S. aureus* strains is increasing. In particular, methicillin- and vancomycin-resistant *S. aureus* strains (MRSA or VRSA) have become a major healthcare problem. MRSA deaths in the UK peaked in 2006 with 1652 deaths attributed to MRSA (Cole, 2013). However, policy changes have led to a year-on-year decrease in deaths with just 292 deaths due to MRSA in 2012 (Cole, 2013). Recently, overall rates of *S. aureus* bacteraemia have risen for the last five years, with 19.9 cases per 100,000 population (Public Health England, 2018). This highlights the threat of methicillin-sensitive *S. aureus* (MSSA) to human health despite the fact it is more readily treatable with antibiotics.

MRSA is associated with a higher bacteraemia mortality rate than MSSA, although it is unclear whether this is due to MRSA-specific factors or due to a generally worse response to antibiotic treatment (van Hal *et al.*, 2012). Daptomycin and vancomycin are recommended for treatment of MRSA bacteraemia (Holland *et al.,* 2014). Methicillin resistance is encoded by mobile genetic elements known as SCC*mec* elements. These elements usually encode *mecA* and *ccr* recombinase genes and are grouped based on the sequences of these genes. MRSA infections that are hospital acquired (HA-MRSA) and community acquired (CA-MRSA) have been reported. HA-MRSA strains generally encode Group I, Group II and Group III SCC*mec* elements, whilst CA-MRSA strains encode Group IV and Group V SCC*mec* elements (Hiramatsu *et al.,* 2001; Daum *et al.*, 2002). It is thought that the smaller Group IV and Group V SCC*mec* elements have a lower fitness cost than those found in HA-MRSA (Lee *et al*., 2007a). This allows CA-MRSA strains to maintain a higher virulence level through gaining various virulence genes, such as PVL (Vandenesch *et al.,* 2003). At least 90% of CA-MRSA infections are skin infections, which is much higher than the rate seen with HA-MRSA infections (Fridkin *et al*., 2005). This altered epidemiology may be due to different virulence factor profiles in the two subsets of *S. aureus* strains.

Vancomycin is a glycopeptide antibiotic that binds to the two D-ala residues at the end of the peptide stems in *S. aureus* peptidoglycan (PG), preventing cell wall cross-linking and compromising the cell wall integrity (Reynolds, 1961). It is commonly used to treat MRSA infections, but recently the emergence of VRSA strains and vancomycin intermediate-resistance *S. aureus* strains (VISA) has become more common. VISA strains usually arise following prolonged infection and vancomycin

treatment (Howden *et al.*, 2010). VISA strains have multiple mutations in several genes resulting in a decreased sensitivity to vancomycin but not complete resistance (Katayama *et al.*, 2016). On the other hand, VRSA strains are completely resistant to vancomycin having acquired the *vanA* gene and operon, following conjugation of the vancomycin resistance enterococci conjugative plasmid containing the transposon Tn*1546* (Zhu *et al.*, 2010). Tn*1546* is either maintained on the enterococcal plasmid or through transposition to a host plasmid. The *vanA* operon contains 7 genes which ultimately replace the final residue on the PG stem peptide with D-Lac, meaning vancomycin cannot bind and the crosslinking is not inhibited (Bugg *et al.*, 1991). VRSA strains are rare, with only 14 isolates being reported by 2015, 13 years after the first recorded instance (Walters *et al.,* 2015). Linezolid can be used quite successfully to treat VISA infections (Howden *et al.*, 2004).

In hospitals, the cause of a *S. aureus* infection can often be attributed to catheters or prosthetic implants (Tornero *et al.,* 2012). Following swift removal of these objects, infection is treated with antibiotics. *S. aureus* is responsible for around 13% of urinary tract infections and this has been linked to chronic urinary catheter use (Ackermann and Monroe, 1996). Replacement of infection-causing implants can be both dangerous and costly and thus research into preventing biofilm formation on medical implants is vital. Many antimicrobial surface polymers have been developed to try to reduce the risk of *S. aureus* infection (Bhattacharya *et al.*, 2015).

Research into *S. aureus* vaccines has yielded several promising vaccine candidates, however, none have been shown to prevent infection in clinical trials (Fowler and Proctor, 2014). It has been suggested that a vaccine against all *S. aureus* infections is out of reach and that a prophylactic for specific types of infections may be more realistic (Pier, 2013). For example, a vaccine that targets against soft tissue infections could be useful for at risk patients (Lacey *et al.*, 2016).

Currently, most *S. aureus* infections remain treatable with antibiotics however, the mortality rates of *S. aureus* bacteraemia are around 10 to 30% even with antibiotic treatment (van Hal *et al.,* 2012). Careful surveillance of antibiotic resistance in *S. aureus* strains is required to ensure the long-term efficacy of antibiotic treatment. The recent successful efforts to curb the rates of MRSA infection prove that prophylactic treatment and infection control are also important in preventing *S. aureus* infections.

1.1.3 Regulation of virulence factors in *S. aureus*

S. aureus has a wide array of virulence factors used to aid adhesion to the host cells, evade the host immune system and degrade host tissues. The breadth of adhesins, evasins and toxins in the *S. aureus* arsenal facilitates the diverse infection types it can produce. Expression of these virulence factors must be tightly controlled in order to conserve energy and to ensure successful infection. In *S. aureus,* virulence factors are most commonly regulated on the transcriptional level in response to growth

conditions or growth phase (Bronner *et al.*, 2004). Two-component systems such as Agr, ArlRS, LytRS and Sae are responsible for the large majority of virulence factor regulation. However, the sigma factor SigB and other DNA binding molecules also play a role. The regulatory network of virulence factors is complex, allowing for fine-tuning of the response to different stimuli.

Two-component systems typically consist of a sensor histidine kinase, which can sense environmental changes, and a response regulator. Perhaps the best characterised two-component system in *S. aureus* is the quorum sensing *agr* system (Fig. 1.1.3). The *agr* locus encodes 5 genes (*agrB, agrD, agrC, agrA* and *hld*) and is controlled by two promoters (P2 and P3). Transcription from P2 gives the transcriptional unit RNAII which encodes AgrB, AgrD, AgrC and AgrA, whereas transcription from P3 yields RNAIII which encodes the delta haemolysin peptide Hld but is also the effector of the *agr* system (Peng *et al.*, 1988). AgrB is a transmembrane protein that matures AgrD into autoinducing peptide (AIP) and secretes it (Ji *et al.*, 1995). When extracellular AIP reaches a threshold level, the histidine kinase of the system, AgrC, forms a homodimer and is autophosphorylated (Lina *et al.*, 1998). The phosphate residue is then transferred from the histidine of AgrD to the aspartate residue of AgrA, allowing AgrA to activate transcription from P2 and P3. RNAIII acts to increase expression of extracellular toxins such as alpha and beta toxins Hla and Hlb (Morfeldt *et al.*, 1995) but decrease expression of cell wall components such as fibronectin binding protein FnbA and FnbB (Wolz *et al.*, 2000). Interestingly, the SaeRS (*S. aureus* exoprotein expression) two-component system is essential for transcription of *hla* and *hlb*, despite having no effect on *agr* expression, suggesting SaeRS acts independently of the *agr* system (Giraudo *et al.*, 1997).

Other two-component systems, such as ArlRS and LytRS, are used to regulate the expression of autolysins that hydrolyse the cell wall during cell division. Mutants in both *arlS* and *lytS* show increased autolysis and cell death, highlighting the necessary regulation of autolysins to ensure they are only active when needed during cell division (Brunskill and Bayles, 1996; Fournier *et al.*, 2000). LytR upregulates the expression of *lrgA* and *lrgB* genes which encode proteins that inhibit the activity of murein hydrolases (Groicher *et al.*, 2000). When the murein hydrolases are inhibited the cells cannot divide and become penicillin tolerant. ArlR represses the expression of autolysins such as LytN (Liang *et al.*, 2005). The *arlRS* locus is transcribed between exponential and post-exponential growth phases, however the environmental signal triggering ArlS autophosphorylation is unknown. The *arl* system downregulates RNAII expression, resulting in decrease in RNAIII expression and RNAIII-regulated virulence genes.

SigB is an alternative sigma factor that has been shown to regulate both virulence factors and various stress response proteins. Microarray analysis has shown that SigB positively regulates certain genes

during exponential phase, whilst negatively regulating others during late exponential growth (Bischoff *et al.*, 2004). SigB activity is highest during stationary phase and *sigB* expression is induced in response to salt and heat shock stress (Senn *et al*., 2005). SigB negatively regulates RNAIII expression and thus influences virulence factor expression in an *agr*-dependent manner (Bischoff *et al.*, 2001).

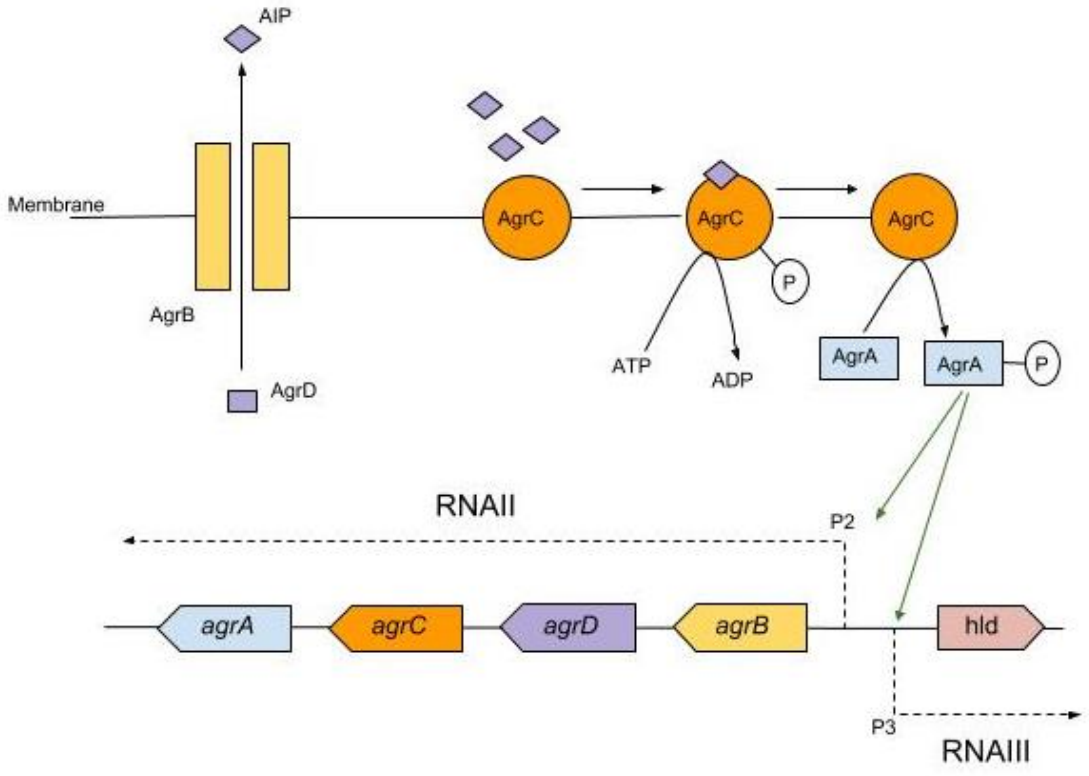

Fig. 1.1.3 The *agr* quorum sensing system. The *agr* locus is controlled by two promoters, P2 and P3, resulting in transcripts RNAII and RNAIII, respectively. AgrD (purple) is matured and secreted by AgrB (yellow) to AIP. When AIP levels reach a threshold AIP binds to AgrC (orange) in the membrane, triggering autophosphorylation with ATP as the phosphate donor. The phosphate is then transferred to AgrA (blue). Phosphorylated AgrA can induce transcription from both P2 and P3.

1.1.4 Bacterial Stress Responses

Bacteria have several stress responses that allow them to rapidly respond to different stimuli. These could be changes in temperature, nutrient availability, competition or attack from the immune system or other bacteria. Bacterial stress responses can alter the gene transcription profile. For example, when resources are limited the expression of virulence genes may be downregulated, and the expression of certain nutrient biosynthetic pathways may be upregulated.

1.1.4.1 The SOS response

The SOS response is triggered by DNA damage and an accumulation of single stranded DNA (ss-DNA), which can be caused by a number of stresses such as oxidative stress (Painter *et al.*, 2015) and antibiotics such as ciprofloxacin and mitomycin C (Anderson *et al.*, 2006; Cirz *et al.*, 2007). RecA proteins form a filament along ss-DNA and these filaments activate the autocleavage of the SOS repressor LexA (Little *et al.*, 1980). LexA binds the promoter region of SOS genes limiting their transcription and this repression is released following LexA cleavage (Michel, 2005). The SOS response is halted following DNA repair and the accumulation of uncleaved LexA.

In *S. aureus*, 73 genes are induced by a mitomycin C-induced SOS response and 453 genes are downregulated (Anderson *et al.*, 2006). These include the *recA* and *lexA* genes, as well as *uvrA* and *uvrB* which are part of the nucleotide excision repair machinery (Anderson *et al.,* 2006). However, the SOS response does not just regulate expression of DNA repair genes, and several virulence genes are also upregulated, including a bovine pathogenicity island. Interestingly, the SOS response has also been implicated in the horizontal transmission of *S. aureus* pathogenicity islands (Ubeda *et al.*, 2005). In *S. aureus*, the SOS response also induces the formation of small colony variants (SCVs), which are a sub-population of slow growing cells associated with persistence (Vestergaard *et al.*, 2015). SCVs are commonly linked to chronic infections and antibiotic resistance (Kahl *et al.*, 2016). Sub-inhibitory levels of mitomycin C and fluoroquinolones can induce the production of gentamicin resistant SCVs through the activation of the SOS response (Vestergaard *et al.*, 2015). Therefore, an understanding of the SOS response is vital to understand the rise and spread of antibiotic resistance in *S. aureus.*

1.1.4.2 The cold shock response

In *S. aureus*, the cold shock (10°C for 30 min) response results in the up-regulation of 46 genes (Anderson *et al.*, 2006). The cold shock gene *cspB* is upregulated more than the *cspA* gene (9.3-fold and 2.0-fold, respectively). This is also the case in *E. coli*, where *cspA* is hugely upregulated at 25°C but only slightly upregulated at 15°C (Vasina and Baneyx, 1996). Virulence factors such as sortase and lipase are also upregulated, as well as the SOS response repressor LexA (Anderson *et al.*, 2006).

In *Bacillus subtilis*, it has been hypothesized that the genes differentially expressed in the cold shock response are inversely regulated during the stringent response *i.e.* genes that are downregulated during the cold shock response are upregulated during the stringent response and vice-versa (Weber and Marahiel, 2003). However, this does not appear to be true in *S. aureus*, as only 30 of the 462 genes differentially expressed after cold shock were oppositely regulated during the stringent response (Anderson *et al.,* 2006).

1.1.4.3 The heat shock response

High temperatures can have many negative effects on a bacterial cell, especially protein misfolding. Chaperones such as DnaK, GroES and GroEL can act to prevent misfolding or indeed encourage refolding of misfolded proteins. Chaperones with protease activity such as ClpB, ClpC and ClpP can also degrade misfolded proteins. The heat shock chaperone genes are controlled by two repressors, CtsR and HrcA. HrcA regulates expression of *dnaK* and *groESL* operons, whilst CtsR regulates the expression of the Clp proteases such as *clpB, clpC* and *clpP* (Derre *et al.*, 1999). The *hrcA* and *ctsR* genes themselves are located at the start of the *dnaK* and *clpC* operons, respectively, and thus negatively regulate their own expression. Interestingly, CtsR also controls *dnaK* and *groESL* expression, which differentiates the heat shock response in *S. aureus* from that seen in *B. subtilis* (Chastanet *et al.*, 2003). During the heat shock response, the repression of HrcA and CtsR is released, resulting in an increase in expression of the genes in their regulons. The transcription of 98 genes is upregulated during heat shock response in *S. aureus*, whilst 42 genes are downregulated (Anderson *et al*., 2006). Interestingly, there is an overlap of 11 genes that are upregulated in both cold and heat shock responses, suggesting a general temperature regulated stress response in *S. aureus*. Other overlaps between the heat shock response and other stress responses are mediated by the ClpP protease (Michel *et al.*, 2006). A *clpP* mutant shows reduced expression of *agr* and therefore agr-dependent virulence factors, as well as genes involved in adaptation to anaerobic conditions. Without ClpP there is derepression of the HrcA and CtsR regulons and limited derepression of PerR, Fur, MntR and LexA.

There is a clear overlap in the regulation of the heat shock response and the cold shock and SOS responses. During stringent, heat shock, and cold shock responses in *S. aureus*, the stability of mRNA molecules increases (Anderson *et al.*, 2006). As such, it is not only an increase in transcription that is responsible for high gene transcript numbers, but also an increase in mRNA half-life. Furthermore, competence genes are upregulated during cold shock and heat shock responses in *S. aureus,* and it is thought that this may be a common response to stress in Gram positive bacteria (Anderson *et al.*, 2006; Claverys *et al.*, 2006).

1.2 The Stringent Response

The stringent response is a conserved mechanism that allows bacteria to react to stress conditions. Interestingly, most plants can also affect a stringent response in response to stresses such as wounding, drought and UV irradiation (van der Biezen *et al.*, 2000; Takahashi *et al.*, 2004). The effectors of the stringent response are the alarmone nucleotides guanosine tetraphosphate (ppGpp) and guanosine pentaphosphate (pppGpp), collectively known as (p)ppGpp. A pGpp alarmone is also

synthesised by an *Enterococcus faecalis* enzyme *in vitro* but it has yet to be shown to be produced by the bacteria naturally (Gaca *et al*., 2015).

The stringent response is triggered by a wide variety of environmental signals. Bacteria in different niches utilise the stringent response to react to stresses and signals relevant to their survival. The stringent response was first discovered through investigation of the response of *E. coli* to amino acid starvation. The starved *E. coli* cells produced two nucleotides that appeared as 'magic spots' on a chromatograph and were later identified as ppGpp and pppGpp (Cashel, 1969). Across bacteria, amino acid starvation appears to be a common trigger of the stringent response because amino acids are universally required for growth. However, in the photosynthetic bacteria *Synechococcus elongatus* the stringent response is triggered by darkness, which is a specific response due to its lifestyle (Hood *et al.*, 2016; Puszynska *et al.*, 2017).

In bacteria, the stringent response is characterised by an accumulation of (p)ppGpp and a decrease in GTP pool in the cell (Potrykus and Cashel, 2008). There is a general reduction in transcription, particularly in genes involved in biosynthesis of macromolecules, however other genes are upregulated (Potrykus and Cashel, 2008). Protein translation is also low during the stringent response due to a reduction in rRNA transcription and impaired ribosome maturation (Kästle *et al.*, 2015; Corrigan *et al.*, 2016). Ultimately, these effects result in slow growth during the stringent response, which has now been implicated in various bacterial processes such as biofilm formation and persister formation (Hauryliuk *et al.*, 2015).

1.2.1 Enzymes of the stringent response

(p)ppGpp is synthesised and hydrolysed by members of the RSH superfamily. This superfamily is divided into three groups (Fig. 1.2.1): long RelA/SpoT homologues (long-RSHs); small alarmone synthetases (SASs); and small alarmone hydrolases (SAHs) (Atkinson *et al*., 2011). More than 90% of the bacterial genomes analysed by Atkinson *et al.* were shown to encode at least one member of the RSH superfamily, indicating the near ubiquity of the stringent response across the domain. Bacteria that do not encode for RSH superfamily genes inhabit stable microenvironments or are members of the *Plantomycetes, Verrucomicrobia* and *Chlamydiae* superphylum (Atkinson *et al.*, 2011).

Long-RSH proteins contain a hydrolase domain (HD) (PF13328) and SYNTH domain (PF04607) in their N-terminal domain (NTD). The identity of the domains present in the C-terminal domain (CTD) of long-RSH proteins is described differently throughout the literature. However, generally it is described as comprising a TGS region (ThrRS, GTPase and SpoT: PF02824), CC/ZFD domain (conserved cysteine/zinc finger domain), alpha-helical domain and an ACT/RRM domain (aspartate kinase, chorismate and TyrA: PF13291/RNA recognition motif) based on cyro-EM images of the CTD domain structure (Brown

et al., 2016; Loveland *et al.*, 2016; Arenz *et al.*, 2016). SASs and SAHs are monofunctional and typically only comprise of one domain (SYNTH or HD, respectively) with no C-terminal regulatory region.

Whilst 7 subgroups of SAH enzymes have been predicted in bacteria based on phylogenetic analysis, the presence of active SAHs has not been confirmed in any bacteria yet (Atkinson *et al.*, 2011). A SAH protein called Mesh-1 is present in eukaryotes such as humans and fruit flies, however its function is unclear because these organisms do not appear to produce (p)ppGpp (Sun et al., 2010).

The combination of RSH superfamily member proteins that are present in a given bacterial species can vary. However, Gram negative bacteria tend to contain the same combination of enzymes and the same is true for Gram positive bacteria. Theses difference may explain why the ratio of ppGpp to pppGpp during the stringent response varies across bacteria. Gram negative bacteria favour ppGpp production (Cashel, 1996), whereas Gram positive bacteria favour pppGpp production (Samarrai *et al.*, 2011; Gaca *et al.*, 2012; Corrigan *et al.,* 2015).

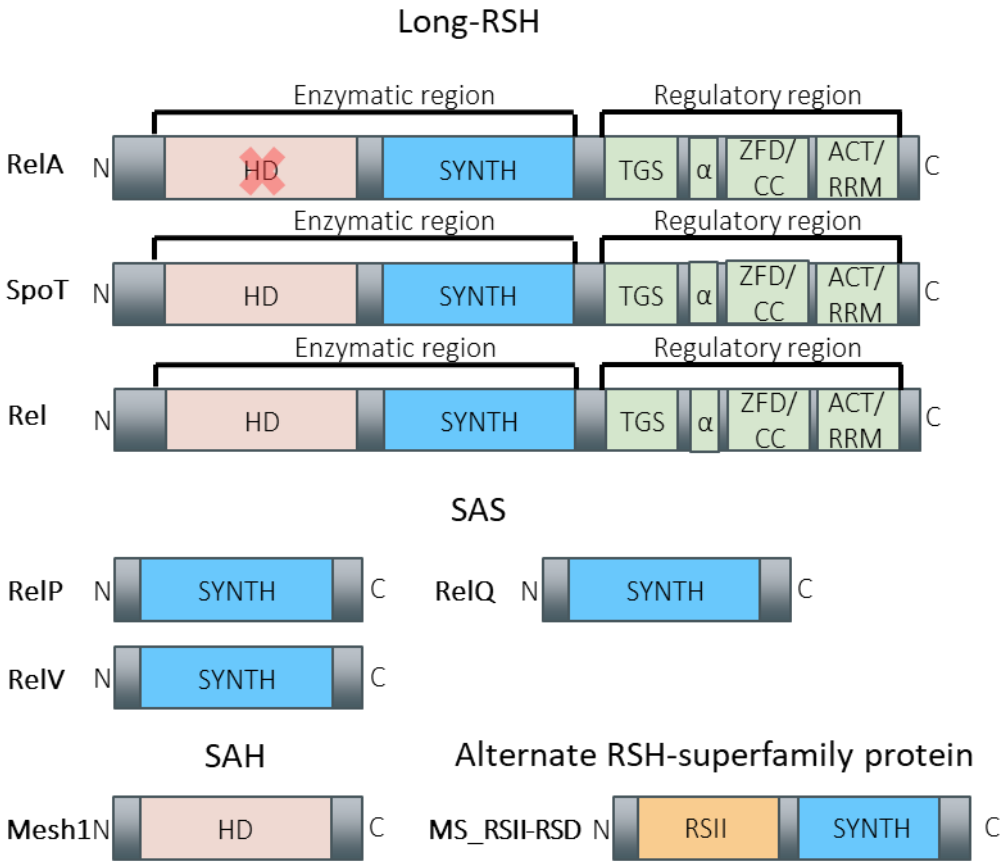

Fig. 1.2.1 Overview of RSH superfamily proteins. Long-RSH proteins (RelA, SpoT, Rel) have an N-terminal enzymatic region with a HD (pink) and a SYNTH domain (blue). The HD domain of RelA is inactive. The C-terminal regulatory region consists of a TGS region (ThrRS, GTPase and SpoT), CC/ZF domain (conserved cysteine/zinc finger domain), alpha-helical domain and an ACT/RRM domain (aspartate kinase, chorismate and TyrA/RNA recognition motif). Small alarmone synthetases (RelP, RelQ and RelV) have a single SYNTH domain. Small alarmone hydrolases (Mesh-1) have a single HD domain. The alternate RSH-superfamily protein MS_RSII-RSD consists of a RSII domains and a SYNTH domain.

1.2.1.1 Gram negative bacteria

Gram negative bacteria, like *Escherichia coli*, commonly contain two long-RSH synthetases. These are RelA and SpoT, homologous enzymes that arose due to a gene duplication event. SpoT is a bifunctional enzyme containing active synthetase and hydrolase domains. Whilst the synthetase activity of RelA is intact, the hydrolysis domain of RelA is inactive. This is due to the mutation of the amino acid residues H and D in the active site to F and P residues making it a monofunctional enzyme (Aravind and Koonin, 1998). There is also a difference in the catalytic sites of the SYNTH domains in RelA and SpoT. RelA and other monofunctional long-RSH proteins have the acidic residues EFDD, whereas SpoT and other bifunctional long-RSH proteins have basic residues RFKD (Sajish *et al.*, 2007). This difference may be responsible for the preference of RelA for GDP as a substrate and of SpoT for GTP as a substrate.

E. coli also encodes a third enzyme involved in (p)ppGpp metabolism called GppA. Althought it does not have a HD or SYNTH domain (and is therefore not a member of the RSH superfamily), it does convert pppGpp to ppGpp through its guanosine pentaphosphate phosphohydrolase activity (Keasling *et al.*, 1993). GppA is not present in Gram positive bacteria.

It is rare for Gram negative bacteria to contain SAS or SAH enzymes, however in the *Vibrio* genus there is a conserved SAS, RelV (Das et al., 2009). RelV was discovered when a *relA* and *spoT* double mutant was still able to accumulate (p)ppGpp following fatty acid starvation, indicating the presence of an as yet undiscovered (p)ppGpp synthetase enzyme.

1.2.1.2 Gram positive bacteria

Gram positive bacteria usually contain one long-RSH protein and two SAS proteins. This is the case for *Streptococcus mutans* (Lemos et al., 2007), *Bacillus subtilis* (Nanamiya et al., 2008), and *S. aureus* (Geiger et al., 2014), where the SAS proteins are referred to as RelP and RelQ. The long-RSH proteins in Gram positive bacteria are more similar to SpoT than RelA because they are bifunctional and usually have the RFKD motif in the SYNTH active site.

In *B. subtilis* the RelQ enzyme was shown to form a tetramer and analysis of the monomer interfaces suggest this homotetramerisation in conserved across RelP and RelQ homologues (Steinchen *et al*., 2015).

The RelP enzyme of both *S. aureus* and *S. mutans* shows higher synthetase activity than the RelQ enzyme *in vitro* (Geiger *et al.*, 2014; Lemos *et al.*, 2007). Both enzymes in *S. aureus* preferentially use GDP as a synthesis substrate over GTP (Geiger *et al.*, 2014). Although a clear phenotype of *relP* or *relQ* mutants has not yet been described in the literature as both enzymes are active in the cell. In the

presence of RelP and RelQ the hydrolase domain of Rel_{Sa} is essential due to the toxic effect of unchecked (p)ppGpp accumulation by RelP and RelQ (Geiger *et al.*, 2014).

Nomenclature of RSH superfamily members has not been consistent across the literature. In *B. subtilis* RelQ is often referred to as YjbM or SAS1 and RelP is referred to as YwaC or SAS2. The long-RSH protein in *S. aureus* was originally annotated as RSH (encoded by *rsh*), but now it is common for long-RSH proteins to be written as Rel with the species in italics and subscript. Here, the (p)ppGpp synthetases genes in *S. aureus* are denoted as *rel*, *relP* and *relQ* and the protein products of these genes are referred to as Rel_{Sa}, RelP and RelQ respectively.

1.2.1.3 Other members of the RSH superfamily

MS_RHII-RSD is unique in that it is the only RSH superfamily member identified thus far that also contains an enzymatic domain not involved in the metabolism of (p)ppGpp (Fig. 1.2.1) (Murdeshwar and Chatterji, 2012). The enzyme in *Mycobacterium smegmatis* has a SYNTH domain fused to a RNase HII domain that is involved in separating R-loops: RNA-DNA hybrid structures. Each of the domains is only active when found in a hexamer of full-length proteins (Krishnan *et al*., 2016). The expression of MS_RHII-RSD is up-regulated during UV stress, when DNA damage leads to the formation of R-loops. The coupling of the SYNTH and RNase HII domains could provide a way of localising (p)ppGpp production at ribosomes stalled at R-loops. (p)ppGpp would destabilise the stalled ribosome allowing the RNase HII domain to resolve the R-loop before translation can continue.

Given the near ubiquity of the stringent response across bacteria it is possible that other RSH superfamily members have been overlooked thus far. Many other functional domain fusions could exist in order to adapt the stringent response to respond to other stimuli specific for survival of a given species.

1.2.2 Transcriptional regulation of (p)ppGpp synthetase genes

Transcriptional regulation is a conserved mechanism for determining when genes are expressed. Genes can be regulated in response to different stimuli or based on growth phase. Here, the transcriptional regulation of RSH-superfamily genes in bacteria is discussed.

1.2.2.1 Transcriptional regulation of long-RSH genes

In *E. coli* 4 promoters have been identified for the *relA gene*; *relA*P1 and *relA*P2 are controlled by sigma 70 while *relA*P3 and *relA*P4 are dependent on sigma 54 (Fig. 1.2.2) (Brown *et al.*, 2014; Metzger *et al.*, 1988; Nakagawa *et al.*, 2006). *relA*P3 and *relA*P4 are activated during nitrogen stress by the two-component system NtrBC (Brown *et al.*, 2014). When NtrB is activated it phosphorylates NtrC, allowing it to bind to an enhancer-like element and inducing transcription (Villadsen and Michelsen, 1977).

Conversely, during nitrogen starvation the transcription of *spoT* is reduced (Brown *et al.*, 2014). This opposing regulation of the long-RSH genes in *E. coli* may be due to the presence of a functional hydrolase domain in SpoT, which is mutated in RelA. An increase in *spoT* expression could hinder the (p)ppGpp accumulation required to trigger the stringent response through unwanted hydrolase activity, and so *spoT* is regulated differently to *relA* during nitrogen starvation.

The expression of *relA* is regulated temporally through *relA*P1 and *relA*P2. An UP element before *relA*P1 ensures constitutive expression, whereas transcription from *relA*P2 occurs in late exponential phase (Nakagawa *et al.*, 2006). Transcription from *relA*P2 is regulated by multiple factors. In a CRP or H-NS mutant there is almost no transcription from *relA*P2 at all (Nakagawa *et al.*, 2006). Overexpression of H-NS did not complement the *crp* mutant, suggesting that H-NS cannot activate transcription from *relA*P2 on its own and requires CRP. An *rpoS* mutant shows increased transcription from *relA*P2 after mid-exponential phase, showing that RpoS represses *relA* expression later on in the growth phase (Nakagawa *et al.*, 2006). *relA*P1 and *relA*P2 are both negatively regulated by 6S RNA, a small noncoding RNA that binds directly to the RNA polymerase-sigma 70 holoenzyme. In a 6S RNA mutant the expression of *relA* is higher leading to an accumulation of (p)ppGpp (Cavanagh, *et al.*, 2010). However, this accumulation is also seen in a 6S RNA and *relA* double mutant, suggesting that the activity of SpoT is somehow controlled by 6S RNA (Neusser *et al.*, 2010).

Transcription of *relA* is also negatively regulated by the HipAB type II toxin-antitoxin module (Lin *et al.*, 2013). HipB binds to a palindromic TATCC//GGATA sequence upstream of the *relA*P3 promoter, blocking transcription. HipA increases the repression of HipB, perhaps by protecting HipB from degradation.

The antibiotic mupirocin inhibits isoleucyl tRNA synthetase activity, resulting in an accumulation of uncharged isoleucyl-tRNAs, thus mimicking isoleucine starvation (Hughes and Mellows, 1978). It is often used to trigger the stringent response in bacteria in order to investigate the effect of amino acid starvation. However, mupirocin appears to have other effects on the cell and in *S. aureus* at least some of the effects of mupirocin are not Rel_{Sa}-mediated (Geiger *et al*., 2010). In *S. aureus*, the transcription of *rel* is induced by mupirocin treatment (Anderson *et al.*, 2006; Reiss *et al.*, 2012). However, amino acid starvation had no effect on the transcription of *rel* in *S. aureus* (Geiger *et al.,* 2014) or on the transcription of the homologous gene in *S. mutans* (Lemos *et al*., 2004).

The alternative sigma factor SigE regulates the expression of *rel* in M*ycobacterium tuberculosis* (Sureka *et al.,* 2007). *sigE* itself is regulated by the two-component system MprBA. Firstly, MprB is phosphorylated by a polyphosphate chain and then this phosphate is passed onto MprA. Phopshorylated MprA can then induce the expression of *rel* (Sureka *et al*., 2007). Polyphosphate

chains accumulate in *M. tuberculosis* during stress, meaning that *rel* transcription is induced during stress as well (Singh *et al*., 2013).

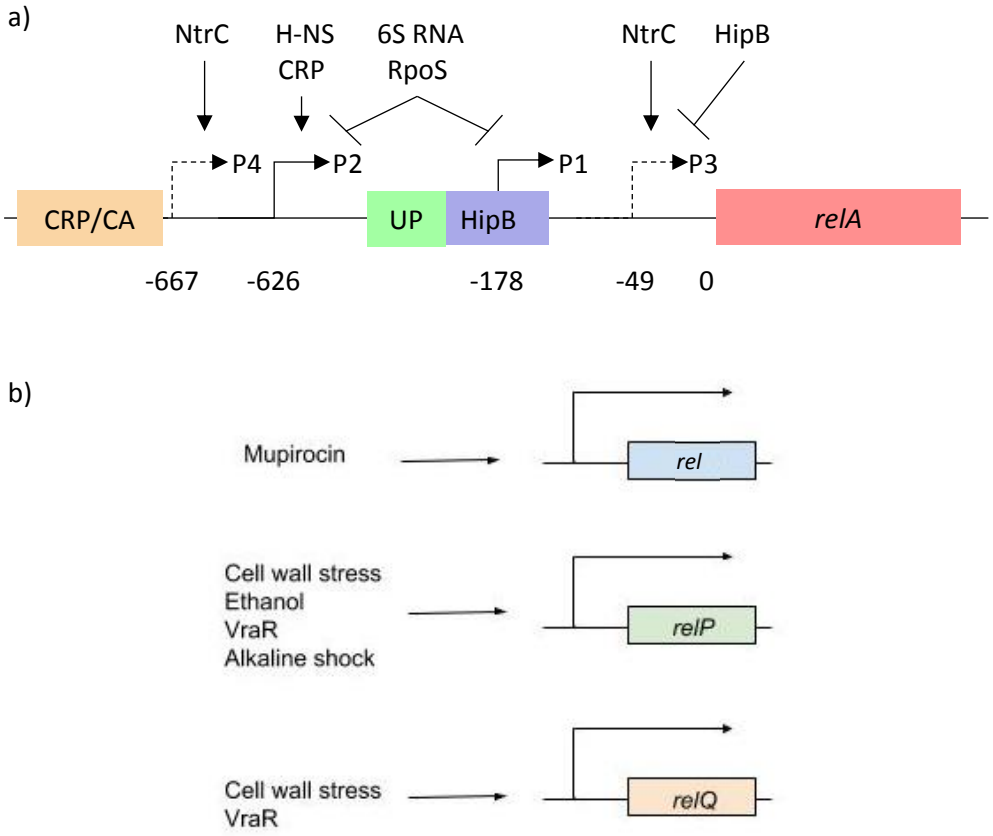

Fig. 1.2.2 Transcriptional regulation of (p)ppGpp synthetase genes in bacteria. a) Detailed diagram of *relA* regulation in *E. coli*. Numbers relate to nucleotide position were the transcription start site is 0. P1 and P2 are regulated by sigma 70 (solid lines) and P3 and P4 are regulated by sigma 54 (dashed lines). Transcription from P3 and P4 is induced by NtrC. HipB represses transcription from P3 by binding the HipB element (blue) upstream. The transcription from P2 is induced by H-NS and CRP but repressed by 6S RNA and RpoS. P1 is also repressed by 6S RNA. The Up element (green) ensure constitutive expression of P1. b) Factors triggering the transcription of *rsh, relP* and *relQ* in Gram positive bacteria.

1.2.2.2 Transcriptional regulation of SAS genes

During normal growth in relaxed conditions the transcription of *relP* and *relQ* is controlled temporally, with *relQ* transcript levels highest during exponential phase (Nanamiya *et al.*, 2008). As *relQ* transcription tails of during late exponential phase, *relP* transcription is induced and then fades as the cells enter stationary phase (Nanamiya *et al.*, 2008). This temporal regulation of *relP* and *relQ* hints that the two enzymes have different biological roles requiring different regulation. For example, overexpression of RelP has been shown to induce the formation of 100S ribosomes in *B. subtilis* but not RelQ overexpression (Tagami *et al*., 2012). 100S ribosomes are ribosome dimers formed during stationary phase growth, which coincides with *relP* induction in *B. subtilis*.

Cell wall stress appears to be an important trigger of SAS transcription in Gram positive bacteria. In *S. aureus* the transcription of *relP* and *relQ* is induced following treatment with cell wall active antibiotics. The induction of *relP* is dependent on VraR, which is the response regulator of the two-component system VraRS (Geiger *et al.*, 2014). The transcription of *relQ* is still induced in a *vraR* mutant although to a lesser extent.

Furthermore, in *B. subtilis*, *relP* is regulated by SigM and SigW (Eiamphungporn and Helmann, 2008; Cao *et al.*, 2002). Both SigM and SigW are involved in responding to cell wall stress caused by a variety of agents, such as the cationic antimicrobial peptide LL-37, the cell wall active antibiotic vancomycin and by alkaline shock (Pietiäinen *et al.*, 2005; Thackray and Moir, 2003; Wiegert *et al.*, 2001). However, the sigma factors responsible for SAS gene regulation are not conserved across Gram positive bacteria. In *S. aureus* the homologous sigma factor to SigM and SigW is SigS (Miller *et al.,* 2012). Based on analysis of the promoter sequences of *relP* and *relQ*, the predicted sigma factor regulator is SigA not SigS (Geiger *et al.* 2014). SigA is the housekeeping sigma factor in *S. aureus* suggesting a constitutive basal expression of both *relP* and *relQ* (Deora and Misra, 1996).

Ethanol treatment is another stress that induces cell wall stress in bacteria (Cao *et al.*, 2017). In *S. aureus*, the transcription of *relP* is induced by ethanol treatment (Pando *et al.,* 2017). Another condition that causes cell wall stress is alkaline shock. Whilst a transcriptional response to alkaline shock has not been reported in other Gram positive bacteria, it is clear that this treatment induces the stringent response in Firmicutes (Nanamiya *et al.*, 2008; Abranches *et al.*, 2009; Anderson *et al.*, 2010). In *B. subtilis*, the (p)ppGpp accumulation following alkaline shock is facilitated by RelP (Nanamiya *et al.*, 2008).

1.2.3 Post-translational regulation of (p)ppGpp synthetases

Once the RSH superfamily gene has been transcribed and the protein has been translated, the activity of the enzymes can still be regulated at a post-translational level. This can be mediated by other proteins, ligands, oligomerisation or intramolecular regulation.

1.2.3.1 Post-translational regulation of long-RSH proteins

Long-RSH proteins have a CTD domain that is considered a regulatory region, facilitating interactions with other proteins to modulate the activity of the HD or SYNTH domains. In bifunctional enzymes, such as SpoT or Rel_{Sa}, this is particularly important to avoid a fruitless cycle of (p)ppGpp synthesis and hydrolysis. Interestingly, the CTD domain alone appears to self-regulate the enzymatic activity of the protein. When the CTD domain is removed from the long-RSH protein, Rel_{Seq}, from *Streptococcus dysgalactiae subsp. equisimilis* the synthetase activity was more than 10 times higher than the full length protein, whereas the hydrolase activity was 150 times lower (Mechold *et al.*, 2002). Therefore,

the full length protein appears to be intrinsically hydrolase-ON synthetase-OFF, meaning the synthetase activity can be switched on when the stringent response is triggered.

Oligomerisation of long-RSH proteins has also been shown to impact enzymatic activity. RelA has been shown to form dimers through interactions between the CTDs of each protein (Yang and Ishiguro, 2001; Gropp *et al.*, 2001). Disrupting the oligomerisation of RelA led to an increase in (p)ppGpp synthesis, whilst overexpressing a CTD fragment was sufficient to reduce (p)ppGpp production (Gropp *et al.*, 2001). Rel_{Mtb} from *M. tuberculosis* forms a homotrimer, again with the monomer having a higher (p)ppGpp synthesis activity than the trimer (Avarbock *et al.*, 2005).

The interaction between RelA and the ribosome is perhaps the best studied post-translational regulation of an RSH superfamily member (Haseltine and Block, 1973). (p)ppGpp synthesis is stimulated and hydrolysis decreases upon binding to a ribosome activating complex (RAC), which consists of the ribosome, mRNA and uncharged tRNA (Fig. 1.2.3.1a) (Avarbock *et al.*, 2000). ppGpp can also induce (p)ppGpp synthesis by RelA when it is bound to the RAC, providing a positive feedback loop to ensure rapid signal amplification (Shyp *et al.*, 2012). Cryo-electron microscopy has determined the interaction interfaces in great detail, showing that there are actually very few contacts between the HD and SYNTH domains and any ribosomal proteins (Arenz *et al.* 2016; Brown *et al.*, 2016; Loveland *et al.*, 2016). Instead the CTD interacts with uncharged tRNA in the A site of the 30S subunit. If the tRNA present at this site is charged, then the interaction is sterically blocked, ensuring that (p)ppGpp synthesis is only stimulated in amino acid starvation conditions.

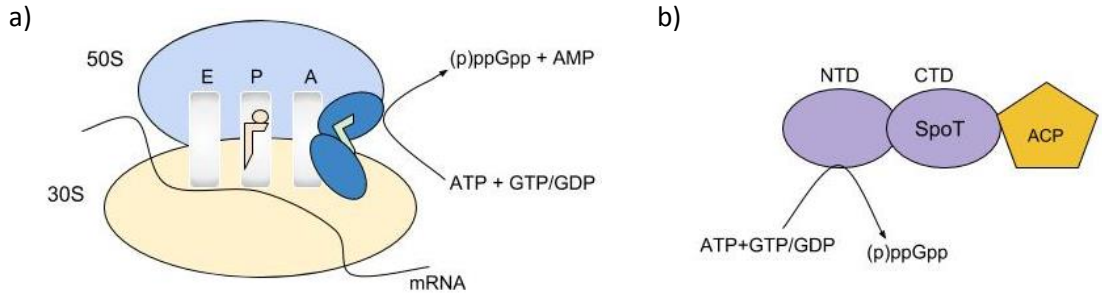

Fig. 1.2.3.1 Post-translational regulation of long-RSH proteins. a) Interaction of RelA (dark blue) with the ribosome activating complex (RAC) increases the synthesis of (p)ppGpp. The RAC consists of the ribosome (50S, light blue; 30S, orange), mRNA and uncharged tRNA (green). A charged tRNA (orange) is situated in the P site of the ribosome. b) Interaction of the CTD of SpoT (purple) with ACP (yellow) increases the synthesis of (p)ppGpp.

In *E. coli*, SpoT mediates the stringent response to fatty acid starvation (Seyfzadeh *et al.,* 1993). The TGS/RRM domain of the SpoT CTD binds to the acyl carrier protein (ACP), inducing (p)ppGpp synthesis (Fig. 1.2.3.1b) (Gully *et al.*, 2003; Butland *et al.,* 2005; Battesti and Bouveret, 2006). Although long-

RSH proteins in Gram positive bacteria also have a TGS/RRM domain, they do not interact with ACP (Battesti and Bouveret, 2009). This is probably due to the fact that these proteins are less basic than SpoT and so cannot bind to the acidic ACP.

ObgE, another SpoT interaction partner in *E. coli,* is a Obg family GTPase (Wout *et al.*, 2004). ObgE inhibits (p)ppGpp synthesis during exponential growth but does not have an effect on the stringent response to amino acid starvation (Jiang *et al.*, 2007). However, ObgE may play a role in determining the ratio of pppGpp to ppGpp, with ObgE mutants showing a higher ratio (Persky *et al.*, 2009). Interestingly, the GTPase activity of ObgE is activated by binding to the ribosome but inhibited by (p)ppGpp (Persky *et al.*, 2009; Gkekas *et al.*, 2017; Corrigan *et al.,* 2016).

Rel_{Bs} from *B. subtilis* binds to ComGA, although it has not been determined if this interaction result in any change in Rel_{Bs} enzymatic activity (Hahn *et al.*, 2015). ComGA is conserved amongst bacteria that are competent and also has a role in regulation of the K-state in *B. subtilis*. ComGA is responsible for a reduction of rRNA gene transcription in a (p)ppGpp-dependent manner, leading to growth arrest.

1.2.3.2 Post-translational regulation of SAS proteins

It was first thought that SAS proteins would be predominantly regulated on a transcriptional level due to the absence of a CTD regulatory region that is found in long-RSH proteins. However, it is now evident that SAS proteins are indeed regulated on a post-transcriptional level by a variety of mechanisms (Fig. 1.2.3.2).

When RelQ from *B. subtilis* forms a tetramer a cleft is formed. Two pppGpp molecules can bind this cleft and allosterically stimulate the synthetase activity of the enzymes by 10-fold *in vitro* (Steinchen *et al.*, 2015). Interestingly, whilst pppGpp but not ppGpp was able to allosterically regulate RelQ from *B. subtilis*, the opposite was true for RelQ from *Enterococcus faecalis* (Gaca *et al.*, 2015). The allosteric cleft is also conserved in RelP from *B. subtilis*, however the negative charge of pocket suggests that a ligand other than (p)ppGpp binds to it. The formation of the RelQ tetramer boosts the synthetase activity, even without allosteric regulation from pppGpp, due to a high positive cooperativity (Steinchen *et al.,* 2015). The positive regulation of an enzyme by its product is rare but allows for rapid signal amplification when required. Presumably a threshold (p)ppGpp concentration must be reached before RelQ is allosterically stimulated, and this must be higher than the basal (p)ppGpp level in the cell.

In *E. faecalis*, RelQ is also negatively regulated by single stranded RNA (ss-RNA), such as mRNA, in the absence of (p)ppGpp (Beljantseva *et al.*, 2017). (p)ppGpp alleviates the negative effect of ssRNA on synthetase activity. The consensus RelQ binding sequence is GGAGG (in particular the successive GG

residues), which is noticeably similar to the Shine-Dalgarno sequence. However, it is unclear whether RelQ binds to mRNAs and whether there is any biological significance to this interaction.

It is clear that the role of RelP and RelQ in the stringent response is more nuanced that previously expected. Further research is required to understand the impact of ligand mediated regulation of SAS on the stringent response in Gram positive bacteria.

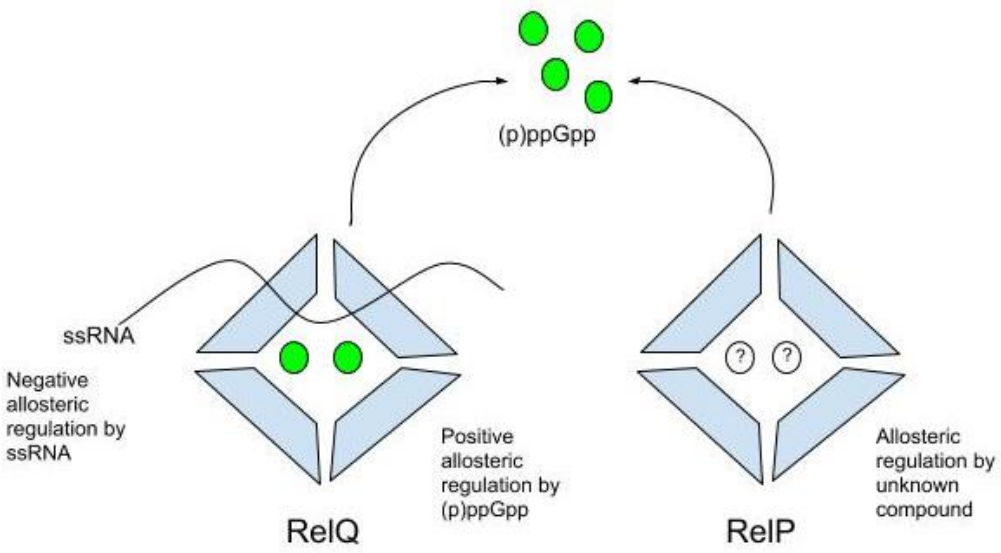

Fig. 1.2.3.2 Post-translational regulation of SAS proteins, RelP and RelQ. RelQ forms a homotetramer allowing 2 molecules of (p)ppGpp (green) to bind and increase (p)ppGpp synthesis by positive allosteric regulation. This cleft is also formed by the RelP tetramer however it is unknown if any molecule binds. RelQ is also negatively regulated by ssRNA.

1.3 Intracellular targets of (p)ppGpp

(p)ppGpp has many targets within the cell, affecting a broad range of cellular processes. Bacteria have evolved to use the universal (p)ppGpp alarmones to trigger different responses according to their ecological niches or lifestyles.

1.3.1 Transcription

1.3.1.1 Gram negative bacteria

The stringent response results in a huge change in transcriptional profile in *E. coli*, with over 500 genes differentially expressed, including a decrease in rRNA synthesis and a concurrent increase in expression of amino acid biosynthesis and transport genes (Durfee *et al.*, 2008). In *E. coli*, (p)ppGpp can bind directly to RNA polymerase (RNAP), although ppGpp is the more potent nucleotide (Fig. 1.3.1) (Mechold *et al.*, 2013; Zuo *et al*., 2013). (p)ppGpp binds in a cleft surrounded by the α- β- and ω-subunits of the RNAP. The ability of a RNAP from a given species to bind to (p)ppGpp can be predicted by the presence of a MAR motif at the N terminal end of the ω-subunit. This MAR motif is conserved amongst Alphaproteobacteria, Betaproteobacteria, Gammaproteobacteria and Deltaproteobacteria

but is absent in other classes such as Firmicutes (Hauryliuk *et al*., 2015). The effect of (p)ppGpp on reducing rRNA gene transcription is potentiated by binding of DksA to RNAP, however the mechanism of this process is not yet understood (Paul *et al*., 2004). DksA and ppGpp act synergistically, with the effect on RNAP transcription with both factors much greater than with either one alone. Indeed, both factors are required for the positive activation of amino acid biosynthesis gene promoters during the stringent response (Paul *et al.,* 2005).

(p)ppGpp appears also to regulate transcription even in relaxed conditions. In *E. coli*, low ppGpp levels trigger the activation of the Lrp regulon, whereas high ppGpp levels are required to activate the RpoS regulon (Traxler *et al.*, 2011).

1.3.1.2 Gram positive bacteria

In Gram positive bacteria, (p)ppGpp does not bind to RNAP and the cofactor DksA is not present. ppGpp has no effect on the stability of the DNA-RNAP open complex in *B. subtilis* and so cannot affect transcription through the same mechanism as in *E. coli* (Krásný and Gourse, 2004). Instead, transcription is controlled through GTP levels (which are lower during the stringent response) through two mechanisms.

Firstly, GTP is the initiating nucleotide of the *rrn* promoter, so when GTP levels are low in the cell rRNA transcription is downregulated due to a slower initiation rate (Krásný and Gourse, 2004). This method of rRNA regulation seems specific to Gram positive bacteria, as the identity of the initiating nucleotide in *E. coli* has no effect on the promoter regulation by (p)ppGpp (Haugen *et al.,* 2008). In *S. aureus*, GTP nucleotides in positions +1 to +4 can have a role in promoter activity and so any other gene with this property would also be downregulated during the stringent response (Kastle *et al.*, 2015).

Secondly, GTP is one of two CodY cofactors, along with branched chain amino acids (isoleucine, leucine and valine) (Geiger and Wolz, 2014). CodY is a gene repressor in Gram positive bacteria with a large regulon (Majerczyk *et al.*, 2010). As the GTP pool in the cell drops during the stringent response, the repression of CodY is released resulting in a huge change in transcriptional profile. In *S. aureus*, 150 genes are upregulated during the stringent response, however only 7 of these do so independently of CodY deprepression (Geiger *et al.*, 2012). 161 genes are down-regulated during the stringent response induced by leucine/valine starvation and all of these are regulated independently of CodY. This is perhaps unsurprising seen as CodY acts as a gene repressor. This clearly highlights that, in Gram positive bacteria, CodY is an important factor for determining gene upregulation during the stringent response but not downregulation.

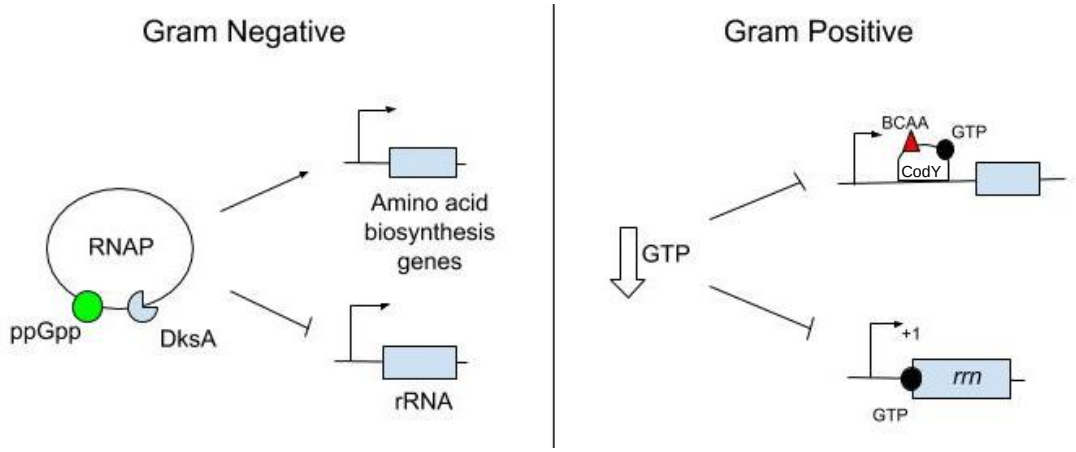

Fig. 1.3.1 Effects of the stringent response on transcription in Gram negative and Gram positive bacteria. In Gram negative bacteria, ppGpp (green) and DksA bind to RNA polymerase to alter the transcription of various genes. The transcription of amino acid biosynthesis genes is increased, while the transcription of rRNA genes is repressed. In Gram positive bacteria the decrease in GTP levels during the stringent response results in a derepression of the CodY regulon and a decrease in transcription of *rrn* and other genes with GTP at the +1 site.

1.3.2 Ribosome maturation and translation

During the stringent response the rate of translation in the cell is reduced in order to survive low nutrient levels. This is achieved through a reduction in the number of mature ribosomes through three key mechanisms (Fig. 1.3.2).

Firstly, during the stringent response the transcription of rRNA is repressed, a key component of ribosome maturation. In Gram negative bacteria this occurs through ppGpp and DksA altering RNAP transcription of rRNA genes (Paul *et al.,* 2004). In Gram positive bacteria transcription of rRNA genes decreases dues to low GTP levels (Krásný and Gourse, 2004).

Secondly, (p)ppGpp directly targets key factors involved in ribosome maturation. In Gram positive bacteria, ppGpp inhibits the formation of 70S ribosomes by directly inhibiting the activity of several GTPases involved in ribosome maturation (Corrigan *et al.*, 2016). The GTPase activity of RsgA, RbgA, Era and HflX is inhibited by ppGpp in *S. aureus*, *B. subtilis,* and *E. faecalis*, indicating that this mechanism for reducing translation is conserved across Firmicutes. Furthermore, the activity of the elongation factors EF-Tu and EFG is inhibited by (p)ppGpp, thus preventing the docking of charged tRNAs and translocation during peptide synthesis (Miller *et al.*, 1973; Rojas *et al.*, 1984). The activity of initiation factor IF2 is also inhibited by (p)ppGpp, preventing the formation of the initiation complex (Legault *et al*., 1972).

Lastly, any mature ribosomes already present in the cell at the start of the stringent response can be sequestered. During the stringent response inactive 70S ribosome dimers form called 100S ribosomes (Tagami *et al*., 2012). In *S. aureus*, the GTPase HflX is involved in splitting the 100S ribosome, however

this activity in inhibited by (p)ppGpp thus maintaining 100S ribosomes during the stringent response (Basu and Yap, 2017). This mechanism is more cost effective than completely dismantling ribosomes and allows a swifter return to normal translation levels when the stringent response ends.

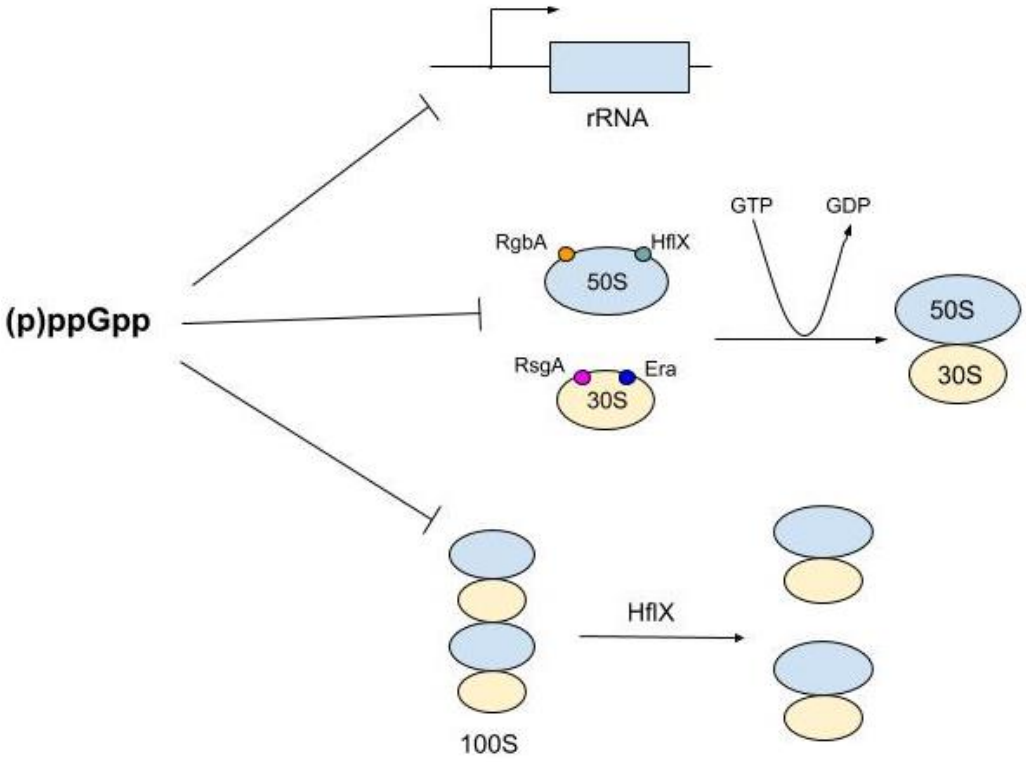

Fig. 1.3.2 Effects of (p)ppGpp on ribosome maturation. (p)ppGpp directly or indirectly inhibits rRNA transcription. (p)ppGpp inhibits the GTPase activity of various small GTPases, preventing correct ribosome maturation. (p)ppGpp inhibits splitting of inactive 100S ribosome dimers by HflX.

1.3.3 Metabolism

During the stringent response there is a shift in metabolism in order to adapt to nutrient limitation or other stresses. This is predominantly regulated on a transcriptional level, however (p)ppGpp does directly impact the activity of various metabolic proteins.

One aspect of metabolism controlled by the stringent response is DNA replication. (p)ppGpp inhibits the of primase activity of DnaG in *B. subtilis*, resulting in the arrest of DNA replication forks (Wang *et al.,* 2007). This inhibition has also been shown *E. coli* and *S. aureus*, indicating that it is a conserved mechanism for halting DNA replication amongst bacteria (Maciag *et al.,* 2010; Rymer *et al.*, 2012).

As (p)ppGpp accumulates in the cell, the GTP pool in the cell is lowered following the use of GTP as a substrate in (p)ppGpp synthesis, but also due to a direct inhibition of GTP synthesis by (p)ppGpp. Three enzymes in the GTP biosynthetic pathway are inhibited by (p)ppGpp: IMP dehydrogenase, GuaB; hypoxanthine phosphoribosyltransferase, HprT; and guanylate kinase, Gmk (Lopez *et al.*, 1981;

Beaman *et al.*, 1983; Kriel *et al.*, 2012). In *B. subtilis* the inhibition of HprT and Gmk is thought to have the largest effect on the GTP pool (Kriel *et al.*, 2012). In *E. coli* the ATP biosynthesis enzyme PurA is also inhibited by (p)ppGpp. (Stayton and Fromm, 1979). ppGpp also inhibits PurF in *E. coli* thus halting *de novo* purine biosynthesis (Wang *et al.*, 2019).

Phospholipid metabolism is also regulated by (p)ppGpp to ensure adaptation to nutrient limitation. The enzymes responsible for the first steps of lipid and phospholipid biosynthesis (PlsB and PgsA, respectively) are inhibited by (p)ppGpp (Merlie and Pizer, 1973; Heath *et al.*, 1994). Presumably, phospholipid biosynthesis is inhibited during the stringent response because the cells are not growing.

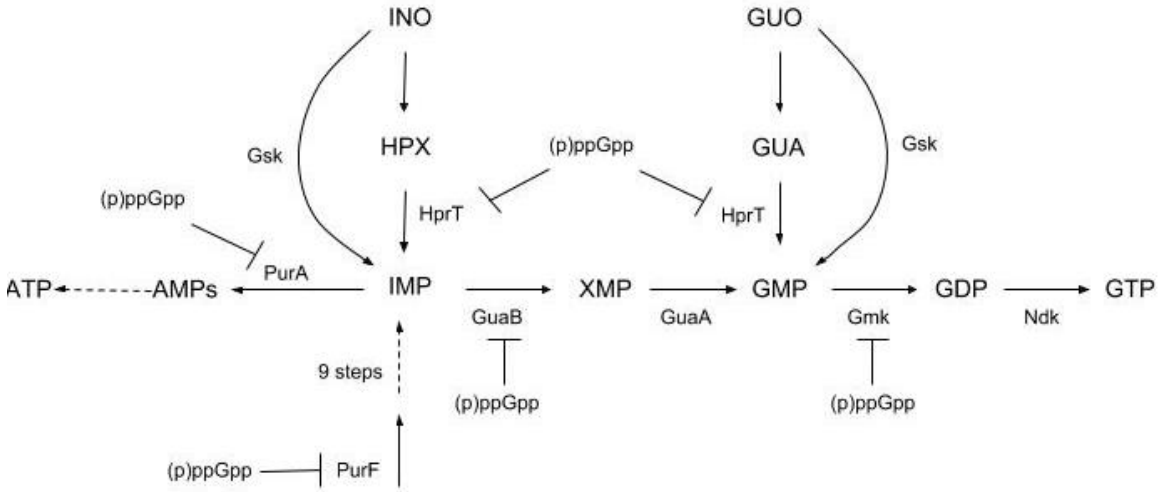

Fig. 1.3.3 The impact of (p)ppGpp on GTP and ATP synthesis. (p)ppGpp inhibits the activity of HprT, GuaB, Gmk,PurA and PurF. HprT converts HPX or GUA to IMP or GMP, respectively. GuaB converts IMP to XMP. Gmk converts GMP to GDP. PurA converts IMP to AMPs. PurF is part of the purine *de novo* synthesis pathway. Cumulatively, the inhibition by (p)ppGpp results in a reduction in GTP and ATP biosynthesis as well as all *de novo* purine biosynthesis.

1.4 The stringent response and bacterial pathogenicity

1.4.1 The impact of the stringent response on virulence

The stringent response has been linked to virulence in many organisms. (p)ppGpp mutant strains in various species, such as *S. aureus* and *M. tuberculosis* show impaired virulence in animal models (Geiger *et al.*, 2010; Klinkenberg *et al.*, 2010). A rel_{syn} mutant (defective in (p)ppGpp synthesis from $RelA_{Sa}$ but hydrolase activity is intact) of *S. aureus* showed reduced virulence compared to the wild type (WT) in mice (Geiger *et al.*, 2010). Interestingly, there was no significant difference in virulence between the WT and *codY* or a *codY*/rel_{syn} double mutant. This suggests that the rel_{syn} single mutant is less virulent because CodY repression is not significantly released, whereas in a background without CodY (and thus no repression of virulence factors) a rel_{syn} mutant has no effect on virulence. Clearly the impact of the stringent response on the transcriptional regulation of virulence factors is key to how (p)ppGpp accumulation influences bacterial virulence.

In *V. cholerae*, a *relA* mutant showed reduced transcription of the hallmark virulence factors cholera toxin and toxin coregulated pilus (Haralalka *et al.*, 2003). This mutant also had attenuated colonisation of the intestine in mice. Similarly, a *relA*/*spoT* double mutant in *Salmonella typhimurium* is avirulent in mice and shows reduced transcription of *hilA* and *invF*, which are key regulators of the expression of pathogenicity islands (Pizarro-Cerdá and Tedin, 2004). However, a *relA* single mutant in *S. typhimurium* did not show any attenuation of virulence (Pizarro-Cerdá and Tedin, 2004). The importance of SpoT for virulence has been demonstrated in several other bacteria, such as *Francisella tularensis*, *Legionella pneumophila* and *Yersinia pestis*, where a *relA/spoT* double mutant is attenuated compared to the WT or *relA* single mutant strains (Charity *et al.*, 2009; Dalebroux *et al.*, 2009; Sun *et al.,* 2009). It is thought that the hydrolase activity of SpoT is required for cell replication to continue after cell growth is stalled during the stringent response and thus SpoT is required for infection expansion.

1.4.2 The stringent response and persistence

Bacterial persistence is mediated by the formation of persister cells. These are a sub-population that are genetically identical to non-persister cells but are tolerant to antibiotic treatment due to slow growth (Fig. 1.4.3a). Many antibiotics target aspects of bacterial metabolism that only occur in growing cells, thus persister cells can survive antibiotic treatment. Research into persister cell formation has highlighted the role of the stringent response in governing persistence in bacteria.

In *E. coli*, the frequency of persister cells is reduced in a *relA* mutant and is reduced even further in a *relA*/*spoT* double mutant (Korch *et al.,* 2003). In a clinical isolate of *S. aureus* responsible for a persistent infection, a mutation in the hydrolase domain of Rel_{Sa} resulted in reduced (p)ppGpp hydrolysis and therefore a constitutive stringent response (Gao *et al.*, 2010). This mutation resulted in a SCV phenotype associated with persistence in *S. aureus* and therefore reduced antibiotic susceptibility and a persistent infection. Antibiotic tolerance is a key phenotype of persistence and vancomycin tolerance in *E. faecalis* is mediated by (p)ppGpp (Abranches *et al.*, 2009).

There are many similarities between persistence and the stringent response, namely, antibiotic tolerance, reversible slow-growth, and a reduction in general cell processes. However, it is important to distinguish the two. The stringent response is triggered in response to stimuli, whereas persister cells form stochastically and are present in any bacterial population. The relationship between the stringent response and persistence is yet to be fully understood in bacteria.

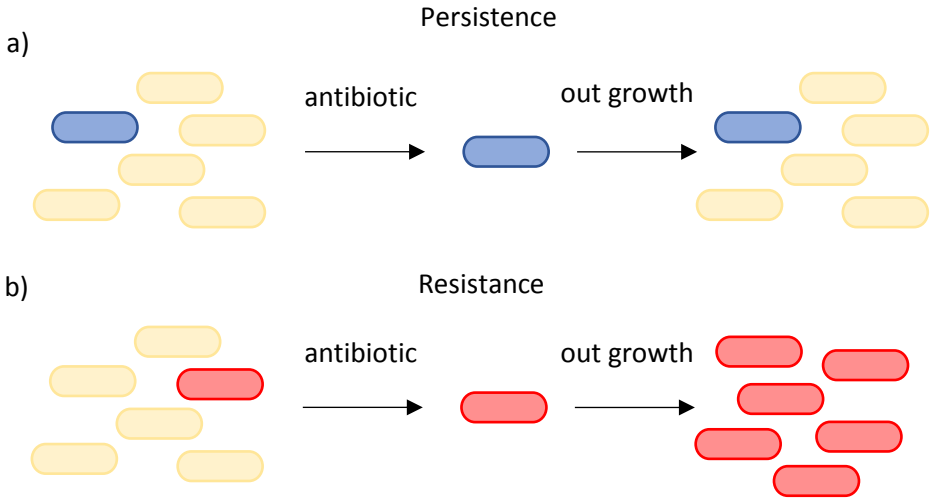

Fig. 1.4.3 Resistance and persistence in bacteria. Antibiotic susceptible cells (yellow), antibiotic resistant cells (red) and persister cells (blue) are treated with antibiotic cells are treated with antibiotics. Only resistant and persister cells survive. a) after outgrowth the following population has inheeited the antibiotic resistance and the whole population is resistant. b) after outgrowth the following population is a mixture of antibiotic susceptible cells and pesister cells. The frequency of persister cells is the same before and after antibiotic treatment.

1.4.3 The stringent response and resistance

Whilst persister cells are genetically identical to the WT cells, resistant cells are not (Fig. 1.4.3b). They have acquired a genetic element that allows the cell to become resistant to antibiotic treatment through four main mechanisms. These mechanisms are: reducing the accumulation of the drug in the cell; inactivating the drug; alteration of the drug target; and altering the pathway the drug targets.

The presence of resistance genes is not determined by the stringent response, however there is evidence that it can impact the resistance level of a strain. For example, many MRSA strains show different levels of resistance to beta-lactam antibiotics despite all encoding SCC*mec* elements. These differences in resistance are mediated, in part, by the stringent response with high levels of (p)ppGpp associated with high beta-lactam resistance (Mwangi *et al*., 2013). Therefore, it could be possible to reduce the methicillin resistance of MRSA by inhibiting the accumulation of (p)ppGpp.

1.5 The stringent response as a drug target

As detailed above, the stringent response plays a major role in the pathogenicity of many bacteria and so is a potential target for anti-microbial therapeutics. Efforts thus far have focused on inhibiting the (p)ppGpp synthetase activity of RSH-superfamily enzymes. However, inhibition of (p)ppGpp hydrolysis could be another valid strategy, because in *S. aureus* the hydrolase domain of Rel_{Sa} is essential in WT strains (i.e. in the presence of RelP and RelQ) (Geiger *et al.*, 2010).

1.5.1 Relacin

Using the crystal structure of Rel_{Seq} from *S. equisimilis* (Hogg *et al.*, 2004), Wexselblatt and colleagues designed an analogue of ppGpp with the intention of blocking the activity of long-RSH proteins (Wexselblatt *et al.*, 2012). In this molecule, named Relacin, the C5ˈ and C3ˈ pyrophosphate moieties of ppGpp are replaced by glycyl-glycine dipeptides, which are linked by a carbamate bridge to the sugar ring. Relacin inhibits (p)ppGpp production by RelA and Rel_{Dra} from *E. coli* and *Deinococcus radiodurans in vitro* and also inhibits (p)ppGpp production in *B. subtilis*. Relacin hinders certain strategies used by bacteria for long-term survival such as sporulation, biofilm formation, and entry into stationary phase growth. However, Relacin had no effect on the production of (p)ppGpp by *E. coli* cells *in vivo*, perhaps due to the drug being unable to enter the *E. coli* cell. Another limitation of Relacin is that it does not inhibit SASs such as RelQ (Gaca *et al.*, 2015). Relacin-2d, which has glutamyl-glutamic acid moieties at C5ˈ and C3ˈ, is more potent than Relacin but has not been shown to be effective against Gram negative bacteria (Wexselblatt *et al.*, 2013).

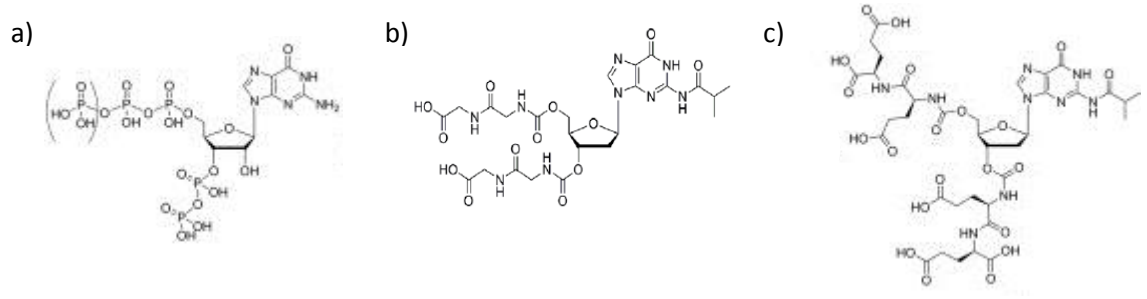

Fig. 1.5.1 Chemical structure of (p)ppGpp analogues. a) Structure of (p)ppGpp. b) Structure of Relacin, the C5ˈ and C3ˈ pyrophosphate moieties of ppGpp are replaced by glycyl-glycine dipeptides. c) Structure of Relacin-2d, the C5ˈ and C3ˈ pyrophosphate moieties of ppGpp are replaced by glutamyl-glutamic acid moieties

1.5.2 Peptide Therapeutics

An immunomodulatory peptide, innate-defence regulator-1018, has been shown to disperse mature biofilms and cause cell death at high concentrations in several bacteria (de la Fuente-Nuñes *et al.*, 2014). It was proposed that the mode of action of the peptide is direct targeting of (p)ppGpp. However, Andresen and colleagues contested this, as 1018 inhibited *E. coli* growth equally in media without or with valine (when (p)ppGpp is or is not essential, respectively) (Andresen *et al.*, 2016b). More potent peptide derivatives of 1018, DJK-5 and DJK-6 protected against *Pseudomonas aeruginosa* infections in *Galleria mellonella* and *Caenorhabditis elegans* invertebrate models and prevented the accumulation of (p)ppGpp (de la Fuente-Nuñes *et al.*, 2015). DJK-5 and 1018 suppressed promoter activity of *spoT* during cutaneous abscess formation in mice (Pletzer *et al.*, 2017). Whilst their mechanism of action is debated, cationic peptides are an interesting therapeutic that are active against biofilms, which are difficult to treat with conventional antibiotics.

1.5.3 Autotrophy-based High Throughput Screening for long-RSH inhibitors

In order to find an effective drug that targets the stringent response, a high-throughput method is needed. Work exploiting the valine auxotrophy of (p)ppGpp^0 *B. subtilis* in a screen of 17,500 compounds highlighted a novel class of antimicrobials with a 4-(6-(phenoxy)alkyl)-3,5-dimethyl-1H-pyrazole core (Andresen *et al.*, 2016a). However, these molecules do not specifically inhibit Rel$_{Bs}$ activity, as further testing showed that they inhibit *B. subtilis* growth equally in media with and without valine. Using the same methods, Relacin and peptide 1018 were shown to not be specific inhibitors of the stringent response in *B. subtilis*. Relacin did not inhibit the growth of a Δ*relP*Δ*relQ* strain in media with or without valine. Peptide 1018 inhibited the growth of Δ*relP*Δ*relQ* and (p)ppGpp^0 strains equally highlighting that Rel$_{Bs}$ is not its target. Clearly, more work is required to find a true inhibitor of long-RSH synthetases, however other ways of exploiting our knowledge of the stringent response should not be overlooked.

1.6 Aims and Objectives of this Study

This study aims to characterise the regulation and function of RSH superfamily enzymes in *S. aureus*, Rel$_{Sa}$, RelP and RelQ. As detailed above, there are major differences in the stringent response in Gram negative and Gram positive bacteria, and subtleties between the stringent response in *S. aureus* and other Gram positive bacteria.

Firstly, this study aims to investigate the regulation of the (p)ppGpp synthetases on a transcriptional level using promoter-reporter gene fusions. We sought to understand how different stresses impact transcription of the synthetases and how they are expressed during growth. We also attempted to identify any transcription factors involved in the regulation of (p)ppGpp synthetase gene expression using transposon insertion mutants. The discovery of VraRS regulation of *relP* and *relQ* in *S. aureus* led to the conclusion that cell wall stress and therefore cell wall active antibiotics, trigger the stringent response in *S. aureus.* In the same way, we hypothesised that gaining an understanding of gene regulation in *S. aureus* would lead to further information about which conditions trigger the stringent response.

Secondly, we sought to investigate how the (p)ppGpp synthetases in *S. aureus* are regulated post-translationally. As highlighted previously, much of what is known about protein-protein interactions that influence the stringent response is only applicable to Gram negative bacteria. It was hypothesised that understanding the regulation of (p)ppGpp synthetases would provide insights into novel environmental stresses that trigger the stringent response in *S. aureus*. Initially, we used a targeted approach to investigate if the (p)ppGpp synthetases interact with each other. We then focused on

identifying novel (p)ppGpp synthetase binding partners, because very few have been identified in Gram positive bacteria and none have been characterised in *S. aureus*.

Having identified several novel Rel_{Sa} and RelP binding partners we focussed on the role of the Rel_{Sa}-RocF interaction in the stringent response. RelA and SpoT interaction partners have been shown to influence the (p)ppGpp synthetase or hydrolase activity of the enzymes. As such, we investigated how the enzymatic activity of Rel_{Sa} or RocF was affected by their interaction in order to gain a better understanding of the importance of this interaction within the context of the stringent response.

Finally, we investigated the role of the stringent response in survival and growth in various growth conditions. We hoped that by using a panel of single, double and triple (p)ppGpp synthetase mutants we would be able to examine the role of each of the synthetases in survival of stress conditions. We hypothesised that the three enzyme have different roles in the stringent response despite all having (p)ppGpp synthesis activity.

Ultimately, this study aims to understand the importance and the regulation of the stringent response in *S. aureus*. The stringent response has been linked to bacterial persistence and antibiotic tolerance resulting in a worse clinical outcome. As such, understanding how the stringent response is triggered and regulated in *S. aureus* is important for tackling this major human pathogen.

Chapter 2 - Methods

2.1 Bacterial strains and growth conditions

Escherichia coli strains were grown at 37°C in Lysogeny Broth (LB), on LB agar (Fisher) or MacConkey agar (Sigma) supplemented with 1% maltose (w/v). The BTH101 *E. coli* strain was usually grown at 30°C to avoid reversion of the *cya*$^-$ mutation. *Staphylococcus aureus* strains were grown at 37°C in tryptic soy broth (TSB), synthetic human urine (SHU), Chemically Defined Media (CDM), human urine (HU) or on tryptic soy agar (TSA) (Scientific Laboratory Supplies). The components of the different CDMs used are listed in Table 2.1.1, Table 2.1.2 and Table 2.1.3. The bacterial cultures were incubated with shaking (250 rpm) at the indicated temperatures. *E. coli* cultures were supplemented where appropriate with the following concentrations: carbenicillin, 50 μg/ml in broth and 150 μg/ml on agar; chloramphenicol, 10 μg/ml; kanamycin 30 μg/ml; gentamicin 20 μg/ml. *S. aureus* cultures were supplemented where appropriate with the following concentrations: chloramphenicol, 7.5 μg/ml; kanamycin 30 μg/ml; erythromycin 10 μg/ml; tetracycline 2 μg/ml.

Bacterial strains were stored by mixing 500 μl of a stationary phase culture with 500 μl of freezer medium (10% bovine serum albumin, 10% monosodium glutamate) and maintaining at -80°C.

Bacterial strains used in this study are listed in Table 2.2.

Table 2.1.1 Chemically defined media for growth of *S. aureus* (Rudin *et al.*, 1974; Schwan *et al.*, 2004)

Ingredients	Concentration (mg/L)
KCl	3000
NaCl	9500
$MgSO_4 \cdot 7H_2O$	1300
$(NH_4)_2SO_4$	4000
Tris	12100
*Glucose	5000
*L-Arg	125
*L-Pro	200
*L-Glu	250
L-Val	150
L-Thr	150
L-Phe	150
L-Leu	150
L-Gly	50

L-Ser	30
L-Asp	90
L-Lys	50
L-Ala	60
L-Trp	10
L-Met	10
L-His	20
L-Ile	30
L-Tyr	50
Thymine	20
Biotin	0.1
Thiamine	2
Nicotinic acid	2
Calcium pantothenate	2
$CaCl_2 \cdot 2H_2O$	22
KH_2PO_4	140
$FeSO_4 \cdot 7H_2O$	6
$MnSO_4 \cdot 4H_2O$	10
Citric acid	6
L-Cys	80

*included where necessary

Table 2.1.2 Chemically defined media for growth of *S. aureus* (Hussain *et al.*, 1991)

Ingredients	Concentration (mg/L)
$MgSO_4 \cdot 7H_2O$	500
*Glucose	10000
*L-Arg	100
*L-Pro	150
*L-Glu	150
L-Val	150
L-Thr	150
L-Phe	100
L-Leu	150
L-Gly	100
L-Ser	100

L-Asp	150
L-Lys	100
L-Ala	100
L-Trp	100
L-Met	100
L-His	100
L-Ile	150
L-Tyr	100
Thiamin hydrochloride	2
Biotin	0.1
Pyridoxal	4
Pyridoxamine dihydrochloride	4
Nicotinic acid	2
Calcium pantothenate	2
Riboflavin	2
Adenine sulphate	20
Guanine hydrochloride	20
$CaCl_2 \cdot 6H_2O$	10
KH_2PO_4	3000
$Na_2HPO_4 \cdot 2H_2O$	10000
$(NH_4)_2SO_4 \cdot$ FeSO4$\cdot 6H_2O$	6
$MnSO_4$	5
L-Cys	50

*included where necessary

Table 2.1.3 Synthetic human urine for growth of *S. aureus* (Ipe and Ulett, 2016)

Ingredients	Concentration (g/L)
NaCl	5.8440
Na_2SO_4	2.4147
Urea	16.8168
KCl	2.8329
$CaCl_2$	0.4439
Creatinine	1.0181
$Na_3C_6H_5O_7$	1.9999
NH_4Cl	1.0698

$MgSO_4$	0.3852
$Na_2C_2O_4$	0.0241
NaH_2PO_4	0.5616
Na_2HPO_4	0.9227
KH_2PO_4	2.1774
$C_5H_4N_4O_3$	0.1009
$NaHCO_3$	1.1341
$MgCl_2{\cdot}6H_2O$	0.6506
$C_3H_6O_3$	0.0991
$FeSO_4{\cdot}7H_2O$	0.0014
*Yeast extract	2.0000

*included where necessary

Table 2.2 Bacterial strains used in this study

Strain	Relevant features	Reference
	Escherichia coli strains	
XL1-Blue	Cloning strain, TetR	Stratagene
BL21 DE3	Protease deficient protein expression strain	Novagen
T7IQ	Protease deficient protein expression strain, lacIq tightly control expression: CamR	New England Biolabs
BTH101	Deletion mutation at bp 99 in the *cya* gene results in a *cya*$^-$ phenotype.	Euromedex
	Staphylococcus aureus strains	
RN4220 Δ*spa*	RN4220 *spa*; protein A negative derivative of RN4220	Grundling and Schneewind, 2007
NMΔΦ4	Newman strain with deletion of phage NM4, which allows integration of pCL55-derived plasmids	Corrigan *et al*., 2013
LAC*	LAC*: Erm sensitive CA-MRSA LAC strain (AH1263)	Boles *et al*., 2010
JE2	LAC* cured of all plasmids	Fey *et al.* 2013
SH1000 GFP	SH1000 with chromosomally inserted *gfp* gene: KanR	Foster strain collection
LAC* rel_{syn}	LAC* with 9 bp deletion in *rel* corresponding to the conserved aa: YQS (aa308-310)	Corrigan *et al.*, 2015
LAC* *relP::erm*	LAC* with Tn insertion in *relP*: ErmR	Corrigan strain collection

LAC* *relQ*	LAC* with *relQ* replaced by tetracycline resistance cassette: TetR	Corrigan strain collection
LAC* rel_{syn} *relP*	LAC* with 9 bp deletion in *rel* corresponding to the conserved aa: YQS (aa308-310) and Tn insertion in *relP*: ErmR	Corrigan strain collection
LAC* rel_{syn} *relQ*	LAC* with 9 bp deletion in *rel* corresponding to the conserved aa: YQS (aa308-310) and *relQ* replaced by tetracycline resistance cassette: TetR	Corrigan strain collection
LAC* *relP relQ*	LAC* with Tn insertion in *relP* and *relQ* replaced by tetracycline resistance cassette: ErmR, TetR	Corrigan strain collection
LAC* rel_{syn} *relP relQ*	LAC* with 9 bp deletion in *rel* corresponding to the conserved aa: YQS (aa308-310), Tn insertion in *relP* and *relQ* replaced by tetracycline resistance cassette: ErmR, TetR	Corrigan strain collection
LAC* Δ*hflX*	LAC* with deletion of *hflX*	Corrigan strain collection
LAC* *codY::erm*	LAC* with Tn insertion in *codY*: ErmR	This study
RN4220 Δ*spa* pCL55*pitet*	RN4220 Δ*spa* containing pCL55*pitet* chromosomal insertion: CamR	Corrigan *et al*., 2013
RN4220 Δ*spa* pCL55*pitet-lacZ*	RN4220 Δ*spa* containing pCL55*pitet*-lacZ chromosomal insertion: CamR	This study
NMΔΦ4 pCL55*prel-lacZ*	NMΔΦ4 containing pCL55*prel-lacZ* chromosomal insertion: CamR	This study
NMΔΦ4 pCL55p*relP-lacZ*	NMΔΦ4 containing pCL55*prelP-lacZ* chromosomal insertion: CamR	This study
NMΔΦ4 pCL55*prelQ-lacZ*	NMΔΦ4 containing pCL55*prelQ-lacZ* chromosomal insertion: CamR	This study
JE2 pCL55*prel-lacZ*	JE2 containing pCL55*prel-lacZ* chromosomal insertion: CamR	This study
JE2 pCL55*prelP-lacZ*	JE2 containing pCL55*prelP-lacZ* chromosomal insertion: CamR	This study
JE2 pCL55*prelQ-lacZ*	JE2 containing pCL55*prelQ-lacZ* chromosomal insertion: CamR	This study
JE2 pCL55*prel-lacZ agrA::erm*	JE2 containing pCL55*prel-lacZ* chromosomal insertion and Tn insertion in the *agrA* gene: CamR, ErmR	This study
JE2 pCL55*prel-lacZ argR::erm*	JE2 containing pCL55*prel-lacZ* chromosomal insertion and Tn insertion in the *argR* gene: CamR, ErmR	This study
JE2 pCL55*prel-lacZ arlR::erm*	JE2 containing pCL55*prel-lacZ* chromosomal insertion and Tn insertion in the *arlR* gene: CamR, ErmR	This study

JE2 pCL55*prel-lacZ clpP::erm*	JE2 containing pCL55*prel-lacZ* chromosomal insertion and Tn insertion in the *clpP* gene: CamR, ErmR	This study
JE2 pCL55*prel-lacZ codY::erm*	JE2 containing pCL55*prel-lacZ* chromosomal insertion and Tn insertion in the *codY* gene: CamR, ErmR	This study
JE2 pCL55*prel-lacZ fur::erm*	JE2 containing pCL55*prel-lacZ* chromosomal insertion and Tn insertion in the *fur* gene: CamR, ErmR	This study
JE2 pCL55*prel-lacZ lytR::erm*	JE2 containing pCL55*prel-lacZ* chromosomal insertion and Tn insertion in the *lytR* gene: CamR, ErmR	This study
JE2 pCL55*prel-lacZ rot::erm*	JE2 containing pCL55*prel-lacZ* chromosomal insertion and Tn insertion in the *rot* gene: CamR, ErmR	This study
JE2 pCL55*prel-lacZ saeR::erm*	JE2 containing pCL55*prel-lacZ* chromosomal insertion and Tn insertion in the *saeR* gene: CamR, ErmR	This study
JE2 pCL55*prel-lacZ sarS::erm*	JE2 containing pCL55*prel-lacZ* chromosomal insertion and Tn insertion in the *sarS* gene: CamR, ErmR	This study
JE2 pCL55*prel-lacZ sarU::erm*	JE2 containing pCL55*prel-lacZ* chromosomal insertion and Tn insertion in the *sarU* gene: CamR, ErmR	This study
JE2 pCL55*prel-lacZ sarX::erm*	JE2 containing pCL55*prel-lacZ* chromosomal insertion and Tn insertion in the *sarX* gene: CamR, ErmR	This study
JE2 pCL55*prel-lacZ sigB::erm*	JE2 containing pCL55*prel-lacZ* chromosomal insertion and Tn insertion in the *sigB* gene: CamR, ErmR	This study
JE2 pCL55*prel-lacZ sigS::erm*	JE2 containing pCL55*prel-lacZ* chromosomal insertion and Tn insertion in the *sigS* gene: CamR, ErmR	This study
JE2 pCL55*prelP-lacZ agrA::erm*	JE2 containing pCL55*prelP-lacZ* chromosomal insertion and Tn insertion in the *agrA* gene: CamR, ErmR	This study
JE2 pCL55*prelP-lacZ argR::erm*	JE2 containing pCL55*prelP-lacZ* chromosomal insertion and Tn insertion in the *argR* gene: CamR, ErmR	This study
JE2 pCL55*prelP-lacZ arlR::erm*	JE2 containing pCL55*prelP-lacZ* chromosomal insertion and Tn insertion in the *arlR* gene: CamR, ErmR	This study
JE2 pCL55*prelP-lacZ clpP::erm*	JE2 containing pCL55*prelP-lacZ* chromosomal insertion and Tn insertion in the *clpP* gene: CamR, ErmR	This study
JE2 pCL55*prelP-lacZ codY::erm*	JE2 containing pCL55*prelP-lacZ* chromosomal insertion and Tn insertion in the *codY* gene: CamR, ErmR	This study
JE2 pCL55*prelP-lacZ fur::erm*	JE2 containing pCL55*prelP-lacZ* chromosomal insertion and Tn insertion in the *fur* gene: CamR, ErmR	This study

JE2 pCL55*prelP-lacZ lytR::erm*	JE2 containing pCL55*prelP-lacZ* chromosomal insertion and Tn insertion in the *lytR* gene: CamR, ErmR	This study
JE2 pCL55*prelP-lacZ rot::erm*	JE2 containing pCL55*prelP-lacZ* chromosomal insertion and Tn insertion in the *rot* gene: CamR, ErmR	This study
JE2 pCL55*prelP-lacZ saeR::erm*	JE2 containing pCL55*prelP-lacZ* chromosomal insertion and Tn insertion in the *saeR* gene: CamR, ErmR	This study
JE2 pCL55*prelP-lacZ sarA::erm*	JE2 containing pCL55*prelP-lacZ* chromosomal insertion and Tn insertion in the *sarA* gene: CamR, ErmR	This study
JE2 pCL55*prelP-lacZ sarS::erm*	JE2 containing pCL55*prelP-lacZ* chromosomal insertion and Tn insertion in the *sarS* gene: CamR, ErmR	This study
JE2 pCL55*prelP-lacZ sarU::erm*	JE2 containing pCL55*prelP-lacZ* chromosomal insertion and Tn insertion in the *sarU* gene: CamR, ErmR	This study
JE2 pCL55*prelP-lacZ sarX::erm*	JE2 containing pCL55*prelP-lacZ* chromosomal insertion and Tn insertion in the *sarX* gene: CamR, ErmR	This study
JE2 pCL55*prelP-lacZ sigB::erm*	JE2 containing pCL55*prelP-lacZ* chromosomal insertion and Tn insertion in the *sigB* gene: CamR, ErmR	This study
JE2 pCL55*prelP-lacZ sigS::erm*	JE2 containing pCL55*prelP-lacZ* chromosomal insertion and Tn insertion in the *sigS* gene: CamR, ErmR	This study
JE2 pCL55*prelQ-lacZ agrA::erm*	JE2 containing pCL55*prelQ-lacZ* chromosomal insertion and Tn insertion in the *agrA* gene: CamR, ErmR	This study
JE2 pCL55*prelQ-lacZ argR::erm*	JE2 containing pCL55*prelQ-lacZ* chromosomal insertion and Tn insertion in the *argR* gene: CamR, ErmR	This study
JE2 pCL55*prelQ-lacZ arlR::erm*	JE2 containing pCL55*prelQ-lacZ* chromosomal insertion and Tn insertion in the *arlR* gene: CamR, ErmR	This study
JE2 pCL55*prelQ-lacZ clpP::erm*	JE2 containing pCL55*prelQ-lacZ* chromosomal insertion and Tn insertion in the *clpP* gene: CamR, ErmR	This study
JE2 pCL55*prelQ-lacZ codY::erm*	JE2 containing pCL55*prelQ-lacZ* chromosomal insertion and Tn insertion in the *codY* gene: CamR, ErmR	This study

JE2 pCL55*prelQ-lacZ fur::erm*	JE2 containing pCL55*prelQ-lacZ* chromosomal insertion and Tn insertion in the *fur* gene: CamR, ErmR	This study
JE2 pCL55*prelQ-lacZ lytR::erm*	JE2 containing pCL55*prelQ-lacZ* chromosomal insertion and Tn insertion in the *lytR* gene: CamR, ErmR	This study
JE2 pCL55*prelQ-lacZ rot::erm*	JE2 containing pCL55*prelQ-lacZ* chromosomal insertion and Tn insertion in the *rot* gene: CamR, ErmR	This study
JE2 pCL55*prelQ-lacZ saeR::erm*	JE2 containing pCL55*prelQ-lacZ* chromosomal insertion and Tn insertion in the *saeR* gene: CamR, ErmR	This study
JE2 pCL55*prelQ-lacZ sarA::erm*	JE2 containing pCL55*prelQ-lacZ* chromosomal insertion and Tn insertion in the *sarA* gene: CamR, ErmR	This study
JE2 pCL55*prelQ-lacZ sarS::erm*	JE2 containing pCL55*prelQ-lacZ* chromosomal insertion and Tn insertion in the *sarS* gene: CamR, ErmR	This study
JE2 pCL55*prelQ-lacZ sarU::erm*	JE2 containing pCL55*prelQ-lacZ* chromosomal insertion and Tn insertion in the *sarU* gene: CamR, ErmR	This study
JE2 pCL55*prelQ-lacZ sarX::erm*	JE2 containing pCL55*prelQ-lacZ* chromosomal insertion and Tn insertion in the *sarX* gene: CamR, ErmR	This study
JE2 pCL55*prelQ-lacZ sigB::erm*	JE2 containing pCL55*prelQ-lacZ* chromosomal insertion and Tn insertion in the *sigB* gene: CamR, ErmR	This study
JE2 pCL55*prelQ-lacZ sigS::erm*	JE2 containing pCL55*prelQ-lacZ* chromosomal insertion and Tn insertion in the *sigS* gene: CamR, ErmR	This study
JE2 *rocF::erm*	JE2 with a Tn insertion in the *rocF* gene: ErmR	NTML

2.2 Plasmids

Plasmids used in this study are listed in Table 2.3

Table 2.3 Plasmids used in this study

Name	Description	Reference
	Escherichia coli plasmids	
pUT18	BACTH vector for fusions to the N-terminus of fragment T18: CarbR	Karimova *et al.*, 2001
pUT18+1	BACTH vector for fusions to the N-terminus of fragment T18 with +1 frameshift: CarbR	This study

pUT18+2	BACTH vector for fusions to the N-terminus of fragment T18 with +2 frameshift: CarbR	This study
pUT18C	BACTH vector for fusions to the C-terminus of fragment T18: CarbR	Karimova *et al.*, 2001
pKT25	BACTH vector for fusions to the C-terminus of fragment T25: KanR	Karimova *et al.*, 2001
pKNT25	BACTH vector for fusions to the N-terminus of fragment T25; KanR	Karimova *et al.*, 2005
pUT18C*zip*	pUT18C containing *zip*: CarbR	Karimova *et al.*, 1998
pKT25*zip*	pKT25 containing *zip:* KanR	Karimova *et al.*, 1998
pUT18*rel*	pUT18 containing *rel*: CarbR	This study
pUT18C*rel*	pUT18C containing *rel*: CarbR	This study
pKT25*rel*	pKT25 containing *rel:* KanR	This study
pKNT25*rel*	pKNT25 containing *rel:* KanR	This study
pUT18*relP*	pUT18 containing *relP*: CarbR	This study
pUT18C*relP*	pUT18C containing *relP*: CarbR	This study
pKT25*relP*	pKT25 containing *relP:* KanR	This study
pKNT25*relP*	pKNT25 containing *relP:* KanR	This study
pUT18*relQ*	pUT18 containing *relQ*: CarbR	This study
pUT18C*relQ*	pUT18C containing *relQ*: CarbR	This study
pKT25*relQ*	pKT25 containing *relQ:* KanR	This study
pKNT25*relQ*	pKNT25 containing *relQ:* KanR	This study
pUT18HD	pUT18 containing *rel* domain HD (aa41-187): CarbR	This study
pUT18CHD	pUT18C containing *rel* domain HD (aa41-187): CarbR	This study
pKT25HD	pKT25 containing *rel* domain HD (aa41-187)*:* KanR	This study
pKNT25HD	pKNT25 containing *rel* domain HD (aa41-187)*:* KanR	This study
pUT18SYNTH	pUT18 containing *rel* domain SYNTH (aa226-357): CarbR	This study
pUT18CSYNTH	pUT18C containing *rel* domain SYNTH (aa226-357): CarbR	This study
pKT25SYNTH	pKT25 containing *rel* domain SYNTH (aa226-357)*:* KanR	This study
pKNT25SYNTH	pKNT25 containing *rel* domain SYNTH (aa226-357)*:* KanR	This study
pUT18TGS	pUT18 containing *rel* domain TGS (aa402-461): CarbR	This study
pUT18CTGS	pUT18C containing *rel* domain TGS (aa402-461): CarbR	This study
pKT25TGS	pKT25 containing *rel* domain TGS (aa402-461)*:* KanR	This study
pKNT25TGS	pKNT25 containing *rel* domain TGS (aa402-461)*:* KanR	This study
pUT18ACT	pUT18 containing *rel* domain ACT (aa657-736): CarbR	This study
pUT18CACT	pUT18C containing *rel* domain ACT (aa657-736): CarbR	This study
pKT25ACT	pKT25 containing *rel* domain ACT (aa657-736)*:* KanR	This study
pKNT25ACT	pKNT25 containing *rel* domain ACT (aa657-736)*:* KanR	This study
pUT18*rocF*	pUT18 containing *rocF*: CarbR	This study
pUT18C*rocF*	pUT18C containing *rocF*: CarbR	This study
pUT18*cshA*	pUT18 containing *cshA*: CarbR	This study
pUT18C*cshA*	pUT18C containing *cshA*: CarbR	This study
pUT18*era*	pUT18 containing *era*: CarbR	This study
pUT18C*era*	pUT18C containing *era*: CarbR	This study
pET28b-*relP*	C-terminal His tag on *relP:* KanR	This study
pET28b	Protein expression plasmid giving a C-terminal His tag: KanR	Novagen
pVL847-*rel*	N-terminal MBP-His tag on *rel*: GnR	This study

pVL847	Protein expression plasmid derived from pET19 giving an N-terminal MBP-His tag: GnR	Lee *et al.*, 2007b
pGEX-2TK-*rocF*	N-terminal GST tag on *rocF*: CarbR	This study
pGEX-2TK	Protein expression plasmid giving an N-terminal GST tag: CarbR	Pharmacia
	Staphylococcus aureus plasmids	
pMUTIN4	Suicide plasmid containing *lacZ* gene: CarbR, CamR	Vagner et al., 1998
pCL55*pitet*	pCL55 with an iTet promoter sequence: CarbR, CamR	Corrigan *et al*., 2013
pCL55*itet-lacZ*	pCL55 with *lacZ* under the control of the iTet promoter: CarbR, CamR	This study
pCL55*prel-lacZ*	pCL55 with *lacZ* under the control of the *rel* promoter: CarbR, CamR	This study
pCL55p*relP-lacZ*	pCL55 with *lacZ* under the control of the *relP* promoter: CarbR, CamR	This study
pCL55*prelQ-lacZ*	pCL55 with *lacZ* under the control of the *relQ* promoter: CarbR, CamR	This study
pAF257	Negative control for luciferase assay. Contains SmBit and *hupA*-LgBit under the control of an Atet inducible promoter: CamR	Oliviera Paiva *et al.*, 2019
pAF259	Positive control for luciferase assay. Contains LgBit-SmBit under the control of an Atet inducible promoter: CamR	Oliviera Paiva *et al.*, 2019
pAP118	Luciferase assay vector. Contains *hupA*-SmBit and *hupA*-LgBit under the control of an Atet inducible promoter: CamR	Oliviera Paiva *et al.*, 2019
pAF257*rel*	Negative control for luciferase assay. Contains SmBit and *rel*-LgBit under the control of an Atet inducible promoter: CamR	This study
pAF257*rocF*	Negative control for luciferase assay. Contains SmBit and *rocF*-LgBit under the control of an Atet inducible promoter: CamR	This study
pAF257*cshA*	Negative control for luciferase assay. Contains SmBit and *cshA*-LgBit under the control of an Atet inducible promoter: CamR	This study
pAP118*relrel*	Luciferase assay vector. Contains *rel*-SmBit and *rel*-LgBit under the control of an Atet inducible promoter: CamR	This study
pAP118*relrocF*	Luciferase assay vector. Contains *rel*-SmBit and *rocF*-LgBit under the control of an Atet inducible promoter: CamR	This study
pAP118*relcshA*	Luciferase assay vector. Contains *rel*-SmBit and *cshA*-LgBit under the control of an Atet inducible promoter: CamR	This study

2.3 DNA manipulation

2.3.1 Polymerase Chain Reaction (PCR)

Primers were purchased from Eurofins and are listed in Table 2.4. PCR reactions were typically carried out in 50 µl reaction volumes with approximately 10 ng of plasmid DNA or 100 ng of genomic DNA as

a template. Forward and reverse primers were each present at a final concentration of 0.5 µM and 25 µl of 2X Phusion Master Mix with HF Buffer (ThermoScientfic) was used. T100 Thermal Cycler (Biorad) was programmed with a 2 min initial denaturation step at 94°C followed by 5 cycles of denaturation (30 seconds, 94°C), annealing (30 seconds, 45°C) and elongation (15-30 seconds per kb, 72°C). The annealing temperature for the following 25 cycles was typically 53°C. A final extension step was carried at 72°C for 1 min per kb. PCR products were purified using the GeneJet gel extraction kit (ThermoScientific) according to the manufacturer's instructions.

For PCRs which did not require high fidelity, such as colony PCRs, Taq polymerase was used. The 2X Taq master mix (~0.1 U/µl Taq polymerase; 20 mM Tris-HCl pH 9; 100 mM KCl, 0.5 M sucrose, 4 mM $MgCl_2$, 0.01% cresol red, 0.02% gelatin, 0.02% Tween 20, 400 µM dATP; 400 µM dGTP; 400 µM dCTP; 400 µM dTTP) was used as described above except an extension time of 1 min per kb was used in the elongation steps of the cycle.

2.3.2 Agarose gel electrophoresis

TAE buffer (40 mM Tris-acetate pH 8, 1 mM EDTA) with 0.5-2% (w/v) agarose (VWR) and a 1:10,000 dilution of Sybr Safe DNA stain (Invitrogen) was used to pour gels for electrophoresis. The percentage of agarose used was dependent of the size of the DNA fragments being separated. 6X DNA loading dye (ThermoScientific) was added to DNA samples before loading or 6X UView DNA loading dye (Biorad) was used in the case of gel extractions. GeneRuler 1 kb DNA ladder (ThermoScientific) was used to infer DNA band size. Electrophoresis was performed at 110 V for at least 15 minutes in TAE buffer. The DNA bands were imaged using a ChemiDoc MP Imager (Biorad).

2.3.3 Purification of PCR products

PCR products were purified using the GeneJet PCR Purification kit (ThermoScientific) as per the manufacturer's instructions except that ddH_2O was used to elute the DNA.

2.3.4 Isolation of plasmid DNA

Plasmid DNA was isolated from *E. coli* cells using the GeneJet Plasmid Miniprep Kit (ThermoScientific) or Midiprep Kit (QIAGEN) as per the manufacturer's instructions. For plasmid preparations from *S. aureus* the cells were lysed using 50 µg/ml of lystostaphin in TSM buffer (50 mM Tris pH 7.5, 0.5 M sucrose, 10 mM $MgCl_2$) for 1 h at 37°C before using the GeneJet Plasmid Miniprep Kit (ThermoScientific) as per the manufacturer's instructions. A culture volume of 5 ml or 200 ml was used for minipreps and midipreps, respectively. Plasmids were eluted with appropriate volumes of ddH_2O or TE buffer (10 mM Tris-Cl pH 7.5, 1 mM EDTA).

2.3.5 Isolation of genomic DNA

Genomic DNA (gDNA) was isolated from 5 ml stationary phase cultures of *S. aureus* cells using the Wizard Genomic DNA Extraction Kit (Promega). The kit was used as per manufacturer's instructions except that harvested cells were resuspended in 100 µl of TSM buffer (50 mM Tris pH 7.5, 0.5 M sucrose, 10 mM $MgCl_2$) and cells were incubated with 50 µg/ml of lysostaphin for 30 min at 37°C in order to digest the cell wall peptidoglycan prior to DNA extraction.

2.3.6 Digestion of DNA with Restriction Enzymes

Restriction digestion of plasmid DNA, insert DNA or gDNA for use in cloning was carried out in a 100 µl reaction volume with 10 µl CutSmart buffer or other appropriate buffer (New England Biolabs), 1-10 µg of DNA and 1 U of restriction enzyme per 1 µg of DNA being digested (New England Biolabs). When a restriction digest was used for screening plasmids, the reaction volume was scaled down to 20 µl. Reactions were incubated at 37°C for 1 h and then purified using the GeneJet Plasmid Miniprep Kit (ThermoScientific) as per the manufacturer's instructions.

2.3.7 DNA fragment ligation

Ligations of digested insert DNA and digested plasmid DNA were carried out in a reaction volume of 25 µl with 1 µl T4 ligase (New England Biolabs), 2.5 µl 10x T4 Ligase Buffer (New England Biolabs) and a 3:1 molecular ratio of insert DNA to plasmid DNA with 25 ng of plasmid DNA. Reactions were incubated at room temperature for 1 h or at 16°C for 16 h and then heat inactivated at 65°C for 20 min before being stored at -20°C.

2.3.8 Colony screening using PCR

Colony PCRs were used in order to quickly screen colonies after transformation or transduction. *E. coli* colonies were added directly to the PCR reaction however *S. aureus* colonies had to be lysed first. This was done by resuspending colonies in 50 µl of TSM (50 mM Tris HCl pH 7.5, 0.5 M sucrose, 10 mM $MgCl_2$) with 100 µg/ml lysostaphin and incubating at 37°C for 1 h. The samples were then centrifuged at 17,000 xg for 2 min and 5 µl of the supernatant was added to the PCR reaction.

Table 2.4 Primers used in this study

Number	Name	Sequence (5'-3')	Restriction Sites
RMC003	R-5'geh	CTTGCTTTCAATTGTGTTCC	
RMC004	F-5'geh	GTTGTTTTTGTACATGGATTTTTAG	
RMC005	R-pCL55	GCGCATAGGTGAGTTATTAGC	
RMC006	3-pCL55seq	CACGTTTCCATTTATCTGTATACGGATC	
RMC074	5-AvrII-lacZ	GGGCCTAGGAGCTTGTTGATACACTAATGCTTTTATA	AvrII

RMC075	3-SacII-lacZ	TCCCCGCGGTTATTTTTGACACCAGACCAACTGGTAA	SacII
RMC078	F-KpnI-RelQ	GGGGGTACCGATATGTATACACCTCGTATC	KpnI
RMC079	R-RelQprom-LacZ	AGTAACTTCCACGCTTAATCCTCCTCTTATTCCATA	
RMC080	F-RelQprom-lacZ	GGAGGATTAAGCGTGGAAGTTACTGACGTAAGATTA	
RMC081	F-KpnI-RelP	GGGGGTACCCATCTCTATCAATTAAGCAC	KpnI
RMC082	R-RelPprom-lacZ	AGTAACTTCCACTTTTATACTAACCTCCGATATATA	
RMC083	F-RelPprom-lacZ	GTTAGTATAAAAGTGGAAGTTACTGACGTAAGATTA	
RMC084	F-KpnI-Rel	GGGGGTACCGAGTTTAATCTCATACGACG	KpnI
RMC085	R- Relprom-lacZ	AGTAACTTCCACATTTATTACTTCGCCTTAAACAAT	
RMC086	F-Relprom-lacZ	GAAGTAATAAATGTGGAAGTTACTGACGTAAGATTA	
RMC087	F-pCL55-insertscreen	GAGCGGATACATATTTGAATG	
RMC258	F-RelXbaI	GGGGTCTAGAGAACAACGAATATCC	XbaI
RMC259	R-RelKpnI	GGGGGTACCTTCCAAACTCTTGTTAC	KpnI
RMC260	F-RelPXbaI	GGGTCTAGAGTATGTAGATCGAAAACC	XbaI
RMC261	R-RelPKpnI	GGGGGTACCTCTGTTATTTCAGAATG	KpnI
RMC262	F-RelQXbaI	GGGTCTAGAGAATCAATGGGATCAG	XbaI
RMC263	R-RelQKpnI	GGGGGTACCTCATTTTCATGTTTTTTAGAACG	KpnI
RMC266	F-RelHD-XbaI	GGGTCTAGATATTGCTTATGAAGCAC	XbaI
RMC267	R-RelHD-KpnI	GGGGGTACCTTAATACCAAGACGATGTG	KpnI
RMC268	F-RelSYNTH-XbaI	GGGTCTAGATGGTAGACCTAAACATATTTAC	XbaI
RMC269	R-RelSYNTH-KpnI	GGGGGTACCTTTTTACCTTCTTTGTAAGC	KpnI
RMC270	F-RelTGS-XbaI	GGGTCTAGAAGTATACGCATTTACCCC	XbaI
RMC271	R-RelTGS-KpnI	GGGGGTACCCTAGTACGTATTTCAAC	KpnI
RMC272	F-RelACT-Xba1	GGGTCTAGATCAAAAATATCAGGTTG	XbaI
RMC309	pUT18+1for	GGGGGATCCCCGGGGAACAACGAATATCC	BamHI
RMC310	pUT18+1rev	GGGGGTACCCCGGGGTTCCAAACTCTTGTTAC	KpnI
RMC338	F-AvrII-CodY	CCCCCTAGGATACAAAAGGAGAAAAATTCATGAG	AvrII
RMC339	R-SacII-CodY	CCCCCGCGGTCCCAGACTCATCGACTTATTTAC	SacII
RMC422	R-RocF-XbaI	GGGTCTAGAGACAAAGACAAAAGCAATTG	XbaI
RMC423	F-rocF-stop-EcoRI	GGGGAATTCTTATAATAAAGTTTCACCAAAAAATG	EcoRI
RMC461	R-RocF-BamHI	GGGGGATCCACAAAGACAAAAGCAATTG	BamHI
RMC475	F-SacI-Rel	GGGGAGCTCCCTAAATCATTGTTTAAGGCGAAG	SacI
RMC476	R-PvuI-linker Smbit	GGGCGATCGAGCTATAGAATTTCTTCAAAAAG	PvuI

RMC477	R-Rel-F-linker	ACCCCCTCGAGAGTTCCAAACTCTTGTTACTGTATA	
RMC478	F-linker-R-Rel	AGAGTTTGGAACTCTCGAGGGGGTTCTAGTGGTGGT	
RMC479	F-PvuI-Rel	GGGCGATCGCCTAAATCATTGTTTAAGGCGAAG	PvuI
RMC480	R-NotI-Rel	GGGGCGGCCGCGTTCCAAACTCTTGTTACTGTATAAAC	NotI
RMC481	F-PvuI-rocF	GGGCGATCGATTACATAGAGCAAAGGGGGACGCTT	PvuI
RMC482	R-NotI-rocF	GGGGCGGCCGCTAATAAAGTTTCACCAAAAAATGTTC	NotI
RMC488	F-PvuI-cshA	GGGCGATCGCAGGTAAAAAGGAGAATTATTTTG	PvuI
RMC489	R-NotI-cshA	GGGGCGGCCGCTTTTTGATGGTCAGCAAATGTGC	NotI

2.4 Preparation and transformation of chemically competent *E. coli* cells with plasmid DNA

E. coli strains were grown overnight in 20 ml LB. The culture was diluted 1:100 into 1 L fresh PSI broth (20 g/L Bacto tryptone, 5 g/L Bacto yeast extract, 20 mM $MgSO_4$, pH 7.6) and incubated at 37°C until an OD_{600} of 0.5-0.7 was reached. Cells were then incubated on ice for 15 min and harvested by centrifugation (6000 x g, 10 min, 4°C). Pelleted cells were resuspended in 200 ml Transformation buffer I (TfbI) (30 mM CH_3COOK, 100 mM RbCl, 10 mM $CaCl_2$, 50 mM $MnCl_2$, 15% glycerol, pH 5.8). Cells were incubated on ice for 15 min and harvested again by centrifugation (6000 x g, 10min, 4°C). Cell pellet was resuspended in 25 ml TfbII (10 mM MOPS, 75 mM $CaCl_2$, 10 mM RbCl, 15% glycerol, pH 6.5) and 500 µl aliquots were snap-frozen in a dry ice/ethanol bath and stored at -80°C. To transform these chemically competent cells, 100 µl of cells were incubated on ice for 30 min with 12 µl of the ligation reaction. Cells were then heat shocked for 45 sec at 42°C, followed by a 5 min incubation on ice. 900 µl of SOC media (5 g/L Bacto yeast extract, 20 g/L Bacto tryptone, 0.25 g/L NaCl, 20 mM glucose, 2.5 mM KCl, pH 7.5) was added and cells were incubated at 37°C for 1 h before plating onto LB agar plates with the appropriate antibiotics. Plates were incubated at 37°C overnight to allow growth of single colonies.

2.5 Preparation and transformation of electrocompetent *S. aureus* with plasmid DNA

A stationary phase culture of *S. aureus* RN4220 cells was diluted 1:100 into 200 ml of TSB and incubated at 37°C for 3 hours. Cells were then harvested by centrifugation (6000 x g, 10 min, 4°C). Cells were then washed twice with 200 ml of Wash solution (0.5 M sucrose) then washed again in 100 ml Wash solution. Cells were pelleted through centrifugation (6000 x g, 10 min, 4°C) and suspended in 2 ml Wash solution. 120 µl aliquots were snap-frozen in a dry ice/ethanol bath and stored at -80°C. Before transformation, plasmids were dialysed against ddH_2O using a Millipore 0.025 µm filter (Fisher) in order to remove salts. 4-12 ng of plasmid DNA was added to 110 µl of competent cells in a

MicroPulser electroporation cuvette (Biorad) which has an electrode gap of 1 mm. The cells were pulsed at 2.5 kV with 100 Ω resistance and 25 mF capacitance. Cells were recovered using 900 µl of Brain Heart Infusion broth (BHI) supplemented with 0.5 M sucrose and incubated at 37°C for 1 h. Cells were then plated out onto TSA plates with the appropriate antibiotics.

2.6 Phage transduction

S. aureus strains were grown overnight in a mixture of LB and TSB, with a ratio of 2:1 (LB/TSB), supplemented with 5 mM $CaCl_2$ and the appropriate antibiotics. The culture was then diluted 1:50 into 4.5 ml fresh LB/TSB 5 mM $CaCl_2$ and grown for 3 h at 37°C. 500 µl of culture was incubated for 30 min at room temperature with 100 µl of phage 85, 80α or 11 lysates at the highest dilution that would result in confluent lysis. This mixture was added to 5 ml of top agar (0.8% NaCl, 0.8% Bacto-agar), poured on a warm TSA plate with the appropriate antibiotic and incubated at 37°C overnight. The top layer of a confluently lysed plate was removed using 3 ml of TMG buffer (10 mM Tris pH7.5, 10 mM $MgSO_4$, 0.1% gelatin) and centrifuged for 10 min at 13,000 x g and at 4°C. The phage lysate supernatant was filtered through a 0.22 µm syringe filter (Merck) and stored at 4°C.

Recipient *S. aureus* strains were grown overnight in 24 ml LB/TSB, 5 mM $CaCl_2$ at 37°C. Cells were concentrated 5-fold in fresh LB/TSB 5 mM $CaCl_2$ and 250 µl of concentrated culture was incubated with 200 µl or 400 µl of phage lysate (for Newman and LAC* recipient strains respectively) for 20 min at 37°C. Cells were washed twice with 1 ml 40 mM sodium citrate and then plated onto 40 mM sodium citrate TSA plates with the appropriate antibiotics and incubated at 37°C overnight or longer until single colonies were visible. Transductants were restreaked at least three times onto 40 mM sodium citrate TSA plates with antibiotic to cure phage.

2.7 Protein purification

2.7.1 Recombinant protein expression

Stationary phase cultures of *E. coli* strains with the appropriate expression plasmid were diluted to OD_{600} 0.05 in 1-3 L fresh LB supplemented with the appropriate antibiotics. For RelP and RocF expression, the culture was incubated at 37°C and protein expression was induced with 1 mM IPTG for 3 h after the culture reached an OD_{600} of 0.5. For $Rel_{Sα}$ expression, the culture was grown for 16 h at 30°C before induction with 1 mM IPTG for 6 h. Cells were harvested through centrifugation (6000 x g, 10 mins, 4°C), washed with 45 ml buffer (50 mM Tris pH 7.5, 150 mM NaCl, 5% glycerol) and pelleted again (4700 x g, 10 min, 4°C) before storing at -20°C.

2.7.2 His-tagged proteins

Frozen cell pellets were defrosted on ice and resuspended in 5 ml Buffer A (50 mM Tris pH 7.5, 150 mM NaCl, 5% glycerol, 10 mM imidazole) with one cOmplete, Mini, EDTA-free Protease I tablet (Sigma), lysed with 100 µg lysozyme and then sonicated for 10 min (1 min on, 1 min off). The sample was then centrifuged (14000 x g, 40 min, 4°C) and the supernatant was filtered using a 0.45 µm syringe filter (Merck). The cell lysate was loaded onto a 1 ml HisTrap HP Ni^{2+} column (GE Healthcare) and eluted using a gradient of Buffer B (50 mM Tris pH 7.5, 150 mM NaCl, 5% glycerol + 500 mM imidazole). Appropriate fractions were collected based on the peaks observed in the chromatogram. Protein containing fractions were dialysed in storage buffer (50 mM Tris pH 7.5, 200 mM NaCl, 5% glycerol) then concentrated using a 10 kDa Amicon ultracentrifuge filter (Merck). The purified protein was then snap-frozen in a dry ice/ethanol bath and stored at -80°C.

2.7.3 GST-tagged proteins

Frozen cell pellets were defrosted on ice and resuspended in 5 ml phosphate buffered saline (PBS; 0.01 M phosphate buffer: 0.0027 M KCl and 0.137 M NaCl, pH 7.4), lysed with 100 µg lysozyme and then sonicated for 10 min (1 min on, 1 min off). The sample was then centrifuged (14000 x g, 40 min, 4°C) and the supernatant was filtered using a 0.45 µm syringe filter (Merck). The cell lysate was loaded onto a 1 ml GSTrap HP column (GE Healthcare) and eluted using Buffer B (50 mM Tris pH 8.0, 10 mM reduced glutathione). Appropriate fractions were collected based on the peaks observed in the chromatogram. Protein containing fractions were dialysed in storage buffer (50 mM Tris pH 7.5, 200 mM NaCl, 5% glycerol) then concentrated using a 10 kDa Amicon ultracentrifuge filter (Merck). The purified protein was then snap-frozen in a dry ice/ethanol bath and stored at -80°C.

2.8 Protein characterisation

2.8.1 SDS-PAGE

Protein size and purity was analysed by polyacrylamide gel electrophoresis (PAGE) using sodium dodecyl sulfate (SDS) as the denaturing agent. Samples for SDS-PAGE were boiled for 5 min in an equal volume of 2X loading dye (10% (v/v) glycerol, 5% (v/v) β-mercaptoethanol, 0.01% bromophenol blue, 2% (w/v) SDS, 62.5 mM Tris-HCl pH 6.8) to fully denature the samples. The resolving gel was prepared with varying concentrations of acrylamide, depending on the size of the protein to be resolved, along with 25% (v/v) lower buffer (1.5 M Tris pH 8.8, 0.12 M NaCl, 8 mM EDTA pH 8, 0.4% (w/v) SDS), 0.1% (w/v) ammonium persulfate (APS) and 0.1% TEMED. The stacking gel was prepared with 5.6% acrylamide, 25% (v/v) upper buffer (0.5 M Tris pH 6.8, 0.12 M NaCl, 8 mM EDTA pH 8, 0.4% (w/v) SDS), 0.1% (w/v) ammonium persulfate (APS) and 0.1% TEMED. The electrophoresis was performed at 190 V until the dye front reached the bottom of the gel. Gels were stained where appropriate with 10%

(v/v) acetic acid, 45% (v/v) methanol, 45% (v/v) ddH_2O and 2.5 g/L Coomassie Brilliant Blue R-250 and destained using the same preparation without Coomassie Brilliant Blue R-250.

2.8.2 Transfer to PDVF membrane

After separating the proteins in a sample using SDS-PAGE they were transferred to a PVDF membrane in order to perform a Western blot using a wet transfer method. The PVDF membrane was soaked in methanol for 30 sec, rinsed in ddH_2O and then equilibrated in transfer buffer (25 mM Tris, 192 mM glycine, 10% (w/v) glycine). The gel was also rinsed in transfer buffer before it was stacked against the PVDF membrane with three sheets of transfer buffer soaked Whatmann filter paper. The transfer was carried out at a constant current of 400 A in transfer buffer for 1 h.

2.8.3 Western blot analysis

Following transfer to the PVDF membrane the membrane was blocked with 5% skimmed milk in TBST (20 mM Tris-HCl pH 7.6, 0.14 mM NaCl, 0.1% Tween 20) for 1 h at room temperature with shaking. The membrane was then incubated in 5% skimmed milk in TBST with 1:2500 primary antibody (Monoclonal Anti-polyHistidine–Peroxidase antibody produced in mouse, Sigma) for 16 h at 4°C. The membrane was washed in TBST 3 times and then developed with Clarity Western ECL Blotting Substrate (Biorad). Western blots were imaged using the ChemiDoc MP Imager (Biorad) and the band intensity was measured using ImageJ software (NIH).

2.9 Protein pulldown assay

For each sample, 10 µl of Glutathione-tagged Sepharose beads (GE Healthcare) were washed in 1000 µl of 1X wash buffer (25 mM Tris pH 7.5, 150 mM NaCl, 1 mM EDTA pH 8, 0.5% Triton), pelleted by centrifugation at 1250 x g for 30 sec, and all liquid was removed. This process was repeated 5 times. 100 µl of 2X wash buffer was added to the beads along with purified RocF or GST protein to a final concentration of 4 µM and ddH_2O to bring to volume to 200 µl. Each sample was then incubated at 4°C with rotation for 4 h before washing with 1X wash buffer 5 times. Next, 100 µl of 2X wash buffer was added to the beads along with purified Rel_{Sa} protein to a final concentration of 2 µM and ddH_2O to bring to volume to 200 µl. For samples with ppGpp, a final concentration of 1 µM was used. Each sample was then incubated at 4°C with rotation for 16 h before washing with 1X wash buffer 5 times. Protein was eluted from the beads using 20 µl of elution buffer (25 mM Tris pH 7.5, 150 mM NaCl, 1 mM EDTA pH 8, 0.5% Triton, 1 M reduced glutathione, adjusted to pH 8) and allowing 5 min elution time. Elutions were run on an SDS PAGE gel for analysis by Western blot in order to quantify the amount of protein eluted.

2.10 Genomic DNA fragment bacterial adenylate cyclase two hybrid screen

2.10.1 Constructing the gDNA fragment library

gDNA was extracted from *S. aureus* strain LAC* as described in Section 2.3.5. 60 µg of gDNA was partially digested by incubation with Sau3AI (NEB) at 37°C for 20 min. Digested gDNA was separated on a 0.8% agarose gel and fragments of 500 to 1000 bp and 1000 to 3000 bp were gel extracted and purified. This was repeated five times from separate genomic preparations and DNA fragments from all digestions were pooled. Bacterial adenylate cyclase two hybrid (BACTH) plasmids pUT18, pUT18+1, pUT18+2 and pUT18C were incubated for 16 h at 37°C with BamHI (New England Biolabs) and dephosphorylated with Antarctic Phosphatase (New England Biolabs) for 90 min to prevent relegation of the sticky ends. Sau3AI-digested gDNA fragments were ligated into the BamHI-digested BACTH vectors using T4 ligase (New England Biolabs) and then transformed into *E. coli* DH5α competent cells (New England Biolabs) and plated onto LB agar with 150 µg/ml carbenicillin. Resulting colonies were pooled and the library plasmids were isolated using the GeneJET plasmid purification kit (ThermoScientific).

2.10.2 Using the library to screen for target protein interaction partners

50 ng of the library plasmid DNA was used to transform 10 µl of competent BTH101 cells containing either a pKT25 or pKNT25 plasmid with the target protein as described in Section 2.4. The transformation was plated onto 10 MacConkey agar plates with 1% maltose (w/v) and the plates were incubated at 30°C until pink colonies started to appear. Pink colonies were restreaked onto LB agar with 150 µg/ml carbenicillin, 30 µg/ml kanamycin, 0.5 mM IPTG and 40 µg/ml X-gal and incubated at 30°C overnight. Any resulting blue colonies were screened by colony PCR as described in Section 2.3.8 to confirm they contained a genome fragment in the library plasmid. The genome fragment was then sequenced to identify the gene interacting with the target protein.

2.11 Targeted bacterial adenylate cyclase two hybrid

BACTH vectors were co-transformed into *E. coli* BTH101 cells and plated onto LB agar with 150 µg/ml carbenicillin and 30 µg/ml kanamycin. Plates were incubated at 30°C overnight to allow growth of single colonies. Colonies were used to inoculate LB with 150 µg/ml carbenicillin and 30 µg/ml kanamycin containing 0.5 mM IPTG which was incubated overnight at 30°C with shaking. 5 µl of the stationary phase culture was spotted onto LB agar with 150 µg/ml carbenicillin, 30 µg/ml kanamycin, 0.5 mM IPTG and 40 µg/ml X-gal. The culture spots were allowed to dry before the plates were incubated at 30°C for up to 48 h. Images of the plates were captured using the Perfection v7000 scanner (Epsom).

2.12 β-galactosidase assays

2.12.1 Sample preparation

Stationary phase cultures of *lacZ*-fusion strains were used to inoculate fresh TSB medium at OD_{600} of 0.05. For RN4220 control strains and JE2 NTML strains, the cultures were grown for 4 h with and without 200 ng/ml Atet at 37°C. For shock experiments with the Newman strains the cultures were grown until OD_{600} 0.5 and then were shocked with antibiotic treatment or pH change and incubated at 37°C for 30 min. Antibiotics were used at the following concentrations: 60 µg/ml mupirocin, 62.5 µg/ml cerulenin, 20 µg/ml vancomycin and 1.5 µg/ml oxacillin. Alkaline shock was produced by adjusting the pH of the media to 9.9 with 1 N NaOH. Colony forming units (CFUs) were calculated by plating serial dilutions onto agar plates and incubating overnight at 37°C. After measuring the OD_{600}, 1 ml of culture was pelleted and stored at -20°C.

2.12.2 β-galactosidase assays

Pellets were thawed and resuspended in 500 ml ABT buffer (60 mM K_2HPO_4, 40 mM $KHPO_4$, 100 mM NaCl, 0.1% Triton-X) and incubated at 37°C for 30 min with lysostaphin at a final concentration of 50 µg/ml to lyse the cells. Samples were then centrifuged for 10 min at 17000 x g and 100 µl of lysed sample added to 80 µl ABT and 20 µl of a 0.4 mg/ml stock of 4-methyl umbelliferyl β-D galactopyranoside (MUG) in a black 96-well plate. The plate was then incubated at 25°C for 1 h and the fluorescence was measured, with an excitation wavelength of 355 nm and an emission wavelength of 460 nm, using the Victor X3 multilabel plate reader (Perkin Elmer). The fluorescence reading of a blank (180 µl ABT, 20 µl of a 0.4 mg/ml stock of MUG) was subtracted from the sample fluorescence readings to account for natural degradation of the MUG. The fluorescence of known concentrations of 4-methylumbilliferone (MU) was measured to create a calibration curve for determining β-galactosidase activity. The activity was determined as: β-galactosidase activity per CFU = MUG hydrolysed (pmol) / sample volume (ml) x incubation time (min) x CFU per ml or β-galactosidase activity per OD_{600} = MUG hydrolysed (pmol) / sample volume (ml) x incubation time (min) x OD_{600}.

2.13 Luciferase assays

Strains were grown in 5 ml of TSB with 10 µg/ml chloramphenicol overnight. Stationary phase cultures were used to inoculate fresh TSB with 10 µg/ml chloramphenicol and 100 ng/ml Atet to an OD_{600} of 0.05. Cultures were grown at 37°C with shaking for 1.5 h, before the OD_{600} of the cultures was measured. The OD_{600} of the cultures was normalised to 0.1 in fresh TSB. 50 µl of the normalised culture was mixed with 50 µl of the buffer provided by the Nano-Glo Luciferase Assay System (Promega). Luminescence was measured using a Victor X3 multilabel plate reader (Perkin Elmer). Luciferase activity (LU) was reported as the raw readout out of luminescence.

For assays using different growth media (TSB, TSB pH 5.6 or SHU), the assay was carried out as described except the cultures were not normalised after 1.5 h growth at 37°C. Instead the OD_{600} was measured and 50 µl of the culture was used directly in the assay. The luminescence recorded was divided by the final OD_{600} measurement to give the Luciferase activity per OD_{600} (LU/OD).

For assays using CDM (CDMG, CDM, CDM-R), strains were grown in CDMG overnight and this was used to inoculate fresh CDMG with 10 µg/ml chloramphenicol and 100 ng/ml Atet to an OD_{600} of 0.05. These cultures were grown for 4 h at 37°C before the OD_{600} was measured and the cells were pelleted and washed twice with CDMG, CDM or CDM-R. The cells were resuspended to OD_{600} 0.4 in CDMG, CDM or CDM-R and grown for 15 min at 37°C. The final OD_{600} was recorded and 50 µl of the culture was used for the luciferase assay. The luminescence recorded was divided by the final OD_{600} measurement to give the Luciferase activity per OD_{600} (LU/OD).

2.14 *S. aureus* growth analysis

Strains were streaked out onto TSA plates with appropriate antibiotics and grown overnight at 37°C. Single colonies were used to set up cultures in 5 ml of growth media with appropriate antibiotics. Stationary phase cultures were used to inoculate fresh media to OD_{600} of 0.05 and the cultures were grown at 37 C with shaking. OD_{600} measurements were taken at regular intervals. Colony forming units (CFUs) were calculated by plating serial dilutions onto agar plates and incubating overnight at 37°C.

2.15 Thin layer chromatography

Thin layer chromatography (TLC) allows separation of non-volatile mixtures. Samples were spotted 1-2 cm from the bottom of the TLC PEI cellulose plate (VWR) and placed in a tank with running buffer (1.5 M KH_2PO4, pH 3.6). The buffer was allowed to rise until 1 cm from the top of the plate before removing the plate from the tank. After the plate dried it was exposed to an imaging plate (IP, Fujifilm) for at least five minutes. The IP was then imaged using Typhoon FLA 7000 Phosphoimager (GE Healthcare).

2.16 Synthesis of radiolabelled (p)ppGpp

Radiolabelled GTP (α-^{32}P, PerkinElmer) was diluted 1 in 2 in ddH_2O and 8.3 µl of this dilution was mixed with 2 µM Rel_{Seq}, 8 mM cold ATP, and binding buffer (25 mM Bis-Tris propane pH 9, 100 mM NaCl, 15 mM $MgCl_2$) and ddH_2O was added to bring the volume to 500 µl. The reaction was incubated overnight at 37°C. The nucleotide was separated from the protein using a 3 KDa filter (VWR) leaving radiolabelled pppGpp. pppGpp was incubated with purified recombinant GppA from *E. coli* at a final concentration of 1 µM for 1 h at 37°C. Again, the ppGpp nucleotide was separated from the protein using a 3 KDa filter. In order to measure the percentage conversion, GTP and the synthesised pppGpp and ppGpp

were run on a TLC plate. Using the software ImageQuant (GE Healthcare) the percentage conversion is calculated for each lane. A conversion of 85% or above was deemed suitable for use in DRaCALA and nucleotide hydrolysis assays. Nucleotides were stored at -20°C.

2.17 DRaCALA with radiolabelled ligand

10 µM of protein and ~2.78 nM radiolabelled nucleotide were incubated in binding buffer at room temperature for 5 min before 2.5 µl was spotted in duplicate on nitrocellulose membrane (GE Healthcare). Spots were allowed to dry before being exposed to the IP for at least 5 min. The IP was then imaged using Typhoon FLA 7000 Phosphoimager (GE Healthcare). The program ImageQuant (GE Healthcare) was used to quantify the spots, allowing quantification of the fraction of nucleotide bound by the equations below:

$$F_{B} = \frac{I_{inner} - I_{background}}{I_{total}}$$

and

$$I_{background} = A_{inner} \times \frac{(I_{total} - I_{inner})}{(A_{total} - A_{inner})}$$

Therefore,

$$F_{B} = \frac{I_{inner} - \left[A_{inner} \times \frac{(I_{total} - I_{inner})}{(A_{total} - A_{inner})}\right]}{I_{total}}$$

Where I = Intensity, A = Area, and F_B = Fraction Bound

2.18 DRaCALA with fluorescently labelled ligand

Assay performed as above except 10 mM fluorescently labelled ligand (Dansyl-arginine diluted in methanol, SigmaAldrich) and 75 µM protein was used. For assays where binding was competed with unlabelled L-Arg, 75 µM protein, 10 mM dansyl-arginine were mixed followed by addition of 1 µl of either storage buffer (50 mM Tris pH 7.5, 200 mM NaCl, 5% glycerol) or 1 M L-arginine (final concentration 100 mM). Samples were then incubated at room temperature for 5 min and then spotted onto nitrocellulose membrane. For assays where binding was competed with unlabelled amino acids, 10 µM protein, 1 mM dansyl-arginine were mixed followed by addition of 1 µl of either storage buffer or 200 mM L-Arg, L-Leu, L-Ile, L-Ser or L-Val (final concentration 20 mM). Samples were then incubated at room temperature for 5 min and then spotted onto nitrocellulose membrane. After drying, spots were imaged using a ChemiDoc MP Imager (Biorad) (excitation wavelength: 488; emission wavelength: 530). The program ImageLab (Biorad) was used to quantify to spots, allowing quantification of the fraction of ligand bound using the equation described in 2.17.

2.19 Nucleotide hydrolysis by Rel_{Sa}

2.19.1 GTP hydrolysis by Rel_{Sa}

1 µM Rel_{Sa} with or without 1 µM RocF, RelP, ppGpp or L-arg (diluted in storage buffer) was incubated in hydrolysis buffer (final concentrations: 50 mM Tris-HCl (pH 8), 10 mM $MgCl_2$, 1 mM $MnCl_2$, 1 mM DTT, and 0.1 mM EDTA). 1 µl of α-^{32}P GTP was added just before incubating for 5 min or 1 h at 37°C before spotting onto a TLC plate. TLC was run as described in Section 2.15. Using the software ImageQuant (GE Healthcare) the percentage hydrolysis was calculated for each lane.

2.19.2 (p)ppGpp hydrolysis by Rel_{Sa}

0.05 µM Rel_{Sa} with or without 0.05 µM RocF, RelP, ppGpp or L-arg (diluted in storage buffer) was incubated in hydrolysis buffer (final concentrations: 50 mM Tris-HCl (pH 8), 10 mM $MgCl_2$, 1 mM $MnCl_2$, 1 mM DTT, and 0.1 mM EDTA). 1 µl of α-^{32}P ppGpp or pppGpp was added just before incubating for 5 min or 1 h at 37°C before spotting onto a TLC plate. TLC was run as described in Section 2.15. Using the software ImageQuant (GE Healthcare) the percentage hydrolysis was calculated for each lane.

2.20 Arginase assay

2.20.1 Arginase assay with recombinant protein

An arginase activity assay kit (SigmaAldrich) was used to measure arginase activity in a microtiter plate. To determine the linear range of the assay 40 µl of RocF at an initial concentration of either 2, 5, 10, 15 or 20 nM was incubated for 1 h at 37°C with 10 µl of 5X of sample buffer from the kit. To determine activity with Mn or Ni as a cofactor, 40 µl of 10 nM RocF was incubated for 1 h at 37°C with 10 µl of 5X of sample buffer from the kit made up with 125 mM $MnCl_2$ or 125 mM $NiCl_2$ in place of the Mn solution provided by the kit (final concentration of $MnCl_2$ and $NiCl_2$ in the reaction is 5 mM; final concentration of RocF is 8 nM). To determine the effect of different proteins or ligands on RocF activity, 20 µl of 20 nM RocF or storage buffer was incubated for 2 h at 37°C with 10 µl of 5X of sample buffer from the kit and 20 µl of 20 nM Rel_{Sa}, RelP, L-arg or ppGpp (final concentration of RocF, Rel_{Sa}, RelP, L-arg and ppGpp is 8 nM). For each reaction a reaction was set up without 5X sample buffer to act as a blank. A blank of 50 µl ddH_2O and a 50 µl 1 mM urea standard was also included. The reaction was stopped by adding 100 µl of reagent A and 100 µl of reagent B from the kit. The samples were then incubated at room temperature for 1 h before the absorbance was measured at 430 nm using the SpectraMax plate reader (Molecular Devices). One unit of Arginase is the amount of enzyme that will convert 1 µmole of L-arginine to ornithine and urea per minute at pH 9.5 and 37 °C.

The arginase activity is determined with the following equation:

$$\text{Activity} = \frac{(A_{430})_{sample} - (A_{430})_{blank}}{(A_{430})_{standard} - (A_{430})_{water}} \times \frac{(1\ mM \times 50 \times 10^3)}{(V \times T)}$$

Where:

T = Reaction time in minutes

V = sample volume (μL) added to well (40 μL)

1 mM = concentration of Urea Standard

50 = reaction volume (μL)

10^3 = mM to μM conversion factor

2.20.2 Arginase assay with cell lysates

Strains were grown in CDMG or CDM at 37°C overnight. Cells were pelleted, washed in sterile PBS (0.01 M phosphate buffer: 0.0027 M KCl and 0.137 M NaCl, pH 7.4), and resuspended to OD_{600} 5 in TSM (50 mM Tris pH 7.5, 0.5 M sucrose, 10 mM $MgCl_2$) with 10 μg/ml lysostaphin and 100 mM PMSF. Samples were incubated at 37°C for 1 h to lyse them, before centrifuging at 13,000 xg for 10 min. 40 μl of the lysate was used in the arginase activity assay kit as detailed above. The arginase activity of the samples was normalised by the protein concentration of the lysate. This was measured using Protein Assay Dye Reagent (Biorad) as per the manufacturer's instructions with a standard curve of bovine serum albumin concentrations.

2.21 Biolog Phenotype Microarrays

Biolog Phenotype Microarrays (PM) were carried out as per the manufacturer's instructions with minor adaptations. (p)ppGpp^0 and Δ*hflX* strains were streaked onto TSA plates with appropriate antibiotics and incubated overnight at 37°C. Single colonies were picked and resuspended in supplied media to an OD_{600} of 0.1. This cell suspension was added to a PM additive, supplied media and tetrazolium dye. 100 μl of this suspension was added to each well and the plate was incubated for 24 h at 37°C. As cells actively respire the dye (yellow) is reduced to formazan (purple) and this colour change was measured every 15 mins at OD_{595} using a 96 well plate reader (TECAN).

2.22 Urease activity assay

Stationary phase cultures were normalised to an OD_{600} of 5 and 5 μl was plated onto Christensen's agar (1.5% agar, 0.2% KH_2PO_4, 0.1% peptone, 0.5% NaCl, 0.0012% phenol red) with or without 2% urea and with or without 0.1% glucose. The spots were allowed to dry before the plates were incubate at 37°C for 16 h. Urease activity results in the pH indicator turning from yellow to pink as the urea in the agar is converted to ammonia. Images of the plates were captured using the Perfection v7000 scanner

(Epsom). ImageJ software (NIH) was used to quantify the area of the halos of urease activity which was then divided by the area of the culture spot to give a quantification of urease activity.

2.23 Statistical analysis

Statistical analysis of data was determined using Student t-tests or one-way ANOVA. Statistical tests were performed with GraphPad Prism 7 (GraphPad Software Inc.). Significance was denoted as follows: * $p < 0.05$; ** $p < 0.01$; *** $p < 0.001$; **** $p < 0.0001$.

Chapter 3 - Transcriptional regulation of *rel*, *relP* and *relQ*

3.1 Introduction

Transcriptional regulation is a universal way for living organisms to control gene expression. It ensures that each cell does not waste nutrients or energy transcribing genes that are not needed at that time. Transcriptional regulation can control whether or not a gene is transcribed but also how many RNA molecules are synthesised, ultimately affecting the number of proteins in the cell. Genes can be regulated temporally, during different growth phases, or in response to stimuli. Controlling the transcription of the (p)ppGpp synthetase genes gives another layer of control to the stringent response.

Previous work has shown that the expression of RelP and RelQ from *S. aureus* is controlled in part by the two-component system VraRS (Geiger *et al.*, 2014). The VraRS system is responsible for a change in transcriptional profile during cell envelope stress. Indeed, vancomycin and oxacillin, two antibiotics which target the cell wall, also trigger the expression of *relP* and *relQ* in a VraRS-dependent manner (Geiger *et al.*, 2014). This example highlights how investigating transcriptional regulation can help in the discovery of novel triggers of the stringent response.

As discussed in Section 1.2.1.1, the *E. coli* gene, *relA* has four promoters; *relA*P1 and *relA*P2 (sigma 70 regulated) and *relA*P3 and *relA*P4 (sigma 54 regulated) (Brown *et al.*, 2014; Metzger *et al.*, 1988; Nakagawa *et al.*, 2006). *relA*P2 is upregulated by H-NS and CRP, whilst 6S RNA downregulates transcription from *relA*P1 and *relA*P2 (Nakagawa *et al.*, 2006; Cavanagh, *et al.*, 2010). During nitrogen starvation transcription from *relA*P3 and *relA*P4 is activated by NtrC (Brown *et al.*, 2014; Villadsen and Michelsen, 1977). This complex network highlights that transcriptional regulation is an import aspect of regulating the action of long-RSH proteins, despite the CTD regulatory domain which allows post-translational regulation. Importantly, the transcription of *spoT* is not regulated in the same way as *relA* during nitrogen starvation (Brown *et al.*, 2014). Rel_{Sa} is bifunctional, like SpoT, and so its transcriptional regulation may differ from that of *relA* in *E. coli*.

In this chapter we aim to investigate how *rel*, *relP*, and *relQ* are regulated on a transcriptional level. To do this, reporter fusions of the promoters of the three genes fused to the *lacZ* reporter gene were constructed. These were used to assay promoter activity during different growth phases, during various stresses and in various chemically defined media in a WT *S. aureus* background. These fusions were also used to try to identify the transcription factors (TFs) involved in regulation of the (p)ppGpp synthetase genes, by using them in TF mutant backgrounds.

3.2 Construction of synthetase promoter-*lacZ* fusions

In order to assess the level of transcription from the synthetase promoters in different conditions and stresses, transcriptional reporter plasmids were constructed. These consisted of the promoter region of each synthetase fused to the *lacZ* gene (Fig. 3.2a). The *relQ* gene is situated in a polycistronic operon (SAUSA300_0906, *relQ*, *ppnK*, SAUSA300_0909, *mgtE* and SAUSA300_0911) that is known to be co-transcribed in *B. subtilis* (Nanamiya et al., 2008). As such, the promoter region upstream of the SAUSA300_0906 gene was taken as the promoter region of *relQ*. The *rel* gene (SAUSA300_1590) is at the start of an operon with *dtd* (SAUSA300_1589) and *lytH* (SAUSA300_1588). In *E. coli* the *relA* gene has 4 promoters (Brown *et al.*, 2014; Metzger *et al.*, 1988; Nakagawa *et al.*, 2006) and so the region from *rel* to *apt* (SAUSA300_1591) was taken as the promoter region. The region between the *relP* gene (SAUSA300_2446) and the preceding gene SAUSA300_2447 was taken as the promoter. This approach increased the chances that any undescribed promoters of these genes would be included.

In order to construct these fusions, the *lacZ* reporter gene was amplified from plasmid pMUTIN4 (Fig. 3.2b). This allowed introduction of a SacII restriction site at the 3' end of the DNA. The promoter regions of *relQ*, *relP* and *rel* were amplified from the genomic DNA of the community-acquired methicillin resistant *S. aureus* (CA-MRSA) strain LAC* using primers that introduced a 5' KpnI site. These promoter fragments were fused to the *lacZ* using PCR Splicing by Overlap Extension (PCR-SOE) (Fig. 3.2b and c). The PCR products were subsequently digested with KpnI and SacII and ligated with the pCL55 vector that had also been digested with these enzymes, creating plasmids pCL55p*rel-lacZ*, pCL55p*relP-lacZ* and pCL55p*relQ-lacZ*.

The control plasmid pCL55p*itet-lacZ,* which places the *lacZ* gene under the control of an anhydrotetracycline-inducible promoter was constructed by amplifying the *lacZ* gene with primers RMC074 and RMC075. This introduced AvrII and SacII restriction sites to the 5' and 3' ends of the DNA respectively and allowed for cloning into the pCL55p*itet* vector.

pCL55 is a single site integration vector used to allow the stable insertion of a plasmid into the chromosome of *S. aureus.* The plasmid inserts in the *geh* locus through recombination between the *attB* and *attP* sites on the chromosome and the plasmid respectively (Fig. 3.2d). Incorporation of the reporter fusion at a distal site leaves the native gene intact which is important for *rel* because it is essential in the presence of *relP* and *relQ* (Geiger *et al*., 2012). This approach also ensures that any change in transcription observed is due to the conditions being tested and not because of an abnormal stringent response which might occur in a (p)ppGpp synthetase mutant. Following transformation of the mutagenised laboratory strain RN4220 with a pCL55 plasmid, colonies were screened to check for

plasmid insertion by extracting chromosomal DNA and amplifying using primer RMC004 (*geh* specific) with either RMC003 (*geh* specific) or RMC005 (insert specific). Successful plasmid integration results in a PCR product of around 1750 bp with the primers RMC004/RMC005 and nothing for RMC004/RMC003, while the WT strain will yield a 1151 bp PCR product with primers RMC004/RMC003 but nothing with RMC004/RMC005 (Fig. 3.2d and e). Once confirmed, all successfully integrated constructs were phage transduced into the more clinically relevant methicillin-sensitive *S. aureus* strain Newman. Phage transduced Newman strains were also screened for correct plasmid insertion as described above.

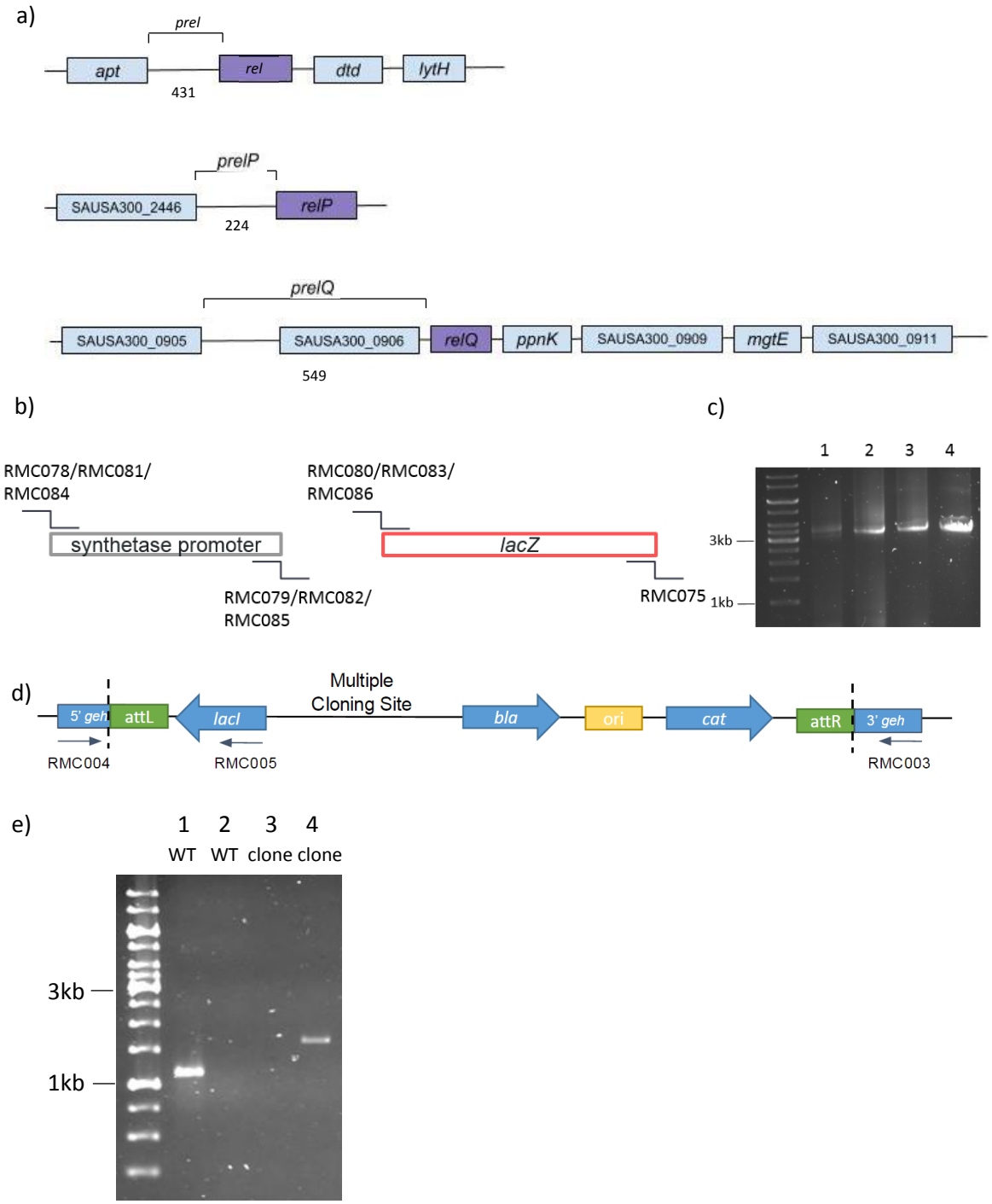

Fig. 3.2 Construction of transcriptional fusions using PCR SOE. a) Operon structure of *rel, relP* and *relQ*. Promoter regions used to construct the promoter fusions are denoted as *prel, prelP* and *prelQ.* The size of the promoter region (nt) is denoted below. b) Schematic diagram showing the primers used for fragment amplification and PCR SOE reactions. c) Agarose electrophoresis gels of PCR-SOE fragments. Lane 1: p*rel-lacZ*, Lane 2: p*relP-lacZ*, Lane 3: p*relQ-lacZ*, Lane 4: lacZ. d) Diagram of the pCL55 vector inserted in the chromosome. Dashed lines indicate the boundary between chromosomal and plasmid derived DNA. The *attB* site on the chromosome recombines with the *attP* site on the pCL55 plasmid resulting in plasmid integration and the formation of *attL* and *attR* sites. Screening by PCR with RMC004 and RMC003 primers results in an 1151 bp band if there is no insertion. With primer pair RMC004 and RMC005 a PCR product of around 1750 bp can be amplified when the plasmid has successfully inserted. e) Example of agarose electrophoresis gel of colony screening. gDNA of WT RN4220 and transformed RN4220 was amplified using primers RMC003/RMC004 (Lanes 1 & 3 respectively) or RMC004/RMC005 (Lanes 2 & 4 respectively).

3.3 Optimisation of β-galactosidase activity assay

In order to assess the levels of transcription from the synthetase promoters under different conditions the β-galactosidase activity of samples was measured. When transcription from the promoter is high transcription of the *lacZ* gene is high. *lacZ* encodes a β-galactosidase, a glycoside hydrolase enzyme which hydrolyses glycosidic bonds. In this assay, 4-methylumbelliferyl-β-D-galactopyranoside (MUG) is used as the substrate which is hydrolysed to fluorescent 4-methylumbelliferone (MU). The fluorescence is measured and compared to a standard curve generated from serial dilutions of MU. This allows the fluorescence reading to be converted to a concentration of MU. The activity was determined as: β-galactosidase activity per CFU = MUG hydrolysed (pmol) / sample volume (ml) x incubation time (min) x CFU per ml or β-galactosidase activity per OD_{600} = MUG hydrolysed (pmol) / sample volume (ml) x incubation time (min) x OD_{600}. This acts as a proxy to measure transcription from the (p)ppGpp synthetase promoters.

Initially, the suitability of the assay was investigated using RN4220 pCL55p*itet* and RN4220 pCL55p*itet*-*lacZ* strains as a negative and positive control, respectively. β-galactosidase activity was measured in the presence and absence of 200 ng/ml anhydrotetracycline (Atet), the inducer of the p*itet* promoter (Fig. 3.3). As expected, only background β-galactosidase activity was observed for the negative control in either the absence or presence of Atet, with no significant difference between the two conditions (Fig. 3.3). In contrast, a significant increase in β-galactosidase activity was seen for the positive control in the presence of Atet compared to without Atet (p = 0.0083). The activity observed in the absence of Atet suggests that p*itet* promoter used is leaky. These data confirm that the *lacZ* assay is functional, as an increase in promoter activity does indeed result in a significant increase in β-galactosidase activity.

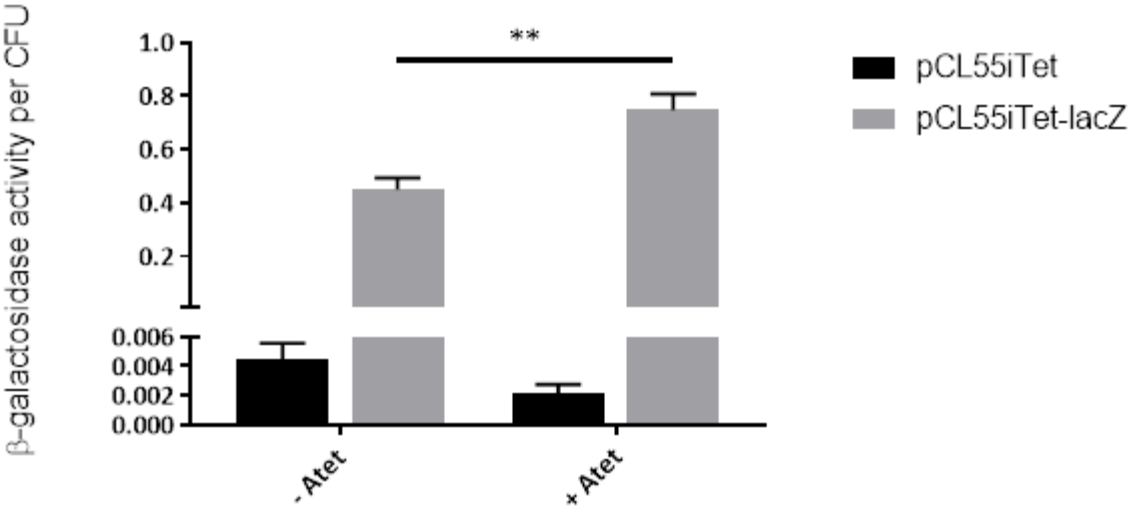

Fig. 3.3 Transcriptional activity from control constructs. The β-galactosidase activity per CFU of RN4220 strains with chromosomally inserted pCL55p*itet* (negative control; black) and pCL55p*itet-lacZ* (positive control; grey) was measured with and without 200 ng/ml Atet. β-galactosidase activity was calculated as one unit= pmol of MUG hydrolysed/ (sample volume (ml) x incubation time (h) x CFUs per ml). The β-galactosidase activity per CFU of the RN4220 *pCL55pitet-lacZ* strain was significantly higher in the presence of Atet. This experiment was performed four times, with means and standard deviations plotted. Statistical significance tested by unpaired T test ** $p < 0.01$

3.4 Transcription of synthetases during normal growth in TSB

Having confirmed that this assay can be used to assess promoter activity, we used it to investigate the activity of the (p)ppGpp synthetase promoters during different growth stages. Newman *pCL55prel-lacZ*, Newman pCL55p*relP-lacZ* and Newman pCL55p*relQ-lacZ* were grown in TSB for 8 h with OD_{600} and β-galactosidase activity per OD_{600} measurements taken at regular intervals. This allows comparison between the promoter activity and the growth phase.

In *E. coli*, two of the promoters of *relA*, *rel*AP3 and *rel*AP4, are induced during nitrogen starvation (Brown *et al.*, 2014). The promoter *rel*AP1 is constitutively active throughout growth whilst *rel*AP2 is induced in the transition between exponential phase and stationary phase (Nakagawa *et al.*, 2006). Here we show that, unlike $relA_{Ec}$, the transcription of *rel* is not affected by the growth phase of the bacteria in *S. aureus*. The activity of the *rel* promoter was not significantly different at any time point and remained low throughout the course of the experiment (Fig. 3.4a). Interestingly, the level of transcription was also lower than that of *relP* and *relQ.*

The activity of the *relP* promoter increased to a peak at around 4 h, corresponding to late exponential phase (Fig. 3.4b), whilst the peak of *relQ* promoter activity was around 3.5 h (Fig. 3.4c), corresponding to exponential phase. The activity of both these promoters decreased as the cells entered stationary phase. This finding is in accordance with work in *B. subtilis*, showing that *relQ* is transcribed during exponential phase and *relP* is transcribed during late exponential phase in unstressed conditions

(Nanamiya *et al.*, 2008). In *E. coli*, (p)ppGpp regulates growth rate and the reduction in RNA/protein and RNA/DNA ratios usually seen as cells switch from fast to slow growth is not seen without (p)ppGpp (Potrykus *et al.*, 2011). The induction of *relQ* and *relP* transcription in *S. aureus* could play a role in slowing the growth rate as cells enter the stationary phase.

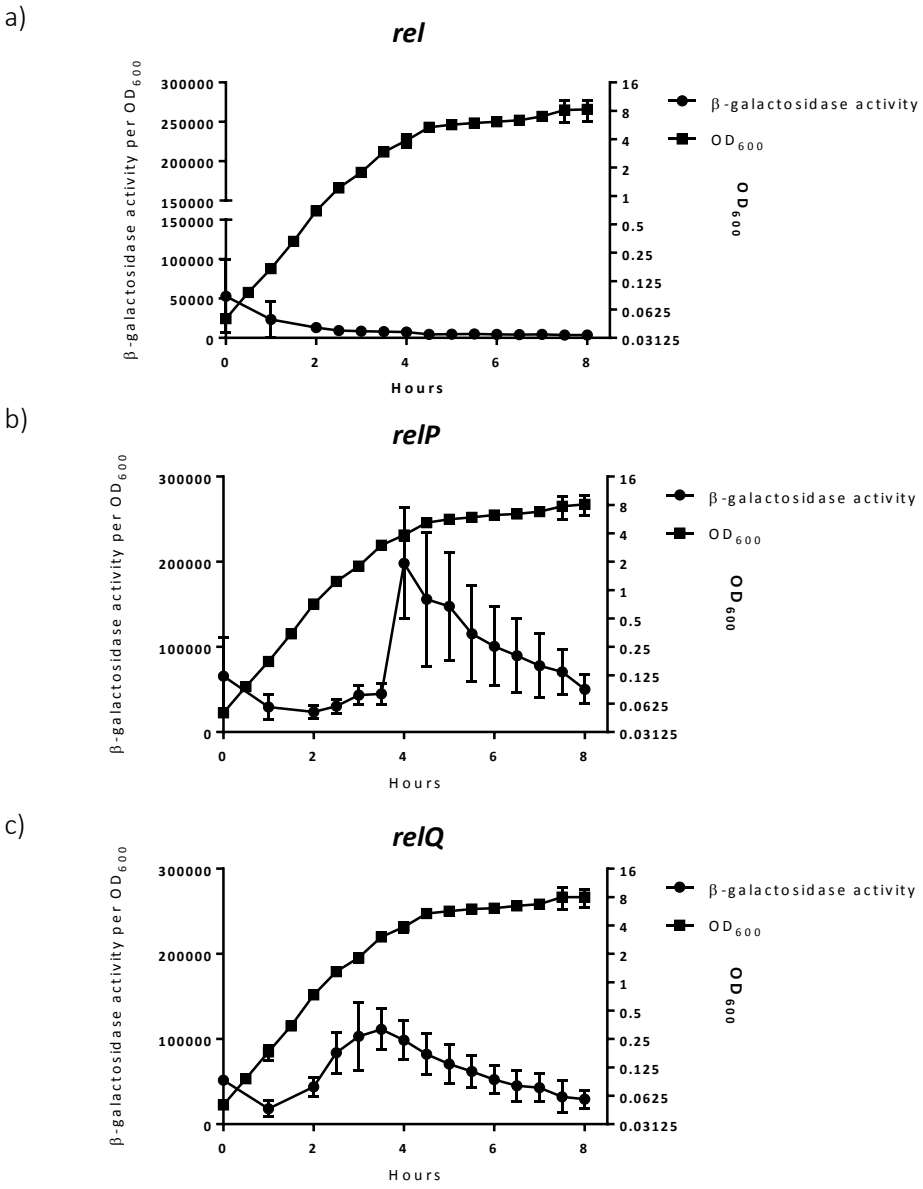

Fig. 3.4 (p)ppGpp synthetase promoter activity over time during growth in TSB. Promoter activity of *rel* (a)*, relP* (b) and *relQ* (c). β-galactosidase activity per OD_{600} is plotted on the left Y axis (circles; linear). OD_{600} is plotted on the right Y axis (squares; log2). β-galactosidase activity per OD_{600} was measured every hour for the first two hours, then every 30 min whilst OD_{600} was measured every 30 min. All three strains showed the same growth over the 8 hours. β-galactosidase activity was calculated as one unit= pmol of MUG hydrolysed/ (sample volume (ml) x incubation time (h) x OD_{600}). a) The β-galactosidase activity per OD_{600} did not change significantly over time. b) The β-galactosidase activity per OD_{600} peaked at 4 h as the cells were in late exponential stage and declined as the cells entered stationary phase. c) The β-galactosidase activity per OD_{600} peaked between 3-4 hours as the cells were in late exponential phase and declined as the cells entered stationary phase. This experiment was performed four times, with means and standard deviations plotted.

3.5 Transcription of synthetases during stress conditions

Following this, the β-galactosidase activity was determined for strains Newman pCL55p*rel-lacZ*, Newman pCL55p*relP-lacZ* and Newman pCL55p*relQ-lacZ* under a number of different conditions that have previously been reported to affect the stringent response (Fig. 3.5). These included a 30 min treatment with 60 µg/ml of mupirocin, 20 µg/ml of vancomycin, 1.5 µg/ml of oxacillin, 62.5 µg/ml of cerulenin, 25% of human serum and alkaline shock. Mupirocin is an antibiotic which inhibits the isoleucyl t-RNA synthetase thus stopping protein synthesis (Hughes and Mellows, 1980). It has been used to mimic amino acid starvation and trigger the stringent response extensively. Here we use 60 µg/ml which induced transcription of *rel* by 2.4-fold in *S. aureus* UAMS-1 (Anderson *et al.,* 2006). Vancomycin and oxacillin are cell wall active antibiotics that prevent cell-wall crosslinking. Cell wall stress has been shown to trigger the stringent response in *S. aureus* (Geiger *et al.*, 2014). Cerulenin is an antibiotic which is used to mimic fatty acid starvation due to its inhibition of the fatty acid biosynthesis enzyme FabF. In *B. subtilis* and *E. coli* the stringent response has a role in survival of fatty acid stress (Pulschen *et al.*, 2017; Seyfzadeh *et al.*, 1993). Human whole blood induced the stringent response in *Streptococcus agalactiae* (Hooven *et al.*, 2018). Vancomycin and oxacillin concentrations used were 5 X Minimum Inhibitory Concentration (MIC) of the *S. aureus* Newman strain, while the cerulenin concentration used was 1 X MIC. For the alkaline shock a pH of 9.9 was used, which was reported to increase the transcription of the *relQ* gene, *ywaC*, in *B. subtilis* and to also result in a ppGpp accumulation (Nanamiya *et al.,* 2008).

The promoter activity of *rel* was relatively low and was not significantly altered during any conditions tested (Fig. 3.5a). This suggests that the Rel_{Sa}-dependent accumulation of (p)ppGpp upon mupirocin treatment reported in *S. aureus* is not due to an increase in transcription of *rel* (Reiss *et al.*, 2012). Indeed, this was shown by microarray analysis of the *S. aureus* COL strain after treatment with 0.03 µg/ml of mupirocin, as there was only a 1.3-fold increase in *rel* expression (Reiss *et al.*, 2012). However, when the *S. aureus* UAMS-1 strain was shocked with 60 µg/ml of mupirocin for 30 mins there was a 2.4-fold increase in *rel* transcription (Anderson *et al.*, 2006). The authors note that when a lower concentration of mupirocin was used, they saw no increase in *rel* transcription. As such, a high level of mupirocin is required for a change of transcriptional activity of *rel* in certain strains of *S. aureus*. The *S. aureus* strain used by Anderson *et al*., UAMS-1, is in clonal complex 30, whereas the Newman strain used in this study is in clonal complex 8, which may explain the differences in *rel* regulation.

Upon treatment of the cells with vancomycin a 65-fold increase in the activity of the *relP* promoter was observed ($p < 0.0001$), while oxacillin treatment resulted in a 100- and 4- fold increase in the

activity of the *relP* and *relQ* promoters, respectively (p = 0.0041 and p = 0.0100, respectively) (Fig. 3.4b and c). These results provide a quantification of the transcriptional induction of *relP* and *relQ* previously seen after vancomycin and ampicillin through Northern blot analysis (Geiger *et al*., 2014). Alkaline shock did not alter the transcription from any of the promoters. This is in accordance with previous microarray work which showed that the accumulation of ppGpp during alkaline shock is not regulated transcriptionally in *S. aureus* (Anderson *et al.*, 2010). The transcriptional induction of the *relP* homologue, *ywaC*, seen in *B. subtilis* during alkaline shock at pH 9.9 (Nanamiya et al., 2008) is not seen in *S. aureus* under the conditions used here.

The transcription of *rel* in *S. agalactiae* was induced when grown in human whole blood (Hooven *et al.*, 2018) however human serum had no effect on the transcription from *rel* and *relQ* promoters in *S. aureus* here. Human serum did significantly induce the transcription from the *relP* promoter (p = 0.0118) but not as much as oxacillin and vancomycin treatment.

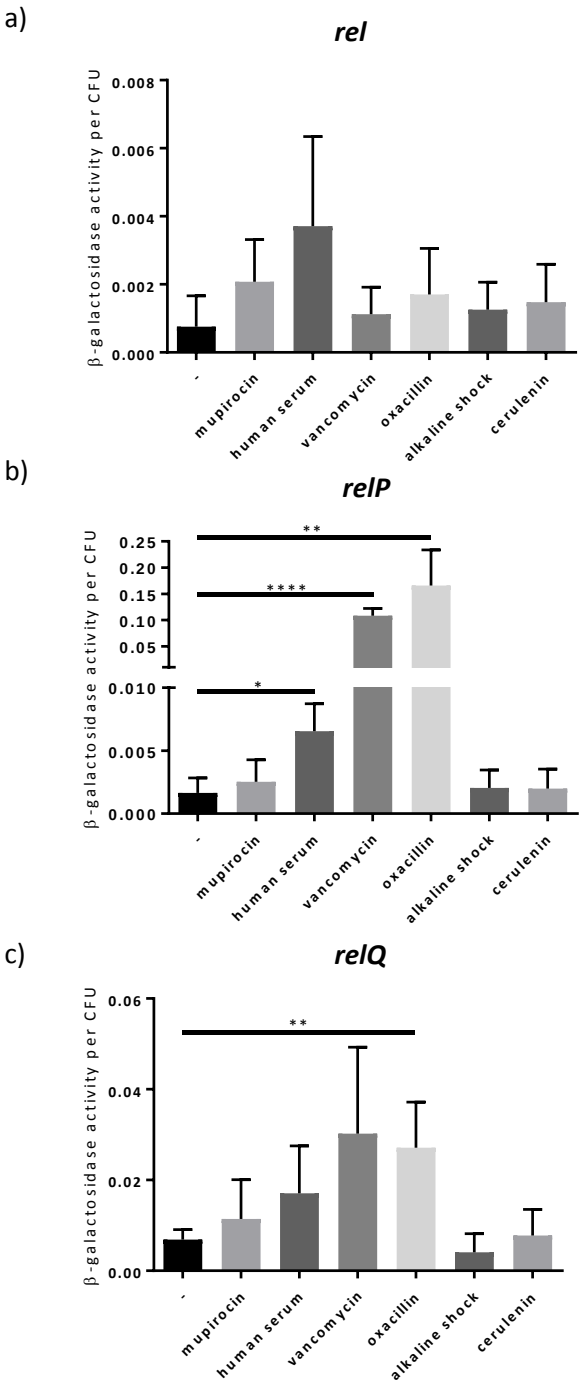

Fig. 3.5 Transcriptional activity of the (p)ppGpp synthetase promoters during various stresses. The β-galactosidase activity per CFU of Newman strains with chromosomally inserted pCL55p*rel-lacZ* (a), pCL55p*relP-lacZ* (b), and pCL55p*relQ-lacZ* (c) after treatment with various stresses. β-galactosidase activity was calculated as one unit = pmol of MUG hydrolysed/ (sample volume (ml) x incubation time (h) x CFUs per ml). Concentrations of 60 µg/ml mupirocin, 20 µg/ml vancomycin, 1.5 µg/ml oxacillin, and 62.5 µg/ml cerulenin were used. For alkaline shock, the pH of the cultures was adjusted to 9.9 with 1 N NaOH. Human serum was added to a final concentration of 25%. a) Transcription from the *rel* promoter is not significantly altered by any of the stresses used here. b) Transcription from the *relP* promoter is significantly increased after treatment with human serum, vancomycin and oxacillin. c) Transcription from the *relQ* promoter is significantly increased after treatment with oxacillin. These experiments were performed four times, with means and standard deviations plotted. Statistical significance tested by unpaired T test * $p < 0.05$; ** $p < 0.01$; **** $p < 0.0001$

3.6 Investigation of transcription factors involved in transcription of synthetases

Any transcriptional regulation of the (p)ppGpp synthetase genes must be mediated by transcription factors. The program DNA-binding Domain (DBD) predicts that there are around 128 TFs encoded in the *S. aureus* genome (Wilson *et al.*, 2008). We decided to narrow down this list to a list of 15 TFs which are important regulators of virulence and stress responses in *S. aureus*. We also ensured that the TFs chosen were represented in the Nebraska Transposon Mutant Library (NTML). The NTML was made using the mariner-based transposon (Tn) *bursa aurealis* to create Tn mutants with insertions near the 5' end of the gene (Bae *et al*. 2008; Fey *et al.*, 2013). The NTML strains are in the *S. aureus* strain JE2, which was created by curing the USA300 strain LAC of its plasmids (Fey *et al.*, 2013).

Having finalised our list of TFs, we recovered the corresponding NTML strains and inserted the reporter gene promoter fusions (pCL55p*rel-lacZ*, pCL55p*relP-lacZ*, and pCL55p*relQ-lacZ*) using phage transduction as described in Section 3.2. The control plasmids pCL55pitet-lacZ and pCL55pitet were transferred into the JE2 strain by phage transduction. The reporter fusions were now in a background in which one TF was not functional. If the TF was involved in the transcriptional regulation of the gene, then the deletion strain would have lower or higher promoter activity when compared to the JE2 strain with the promoter fusion. This approach allows us to assess both positive and negative regulators of the (p)ppGpp synthetase genes.

Two TFs were found to significantly increase the activity from the *rel* promoter when deleted (*argR*, $p = 0.0002$; *arlR*, $p = 0.0407$) (Fig. 3.6a). Five TFs were found to significantly increase the activity from the *relP* promoter when deleted (*agrA*, $p = 0.0050$; *arlR*, $p < 0.0001$; *clpP*, $p = 0.0169$; *lytR*, $p = 0.0304$; *sigB*, $p < 0.0001$) (Fig. 3.6b). Five TFs were found to significantly increase the activity from the *relQ* promoter when deleted (*codY*, $p = 0.0002$; *fur*, $p = 0.0488$; *lytR*, $p = 0.0271$; *saeR*, $p = 0.0021$; *sigS*, $p = 0.0358$) (Fig. 3.6c). The deletion of all of these TFs led to an increase in promoter activity, suggesting that in the WT strain they act as repressors of gene expression.

ArlR is part of a two component system ArlRS which regulates virulence genes involved in adhesion and virulence (Fournier *et al.*, 2001). Microarray analysis of the regulon of ArlR has shown that none of the (p)ppGpp synthetase genes are regulated by ArlR. It is not clear why ArlR appears to repress expression of transcription of *rel* and *relP* here (Fig. 3.6a and b). Microarray data revealed that *lytR* and *agrA* are upregulated by ArlR (Liang *et al*., 2005). LytR is part of the two component system LytRS which is involved in cell wall metabolism (Brunskill and Bayles, 1996). It appears that LytR represses the transcription of *relP* and *relQ* in WT *S. aureus* (Fig. 3.6b and c). AgrA is the regulator of a quorum sensing system in *S. aureus* (Recsei *et al.*, 1986). Phosphorylated AgrA induces the transcription of

agrC, *RNAIII*, *hla*, *spa, psmβ12*, *psmα1234* and itself *agrA* (Tan *et al.*, 2018). RNAIII represses or activates the expression of certain virulence genes, for example it represses *rot* expression (Boisset *et al.*, 2007). Whilst the results here suggest that *relP* is repressed by AgrA (Fig. 3.6b), microarray analysis has shown that none of the (p)ppGpp synthetase genes are in the AgrA regulon (Dunman *et al.*, 2001).

Another TF gene that ArlR regulates is *sigS;* in an *arlR* mutant the transcription of *sigS* was increased, suggesting ArlR is a repressor of *sigS* transcription (Burda *et al.*, 2014). SigS is an alternate sigma factor that is involved in disease causation (Shaw *et al.*, 2008). The transcription of *sigS* has been shown to be induced by cell wall stress and DNA damage (Miller *et al.*, 2012). Here, we show that SigS may also act as a repressor of *relQ* transcription (Fig. 3.6c). The other sigma factor we looked at here was SigB. SigB is an alternative sigma factor in *S. aureus*; microarray analysis has shown that its regulon does not contain the *rel*, *relP*, and *relQ* genes (Bischoff *et al.*, 2004). However, in a *sigB* Tn insertion strain the promoter activity of *relP* increased significantly, suggesting SigB represses *relP* expression (Fig 3.6b).

CodY is a repressor that binds branched chain amino acids and GTP as cofactors required for gene repression. However, during the stringent response, when levels of GTP are low CodY repression is released, resulting in a change in transcriptional profile (Geiger and Wolz, 2014). Previously, it has been shown that the *rel*, *relP*, and *relQ* genes are not in the CodY regulon (Geiger *et al.*, 2012). This corresponds to the results seen here, except that *relQ* appears to be negatively regulated by CodY (Fig. 3.6c). The *S. aureus* strain used by Geiger *et al.*, is HG001 which belongs to the same clonal complex as the JE2 strain used here (clonal complex 8). It is unclear why these two closely related strains would regulate *relQ* differently but it may also be due to the different growth medium used by Geiger *et al.*. CodY downregulates the expression of *saeS, agr* and *rot* whilst upregulating the expression of *sarS and lytS* (Majerczyk *et al.*, 2010). SaeS is part of a two component system along with SaeR and is required for activation of SaeR through phosphorylation (Sun *et al.*, 2010). Here, SaeR appears to negatively regulate the expression of *relQ* (Fig. 3.6c).

Fur regulates genes involved in iron transport in *S. aureus* (Xiong *et al.*, 2000). Fur binds to iron and represses expression of iron uptake genes and certain virulence factors (Hantke, 1981). The transcription of *relQ* is negatively regulated by Fur (Fig. 3.6c).

ArgR regulates operons involved in arginine biosynthesis and metabolism such as *artQM*, *cudT*, *rocD-arcCJB*, *arcABDCR*, *argGH*, and *argR-recN* (Ravcheev *et al.*, 2011). ArgR also appears to negatively regulate the transcription of *rel* (Fig. 3.6a).

ClpP is a protease which can degrade misfolded proteins during stress or it can degrade transcriptional regulators (Gottesman, 1996). In a *clpP* mutant *S. aureus* strain the *agr* locus is repressed, as well as several other gene regulators such as *lytS, arlR, sarR* and *sigB* (Michel *et al.*, 2005). The expression of *sarA*, *codY* and *sarT* are also altered in a *clpP* mutant but their expression is increased (Michel *et al.* 2005). In *E. faecalis*, the expression of *clpP* is induced during the stringent response (Gaca *et al.*, 2012). Here we show that ClpP represses the expression of *relP* in *S. aureus* (Fig. 3.6b). This repression may be indirect, with ClpP promoting expression of *lytR, arlR, sigB* and *agrA* which then repress *relP* expression (Fig. 3.6b).

During mupirocin stress the transcription of *agrA, arlRS, saeRS* and *sigB* all increase (Anderson *et al*., 2006; Reiss *et al*., 2012). This would presumably result is a downregulation of the (p)ppGpp synthetase genes given that all of these TFs repress expression of *rel, relP,* or *relQ* (Fig. 3.6). This may explain why there was no change in transcription seen for any of the genes following mupirocin treatment (Fig. 3.5).

Of the 10 TFs found to have an effect on the (p)ppGpp synthetase genes here, 2 had Tn insertions that would appear to cause polar effects. These were *arlR* and *saeR*, which are both the first gene in an operon with the sensor component of their respective two-component systems. As such, any polar effects may just act to impair the two-component system and so the Tn mutants can still be used in this screen. Of course, unexpected polar effect may occur in all the strains used and so clean deletions should be used to confirm the hits found here.

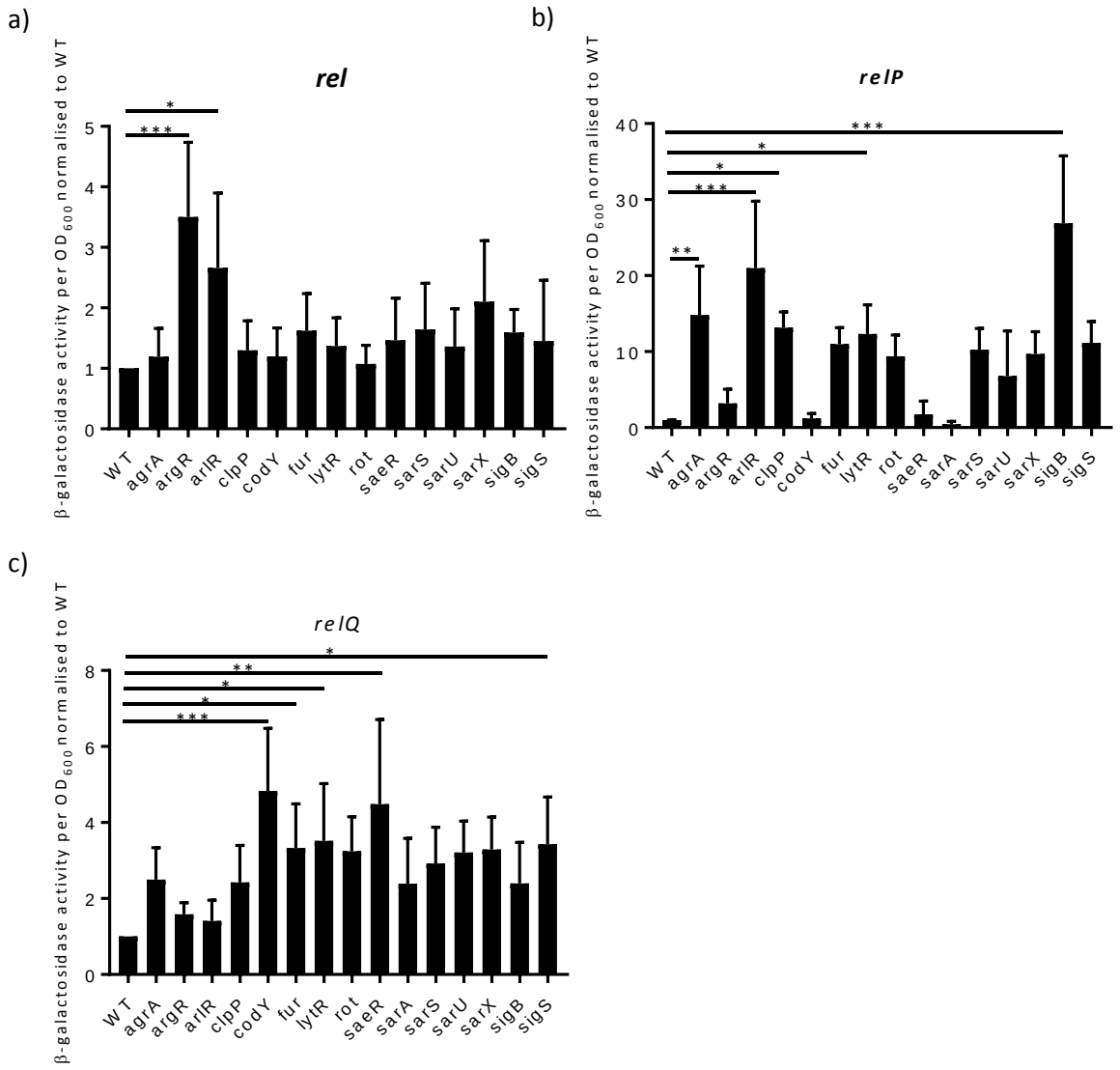

Fig. 3.6 The effect of transcription factor mutations on the promoter activity of *rel*, *relP*, and *relQ*. The β-galactosidase activity per OD_{600} of JE2 strains with chromosomally inserted pCL55p*rel-lacZ* (a), pCL55p*relP-lacZ* (b), and pCL55p*relQ-lacZ* (c) in a WT JE2 background or JE2 with various transposons insertions in transcription factors. β-galactosidase activity was calculated as one unit = pmol of MUG hydrolysed/ (sample volume (ml) x incubation time (h) x OD_{600}) which was then normalised to the WT strain. a) The β-galactosidase activity per OD_{600} normalised to WT is significantly higher in a JE2 background with *argR* and *arlR* disrupted by a Tn insertion versus the WT background. b) The β-galactosidase activity per OD_{600} normalised to WT is significantly higher in a JE2 background with *agrA, arlR, clpP, lytR* and *sigB* disrupted by a Tn insertion versus the WT background. c) The β-galactosidase activity per OD_{600} normalised to WT is significantly higher in a JE2 background with *codY, fur, lytR, saeR* and *sigS* disrupted by a Tn insertion versus the WT background. These experiments were performed at least three times, with means and standard deviations plotted. Statistical significance tested by ordinary one-way ANOVA * $p < 0.05$; ** $p < 0.01$; *** $p < 0.001$

3.7 Discussion

In this chapter we have confirmed that the transcription of *relP* and *relQ* is induced by cell wall active antibiotics, as well as showing that 25% human serum induces the transcription of *relP*. We have also shown that in *S. aureus*, the expression of *relP* and *relQ* is controlled temporally with an induction in

late exponential phase and exponential phase respectively. We have identified 10 TFs that may be involved in the transcriptional regulation of the three (p)ppGpp synthetase genes (2 for *rel*, 5 for *relP*, 5 for *relQ)*.

Here we have shown that some stresses that affect (p)ppGpp synthetase gene expression in other organisms, such as alkaline shock increasing the expression of *ywaC* (*relP* homologue) in *B. subtilis*, do not have an impact in *S. aureus* (Nanamiya *et al.,* 2008). However, before alkaline shock *B. subtilis* was grown in S7 minimal medium where as in this study the *S. aureus* strains were grown in TSB which is a rich medium. This may have impacted the differences seen in transcriptional regulation following alkaline shock.

Another example is that cerulenin did not affect the transcription of any of the (p)ppGpp synthetases despite the stringent response being important for fatty acid starvation survival in *E. coli* and *B. subtilis* (Pulschen *et al.*, 2016; Seyfzadeh *et al.*, 1993). Previously cerulenin was shown to have no effect on the (p)ppGpp pool in *S. aureus* (Greenwood and Gentry, 2002). This may explain why no transcriptional changes were seen with cerulenin treatment as it does not trigger an accumulation of (p)ppGpp in *S. aureus*. However, cerulenin treatment does not trigger an accumulation of (p)ppGpp in *B. subtilis* but the stringent response enzymes are required for survival of fatty acid starvation (Pulschen *et al.*, 2017). The authors suggest that it is a reduction in GTP levels that is responsible for survival and the stringent response enzymes are required for this change. As such, the stringent response may play a role in survival of fatty acid starvation in *S. aureus,* but it is not mediated through (p)ppGpp accumulation or an increase in transcription of the synthetase genes.

The *rel* gene in *S. aureus* was not induced by the stresses tested here and its expression did not change during different growth phases. The expression from the *rel* promoter was low throughout growth but was highest at the start of growth, although this was not significant. This may be due to expression levels of the stationary phase culture used to set up the growth curve and so it would be interesting to look at *rel* promoter activity after 16 h growth. In the case of Rel_{Sa}, post-translational regulation could be more important, which would allow for a quicker response that is more switch-like. Post-translational regulation is mostly likely mediated through the CTD of Rel_{Sa}, allowing the protein to quickly sense changes and respond by altering hydrolase or synthetase activity. However, some transcriptional regulation is provided by ArgR and ArlR as highlighted by the transcription factor screen.

Using the NTML to screen for transcription factors involved in the regulation of *rel*, *relP*, and *relQ* allowed for multiple TFs to be investigated without having to make multiple clean knockout strains.

This allowed us to screen many more TFs more rapidly. However, the results shown here should only be interpreted as an initial screen. The TFs identified here as having an impact on the transcription of the three (p)ppGpp synthetase genes have not get been confirmed by other methods. A clean deletion of the TFs should be made to limit any polar effect the transposon insertions used here may have. RT-PCR could also be used to more sensitively measure transcription levels directly. Direct binding between the TF and the promoter region of the gene should be demonstrated. This can be done using an electrophoretic mobility shift assay, in which fluorescently labelled promoter DNA is incubated with and without the TF. If the TF binds to the DNA it will alter the mobility of the promoter DNA when analysed by electrophoresis. Use of various truncated or mutated DNA fragments would allow the promoter binding site to be determined.

Previously it has been predicted that *relP* and *relQ* are controlled by the housekeeping sigma factor SigA based on their promoter sequences (Geiger *et al.*, 2014). However, *sigA* is an essential gene and therefore we could not assess its effect on the expression of the (p)ppGpp synthetase genes with the method used here. To investigate essential genes electrophoretic mobility, shift assays would have to be used to check promoter binding.

Whilst the number of TFs that impact the promoter activity of *rel*, *relP* and *relQ* may seem high, it is common in these regulatory networks to allow fine tuning and a response to multiple stimuli. Interestingly, only two TFs regulated more than one gene, ArlR and LytR. Both of these transcription factors are involved in regulating autolysin activity and thus may play a role in cell wall stress response.

A limitation of the screen used here is that it can only identify protein transcriptional regulators. RNA molecules that may affect transcription cannot be identified which overlooks a potentially important form of regulation. In *E. coli* the small non-coding RNA molecule 6S inhibits *relA* transcription by binding to the sigma 70 – RNAP complex (Cavanagh et al., 2010). In strains without 6S RNA there is an increase in *relA* transcription and an increase in ppGpp levels, even in *relA* deletion strains (Cavanagh *et al*., 2010; Neusser *et al*., 2010)

In conclusion, the *rel*, *relP* and *relQ* promoter *lacZ* fusions made here are useful tools for looking at promoter activity in different conditions and genetic backgrounds. The TF screen has provided several interesting hits to investigate further which may provide a better understanding of the stringent response in *S. aureus*. However, transcriptional regulation is just one factor of the regulation of the stringent response and in the next chapter we will focus on post-translational regulation.

Chapter 4 – The role of the stringent response in metabolism

4.1 Introduction

The stringent response has been shown to be triggered by varied stimuli in different bacteria (Boutte and Crosson, 2013). These stimuli can be specific to their ecological niches such as darkness triggering the stringent response in the photosynthesising bacteria *Synechococcus elongatus* (Hood *et al*., 2016). They can also be broader, such as nutrient limitation which is a common stimulus of the stringent response across the bacterial domain. During nutrient limitation the stringent response can trigger a change in transcriptional profile in order to utilise alternative carbon or nitrogen sources. Understanding the conditions which trigger the stringent response can provide clues to how it is regulated and vice versa.

In order to understand more on growth conditions where ppGpp is required for viability we decided to test the growth of a triple (p)ppGpp synthetase mutant. In this strain the *relQ* gene is replaced by a tetracycline resistance cassette, the *relP* gene is disrupted by a transposon insertion, and the synthetase domain of the *rel* gene is inactivated by a single amino acid mutation. This strain is completely unable to produce (p)ppGpp and is therefore referred to as a (p)ppGpp^0 strain. The (p)ppGpp^0 strain cannot effect a stringent response and so it will not be able to grow in any condition which requires activation of the stringent response. In order to screen a large number of growth conditions quickly we used Phenotype Microarray (PM) for Microbial Cells plates (Biolog). These are 96 well plates, with each well of the plate containing a different growth media. The plates we used here are plates PM1, PM2A, PM3B, PM4A and PM9. PM1 and PM2A were used to assess the use of various compounds as a carbon source. PM3B examined the use of different nitrogen sources and PM4A had a combination of different phosphorus and sulphur sources. PM9 had various osmolytes in each well to assess the ability of the strains to resist different osmotic stresses. Plates assessing the ability of the strains to use various nutrient sources were used due to the role of the stringent response in sensing nutrient starvation. PM9 was used because osmolytes could cause cell wall stress which has been shown to induce the stringent response in *S. aureus*, via VraRS activation of *relP* and *relQ* transcription following the use of cell wall active antibiotics (Geiger *et al.*, 2014).

A cell suspension of OD_{600} 0.1 was added to a PM additive that is specific to each PM plate, supplied media and 3-(4,5-dimethylthiazol-2-yl)-2,5-diphenyltetrazolium bromide (MTT) tetrazolium dye, before this mixture was added to each well of the plate. As the cells actively respire the MTT tetrazolium dye is reduced to formazan resulting in a colour change from yellow to purple. This colour

change represent metabolism rather than direct growth. The plates were incubated for 24 h at 37 °C and the OD_{595} was measured every 15 min.

Here we compare the metabolism of (p)ppGpp^0 in the PM plates to that of a *ΔhflX* mutant. In this mutant the *hflX* gene has been replaced with an *ermR* cassette. HflX is a GTPase involved in ribosome maturation that has been shown to be inhibited by (p)ppGpp resulting in reduced ribosome maturation (Corrigan *et al.*, 2016). The *hflX* mutant was used because it was being investigated by another member of the laboratory. Ideally, the metabolism of the (p)ppGpp^0 strain would be compared to the WT LAC* strain however this was not possible due to limited resources. Nonetheless, the *ΔhflX* mutant can act as a control to differentiate between ribosome maturation dependent and independent effects of the stringent response.

4.2 Metabolism of (p)ppGpp^0 in Biolog plates

4.2.1 Metabolism with various carbon sources

Biolog plates PM1 and PM2A contained various carbon sources including amino acids and sugars in each well. The (p)ppGpp^0 strain showed defective metabolism with 8 different carbon sources (Fig. 4.2.1) compared to the Δ*hflX* strain. Five of the carbon sources were amino acids (L-asp, L-ser, glycine, homoserine and L-ile) (Fig. 4.2.1a) and 3 were other carbon containing molecules (tyramine, α-methyl-D-glucoside and 2-hydroxy benzoic acid) (Fig. 4.2.1b). The metabolism of (p)ppGpp^0 was not defective compared to *ΔhflX* with other amino acids, such as L-asn, which is included in Fig. 4.2.1a, showing that not all amino acid catabolism is dependent on the stringent response.

L-Asp is a negatively charged amino acid however the negatively charged amino acid L-Glu was used effectively by both (p)ppGpp^0 and *ΔhflX,* suggesting that the defect seen with L-Asp is not due to its negative charge. Glycine is the simplest possible amino acid and showed similar metabolism defect as L-Asp. L-Ser and homoserine have an uncharged polar side chain however this characteristic cannot be responsible for the metabolism defect seen with (p)ppGpp^0 because L-Asn also has an uncharged polar side chain and can be used by both (p)ppGpp^0 and *ΔhflX* as a carbon source.

In the absence of a preferred carbon source L-Gly and L-Ser are catabolised into the intermediate pyruvate (as are alanine, threonine, and cysteine) (Fig. 4.2.1c). L-Thr is converted to L-Gly by threonine aldolase which is then converted to L-ser by glycine cleavage enzymes, GcvT or GcvH (Halsey *et al.*, 2017). L-Ser is then converted to pyruvate by SdsAA or SdsAB which then feeds in to the central metabolism. Although both L-Ser and L-Gly are not used as carbon sources effectively by the (p)ppGpp^0 strain this is probably not due to an effect on the catabolism of the amino acids because L-

Thr at the start of the chain can be used as a carbon source by (p)ppGpp^0. Again, the defect in (p)ppGpp^0 metabolism with L-Asp as a carbon source cannot be explained by a defect in catabolism due to the ability of the strain to utilise L-Asn as a carbon source. Both L-Asn and L-Asp are catabolised into oxaloacetate with L-asn being catabolised to L-Asp by AsnA, which is then converted to oxaloacetate by AspA (Fig. 4.2.1d) (Halsey *et al.*, 2017). Given these examples of L-Gly, L-Ser and L-Asp catabolism not being compromised in the (p)ppGpp^0 strain, the defect in metabolism may be due to impaired import of the amino acids.

L-Ile has an uncharged, non-polar side chain and is hydrophobic. It is one of three branched chain amino acids along with L-Val and L-Leu. Interestingly, the only BCAA which (p)ppGpp^0 could not use as a carbon source as effectively as *ΔhflX* was L-Ile. Previous work has shown that when *S. aureus* is grown in media without L-Val or L-Leu the stringent response is induced, suggesting these are important amino acids for *S. aureus* even in the presence of glucose (Geiger *et al*., 2010). BCAA availability is particularly important for the stringent response of Gram positive bacteria because BCAAs are one of the co-factors of the regulator CodY (along with GTP). The *S. aureus* CodY repressor most likely uses L-Ile as a cofactor along with GTP (Pohl *et al.*, 2009), rather than L-Val or L-Leu. During the stringent response CodY repression is released due to a drop in GTP pool and/or L-Ile pool. Perhaps in the presence of an abundance of L-Ile as a carbon source, CodY repression is not released in the (p)ppGpp^0 strain due to a lack of an effective stringent response. During the stringent response induced by L-Leu/L-Val starvation the expression of the *ilvE* gene increases following derepression by CodY (Geiger *et al.*, 2012). IlvE is a BCAA aminotransferase that has been shown to be important for BCAA catabolism in *Staphylococcus carnosus* (Madsen *et al.*, 2002). Thus, without CodY derepression, L-Ile may not be utilised as a carbon source efficiently, as *ilvE* is not expressed.

The (p)ppGpp^0 also showed a metabolism defect with 3 other, non-amino acid, carbon sources. α-methyl-D-glucoside (αMG) is a glucose-derived monosaccharide that has previously been shown to induce glucose phosphate stress. During α MG-induced glucose phosphate stress SgrR rapidly induces the expression of *sgrS* which encodes a sRNA that is the effector of the glucose stress response (Vanderpool and Gottesman, 2004). In *E. coli*, the stringent response has been implicated in the regulation of *sgrRS* through DskA (Kessler *et al.*, 2017). It could be that in *S. aureus* the stringent response is also required for survival of αMG induced glucose phosphate stress albeit independently of DskA.

Tyramine is an amine that is produced from the decarboxylation of the amino acid tyrosine. Tyrosine was not included as a carbon source on the PM plates and so it is not possible to determine if the metabolism defect seen with tyramine as a carbon source is specific. 2-hydroxybenzoic acid (also

known as salicylic acid) has been shown to reduce *codY* expression in *S. aureus* biofilms, resulting in derepression of the CodY regulon (Dotto *et al.*, 2017). The metabolism defect seen with salicylic acid as a carbon source may not be due to the catabolism of the molecule itself, but rather how it impacts *codY* regulation in the (p)ppGpp^0 strain. Interestingly, in plants, the stringent response, and resulting ppGpp accumulation, leads to a decrease in salicylic acid levels in the chloroplasts (Boniecka *et al.*, 2017).

Of the 192 carbon sources tested here, only 8 could not be used as effectively by a strain with a non-functional stringent response, compared to the *ΔhflX* strain. This suggests that, in general, the stringent response is not required for a switch to secondary carbon source metabolism. However, the stringent response could play a role in the metabolism of at least 8 different carbon sources through various mechanisms. The genes encoding the transporters of these molecules or other metabolic genes involved in their catabolism, could be regulated by the stringent response. Also, (p)ppGpp may directly inhibit or activate these transporters or metabolic enzymes. It is important to note that none of the carbon sources tested here resulted in no metabolism at all. This suggests that either spontaneous mutants arose or that the stringent response is not essential for metabolism with these carbon sources.

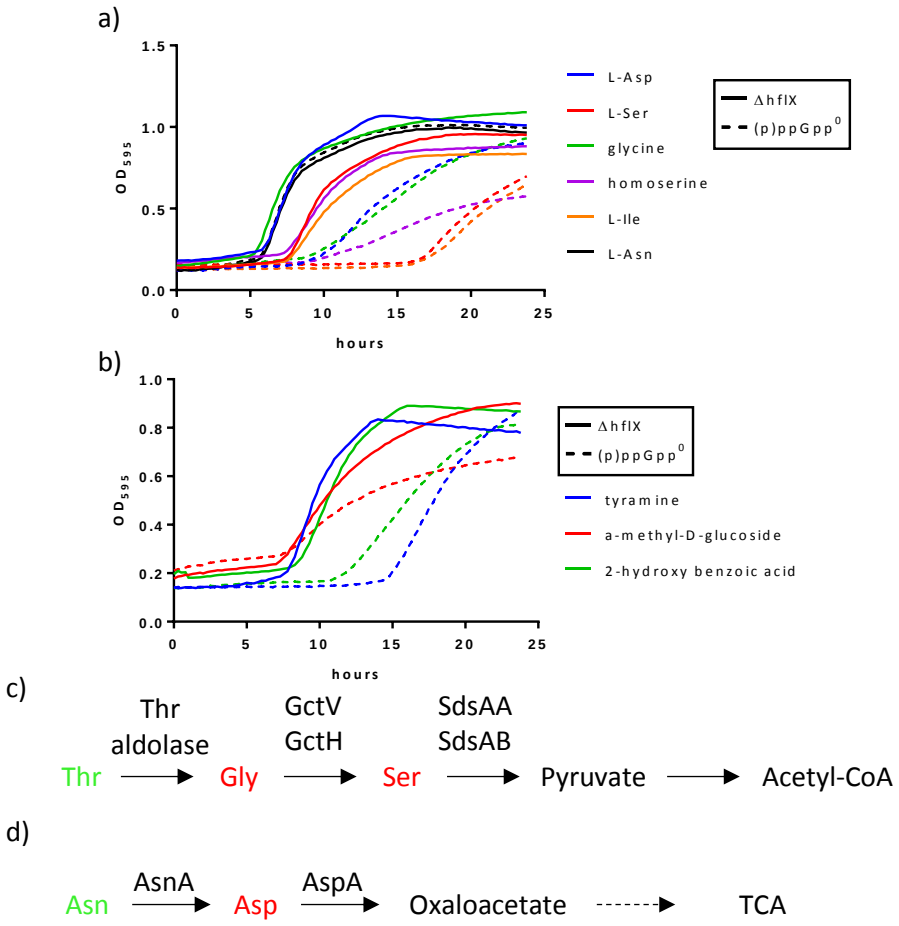

Fig. 4.2.1 Metabolism on Biolog plates PM1 and PM2A with various carbon sources. Metabolism of Δ*hflX* (solid lines) and (p)ppGpp^0 (dashed lines) was recorded over 24 h with OD_{595} readings taken every 15 min. a) Metabolism with various amino acids as a carbon source. The metabolism of (p)ppGpp^0 was impaired compared to Δ*hflX* with L-Asp (blue), L-Ser (red), glycine (green), homoserine (purple) and L-Ile (yellow) as the carbon source. The metabolism of both strains was not impaired with L-asn (black) as the carbon source. b) Metabolism with other carbon sources. The metabolism of (p)ppGpp^0 was impaired compared to Δ*hflX* with tyramine (blue), α-methyl-D-glucoside (red) and 2-hydroxy benzoic acid (green). Experiments were performed once. c) Metabolism diagram of Thr, Gly and Ser catabolism. Thr aldolase converts Thr to Gly. GctV or GctH convert Gly to Ser. SdsAA or SdsAB convert Ser to pyruvate. Amino acids that could be utilised as a carbon source by (p)ppGpp^0 are shown in green and those that could not are shown in red. d) Schematic diagram of Asn and Asp catabolism. AsnA converts Asn to Asp. AspA converts Asp to oxaloacetate which feeds into the citric acid cycle (TCA). Amino acids that could be utilised as a carbon source by (p)ppGpp^0 are shown in green and those that showed defects are shown in red.

4.2.2 Metabolism with various nitrogen sources

Next, we assessed how the (p)ppGpp^0 strain and the Δ*hflX* strain grew with various different nitrogen sources using the Biolog plate PM3B. Nitrogen limitation stress has been shown to induce the stringent response in *E. coli* (Brown *et al.*, 2014) and so we hypothesised that the (p)ppGpp^0 mutant may not be able to grow on certain nitrogen sources. The plate contained various nitrogenous compounds including amino acids, amines and various dipeptides. 29 nitrogenous compounds were found to result in a difference in metabolism between the (p)ppGpp^0 and Δ*hflX* strains (Fig. 4.2.2). The metabolism of (p)ppGpp^0 was worse than that of Δ*hflX* with 26 compounds and nitrogen sources, whereas with 3

compounds (L-Cys, histamine, N-acetyl-D-L glutamic acid) the opposite was true. No metabolism of (p)ppGpp^0 was seen with 5 compounds (guanosine, guanine, L-Ile, L-Ser and L-Tyr).

20 common amino acids were tested as a nitrogen source, of which 7 resulted in a metabolism defect for (p)ppGpp^0 (L-Ala, L-Ile, L-Leu, L-Met, L-Ser, L-Tyr and L-Val) and 1 (L-Cys) had the opposite effect (Fig. 4.2.2a). Interestingly, although the (p)ppGpp^0 strain showed a metabolism defect when grown on L-Asp or L-Gly as a carbon source, this was not the case when these amino acids were used as nitrogen sources. No metabolism of (p)ppGpp^0 was observed with L-Ile, L-Ser or L-Tyr suggesting that the stringent response is essential for using these amino acids as nitrogen sources. The (p)ppGpp^0 strain grew well on L-Cys as a nitrogen source, whilst the Δ*hflX* strain showed a metabolism defect, which either suggests that the stringent response may impede utilisation of L-Cys as a nitrogen source or that there is an unexpected metabolism defect with Δ*hflX*. 3 uncommon amino acids (D-Ala, D-Lys and L-homoserine) were also shown to result in a metabolism defect in (p)ppGpp^0 when used as a nitrogen source (Fig. 4.2.2b). This was not true of all D-isomer amino acids tested and thus is probably specific to D-Ala and D-Lys. Whilst (p)ppGpp^0 showed a similar metabolism defect when grown on L-Ala or D-Ala as a nitrogen source, metabolism with D-Lys but not L-Lys was defective. It is unclear why the (p)ppGpp^0 strain would be able to utilise L-Lys as a nitrogen source but not D-Lys. Use of L-Ile, L-Ser and homoserine as either a carbon or nitrogen source resulted in a metabolism defect for the (p)ppGpp^0 strain, indicating that the stringent response is important for any catabolism of these amino acids.

Of the 12 dipeptides tested as nitrogen sources only 6 resulted in a metabolism defect for (p)ppGpp^0 (Fig. 4.2.2c). Interestingly, the N terminal amino acid did not determine utility as a nitrogen source. For example, Ala-Gln and Gly-Asn were used equally as well by both strains whereas Ala-Glu and Gly-Met were not. During the stringent response in *S. aureus* the CodY repression of *oppBCDF* is released (Geiger *et al.*, 2012). The *oppBCDF* operon encodes an oligopeptide ABC transporter that can transport peptides into the cell. In the (p)ppGpp^0 strain, the repression of CodY may not be released correctly resulting in poor uptake of certain dipeptides. In order to further investigate the ability of the (p)ppGpp^0 strain to use various dipeptides as a nitrogen source, the Biolog plate PM6 could be used as this plate contains 94 other dipeptides.

The use of various amines, nucleotides and nucleosides as nitrogen sources was also assessed (Fig. 4.2.2d). The metabolism of (p)ppGpp^0 was better than Δ*hflX* with histamine as a nitrogen source. The opposite was true with 8 other nitrogenous compounds (tyramine, cytidine, guanine, guanosine, uridine, inosine, xanthine and xanthosine) with no (p)ppGpp^0 metabolism at all seen with guanine and guanosine as nitrogen sources. Whilst guanine, guanosine, inosine, xanthine and xanthosine are all

purine based molecules, this does not explain why they are not good nitrogen sources for the (p)ppGpp^0 strain because the purines adenine and adenosine where used by (p)ppGpp^0 as effectively as the Δ*hflX* strain. Similarly, cytidine and uridine are both pyrimidine based molecules but other pyrimidines tested, such as thymidine, were equally good nitrogen sources for both strains. Interestingly, with the pyrimidine bases (cytosine and uracil) as a nitrogen source there was no metabolism difference between the strains, however with the nucleosides (cytidine and uridine) there was a metabolism defect for (p)ppGpp^0.

Finally, the metabolism of the two strains was found to be different with 3 uncommon nitrogenous compounds as nitrogen sources (Fig. 4.2.2e). With D,L- α-amino-N-butyric acid (homoalanine) and α-amino-N-valeric acid as the nitrogen source the metabolism of the (p)ppGpp^0 strain was impaired compared to the Δ*hflX* strain, whilst the opposite was true with N-acetyl-D-L glutamic acid. D,L- α-amino-N-butyric acid is an amino acid with a side chain that is one carbon longer than alanine. Alanine was also not used effectively as a nitrogen source by (p)ppGpp^0 and the mechanism may be linked. N-acetyl-D-L glutamic acid is the first precursor of arginine biosynthesis, however L-arg was used equally well as a nitrogen source by both strains.

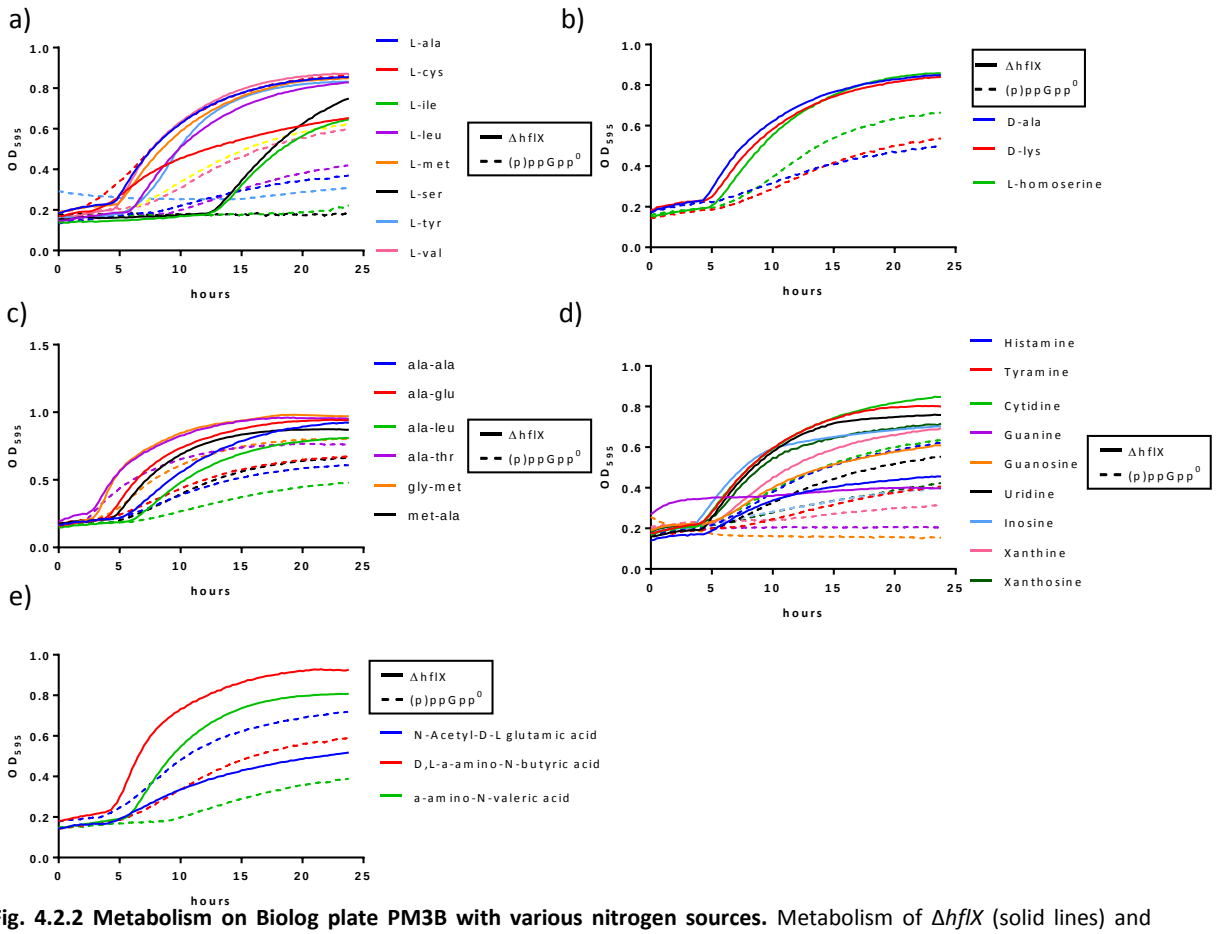

Fig. 4.2.2 Metabolism on Biolog plate PM3B with various nitrogen sources. Metabolism of Δ*hflX* (solid lines) and (p)ppGpp^0 (dashed lines) was recorded over 24 h with OD_{595} readings taken every 15 min. a) Metabolism with various amino acids as a nitrogen source. The metabolism of (p)ppGpp^0 was impaired compared to Δ*hflX* with L-Ala (blue), L-Ile (green), L-Leu (purple), L-Met (orange), L-Ser (black), L-Tyr (light blue), L-Val (pink) as the nitrogen source. The metabolism of Δ*hflX* was impaired compared to (p)ppGpp^0 with L-Cys (red) as the nitrogen source. b) Metabolism with various other amino acids as a nitrogen source. The metabolism of (p)ppGpp^0 was impaired compared to Δ*hflX* with D-Ala (blue), D-Lys (red), L-homoserine (green) as a nitrogen source. c) Metabolism with various dipeptides as a nitrogen source. The metabolism of (p)ppGpp^0 was impaired compared to Δ*hflX* with Ala-Ala (blue), Ala-Glu (red), Ala-Leu (green), Ala-Thr (purple), Gly-Met (orange) and Met-Ala (black) as a nitrogen source. d) Metabolism with various amines and bases as a nitrogen source. The metabolism of (p)ppGpp^0 was impaired compared to Δ*hflX* with tyramine (red), cytidine (green), guanine (purple), guanosine (yellow), uridine (black), inosine (light blue), xanthine (pink) and xanthosine (dark green) as a nitrogen source. The metabolism of Δ*hflX* was impaired compared to (p)ppGpp^0 with histamine (blue) as a nitrogen source. e) Metabolism with various nitrogenous compounds as a nitrogen source. The metabolism of (p)ppGpp^0 was impaired compared to Δ*hflX* with D,L- α-amino-N-butyric acid (red) and α-amino-N-valeric acid (green) as a nitrogen source. The metabolism of Δ*hflX* was impaired compared to (p)ppGpp^0 with N-acetyl-D-L glutamic acid (blue) as a nitrogen source. Experiments were performed once.

4.2.3 Metabolism with various phosphorous sources

Biolog plate PM4A was used to assess the ability of the (p)ppGpp^0 and Δ*hflX* strains to grow and metabolise on various phosphorous (Fig. 4.2.3) and sulphur sources (Fig. 4.2.4). 18 phosphorous sources were found to result in altered metabolism between the strains. The metabolism of (p)ppGpp^0 was better than Δ*hflX* with 8 of the phosphorous sources (adenosine-2'-monophosphate, adenosine-3'-monophosphate, adenosine-5'-monophosphate, adenosine-2',3'-cyclic monophosphate, adenosine-3',5'-cyclic monophosphate, cytidine-2'-monophosphate, cytidine-5'-monophosphate and

uridine-5'-monophosphate) and the reverse was true for 10 of the phosphorous sources (guanosine-2'-monophosphate, guanosine-3'-monophosphate, guanosine-5'-monophosphate, guanosine-2',3'-cyclic monophosphate, guanosine-3',5'-cyclic monophosphate, cytidine-3'-monophosphate, cytidine-2',3'-cyclic monophosphate, cytidine-3',5'-cyclic monophosphate, uridine-2',3'-cyclic monophosphate and uridine-3',5'-cyclic monophosphate).

Although other phosphorous containing compounds were used, such as various inorganic phosphates, the only molecules which resulted in metabolism differences between the two strains were nucleotides. All five adenosine nucleotides tested showed a metabolism defect for Δ*hflX* compared to the (p)ppGpp^0 strain (Fig. 4.2.3a), whereas the opposite was true for all five guanosine nucleotides (Fig. 4.2.3b). Adenosine and guanosine nucleotides are both based on purine bases but seem to have the opposite effect on (p)ppGpp^0 when used as a phosphate source. (p)ppGpp inhibits various purine synthesis enzymes (see Section 1.3.3), however the impact of this on catabolism in unclear.

For the pyrimidine based nucleotides the picture is slightly more complex. In the case of cytidine-based (Fig. 4.2.3c) and uridine-based (Fig. 4.2.3d) nucleotides the position of the phosphate groups seemed to influence how the strains could utilise them as phosphate sources. With cytidine-5'-monophosphate and uridine 5'-monophosphate as the phosphate source, the metabolism of the Δ*hflX* strain was impaired compared to the (p)ppGpp^0 strain. The opposite was true with cytidine/uridine-2',3'-cyclic monophosphates and cytidine/uridine-3',5'-cyclic monophosphates. However, this phenotype is not solely based on whether the nucleotide is cyclic or not because cytidine-2'-monophosphate and cytidine-3'-monophosphate also had opposite phenotypes. Whilst all of the adenosine-, guanosine- and cytidine-based nucleotides tested as a phosphate source resulted in a difference in metabolism between the two strains, only 3 of the 5 uridine based nucleotides did (Fig. 4.2.3d).

In *E. coli*, ppGpp inhibits the uptake of purine and pyrimidine molecules through inhibition of phosphoribosyltransferases (Hochstadt-Oze and Cashel, 1972). Adenine phosphoribosyltransferase is inhibited by ppGpp but to a lesser extent than guanine phosphoribosyltransferase and uracil uptake is also more severely inhibited by ppGpp than cytosine uptake (Hochstadt-Oze and Cashel, 1972). If this were the case in *S. aureus* we would expect the (p)ppGpp^0 to have a larger increase in uracil and guanine uptake resulting in more efficient metabolism with uridine and guanosine molecules as phosphorous sources. However, this is not the case, suggesting that the way purine and pyrimidine uptake is regulated in *S. aureus* is different to in *E. coli*.

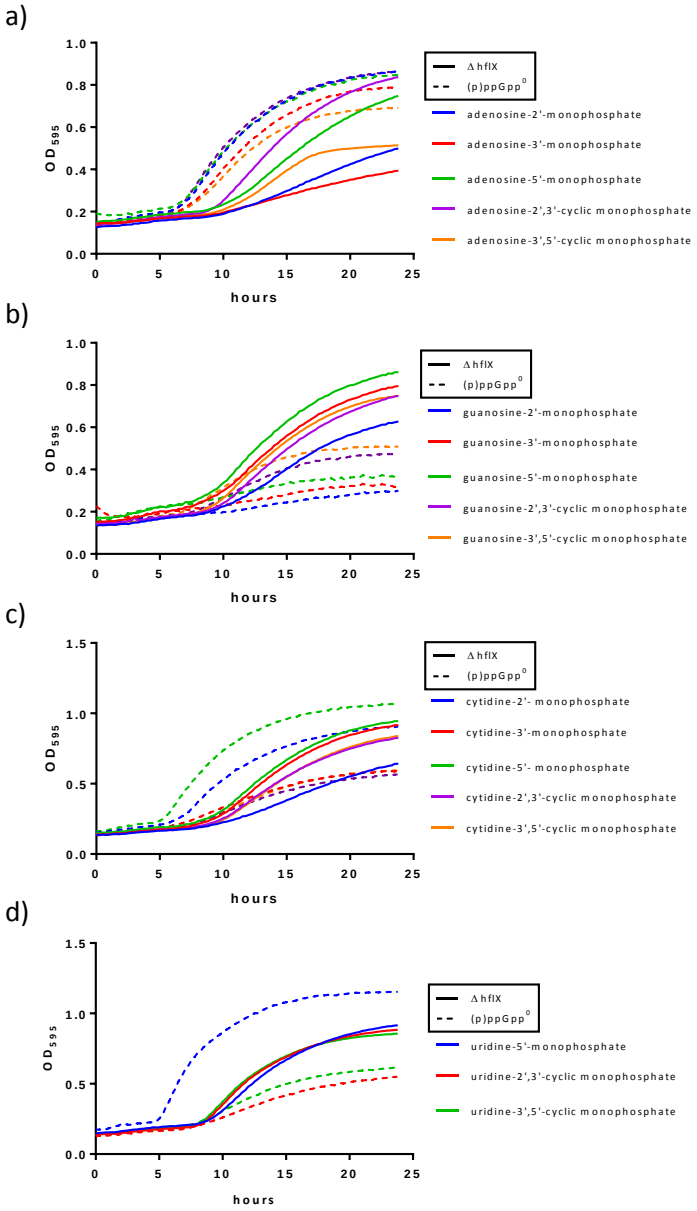

Fig. 4.2.3 Metabolism on Biolog plate PM4A with various phosphorous sources. Metabolism of Δ*hflX* (solid lines) and (p)ppGpp^0 (dashed lines) was recorded over 24 h with OD_{595} readings taken every 15 min. a) Metabolism with various adenosine nucleotides as a phosphorous source. The metabolism of Δ*hflX* was impaired compared to (p)ppGpp^0 with adenosine-2'-monophosphate (blue), adenosine-3'-monophosphate (red), adenosine-5'-monophosphate (green), adenosine-2',3'-cyclic monophosphate (purple) and adenosine-3',5'-cyclic monophosphate (yellow) as a phosphorous source. b) Metabolism with various guanosine nucleotides as a phosphorous source. The metabolism of (p)ppGpp^0 was impaired compared to Δ*hflX* with guanosine-2'-monophosphate (blue), guanosine-3'-monophosphate (red), guanosine-5'-monophosphate (green), guanosine-2',3'-cyclic monophosphate (purple) and guanosine-3',5'-cyclic monophosphate (yellow) as a phosphorous source. c) Metabolism with various cytidine nucleotides as a phosphorous source. The metabolism of Δ*hflX* was impaired compared to (p)ppGpp^0 with cytidine-2'-monophosphate (blue) and cytidine-5'-monophosphate (green) as a phosphorous source. The metabolism of (p)ppGpp^0 was impaired compared to Δ*hflX* with cytidine-3'-monophosphate (red), cytidine-2',3'-cyclic monophosphate (purple) and cytidine-3',5'-cyclic monophosphate (yellow) as a phosphorous source. d) Metabolism with various uridine nucleotides as a phosphorous source. The metabolism of Δ*hflX* was impaired compared to (p)ppGpp^0 with uridine-5'-monophosphate (blue) as a phosphorous source. The metabolism of (p)ppGpp^0 was impaired compared to Δ*hflX* with uridine-2',3'-monophosphate (red), uridine-3',5'-monophosphate (green) as a phosphorous source. Experiments were performed once.

4.2.4 Metabolism with various sulphur sources

The Biolog plate PM4A was also used to identify which sulphur sources could be used by the (p)ppGpp^0 and Δ*hflX* strains. Here, 8 compounds were found to be used by Δ*hflX* more effectively than (p)ppGpp^0 as a sulphur source (Fig. 4.2.4). These were L-cysteic acid, L-cysteine sulfonic acid, N-acetyl-D,L-methionine, L-methionine sulfoxide, L-methionine sulfone, 2-Hydroxyethane sulfonic acid, 2-methane sulfonic acid and tetramethylene sulfone. L-cysteic acid, and L-cysteine sulfonic acid are amino acid derivatives of L-cysteine, which itself was used effectively as a sulphur source by both the (p)ppGpp^0 and Δ*hflX* strains. In the same way, neither strain showed a metabolism defect when grown with L-methionine as a sulphur source, but the (p)ppGpp^0 strain did have a metabolism defect when grown with N-acetly-D,L-methionine, L-methionine sulfoxide, L-methionine sulfone.

There is currently no evidence to show that sulphur starvation triggers the stringent response in bacteria. *S. aureus* can use sulphate, sulphonates, sulphide, thiosulphate, cysteine and cystine as sulphur sources (Soutourina *et al.*, 2009). This ability is not lost in the (p)ppGpp^0 strain suggesting the stringent response is not required for this element of *S. aureus* metabolism. The sulphur containing compounds that resulted in a metabolism defect for (p)ppGpp^0 are not as abundant as the other sulphur sources tested and it is therefore unlikely that the stringent response is involved in sensing or responding to sulphur starvation.

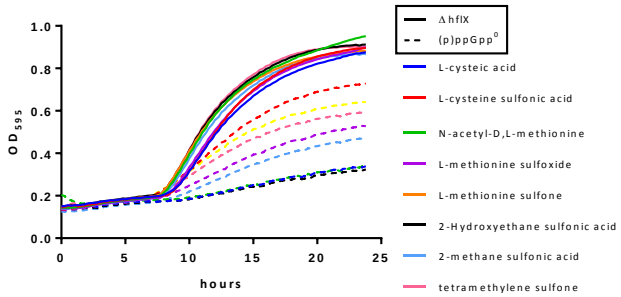

Fig. 4.2.4 Metabolism on Biolog plate PM4A with various sulphur sources. Metabolism of Δ*hflX* (solid lines) and (p)ppGpp^0 (dashed lines) was recorded over 24 h with OD_{595} readings taken every 15 min. The metabolism of (p)ppGpp^0 was impaired compared to Δ*hflX* with L-cysteic acid (blue), L-cysteine sulfonic acid (red), N-acetyl-D,L-methionine (green), L-methionine sulfoxide (purple), L-methionine sulfone (yellow), 2-Hydroxyethane sulfonic acid (black), 2-methane sulfonic acid (light blue) and tetramethylene sulfone (pink) as a sulphur source. Experiment was performed once.

4.2.5 Metabolism with various osmolytes

Finally, PM9 was used to identify how (p)ppGpp^0 and Δ*hflX* strains grew in the presence of various osmolytes. From PM9, the osmolyte sodium lactate was found to reduce the metabolism of the (p)ppGpp^0 strain compared to the *ΔhflX* strain in a dose dependent manner (Fig. 4.2.5a). As the percentage of sodium lactate increased from 1% to 12%, the metabolism of both strains was impaired

but the (p)ppGpp^0 strain showed an increased lag phase and shallower exponential phase curve. However, no other osmolyte affected the metabolism of the (p)ppGpp^0 mutant more than the metabolism of Δ*hflX*, suggesting that the effect seen in the presence of sodium lactate is not due to osmotic stress but a lactate-specific mechanism. This is demonstrated in Fig. 4.2.5b, where NaCl was tested as an osmolyte on PM9 and showed no difference between the two mutants tested even up to 10% NaCl. (p)ppGpp has been shown to help protect *E. coli* from osmotic stress caused by NaCl (Tarusawa *et al.*, 2016) but the results here show that (p)ppGpp is not required for metabolism in up to 10% NaCl in *S. aureus*.

In order to confirm the phenotype seen in Fig. 4.2.5a, the growth of the (p)ppGpp^0 mutants was then compared to that of the WT LAC* strain in TSB supplemented with 10% sodium lactate (Fig. 4.2.5c). A small but repeatable growth defect was seen for the (p)ppGpp^0 mutant compared to the WT after 6 h growth with 10% Na-lactate (p = 0.0349). A slight growth defect was also seen after 8 h growth for (p)ppGpp^0 compared to LAC* grown without Na-lactate (p = 0.0366). The growth defect of the (p)ppGpp^0 strain in 10% Na-lactate is less severe than that seen in Fig. 4.2.5a and this is probably due to the use of TSB medium. TSB is a richer medium than that used for the PM plate with may help the bacteria withstand the high concentration of Na-lactate. This could also explain why there is a long lag phase of around 12 h (Fig. 4.2.5).

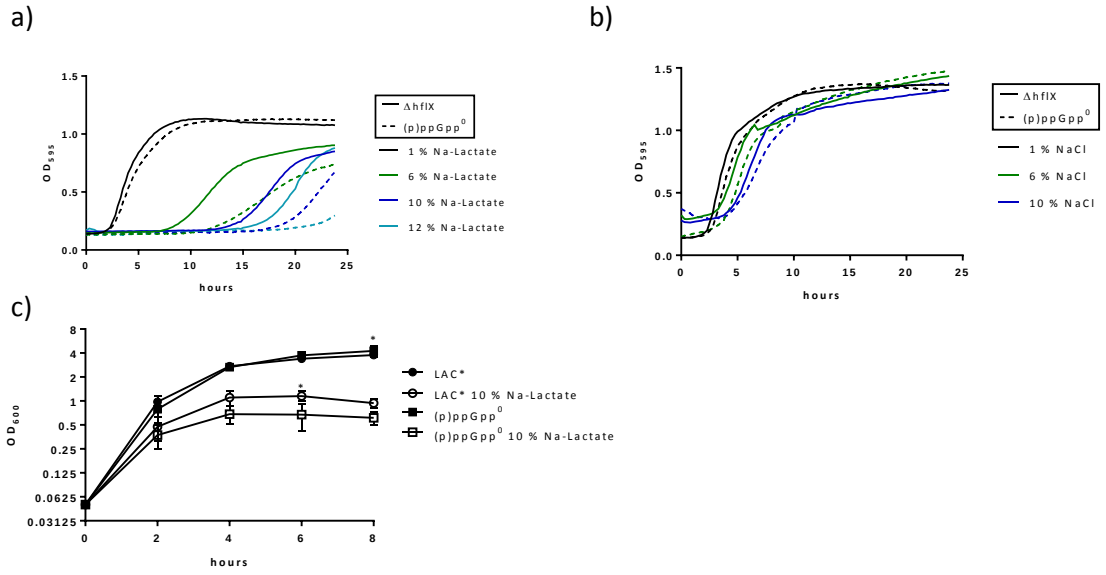

Fig. 4.2.5 Growth and metabolism in the presence of osmolytes. a) Metabolism of Δ*hflX* (solid lines) and (p)ppGpp^0 (dashed line) in PM9 wells F1 (1% Na-lactate; black), F6 (6% Na-lactate; green), F10 (10% Na-lactate; dark blue) and F12 (12% Na-lactate; light blue). b) Metabolism of Δ*hflX* (solid lines) and (p)ppGpp^0 (dashed line) in PM9 wells A1 (1% NaCl; black), A7 (6% NaCl; green) and A12 (10% NaCl; dark blue). c) Growth of LAC* (circles) and (p)ppGpp^0 (squares) in TSB with (unfilled symbols) and without (filled symbols) 10% Na-lactate. Both strains had a growth defect when grown with 10% Na-lactate compared to without but after 6 h (p)ppGpp^0 grew significantly worse than LAC*. Experiments in (a) and (b) were performed once. Experiment in (c) was performed three times, with means and standard deviations plotted. Two-way ANOVA was performed. * $p < 0.05$

4.3 Discussion

Based on the results presented here it is clear that in *S. aureus* the stringent response plays an important role in survival and metabolism during various growth conditions. In total the Biolog PM plates revealed that the (p)ppGpp^0 strain had a metabolism defect when using 52 molecules as either a carbon, nitrogen, phosphorous or sulphur source as effectively as the Δ*hflX* strain. The reverse was true for 11 compounds.

All of the Biolog experiments presented here were only performed once. This means that no statistical analyses could be performed on the data generated and so the results presented should only be interpreted as preliminary. Without repeats of the experiments it is difficult to exclude the possibility of metabolism due to spontaneous mutations in the strains. Repeating the Biolog experiments would also allow the list of conditions that lead to altered metabolism of the strain to be narrowed down following statistical analysis. It would also be important to then compare the (p)ppGpp^0 strain to the WT LAC* strain in order to rule out the effect of the Δ*hflX* mutation, as was done in Fig. 4.2.5c. For conditions in which the *hflX* strain showed a metabolism defect compared to the (p)ppGpp^0 strain, the experiments should be repeated with the WT strain LAC* as a control to rule out any effect the *hflX* mutation has.

Only 8 compounds were found to result in a (p)ppGpp^0 metabolism defect when used as the sole carbon source, whereas 29 compounds were found to effect the metabolism of (p)ppGpp^0 or Δ*hflX* when used as a sole nitrogen source. This suggests that, in general, the stringent response is more important for controlling nitrogen metabolism in *S. aureus* than carbon metabolism. A lot of the genes regulated by CodY are involved in alternate nitrogen metabolism (Sonenshein *et al.*, 2007). During the stringent response the CodY regulon is derepressed resulting in an upregulation of genes involved in nitrogen metabolism. The (p)ppGpp^0 strain may not be able to derepress *codY* as well as the WT or Δ*hflX* strains, which could result in fewer nitrogenous compounds being usable nitrogen sources.

Based on bioinformatics analyses and experimental data it has been predicted that *S. aureus* cannot catabolise 8 amino acids (tryptophan, isoleucine, leucine, lysine, methionine, phenylalanine, tyrosine and valine), even in the absence of glucose as a carbon source (Halsey *et al.*, 2018). However, the results presented here contradict this finding with leucine, lysine, methionine, phenylalanine and valine all successfully used as a carbon source by both the (p)ppGpp^0 and Δ*hflX* strains (Fig. 4.2.1a). Isoleucine was used as a carbon source by Δ*hflX* and although the (p)ppGpp^0 strain had a metabolism defect, it did eventually show some metabolic activity (Fig. 4.2.1a). Tryptophan and tyrosine were not included as carbon sources on either PM1 or PM2A. All of the 8 amino acids without predicted

catabolic pathways were successfully used as nitrogen sources by Δ*hflX*, whilst only lysine and phenylalanine did not result in a metabolism defect with the (p)ppGpp^0 strain (Fig. 4.2.2a).

In conclusion, the stringent response appears to be important for many aspects of metabolism, particularly the use of alternate nitrogen sources. Future work should aim to elucidate whether this regulation occurs on a transcriptional or post-transcriptional level, and whether it is the transport of the nutrients or the catabolic enzymes that are defective in a (p)ppGpp^0 mutant.

Chapter 5 - Protein-protein interactions of (p)ppGpp synthetases

5.1 Introduction

One of the ways the stringent response is regulated is through interaction partners binding to RSH superfamily members to alter their activity (discussed in Section 1.2.3). Currently, little is known about how protein-protein interactions affect the stringent response in Gram positive bacteria.

Evidence is growing that RSH superfamily members often form homooligomers which can influence their activity. RelQ forms homotetramers which are more active than the monomer form of the enzyme (Steinchen *et al.*, 2015). RelP also forms tetramers in *S. aureus* (Manav *et al.*, 2018). Rel proteins from *E. coli* and *M. smegmatis* form dimers which are SYNTHETASE-OFF HYDROLASE-ON (Avarbock *et al.,* 2005; Gropp *et al.*, 2001; Yang *et al.*, 2001).

Aside from oligomerisation, (p)ppGpp synthetase can also be regulated by protein-protein interactions with heterologous proteins. The best characterised Rel interaction partner is the ribosome activating complex (RAC). The RAC is comprised of uncharged tRNA, mRNA and the ribosome itself, representing a stalled ribosome (Avarbock *et al.*, 2000). Binding to the RAC causes the Rel protein to be SYNTHETASE-ON HYDROLASE-OFF, thus triggering the stringent response. Rel binds as a monomer thus halting the inhibition of the dimer form of the protein. Whilst the ribosome is a well characterised activator of the Rel proteins in Gram negative species (Haseltine and Block, 1973), there is no structural evidence of an interaction in Gram positive bacteria. Recently, a co-immunoprecipitation experiment revealed 25 protein interaction partners of Rel_{Sa} (Gratani *et al.* 2018). Of these proteins 12 were ribosomal proteins or translation initiation factors, six were RNA related and seven were DNA related. However, the effect of these interactions was not reported. Interestingly, three of the ribosomal proteins which were shown to interact with Rel_{Sa} (L16, S13 and S12) were also previously shown to interact with Rel_{Ec} (Brown *et al.*, 2016).

The *E. coli* protein SpoT binds to uncharged acyl carrier protein (ACP), which is a cofactor in fatty acid biosynthesis (Butland *et al.*, 2005; Gully *et al.*, 2003). The interaction is mediated through the TGS domain of SpoT and is necessary for (p)ppGpp accumulation during fatty acid starvation (Battesti and Bouveret, 2006). Whilst Gram positive bacteria can trigger the stringent response during fatty acid starvation this response is not mediated through an interaction between ACP and long-RSH proteins (Pulschen *et al.*, 2017). The interaction with ACP only occurs in organisms with two long-RSH proteins (such as *E. coli*; RelA and SpoT) despite the presence of the TGS domain in long-RSH proteins in Gram positive bacteria (Battesti and Bouveret, 2007). This could be due to the fact that the isoelectric point (pI) of SpoT is more basic than other long-RSH proteins, allowing it to bind to the acidic ACP. This example demonstrates that the regulation of the stringent response in Gram negative and Gram

positive bacteria is often very different. It is therefore important to research protein-protein regulation in a Gram positive bacteria, such as *S. aureus*, in order to gain a fuller picture of the stringent response.

The aim of this chapter is to find new (p)ppGpp synthetase interaction partners in *S. aureus* by using targeted and whole genome approaches to ensure a broad reaching screen. Once new binding partners were identified we confirmed the interactions using heterologous and homologous host organisms and *in vitro* techniques. The effect of different conditions and stresses on the binding interactions was investigated in a native *S. aureus* host using the bitLucopt system that was adapted from *Clostridium difficile* for use in *S. aureus*.

5.2 Targeted bacterial two hybrid approach

5.2.1 Targeted bacterial two hybrid between (p)ppGpp synthetases

Initially, we investigated binding between the (p)ppGpp synthetases themselves. To do this, the Bacterial Adenylate Cyclase Two Hybrid (BACTH) system was used (Fig. 5.2.1a). In this system one protein of interest is fused to the T25 domain of adenylate cyclase and another protein is fused to the T18 domain of adenylate cyclase. If the proteins interact then it will bring the two adenylate cyclase domains together allowing production of cAMP. cAMP binds to the Catabolite Activator Protein (CAP), which can then bind to the CAP binding site upstream of the reporter gene *lacZ*, triggering its expression. The reporter strain BTH101 is used as it does not have an active adenylate cyclase (*cya*$^{-}$) due to a mutation at the 99th base pair. This mutation can revert to give a *cya*$^{+}$ phenotype resulting in false positives. Two BACTH vectors (pUT18 or pUT18C and pKT25 or pKNT25) are transformed into BTH101 and expression is induced using IPTG (Fig. 5.2.1b). The four vectors add a T25 or T18 domain to the C or N terminal of the protein of interest, to help reduce the effect of any steric hindrance the tag may have. When the transformed strains are plated on LB agar plates containing 5-bromo-4-chloro-3-indolyl-β-D-galactopyranoside (X-gal), *cya*$^{+}$ colonies will be blue as LacZ can hydrolyse X-gal to produce a blue pigment.

The three (p)ppGpp synthetase genes, *rel*, *relP*, *relQ* where cloned into the BACTH vectors pUT18, pUT18C, pKT25 and pKNT25 by restriction digests and ligation. All combinations of interactions were investigated and a positive control (BTH101 pKT25zip pUT18Czip) and a negative control (BTH101 pKT25 pUT18C) were included (Fig. 5.2.1c). For each repeat of the assay fresh BTH101 cells were transformed to avoid revertants. As expected, based on work in other organisms, both the Rel$_{Sa}$- Rel$_{Sa}$ and RelP-RelP interactions were positive (Fig. 5.2.1c). Rel proteins in *E. coli* and *M. smegmatis* have been shown to form dimers (Avarbock *et al.,* 2005; Gropp *et al.*, 2001; Yang *et al.*, 2001). 4 out of 4 Rel$_{Sa}$-Rel$_{Sa}$ combinations were blue and 3 out of 4 RelP-RelP combinations were blue. RelP was

predicted to form a tetramer based on its homology to RelQ (Steinchen *et al.*, 2015) and this has recently been confirmed in *S. aureus* (Manav *et al.*, 2018). The interaction between Rel_{Sa} and RelP which was observed in 5 out of 8 Rel_{Sa}-RelP has not previously been reported and we are currently unaware of what biological function this interaction might play.

RelQ forms tetramers in *E. faecalis* and *B. subtilis* and the oligomerisation interface is conserved in *S. aureus* (Beljantseva *et* al., 2017; Steinchen *et al.*, 2015). However, no positive phenotype was observed for RelQ-RelQ using the bacterial two hybrid system. This could be due to a lack of expression or due to the T25 or T18 domains sterically hindering any binding. The T18 and T25 tags are 21.8 kDa and 25.6 kDa respectively and so are a similar size to RelP and RelQ (27.2 kDa and 25.2 kDa respectively) but much smaller than Rel_{Sa}. This highlights one of the limitations of the BACTH approach, in that it can result in false negatives.

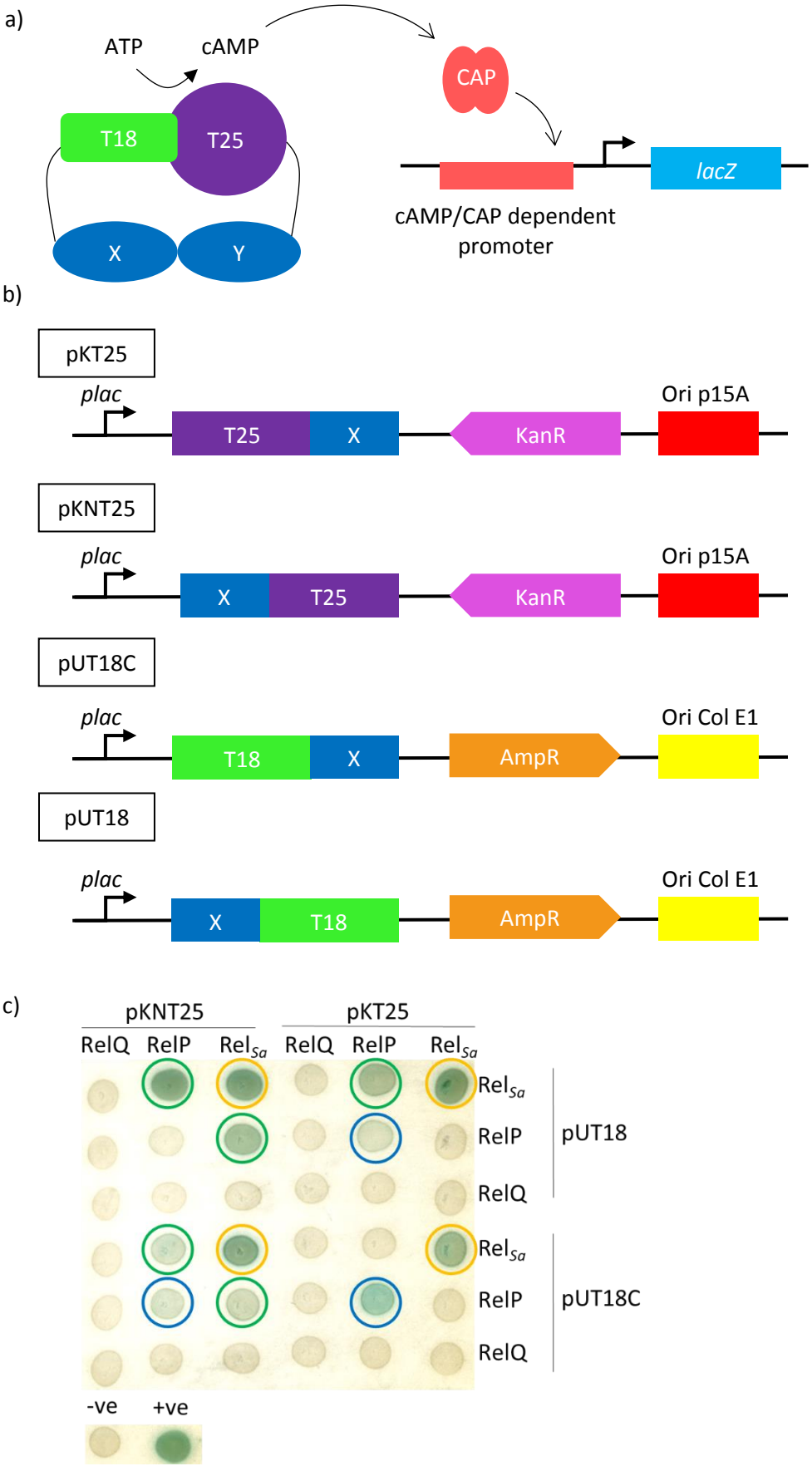
a)
ATP
cAMP
CAP
T18
T25
X
Y
lacZ
cAMP/CAP dependent
promoter
b)
pKT25
plac
T25
X
KanR
Ori p15A
pKNT25
plac
X
T25
KanR
Ori p15A
pUT18C
plac
T18
X
AmpR
Ori Col E1
pUT18
plac
X
T18
AmpR
Ori Col E1
c)
pKNT25
pKT25
RelQ
RelP
RelSa
RelQ
RelP
RelSa
RelSa
RelP
RelQ
pUT18
RelSa
RelP
RelQ
pUT18C
-ve
+ve

Fig. 5.2.1 BACTH between (p)ppGpp synthetases from *S. aureus.* a) schematic diagram of the BACTH system. If proteins X and Y (blue) interact then the T18 (green) and T25 (purple) domains will come together and produce cAMP from ATP. cAMP binds to the CAP protein (pink) which can then activate the transcription of the *lacZ* gene (light blue). b) BACTH vectors: pKT25, pKNT25, pUT18C and pUT18. The protein of interest (X; blue) is fused at the C terminal (pUT18C and pKT25) or the N terminal end (pUT18 and pKNT25) of the T25 (purple) or T18 (green) domains. AmpR (orange) and KanR (pink) genes act as selection marker. pK(N)T25 and pUT18(C) plasmids have an Ori p15A (red) or Ori Col E1 (yellow) origin, respectively. c) BTH101 strains carrying BACTH plasmids spotted on LB agar plates with 150 µg/ml, 30 µg/ml kanamycin, 500 µM IPTG and 40 µg/ml X-gal. Blue colonies are cya^+ and white colonies are cya^-. 4 out of 4 Rel_{Sa}- Rel_{Sa} combinations were blue (circled in orange), 5 out of 8 Rel_{Sa}-RelP combinations were blue (circled in green) and 3 out of 4 RelP-RelP combinations were blue (circled in blue). Representative image of three repeats.

5.2.2 Targeted bacterial two hybrid of Rel_{Sa} domains

In order to narrow down which domains of Rel_{Sa} are responsible for binding to RelP and to Rel_{Sa} itself, four domains of the gene were cloned into the BACTH vectors. The domains chosen were HD (41-187aa), SYNTH (226-357aa), TGS (402-461aa) and ACT (657-736aa) domains based on Pfam domain predictions (Fig. 5.2.2a). Firstly, the pKNT25 based vectors were assayed against the pUT18C and pUT18 vectors (Fig. 5.2.2b). This showed that the interaction between Rel_{Sa} and itself is due to each domain interacting with itself. An ACT-ACT interaction was observed in 2 out of 2 orientations, while HD-HD, SYNTH-SYNTH, and TGS-TGS interactions were seen in 1 out of 2 orientations.

Next, a BACTH assay was performed using the Rel_{Sa} domain pKT25 and pKNT25 vectors against the whole RelP gene in the pUT18 and pUT18C vectors (Fig. 5.2.2c). This suggests that RelP binds to the HD of Rel_{Sa}, which can be seen in 3 out of 4 of the orientations tested. No other interactions were observed using this method.

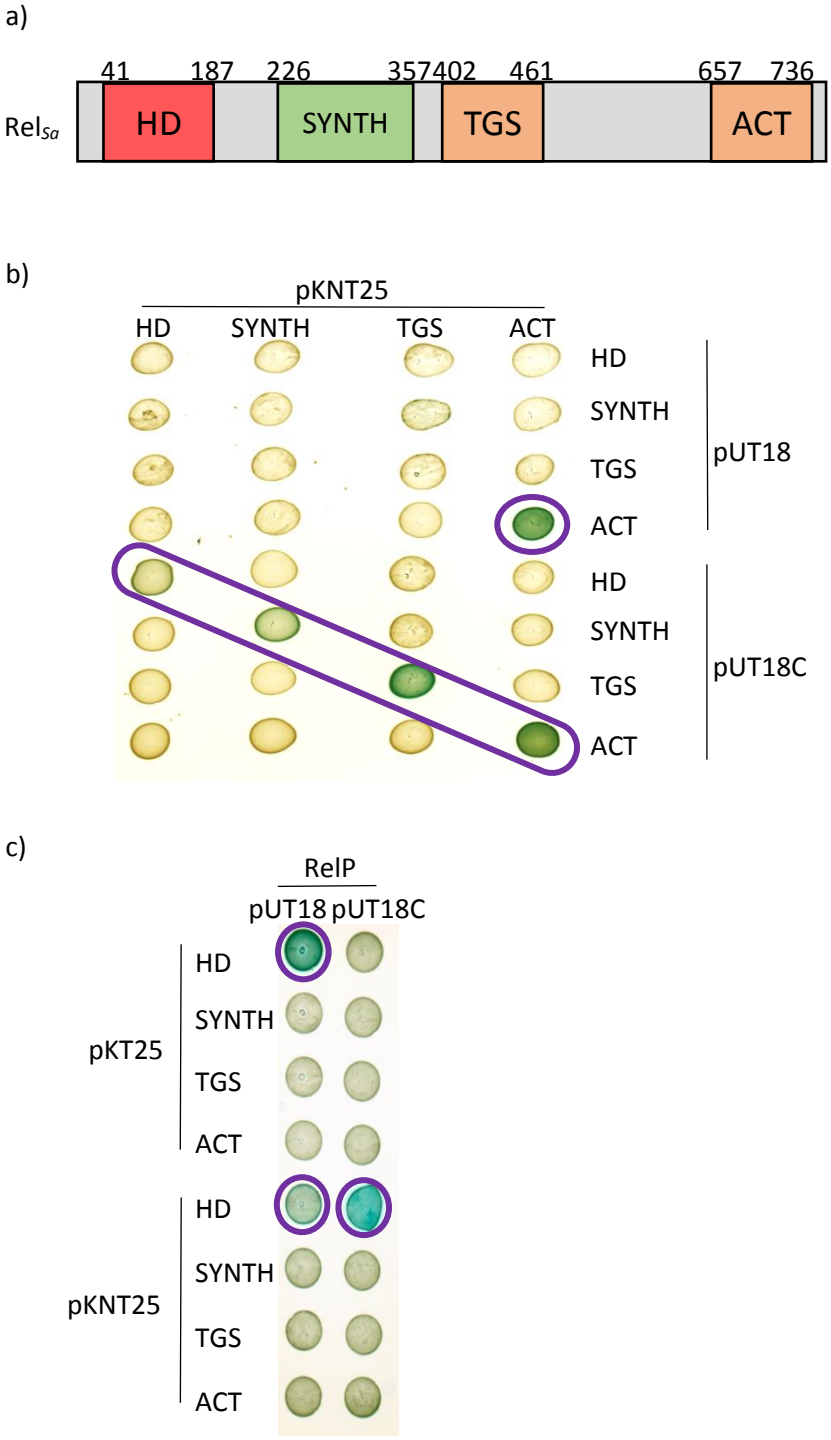

Fig. 5.2.2 BACTH between Rel$_{Sa}$ domains and RelP or Rel$_{Sa}$. a) Domain structure of Rel$_{Sa}$ showing the hydrolase domain (HD; 41-187aa), synthetase domain (SYNTH; 226-357aa), ThrRS, GTPase and SpoT domain (TGS; 402-461aa) and aspartate kinase, chorismate and TyrA domain (ACT; 657-736aa). The segments used in the BACTH vectors are indicated and the numbers refer the amino acid number of the protein. b) BTH101 strains carrying BACTH plasmids spotted on LB agar plates with 150 µg/ml, 30 µg/ml kanamycin, 500 µM IPTG and 40 µg/ml X-gal. Blue colonies are *cya*$^{+}$ (circled in purple) and white colonies are *cya*$^{-}$. An interaction was observed between ACT-ACT (2/2 orientations) and HD-HD, SYNTH-SYNTH, and TGS-TGS (1/2 orientations) c) BTH101 strains carrying BACTH plasmids spotted on LB agar plates with 150 µg/ml, 30 µg/ml kanamycin, 500 µM IPTG and 40 µg/ml X-gal. Blue colonies are *cya*$^{+}$ (circled in purple) and white colonies are *cya*$^{-}$.

5.3 Genome-wide fragment bacterial two hybrid library

In order to search for novel Rel_{Sa} binding protein we wanted to use a genome wide approach in order to increase our chance of success. In order to achieve this, we decided to use a genome fragment library approach. Here, fragments of genomic DNA are randomly inserted into the BACTH vectors to give a library of prey plasmids that can be screened against a bait plasmid containing the gene of interest, and which should cover the whole genome.

5.3.1 Construction of bacterial two hybrid vectors

The genomic fragments used in the library are generated by partial restriction digestion of the genome and so could result in an in frame or out of frame read when ligated into the BACTH vectors. In order to maximise the power of the genome fragment library two new vectors were made, pUT18+1 and pUT18+2, and these were used to build libraries alongside pUT18 and pUT18C (Fig. 5.3.1). Using all four libraries increases the chances of a single random fragment being in frame when inserted into at least one of the BACTH vectors.

pUT18+1 was created by digesting pUT18 with BamHI and KpnI and ligating in a stuffer fragment (*rel*). The stuffer fragment was used so that when the plasmid was digested with SmaI there was an insertion of one base pair in the polylinker region (Fig. 5.3.1a). pUT18+2 was created by digesting pUT18 with Ecl136I and SmaI and religating to remove 10 bps from the polylinker, as previously described (Handford *et al.* 2009) (Fig. 5.3.1b). pUT18+1 has an insertion of one nucleotide that results in a +1 frameshift, whereas pUT18+2 has a 10 bp deletion resulting in a +2 frameshift (Fig. 5.3.1c).

a)

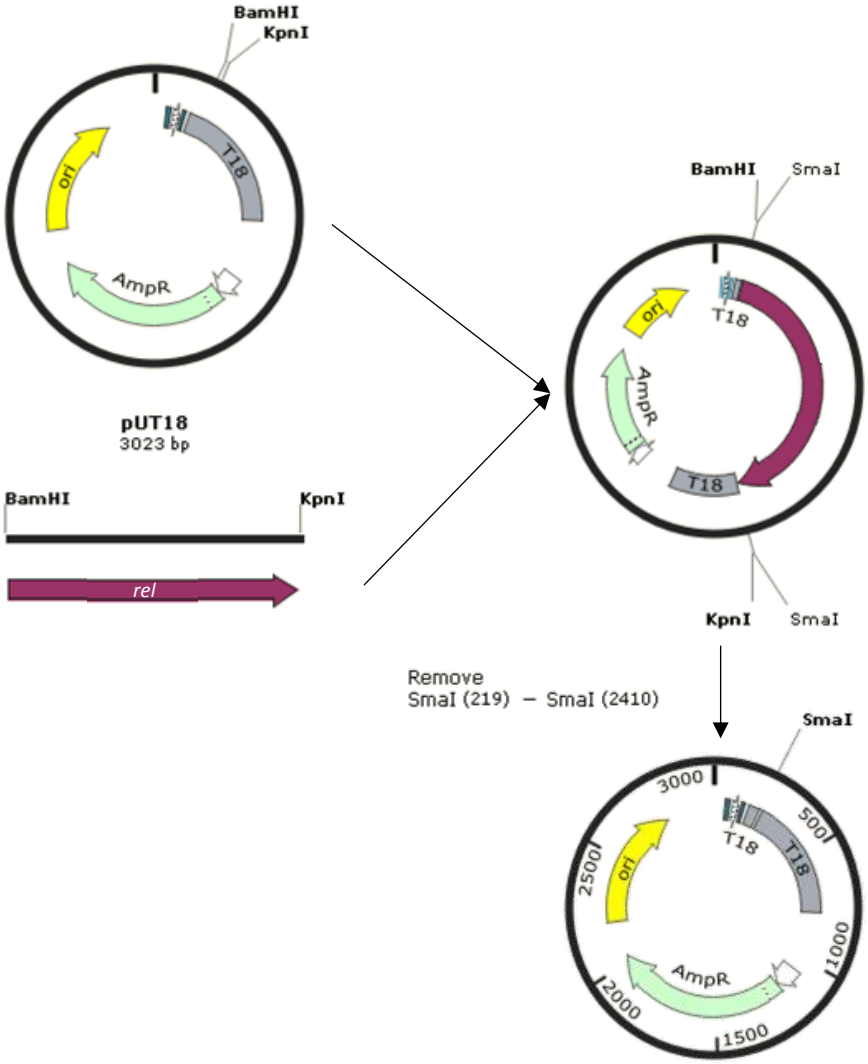

b)

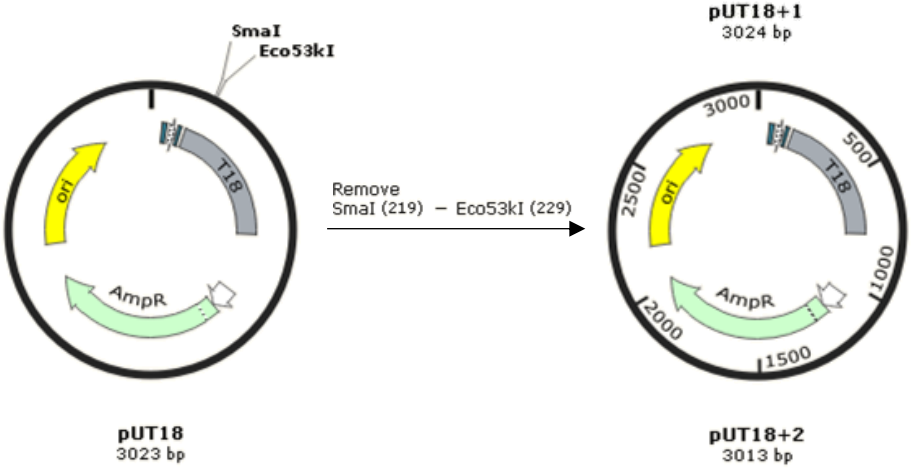

c)

BamHI T18

```
pUT18   TCTAGAGGATCCCC-GGGTACCGAGCTCGAATTCAGCCGCCAGCGAGGCCACGGGCGGCCTGGA
pUT18+1 TCTAGAGGATCCCCGGGGTACCGAGCTCGAATTCAGCCGCCAGCGAGGCCACGGGCGGCCTGGA
pUT18+2 TCTAGAGGATCCCC----------CTCGAATTCAGCCGCCAGCGAGGCCACGGGCGGCCTGGA
```

Fig. 5.3.1 Construction of pUT18+1 and pUT18+2. a) Construction of pUT18+1. pUT18 was digested with BamHI and KpnI and a stuffer fragment (*rel*) was ligated in. This plasmid was then digested with SmaI and religated to add an extra base pair into the polylinker region. b) Construction of pUT18+2. pUT18 was digested with Ecl136I and SmaI to create pUT18+2. c) alignment of pUT18, pUT18+1 and pUT18+2 DNA sequences. BamHI site is highlighted in blue and the first codon of the T18 domain is highlighted in yellow. pUT18+1 has an insertion of one nucleotide whereas pUT18+2 has a 10 bp deletion resulting in a +2 frameshift. Images created using Snapgene.

5.3.2 Construction of genome fragment library

Sau3A1 is a restriction enzyme from *S. aureus* which cleaves DNA at recognition sequence 5'-/GATC-3' sites and with increased efficiency at 5'-/GATCGATC-3' sites. In the *S. aureus* LAC* genome there are 5143 Sau3AI restrictions sites, of which 6 are 5'-/GATCGATC-3' sites. It has been used previously to create genome fragment libraries due to its frequent cutting and the fact that it produces sticky ends that are compatible with BamHI (5'GGATCC-3') cut DNA (Houot *et al.*, 2012). Genomic DNA (gDNA) from *S. aureus* LAC* was partially digested with Sau3AI for 20 minutes and fragments between 0.5 kilobases (kb) and 3 kb were purified by gel extraction. These DNA fragments were ligated with BamHI-cut BACTH vectors (pUT18, pUT18C, pUT18+1 and pUT18+2) and transformed into *E. coli* XL1 Blue cells. This resulted in a library of random gDNA fragments in the vector that could be harvested through a midiprep.

The quality of the libraries was assessed (Table 5.3.2). A subset of colonies were screened by PCR to give the percentage of colonies with inserts. The total number of transformants was divided by this percentage to give an estimate of the number of colonies with genome fragment inserts. The genome coverage was calculated as:

$$\text{genome coverage} = \frac{\mathrm{G} \times \mathrm{i}}{6}$$

where G = genome size (2,809,422) and i = average insert size (1,170), taking into account that the chance a fragment inserts into the plasmid in-frame with the T18 domain is 1/6. The probability of a given fragment being represented in the library in-frame (P_2) was calculated as:

$$P_2 = 1 - (1 - \frac{\mathrm{i}}{G \times 6})^{\mathrm{N}}$$

Where G = genome size (2,809,422), i = average insert size (1,170) and N = the number of colonies with inserts (Houot *et al.*, 2012). The genome coverage and P_2 values of each of the libraries was considered good enough to continue with.

The libraries were then used to transform BTH101 cells which already contained the bait (p)ppGpp synthetases in either the pKT25 or the pKNT25 BACTH vectors. Transformations were plated on MacConkey agar supplemented with 150 µg/ml, 30 µg/ml kanamycin, 500 µM IPTG and 1% maltose.

Only *cya*$^+$ cells can ferment the maltose present, which leads to a decrease in pH which then turns the pH indicator in the MacConkey media bright pink (neutral red). All *cya*$^+$ phenotype colonies were restreaked onto LB agar containing X-gal to confirm the *cya*$^+$ phenotype (blue colonies). These colonies were then checked by colony PCR to ensure that they did contain a fragment of gDNA. Any colonies that did not contain an insert were discarded as they would be *cya*$^+$ due to reversion. The genomic-fragment containing plasmid was then extracted via miniprep and retransformed into a fresh BTH101 background. If the resultant colonies were still *cya*$^+$, then the plasmid was sent for sequencing. The sequence was subsequently checked using the BLAST software to assign it to the genome. Most sequences would result in non-sense reads because they were not in frame with the T18 tag. We hypothesise that these lead to positive phenotypes because the random amino acids just happened to be quite 'sticky'. Hits of this kind were discarded.

Table 5.3.2 Size and quality of genome-wide fragment BACTH libraries

Library	Approximate total no. of clones	Percentage of clones with insert	No. of clones with insert	Genome coverage	P_2
pUT18	19,000	71.2%	13,547	0.94x	0.61
pUT18+1	28,000	78.8%	27,843	1.93x	0.85
pUT18+2	29,000	67.0%	19,430	1.34x	0.74
pUT18C	122,000	76.9%	93,818	6.51x	0.99
Total	198,000	73.5%	154,638	10.73x	0.99

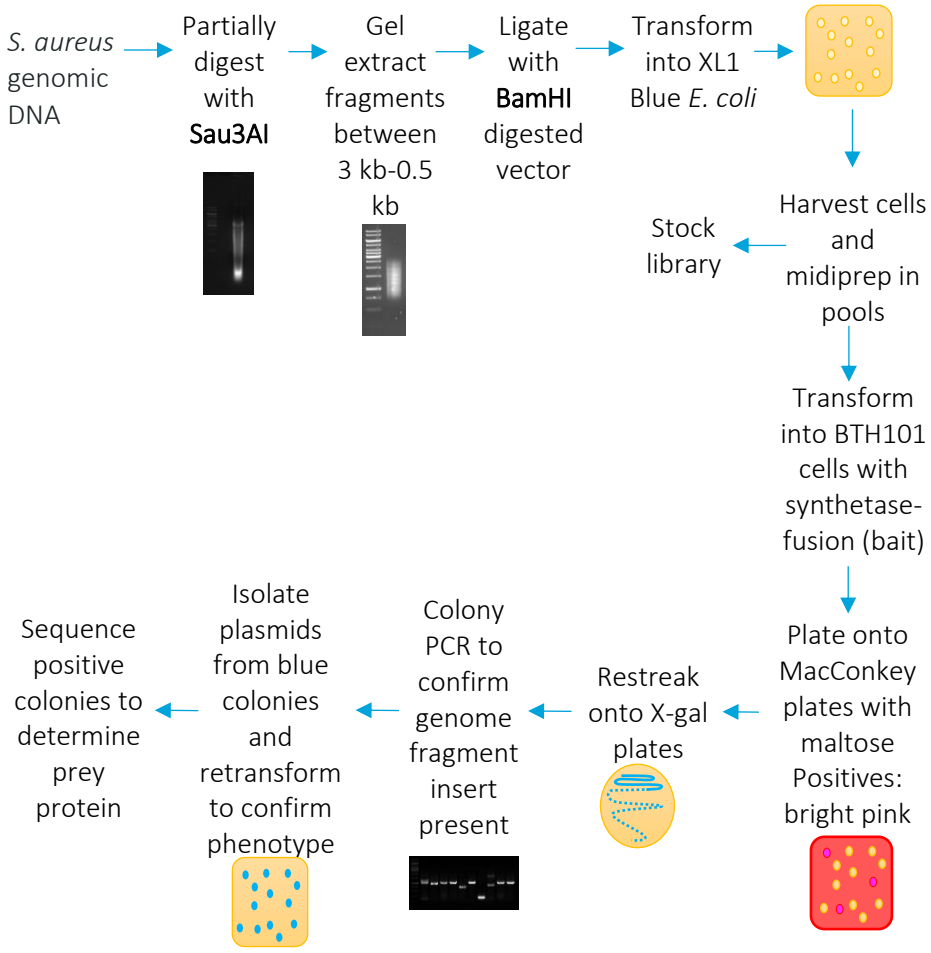

Fig. 5.3.2 Construction of the genome fragment bacterial two hybrid library. Workflow of the screen including construction on the library and the screening process. Genomic DNA from *S. aureus* is digested with Sau3AI and ligated into BamHI cut BACTH vectors. The plasmids are transformed into XL1 Blue *E. coli* cells and then harvested. The library is transformed into BTH101 *E. coli* cells containing the bait BACTH plasmid, before plating on MacConkey agar for selection. Positive colonies were restreaked onto LB agar plates containing 40 µg/ml X-gal. Positives are screened by colony PCR to ensure the library plasmid contains an insert. The plasmid is isolated from positive colonies and retransformed into BTH101 *E. coli* cells containing the bait BACTH plasmid. Positives are then sequenced to identify the genomic fragment in the library.

5.3.3 Interactions of the (p)ppGpp synthetases with the genome fragment library

24 different combinations of library versus bait plasmid were possible but not all were investigated (Table 5.3.3a). 7 different combinations were used, and this resulted in several interesting hits that we chose to follow up on. The hits from screening for Rel_{Sa}, RelP and RelQ interaction partners are listed in Table 5.3.3b. Three unique hits were identified for Rel_{Sa} and six hits were identified for RelP. The Rel_{Sa}-Rel_{Sa} and RelP-RelP interactions pulled out by the screen validated the process because they were already known (Fig. 5.2.1). Genome fragments that contained either the NTD or the CTD of *rel*

were found, corroborating our findings that all the domains of Rel_{Sa} are involved in dimerisation (Fig. 5.2.2).

In addition to Rel_{Sa}, we also identified RocF and CshA as interaction partners of Rel_{Sa}. RocF is an arginase that has been implicated in acid stress survival in *Helicobacter pylori* (McGee *et al.*, 1999). This result was interesting as acidic conditions have previously been shown to induce the stringent response in *H. pylori* (Mouery *et al.*, 2006). CshA is a DEADbox RNA helicase (Kim *et al.*, 2016).

Beyond the RelP-RelP interaction we identified five other RelP interaction partners. The interaction between SraP and RelP seems unlikely to be real, because SraP is located on the cell surface whereas RelP is cytosolic (Siboo *et al.*, 2005). However, SraP must be present in the cytoplasm before it is exported and the interaction could occur if certain stresses prevent proper export of cell wall anchored proteins. 838 nt of the 6816 nt-long *sraP* gene is included in the fragment library meaning that the signal sequence is included but not the cell wall anchoring domain.

The AdhE and transposase (SAUSA300_1309) hits found in the pKT25RelP screen with pUT18+2 were disregarded because they also came up in hits for several different proteins being investigated in the laboratory at the time, suggesting they were unspecific hits. MenA is an enzyme in the biosynthetic pathway of vitamin K_2 (menaquinone) that acts as an electron carrier in the electron transfer chain in bacteria (Meganathan, 2001). RpsA is a 30S ribosomal protein (S1), which binds to and unfolds structured mRNA and is required for translation of most mRNAs in *E. coli* (Duval *et al.*, 2013; Sørensen *et al.,* 1998). This hit is interesting because, although long-RSH protein commonly interact with the ribosome, SASs have not been reported to bind to the ribosome.

No in frame hits were found using the pUT18C library against pKT25RelQ and pKNT25RelQ as bait. This could be for a number of reasons such as that there are no RelQ binding partners in *S. aureus*. Alternatively, any RelQ interactions may not occur in an *E. coli* background or the RelQ-T25 fusions may not be correctly expressed.

Of the hits identified we decided to focus on RocF and CshA. The link between RocF and amino acid metabolism and acid stress was interesting as both are triggers of the stringent response. CshA was also pulled out in a screen for interaction partners of the GTPase Era by Alison Wood in the Corrigan Group.

Table 5.3.3a Library combinations used

	pKT25rel	pKNT25rel	pKT25relP	pKNT25relP	pKT25relQ	pKNT25relQ
pUT18				Yes		
pUT18+1						
pUT18+2			Yes			
pUT18C	Yes	Yes		Yes	Yes	Yes

Table 5.3.3b Hits from genome wide BACTH screen

Bait plasmid	Library	Gene	Locus	Fragment size and gene size	Function
pKT25rel	pUT18C	*cshA*	*SAUSA300_2037*	634-1518 (1518)	DEAD-box RNA helicase
pKNT25rel	pUT18C	*cshA*	*SAUSA300_2037*	634-1518 (1518)	DEAD-box RNA helicase
pKNT25rel	pUT18C	*rel* (NTD)	*SAUSA300_1590*	1-803 (2211)	(p)ppGpp synthetase and hydrolase
pKNT25rel	pUT18C	*rel* (CTD)	*SAUSA300_1590*	1477-2166 (2211)	(p)ppGpp synthetase and hydrolase
pKNT25rel	pUT18C	*rocF*	*SAUSA300_2114*	699-909 (909)	arginase
pKNT25relP	pUT18	*menA*	*SAUSA300_0944*	1-138 (872)	naphthoate octaprenyltransferase
pKNT25relP	pUT18	*relP*	*SAUSA300*_2446	10-693 (693)	(p)ppGpp synthetase
pKNT25relP	pUT18	*rpsA*	*SAUSA300*_1365	1-483 (1176)	30S ribosomal protein S1
pKNT25relP	pUT18	*sraP*	*SAUSA300*_2589	1-838 (6816)	cell wall surface anchor
pKT25relP	pUT18+2	*adhE*	*SAUSA300_0151*	165-2523 (2610)	bifunctional acetaldehyde-CoA/alcohol dehydrogenase
pKT25relP	pUT18+2		*SAUSA300_1309*	180-438 (486)	IS200/IS605 family transposase

5.4 Confirmation and characterisation of Rel_{Sa}-RocF and Rel_{Sa}-CshA interactions

5.4.1 Targeted bacterial two hybrid in *E. coli*

5.4.1.1 Targeted bacterial two hybrid with full length RocF and CshA

Given that the interaction partners pulled out from the screen were from gene fragments, a targeted BACTH approach was performed using the whole gene of interest. Full length *rocF* and *cshA* genes were cloned into the pUT18 and pUT18C vectors, which were then used in a BACTH assay versus the *S. aureus* (p)ppGpp synthetases in the pKT25 and pKNT25 vectors. Rel_{Sa} was included to confirm the interaction pulled out by the screen and RelP and RelQ were included to see if the interaction was specific or applied to all (p)ppGpp synthetases. Both RocF and CshA interacted with Rel_{Sa}, as expected, but did not interact with either RelP or RelQ (Fig. 5.4.1.1a). This result is not surprising as neither RelP nor RelQ have a C terminal regulatory region that has previously been deemed responsible for Rel-protein interactions. In order to narrow down how RocF and CshA bind to Rel_{Sa}, the vectors containing Rel_{Sa} domains discussed in Section 5.2.2 were used in a BACTH assay (Fig. 5.4.1.1b). RocF binds to the HD in 2 out of 4 combinations; to the SYNTH domain in 3 out of 4; to the TGS domain in 3 out of 4; and the ACT domain in 4 out of 4 combinations. CshA binds to the ACT and SYNTH domains of Rel_{Sa} in 1 out of four combinations. These results suggest that RocF and CshA may interact with several points on the Rel_{Sa} protein but this should be confirmed using an *in vitro* method such as a pulldown with truncated Rel_{Sa} protein. We have shown that Rel_{Sa} interacts with CshA, RocF and itself through multiple domains and that the CTD regulatory region is not solely responsible for protein-protein interactions.

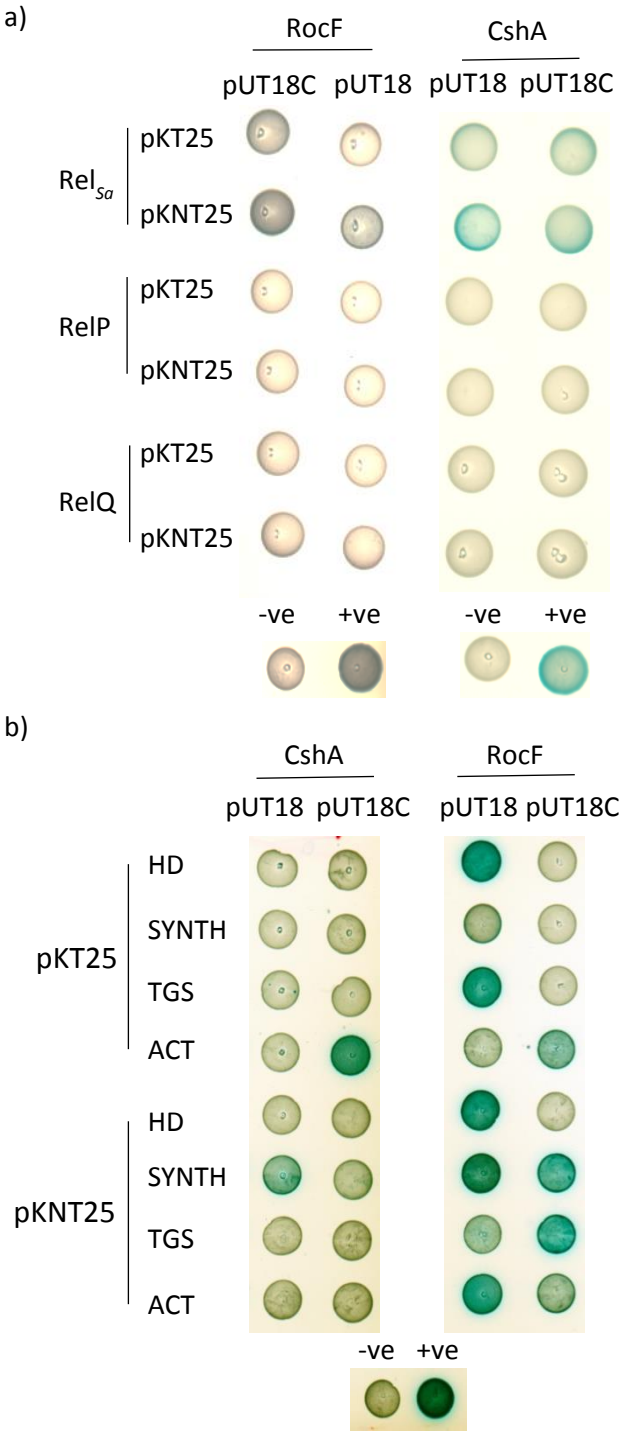

Fig. 5.4.1.1 Targeted BACTH using full length RocF and CshA. BTH101 strains carrying BACTH plasmids spotted on LB agar plates with 150 µg/ml, 30 µg/ml kanamycin, 500 µM IPTG and 40 µg/ml X-gal. Blue colonies are *cya*$^{+}$ and white colonies are *cya*$^{-}$. a) Targeted BACTH using full length RocF and CshA against *S. aureus* (p)ppGpp synthetases. RocF binds to Rel$_{Sa}$ in 3 out of 4 combinations and CshA binds to Rel$_{Sa}$ in 4 out of four combinatons. Neither RocF or CshA bind to RelP or RelQ. Representative image of three repeats. b) Targeted BACTH using full length RocF and CshA against Rel$_{Sa}$ domains. CshA binds to the ACT and SYNTH domains of Rel$_{Sa}$ in 1 out of four combinations. RocF binds to the HD in 2 out of 4 combinations; to the SYNTH domain in 3 out of 4; to the TGS domain in 3 out of 4; and the ACT domain in 4 out of 4 combinations. Representative image of three repeats.

5.4.1.2 Targeted bacterial two hybrid with Era

As mentioned in Section 5.3.3, CshA was also pulled out in a screen for binding partners of Era, performed by A. Wood. Era is a GTPase that is involved in ribosome maturation and its GTPase activity is inhibited by (p)ppGpp (Corrigan *et al.*, 2016). BACTH was used to investigate if Rel_{Sa} interacts with Era as well as CshA. First, full length Rel_{Sa} in pKT25 and pKNT25 was assayed against full length Era in pUT18 and pUT18C (Fig. 5.4.1.2a). Colonies had a *cya*$^{+}$ with 2 out of 4 combinations. Next, the Rel_{Sa} domain BACTH vectors were used to determine which domains of Rel_{Sa} are responsible for binding to Era (Fig. 5.4.1.2b). Era binds to the SYNTH domain in 3 out of 4 combinations; to the TGS domain in 3 out of 4 combinations; and to the ACT domain in 4 out of 4 combinations. However, Era does not bind to the HD of Rel_{Sa}. This suggests that Era binds to Rel_{Sa} through contacts with multiple domains. These results show that Era, CshA and Rel_{Sa} all interact, suggesting they may have a role in coordination of the stringent response or of ribosome maturation. However, it is unclear if they form a complex.

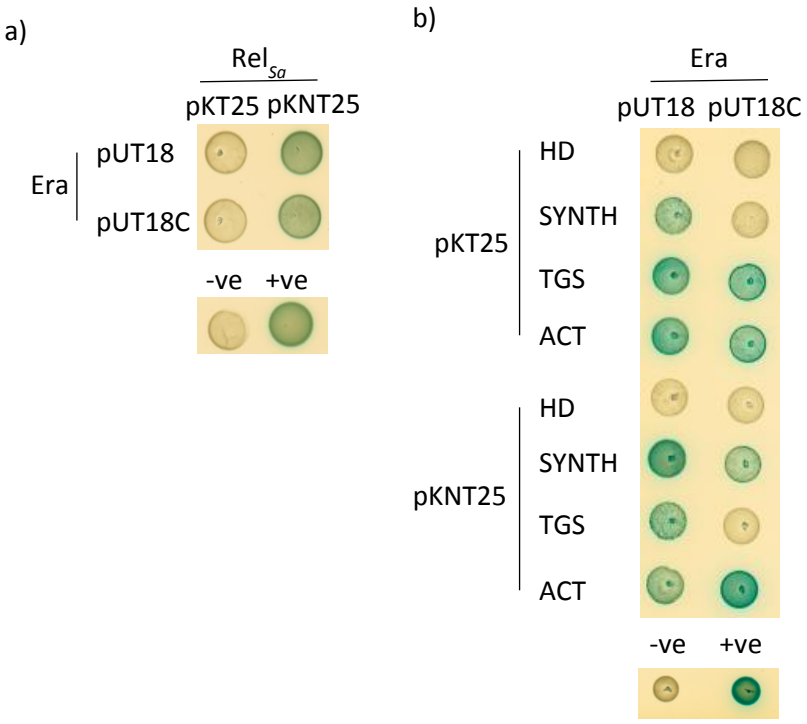

Fig. 5.4.1.2 Targeted bacterial two hybrid with Era BTH101 strains carrying BACTH plasmids spotted on LB agar plates with 150 µg/ml, 30 µg/ml kanamycin, 500 µM IPTG and 40 µg/ml X-gal. Blue colonies are *cya*$^{+}$ and white colonies are *cya*$^{-}$. a) Targeted BACTH using full length Era against Rel_{Sa}. Era binds to Rel_{Sa} in 2 out of 4 combinations. Representative image of three repeats. b) Targeted BACTH using full length Era against Rel_{Sa} domains. Era binds to the SYNTH and TGS domain in 3 out of 4 combinations and to the ACT domain in 4 out of 4 combinations. Representative image of three repeats.

5.4.2 In vitro interaction using GST-tagged pulldown

In order to see if RocF binds to Rel_{Sa} *in vitro* a protein pulldown was performed. Here, glutathione (GSH) tagged Sepharose beads were incubated with RocF-GST, GST, or buffer (beads only) to allow them to bind. The tagged beads were incubated with Rel_{Sa}-MBP-His and with or without ppGpp (Fig. 5.4.2a). After washing the beads, bound protein was eluted using reduced GSH. The eluates were analysed using an anti-His Western blot to identify lanes containing Rel_{Sa}-MBP-His (Fig. 5.4.2b). Bands corresponding to Rel_{Sa}-MBP-His were only present in samples when the beads were tagged with RocF, confirming that Rel_{Sa} does indeed bind to RocF *in vitro.* Quantification of the Western blots showed that Rel_{Sa} bound to RocF significantly more than the beads only and GST controls (p = 0.0092 and p = 0.0104 respectively) (Fig. 5.4.2c). The addition of ppGpp also increased the binding between RocF and Rel_{Sa} compared to Rel_{Sa} alone by 5-fold (p = 0.0003). This suggests that during the stringent response the interaction between Rel_{Sa} and RocF would be stronger.

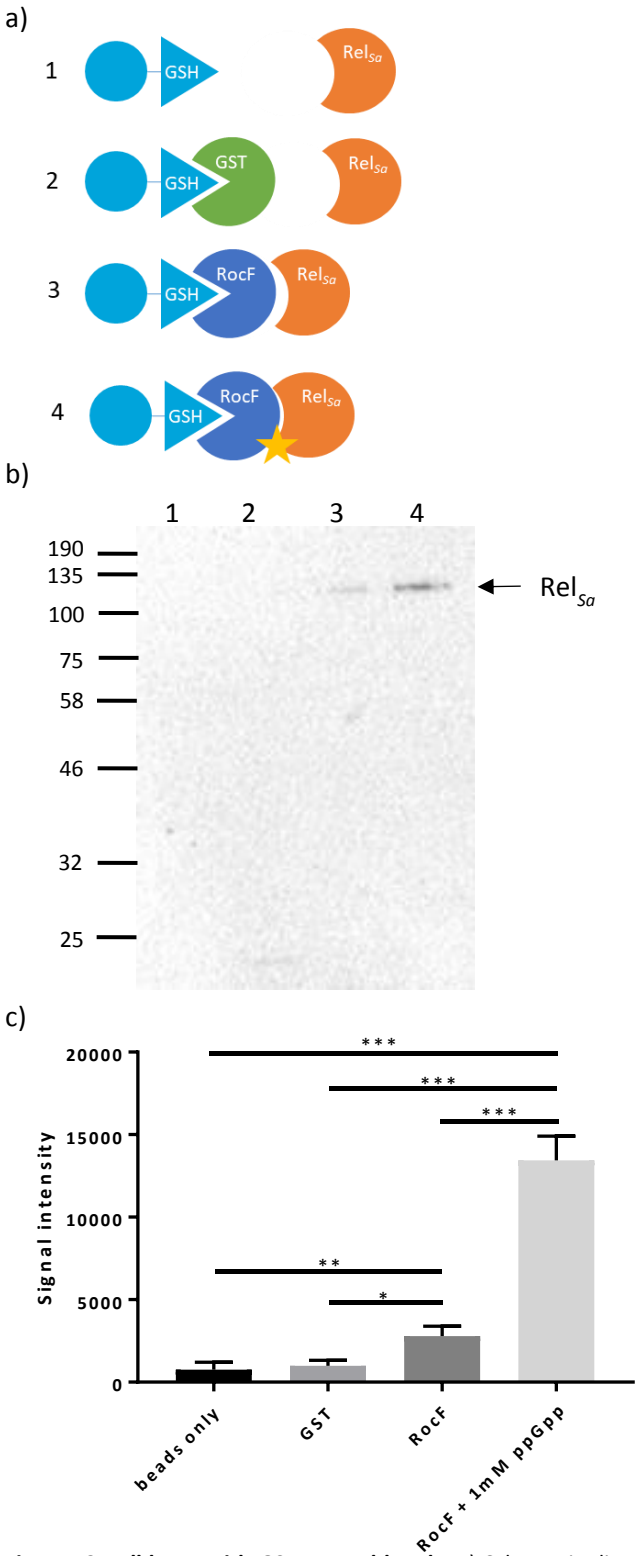

Fig. 5.4.2 Pulldown with GSH-tagged beads. a) Schematic diagram of the pulldown assay. Glutathione (GSH) tagged beads (light blue) is incubated with only buffer (1), GST (green; 2), or RocF (dark blue; 3 and 4). Samples incubated with Rel_{Sa} (orange; 1-3) or Rel_{Sa} and ppGpp (star; 4). b) Representative anti-His Western blot of elutions from the pulldown assay. Protein size ladder represented in KDa with the size of Rel_{Sa} indicated with an arrow. c) Quantification of anti-His Western blots. Rel_{Sa} binds to RocF significantly than the beads only and GST negative controls. The addition of ppGpp significantly increases binding. This experiment was performed three times, with means and standard deviations plotted. Statistical significance tested by unpaired T test * $p < 0.05$; ** $p < 0.01$; *** $p < 0.001$

5.4.3 Using the bitLucopt system to confirm Rel_{Sa} interactions in *S. aureus*

After confirming the Rel_{Sa}-RocF and Rel_{Sa}-CshA interactions in *E. coli*, using a bacterial two hybrid approach, and *in vitro*, using a pulldown technique, we wanted to confirm that the interaction occurs in *S. aureus*. The bitLucopt system was chosen because it allows expression of the tagged proteins in the native host (Oliveira Paiva *et al.,* 2019). The bitLucopt system is similar in principal to the BACTH system in that the proteins of interest are tagged with domains of a protein that come together to form the reporter protein (Fig. 5.4.3a). In the bitLucopt system the reporter is luciferase, which converts furimazine to luminescent furimamide which can be measured by determining the luminescence of the sample. The main difference between the two systems is that in the bitLucopt system the two proteins and their tags are expressed from the same plasmid, meaning that the copy number of the two genes is the same (Fig. 5.4.3b). In the BACTH system the copy number of the pUT18 and pUT18C plasmids is higher than that of the pKT25 and pKNT25 plasmids and so in instances where the T18-fusion protein can form dimers the T25-T18 interaction could be overpowered by fruitless T18-T18 interactions. Whilst having the same gene copy number in the bitLucopt system may help with this problem, it does not guarantee that both genes are expressed equally. The plasmids pAP118 (interacting plasmid; Addgene: 105459), pAF257 (negative control plasmid; Addgene: 105497), and pAF259 (positive control plasmid; Addgene: 105494) were modified by restriction cloning to generate plasmids shown in Fig. 5.4.2b. bitLucopt vectors were first transformed into *S. aureus* strain RN4220 before being re-isolated and transformed into the *S. aureus* strain LAC*. The strains were then tested for luciferase activity (LU) which is given through the raw luminescence readings. All three constructs tested (pAP118*relrel*, pAP118*relrocF*, and pAP118*relcshA*) had a significantly higher luciferase activity compared to their control (pAF257*rel*, pAF257*rocF*, and pAF257*cshA* respectively) (Fig. 5.4.3c). Interestingly, only the Rel_{Sa}-Rel_{Sa} interaction resulted in luciferase activity that was comparable to the positive control of pAF259, suggesting that this interaction is the strongest of the three. These results confirm that the Rel_{Sa}-RocF and Rel_{Sa}-CshA interactions pulled out by the whole genome screen do indeed occur in a *S. aureus* background, as does the Rel_{Sa}-Rel_{Sa} interaction demonstrated using a targeted BACTH approach.

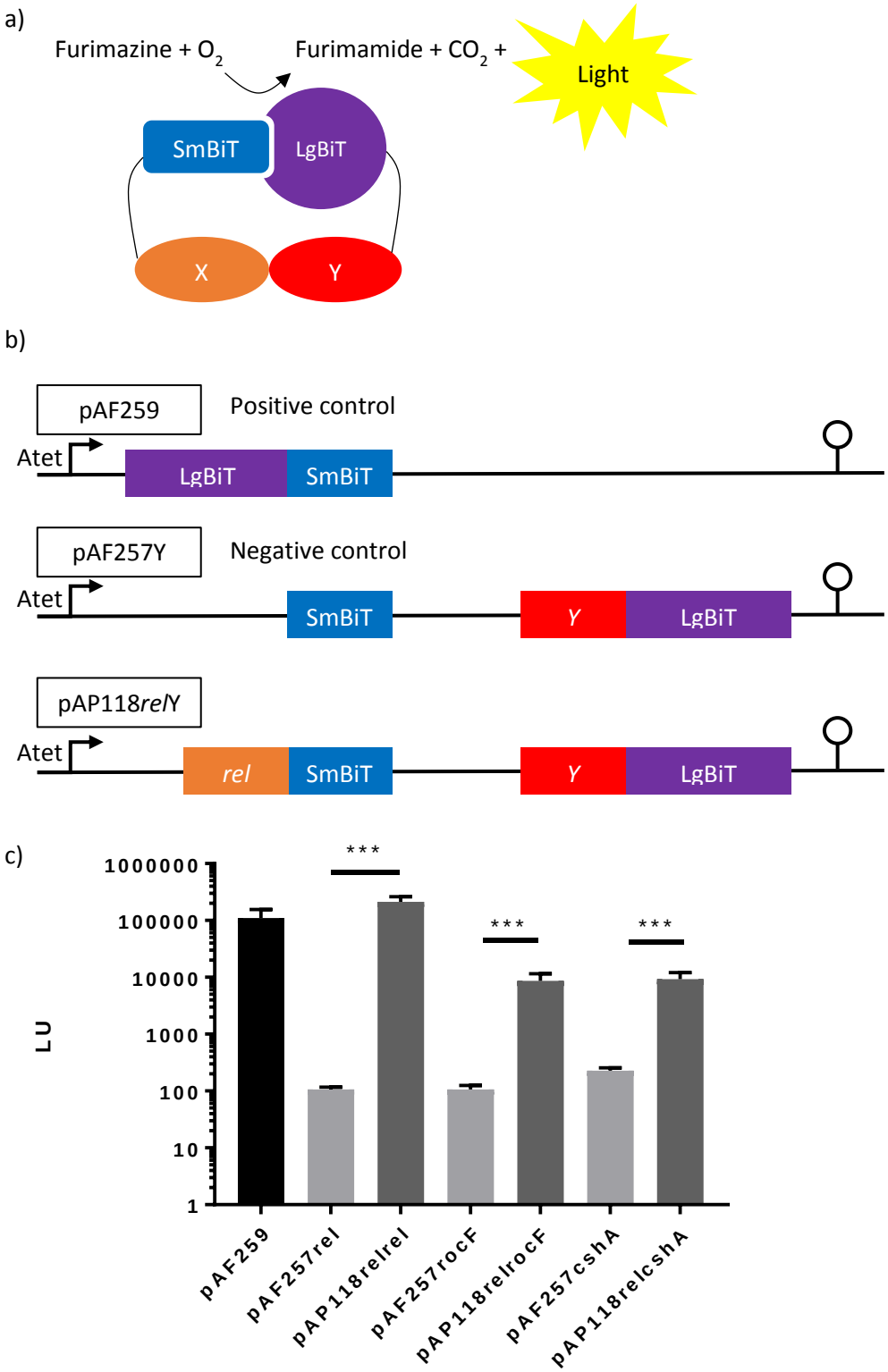

Fig. 5.4.3 Using the bitLucopt system in *S. aureus* to confirm Rel$_{Sa}$ interactions. a) Schematic diagram of the bitLucopt system. Proteins of interest, X (orange) and Y (red) are tagged with domains of luciferase, SmBiT (blue) and LgBiT (purple) respectively. If X and Y interact, SmBiT and LgBiT will come together to form a functional luciferase. The luciferase substrate furimazine is converted into the luminescent furimamide. b) Plasmid constructs used in bitLucopt assays. pAP259 encodes the intact luciferase gene. pAF257Y and pAP118relY represent pAF257rel/pAF257rocF/pAF257cshA and pAP118relrel/pAP118relrocF/pAP118relcshA, respectively, where Y (red) is either *rel, rocF* or *cshA*. c) Luciferase assay to investigate Rel$_{Sa}$ interactions. Expression was induced with 100 ng/ml Atet for 1.5 h. The luciferase activity was significantly higher for strains containing pAP118relrel, pAP118relrocF, and pAP118relcshA than those containing pAF257rel, pAF257rocF, and pAF257cshA. This experiment was performed four times, with means and standard deviations plotted. Statistical significance tested by unpaired T test *** $p < 0.001$

5.5 Discussion

In this chapter we aimed to provide insight into binding partners of the (p)ppGpp synthetases in *S. aureus*. Initially, we confirmed self-interactions reported in other organisms (Rel_{Sa}- Rel_{Sa} and RelP-RelP) and showed a new interaction between Rel_{Sa} and RelP. In order to expand the search for binding partners we set up a genome-wide fragment library to screen for binding partners using BACTH. With this, we identified 2 potential binding partners of both RelP (MenA, RpsA) and Rel_{Sa} (RocF and CshA). An interaction between Rel_{Sa} and Era was also confirmed. Using BACTH and bitLucopt, we confirmed the interaction between Rel_{Sa} and both RocF and CshA *in vivo* and the RocF-Rel_{Sa} was additionally confirmed *in vitro* using a pulldown assay. We were able to begin to investigate how Rel_{Sa} binds to its partners by using Rel_{Sa} domains in the BACTH vectors.

The BACTH system is used extensively here, and so it is important to bear in mind some of its limitations. Firstly, the reporter strain BTH101 is *cya*$^-$ due to a mutation at bp 99 in the gene and so it is not a clean knockout. This means the strain can revert through random mutagenesis, resulting in false positives, although at a low frequency. The impact of this was minimised by performing fresh transformations for each of the three repeats of a targeted BACTH assay. In the library screen, positives were retransformed into a fresh BTH101 background to rule out the effect of reversion before they were sequenced.

Another limitation of this technique is the prevalence of false negative results. This is seen in Section 5.2.1 when no RelQ-RelQ interaction was observed, despite RelQ forming a tetramer *in vivo*. This could be due to poor expression of the tagged proteins or steric hindrance of the tags themselves. Using different combinations of N and C terminal T25 and T18 tags helps reduce the likelihood of false negatives. Most of the interactions shown using BACTH here were not positive in all combinations used, which highlights the impact of the tag.

The genome fragment library screen used here has many benefits but has some limitations. Although theoretically it covers the genome there will be some genes that are missed; for example, here, Rel_{Sa}-RelP and Rel_{Sa}-Era interactions were not pulled out by the screen. This is because some genes will contain too many or too few Sau3AI sites, resulting in fragments which are too short to interact or that were excluded when only fragments between 0.5 kb and 3 kb were used. In some cases, a gene may be included in the fragment but will include the 3' end of the upstream gene. This would result in termination before the gene and the T18 tag. In order to find other hits a library could be made using NheI cut fragments with XbaI cut vectors to make the gDNA fragment library. This would change the fragments represented in the library and may uncover new hits.

Not all combinations of library/bait vectors were investigated because promising hits were pulled out (e.g. Rel_{Sa}-RocF). Trying all combinations may lead to pulling out even more hits from the library. The library can also be used to look for other interaction partners of proteins other than Rel_{Sa}, RelP and RelQ in the future. This would simply require making the pKT25 and pKNT25 vectors with the protein of interest and transforming them into BTH101 cells. A large amount of library DNA was produced and so this is a useful tool in the laboratory for future screens.

Another method to look for novel interaction partners would be to use a co-immunoprecipitation. Co-immunoprecipitation has been used to find Rel_{Sa} binding partners previously (Gratani *et al*. 2018). Pleasingly, CshA was pulled out by co-immunoprecipitation as a Rel_{Sa} interacting protein, adding weight to the results presented here. This co-immunoprecipitation approach also pulled out many ribosomal proteins and enzymes involved in DNA and RNA processing that were not found using our BACTH screen. The advantage of co-immunoprecipitation technique over the genome fragment BACTH library approach is that it can pull out protein interaction partners that need to be in a complex to interact because *S. aureus* lysates are used, and so all the native protein will be present.

Here, we show that the bitLucopt system that was developed in *C. difficile* can be used in *S. aureus* to investigate interactions between proteins. This should prove a useful tool to investigate binding partners in the native host, where conditions for certain interactions maybe be preferential. The Rel_{Sa} interactions with RocF, CshA and itself were all confirmed in the native host, indicating that the BACTH system in *E. coli* can be used to investigate binding partners from other species.

The interaction between RelP and Rel_{Sa} has only been shown in *E. coli* and should be confirmed using at least one more method beyond BACTH. Once it is confirmed, the impact of the interaction on the enzymatic activity of each of the protein should be investigated. It may be that Rel_{Sa}-RelP binding inhibits RelP tetramerisation, therefore inhibiting its (p)ppGpp synthetase activity. Another possibility is that RelP binding to the HD domain of Rel_{Sa} inhibits the hydrolase activity of Rel_{Sa} resulting in an increase in (p)ppGpp. It would also be interesting to follow up on the RelP-MenA and RelP-RpsA interactions identified by the screen, after confirming them using another technique. The *rpsA* gene encodes ribosomal subunit S1 and its transcription is negatively regulated in the presence of ppGpp (Kajitani and Ishihama, 1984). In *S. aureus*, the transcription of *rpsA* is not affected during the stringent response, but the transcription of many other ribosomal subunit genes is downregulated, resulting in a reduction in translation (Geiger *et al.*, 2012). Perhaps, RelP binding to S1 is another way to reduce ribosome maturation and translation during the stringent response. Interestingly, ribosomal protein S1 was not found to bind Rel_{Sa} in a co-immunoprecipitation (Gratani *et al.*, 2018). The RelP-MenA interaction could play role in regulating the production of reactive oxygen species (ROS). In *E. faecalis*,

a (p)ppGpp^0 mutant shows increased ROS production (Gaca *et al.*, 2013). In *E. faecalis*, ROS can be produced by the incomplete reduction of dimethylmenaquinone (Huycke *et al.,* 2001). MenA catalyses the production of dimethylmenaquinone and RelP binding could regulate ROS production.

The Rel$_{Sa}$-CshA, Rel$_{Sa}$-Era and Era-CshA interactions discussed here were investigated further by other members of the Corrigan group (Wood *et al.*, 2018). They found that Era and CshA mutants had a significant increase in ppGpp production compared to the WT following cold shock at 25°C for 1 h. This suggests that the Rel$_{Sa}$-mediated stringent response to cold shock is regulated by Era and CshA. They also saw that, compared to the WT strain, a *rel$_{syn}$* mutant had many additional bands in an rRNA profile after triggering the stringent response with mupirocin at 25°C. These bands correspond to degradation or processing intermediates of the 16S or 23S rRNAs. This suggests that without a functional stringent response, Era and CshA cannot effectively process rRNA during stress conditions.

Aside from the Rel$_{Sa}$-Rel$_{Sa}$ and Rel$_{Sa}$-CshA interactions, no other previously reported RSH superfamily binding partners were found here. For example, no ribosomal proteins were found to interact with Rel$_{Sa}$. ACP and ObgE bind to SpoT in *E. coli* but were not identified as Rel$_{Sa}$, RelP or RelQ binding partners here (Seyfzadeh *et al.,* 1993; Wout *et al.*, 2004). Furthermore, the Rel$_{Bs}$ binding partner ComGA was also not identified as a RSH superfamily binding partner by the BACTH screen (Hahn *et al.*, 2015). Using a targeted BACTH approach may help to determine if these interactions are conserved in *S. aureus*.

The interactions discussed here are not exhaustive and other interaction partners of (p)ppGpp synthetases in *S. aureus* are yet to be discovered. A detailed understanding of the interactions of Rel$_{Sa}$, RelP and RelQ will be vital to understanding the regulation of the stringent response. In the next chapter, we focus on characterising the interaction between Rel$_{Sa}$ and RocF.

Chapter 6 - Characterisation of Rel_{Sa}-RocF interaction

6.1 Introduction

Following confirmation of the Rel_{Sa}-RocF interaction by *in vivo* and *in vitro* methods, the next step was to investigate the biological significance of this interaction and to understand any role RocF plays in the stringent response. A limited number of long-RSH interaction partners are known, of which the ribosome is the best characterised (discussed in Section 1.2.3). All characterised long-RSH interaction partners act to alter the hydrolase or synthetase activity of the protein. For bi-functional enzymes this involves a change between the two opposing enzymatic activities and for mono-functional enzymes it entails an augmentation of synthetase activity. In order to avoid a futile cycle, bi-functional long-RSH enzymes act as a switch, either HYDROLASE-ON SYNTHETASE-OFF or HYDROLASE-OFF SYNTHETASE-ON. Although there are currently no examples of long-RSH altering the activity of an interacting partner, the possibility that Rel_{Sa} modulates RocF activity, and vice-versa, was investigated.

The CTD of long-RSH proteins is important for regulation of the proteins and is sometimes referred to as the C-terminal regulatory region. In this study, we have used BACTH to show that RocF binds to the ACT domain of Rel_{Sa} (Fig. 5.4.1.1b). Recent work has shown that the ACT domain of the *Rhodobacter capsulatus* long-RSH protein, Rel, is regulated by BCCAs (Fang and Bauer, 2018). Isoleucine and valine bind to the ACT domain and stimulate the hydrolase activity of the enzyme. This level of regulation would ensure that the enzyme is in the HYDROLASE-ON SYNTHETASE-OFF state when intracellular amino acid levels are high. Long-RSH proteins from different species show different BCCA binding affinities (Fang and Bauer, 2018). We hypothesised that amino acid binding by the ACT domain is not limited to BCAAs. Given the arginase activity of RocF, looking at L-arginine binding was the obvious place to start to better understand the role of the ACT domain in Rel_{Sa}.

In this chapter, we investigate (p)ppGpp binding to RocF and L-arginine binding to Rel_{Sa} using a Differential Radial Capillary Action of Ligand Assay. The effect of Rel_{Sa} on RocF activity and vice versa was investigated, as well as the effect of other proteins and ligands that are of interest based on previous work presented in this study. All of this work sought to elucidate the role of RocF and Rel_{Sa} in the stringent response.

6.2 (p)ppGpp binding of RocF

As Rel_{Sa} interacts with RocF, we sought to determine if RocF binds to (p)ppGpp using DRaCALA (Fig. 6.2c). Radiolabelled ppGpp and pppGpp were synthesised enzymatically from α-^{32}P GTP (Fig. 6.2a and 6.2b). This labelled ligand was incubated with 10 µM protein for 5 min and then spotted onto a nitrocellulose membrane. The hydrophobic protein will remain at the centre of the spot and unbound

hydrophilic ligand is free to diffuse outward. If the ligand binds to the protein it will remain in the centre of the spot, appearing as a dark centre. As the RocF protein was tagged with GST to enable purification, purified GST was used as a negative control. The ribosome associated GTPase RsgA was used as a positive control as it has been shown to bind to both ppGpp and pppGpp using DRaCALA (Corrigan *et al*. 2016). The fraction of ligand bound to the protein can be calculated using densitometry (Fig. 6.2d). No significant difference in binding of either ppGpp or pppGpp was seen between RocF and GST, showing that RocF does not bind to (p)ppGpp in these conditions. The positive control, RsgA bound significantly to both ppGpp and pppGpp ($p < 0.0001$ and $p = 0.0126$ respectively).

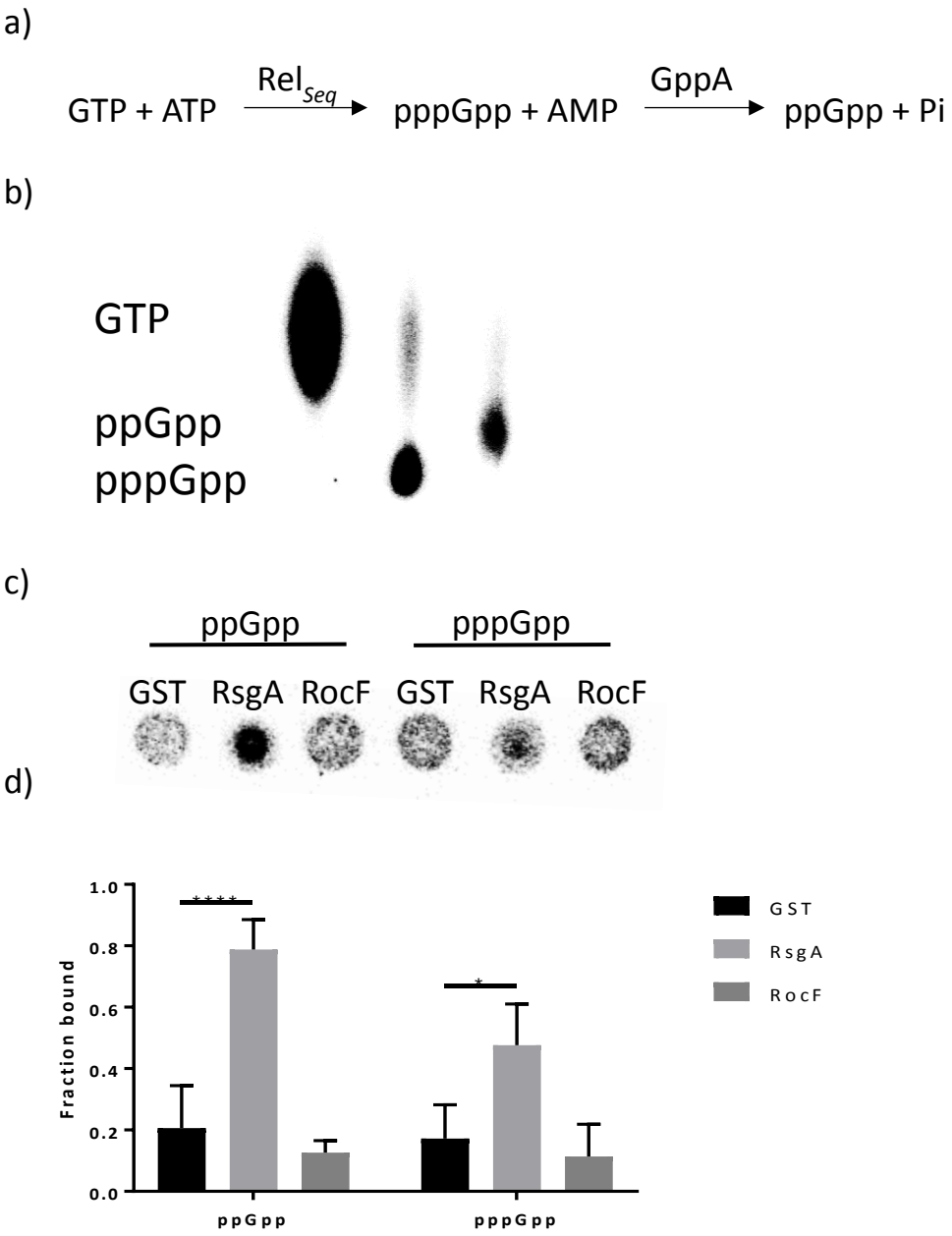

Figure 6.2 DRaCALA and quantification of GST, RocF and RsgA binding to (p)ppGpp. a) Synthesis reaction equation used to make (p)ppGpp. Rel$_{Seq}$ produces pppGpp and AMP from GTP and ATP. GppA hydrolyses pppGpp to produce ppGpp and inorganic phosphate (Pi) b) TLC to calculate percentage conversion to (p)ppGpp. Lane 1 GTP; Lane 2 pppGpp (following incubation with Rel$_{Seq}$); Lane 3 ppGpp (following incubation with GppA) c) Representative image of DRaCALA from four repeats. No interaction is seen with GST and RocF spots with either ppGpp (left) or pppGpp (right). RsgA positive control interacts with both ppGpp and pppGpp. d) Quantification of DRaCALAs. RocF (dark grey) shows no significant binding to (p)ppGpp compared to GST (black). RsgA (light grey) binds significantly to ppGpp and pppGpp. This experiment was performed four times, with means and standard deviations plotted. Statistical significance tested by multiple T tests * $p < 0.05$; **** $p < 0.0001$

6.3 Arginine binding of Rel$_{Sa}$

The ACT domain in the CTD of long-RSH proteins has been shown by recent cryo-EM structures to interact with double stranded rRNA (Arenz et al., 2016; Brown et al., 2016; Loveland et al. 2016). This led to it being referred to as an RNA Recognition Motif (RRM). ACT domains and RRMs share the same

topology, with four anti-parallel β-strands and two α-helices arranged in βαββαβ fold. ACT domains coordinate small ligands in the interface between two β-sheets formed upon dimerisation. A common ligand of ACT domains is serine, however a wide range of amino acids and small ligands such as nickel and thiamine have been shown to bind ACT domains (Grant, 2006). Recently, the ACT domains of long-RSH proteins were shown to bind BCAAs (Fang and Bauer, 2018). BCAA binding was not universal across long-RSH proteins from different species. 7/13 of the CTDs investigated showed no binding to any BCAA. The CTD of Rel_{Sa} bound to leucine with a K_d of 309 µM but did not bind to valine or isoleucine (Fang and Bauer, 2018).

Only BCAA binding was investigated by Fang and Bauer and so based on the interaction observed between Rel_{Sa} and the arginase RocF, we decided to investigate if Rel_{Sa} binds to arginine. A DRaCALA was performed as described in Section 6.2 but with fluorescently labelled arginine (dansyl-arginine) instead of radiolabelled ligand (Fig. 6.3a). A fluorescently labelled ligand has been used in a DRaCALA previously (Fang et al., 2014), and radiolabelled amino acids have also been used (Behr *et al.,* 2017; Bracher *et al.* 2016). First, binding to Rel_{Sa} was determined with RocF included as a positive control and GST and MBP used as negative controls for RocF-GST and Rel_{Sa}–MBP respectively. As expected, significant arginine binding was seen to RocF compared to the GST control (p = 0.0173), confirming the assay could be used to identify proteins that bind to arginine. Rel_{Sa} also bound to arginine significantly compared to the MBP control (p = 0.0028). RelP was also included to see if any arginine binding observed is specific to Rel_{Sa} and not all (p)ppGpp synthetases. RelP did not bind to arginine compared to the buffer control; this is to be expected as RelP does not contain an ACT domain, or indeed any CTD regulatory region, which we hypothesise to be responsible for arginine binding in Rel_{Sa}. In order to confirm that binding to dansyl-arginine was due to arginine binding and not to an unspecific reaction to the fluorescent tag, binding was competed with unlabelled L-arginine at a 10-fold excess (Fig. 6.3b). If the binding is specific to arginine then unlabelled arginine should be able to bind to the protein, resulting in a decrease in the fraction of dansyl-arginine bound. Indeed, unlabelled L-arginine was able to compete with dansyl-arginine binding of both RocF and Rel_{Sa} (p = 0.0054 and p < 0.0001 respectively). As expected, there was no significant reduction in dansyl-arginine binding for RelP when competed with unlabelled L-arginine because RelP does not bind to dansyl-arginine. Finally, the ability of other amino acids to compete with dansyl-arginine binding was assessed (Fig. 6.3c). All three BCAAs were used although only L-leucine has been shown to bind the CTD of Rel_{Sa} (Fang and Bauer, 2018). L-serine was included because it is a common ligand of ACT domains (Grant, 2006). BCAAs cannot be dissolved to high concentrations in water and so the concentration of dansyl-arginine added and the concentration of protein was lowered to a final concentration of 1 mM from 10 mM and 10 µM from 75 µM, respectively, to compensate for the lower concentration of competing amino

acid (final concentration of 20 mM), resulting in the reduced fraction bound values seen. As expected L-valine and L-isoleucine did not cause a significant decrease in the fraction of dansyl-arginine bound to Rel_{Sa} and nor did L-serine. The fact that L-leucine did not affect the fraction of dansyl-arginine bound may be due to a lower affinity or because the two amino acids have different binding sites. The positive control L-Arg did disrupt dansyl-arg binding to Rel_{Sa} ($p = 0.0029$) confirming that the competition assay does work at lower concentrations of ligand and protein.

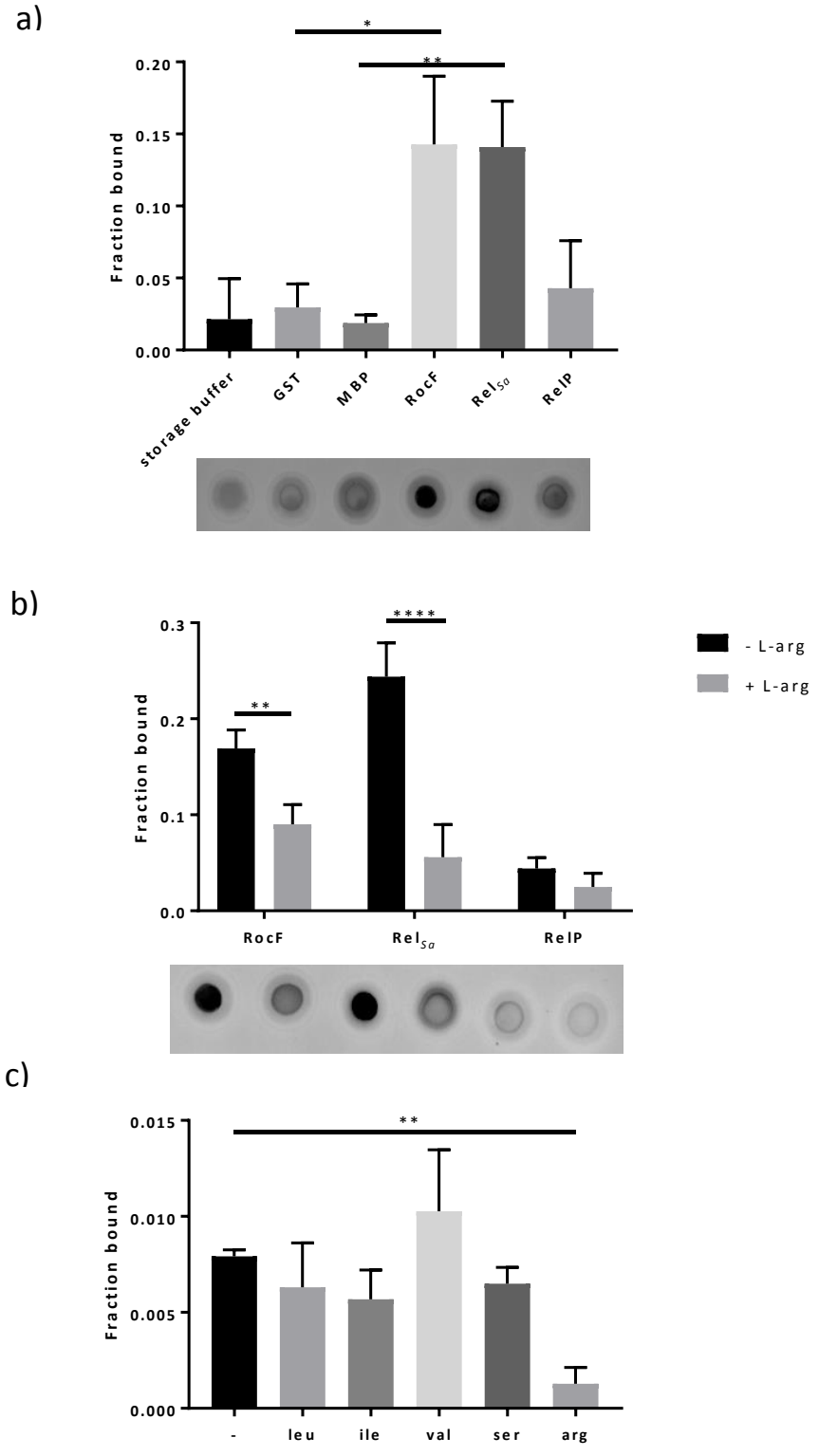

Figure 6.3 DRaCALAs with fluorescently labelled L-arg to investigate L-arginine binding to RocF, Rel$_{Sα}$ and RelP. a) Quantification (above) and a representative image (below) of DRaCALAs. Both Rel$_{Sα}$ and RocF bind to dansyl-arg significantly more than the MBP and GST controls, respectively. RelP does not bind to dansyl-arg. b) Specificity of dansyl-arg binding to RocF, Rel$_{Sα}$ and RelP. Quantification (above) and a representative image (below) of DRaCALAs. Addition of 100 mM unlabelled L-arg (grey) was able to disrupt 10 mM dansyl-arg binding of both RocF and Rel$_{Sα}$ compared to adding only buffer to the reaction (black). RelP does not bind to dansyl-arg and so unlabelled L-arg could not disrupt binding. c) Competition of 1 mM dansyl-arg binding to Rel$_{Sα}$ with 20 mM L-leu, L-ile, L-val, L-ser, and L-arg. Only L-arg disrupted dansyl-arg binding compared to adding only buffer to the reaction (-). Quantification of DRaCALAs. All experiments were performed in triplicate, with means and standard deviations plotted. Statistical significance tested by ordinary one-way ANOVA * $p < 0.05$; ** $p < 0.01$; **** $p < 0.0001$

6.4 Arginase activity of RocF

As mentioned previously, RocF is an arginase (Fig. 6.4a), and so to examine the activity of the *S. aureus* enzyme, *in vitro*, an arginase assay was performed. We initially established the linear range of the assay using various concentrations of RocF. The linear range of enzymatic activity was determined to be 2.5-20 nM and so for future experiments 10 nM RocF was used (Fig. 6.4b).

Homologues of RocF are present in many bacterial species and have been shown to have different cofactor preferences. In *Helicobacter pylori*, RocF activity is highest with Co as a cofactor (McGee *et* al., 1999), while RocF of *Bacillus anthracis* shows highest activity with Ni as a cofactor at both pH 6 and pH 9 (Viator *et al*, 2008). The buffer provided with the arginase kit contains Mn^{2+} as a cofactor, so to assess whether this is the best cofactor for RocF from *S. aureus* the assay was carried out using buffers containing $MnCl_2$ or $NiCl_2$ (final concentration 5 mM). The concentration of Mn^{2+} in the buffer provided by the kit is not known and so a $MnCl_2$ solution was made up so it could be directly compared to the $NiCl_2$ buffer. $CoCl_2$ was not included in the assay as *H. pylori* is unique for its preference for Co (McGee *et* al., 2004) and because in *S. aureus* the metal binding site of RocF is annotated as a manganese binding site. Arginase activity was significantly higher with $MnCl_2$ compared to $NiCl_2$ (p = 0.0127) and so the buffer provided by the kit was used in further experiments (Fig. 6.4c).

The activity of RocF was assayed in the presence of different proteins and ligands (Rel_{Sa}, $RelP_{Sa}$, ppGpp, L-arg, and Rel_{Sa} with ppGpp) to determine if they have any effect on the arginase activity of RocF (Fig. 6.4d). Rel_{Sa} and ppGpp were included together based on previous results showing that ppGpp increased the binding between RocF and Rel_{Sa} in a pulldown assay (Fig. 5.4.2) and so it was hypothesised that ppGpp may also increase any effect of Rel_{Sa} on RocF activity. L-arg and $RelP_{Sa}$ were included based on the fact they both bind to Rel_{Sa}. The arginase activity was measured without RocF to determine a background level and to rule out any non-specific arginase activity of any of the proteins and ligands assayed. All reactions showed significantly higher arginase activity in the presence of RocF ($p < 0.01$ for all) indicating that none of the proteins or ligands were interfering with the assay and any change in arginase activity could be attributed to RocF activity. However, none of the proteins or ligands assayed here influenced RocF arginase activity in these conditions.

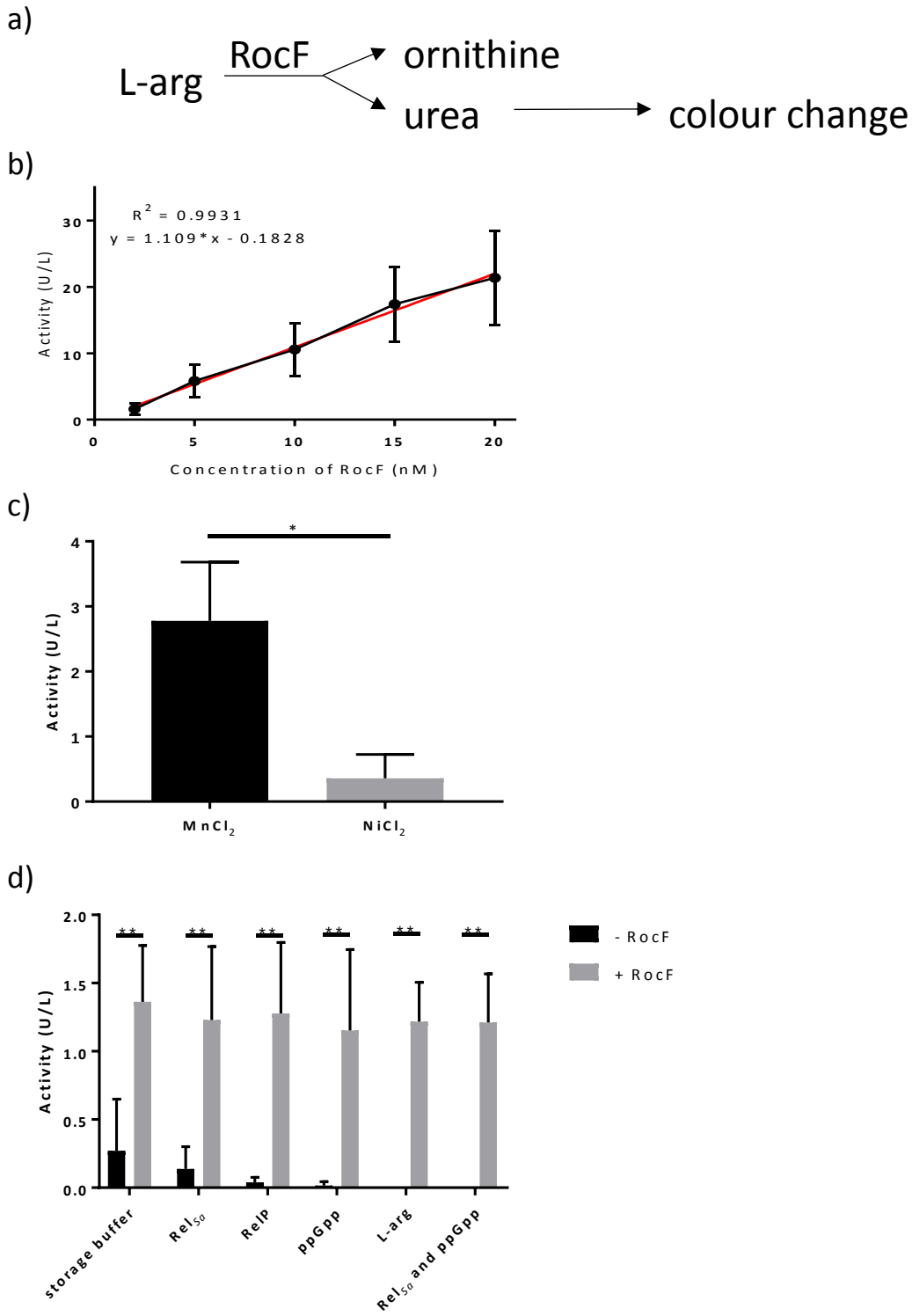

Figure 6.4 Optimisation of arginase activity assay and effect of Rel_{Sa}, RelP, ppGpp, on RocF arginase activity. a) reaction equation of RocF, which converts L-arginine to ornithine and urea. Urea causes a colour change in the arginase assay which is measured at 430 nm. b) determination of linear range for the arginase assay using purified RocF. The trendline (red) was calculated using Graphpad Prism with a line equation of y=1.109*x - 0.1828 and an R^2 value of 0.9931. c) arginase activity of RocF using $MnCl_2$ and $NiCl_2$ as a cofactor. Arginase activity was significantly higher with $MnCl_2$ (black) compared to $NiCl_2$ (grey). d) arginase activity of RocF (10 µM) preincubated with 10 µM Rel_{Sa}, RelP, ppGpp, L-arg, and Rel_{Sa} in combination with ppGpp (grey) and background activity of 10 µM Rel_{Sa}, RelP, ppGpp, L-arg and Rel_{Sa} in combination with ppGpp but without RocF (black). All samples had a significantly higher arginase activity in the presence of RocF but none of the proteins or ligands had an effect on RocF activity. All experiments were performed in triplicate, with means and standard deviations plotted. Statistical significance tested by unpaired T test * $p < 0.05$; ** $p < 0.01$

6.5 Nucleotide hydrolysis activity of Rel_{Sa}

6.5.1 GTP hydrolysis activity of Rel_{Sa}

Another possible effect of the interaction between Rel_{Sa} and RocF is a change in activity of Rel_{Sa}. Originally, we attempted to assay the change RocF may have on the (p)ppGpp synthesis activity of Rel_{Sa}, however preliminary experiments using only Rel_{Sa} resulted in hydrolysis of the radiolabelled GTP used in the assay (data not shown). This supports previous work showing that in vitro Rel_{Sa} is in the HYDROLASE-ON SYNTHETASE-OFF confirmation (Gratani *et al.*, 2018). The enzymatic process responsible for the conversion of GTP to lower weight molecules is not clear and GTP hydrolysis activity of long-RSH proteins has not previously been reported. When (p)ppGpp is hydrolysed by members of the RSH superfamily a pyrophosphate group is released (PPi). These data suggest that Rel_{Sa} is also able to release a single phosphate group (Pi) through hydrolysis of GTP forming GDP (Fig. 6.5.1a).

Following this result, different ligands and proteins were assayed for their impact on Rel_{Sa} GTP hydrolysis activity, namely RocF, RelP, ppGpp, and L-arg. Recently the long-RSH protein in *Rhodobacter capsulatus* was shown to bind to valine and isoleucine, promoting its ppGpp hydrolase activity (Fang and Bauer, 2018). In order to follow up on this observation that amino acids can modulate the activity of long-RSH protein and the observation that L-arginine binds to Rel_{Sa}, L-arginine was included in the GTP hydrolysis activity assay. (p)ppGpp is both a substrate and product of Rel_{Sa} and has been shown to modulate the activity of RSH superfamily members previously (discussed in Section 1.2.3). For example, the synthetase activity of Rel_{Ec} in complex with a 70S ribosome is increased in the presence of ppGpp (Shyp *et al.*, 2012). RelP was included in the assay in order to investigate the biological significance of the interaction between RelP and Rel_{Sa} reported previously (Fig. 5.2.1c). The proteins and ligands were incubated with and without Rel_{Sa} in order to rule out any unpredicted hydrolase activity. Nucleotides can break down over time and through heating and so a buffer control was included to give a baseline of degradation. The percentage of GTP hydrolysed in each reaction was assessed at 5 minutes (Fig. 6.5.1b) and 1 hour (Fig. 6.5.1c) by quantifying a TLC run.

After 5 minutes the presence of RelP significantly increased the percentage of GTP hydrolysed compared to Rel_{Sa} alone (p = 0.0081) although after 1 hour this effect was not seen. Instead, the presence of ppGpp decreased the percentage of GTP hydrolysed compared to Rel_{Sa} alone (p = 0.0065). Finally, after 1 hour RocF seemed to increase GTP hydrolysis in the absence of Rel_{Sa} (p = 0.0224), but not when Rel_{Sa} was present in the reaction. This result was unexpected and may be anomalous as it was not observed with (p)ppGpp hydrolysis (Fig. 6.5.2).

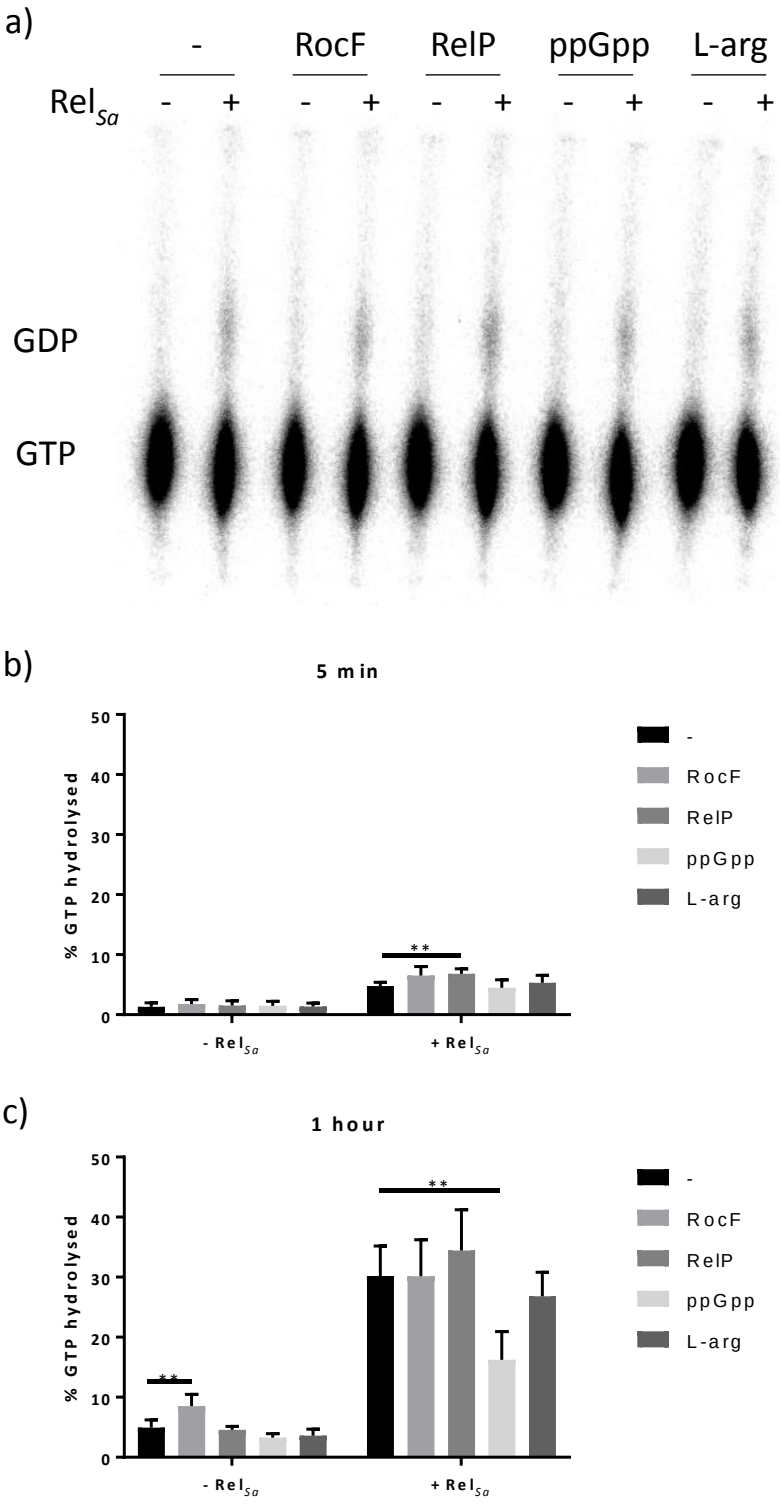

Figure 6.5.1 Assaying the effect of proteins and ligands on GTP hydrolysis by Rel$_{Sa}$. a) Representative TLC showing the effect of RocF, RelP, ppGpp and L-arg or just buffer (-) on GTP hydrolysis to GDP with and without Rel$_{Sa}$ (+ or -) after 5 min. b) percentage of GTP hydrolysed with and without Rel$_{Sa}$ after 5 mins at 37°C in the presence of RocF, RelP, ppGpp and L-arg or just buffer (-). RelP with Rel$_{Sa}$ had a significantly higher percentage of GTP hydrolysis compared to just Rel$_{Sa}$. c) percentage of GTP hydrolysed with and without Rel$_{Sa}$ after 1 hour at 37°C in the presence of RocF, RelP, ppGpp and L-arg or just storage buffer (-). ppGpp with Rel$_{Sa}$ had a significantly lower percentage of GTP hydrolysis compared to just Rel$_{Sa}$. RocF without Rel$_{Sa}$ had a significantly higher percentage of GTP hydrolysis compared to just storage buffer. All experiments were performed four times, with means and standard deviations plotted. Statistical significance tested by unpaired T test * $p < 0.05$; ** $p < 0.01$

6.5.2 (p)ppGpp hydrolysis activity of Rel_{Sa}

Rel_{Sa} hydrolyses ppGpp and pppGpp to GDP and GTP respectively, releasing PPi. This activity is essential for halting the stringent response in relaxed conditions. In fact, the hydrolase domain of Rel_{Sa} is essential to avoid the toxic effects of unchecked (p)ppGpp accumulation by RelP and RelQ (Gentry *et al*., 2000; Geiger *et al*., 2010). A hydrolase assay was carried out but using α^{32}P labelled ppGpp or pppGpp synthesised from α^{32}P labelled GTP (Fig. 6.5.2). The concentration of proteins and ligands used in the GTP hydrolysis assay was reduced 20-fold to a final concentration of 50 nM for the (p)ppGpp hydrolysis assays, due to Rel_{Sa} achieving almost 100% (p)ppGpp hydrolysis even after 5 minutes at a concentration of 1 µM, meaning that any increase in hydrolysis would be masked (data not shown). This huge difference in nucleotide hydrolysis activity may explain the decrease in GTP hydrolysis seen in the presence of ppGpp, as Rel_{Sa} may preferentially hydrolyse the ppGpp present in the reaction over the radiolabelled GTP (Fig. 6.5.1b). There was no significant difference in (p)ppGpp hydrolysis in the presence of RocF, RelP, ppGpp or L-arginine, after 5 minutes or 1 hour under these conditions *in vitro* (Fig. 6.5.2). It may be that (p)ppGpp synthesis activity, rather than (p)ppGpp hydrolysis activity, is affected by these ligands

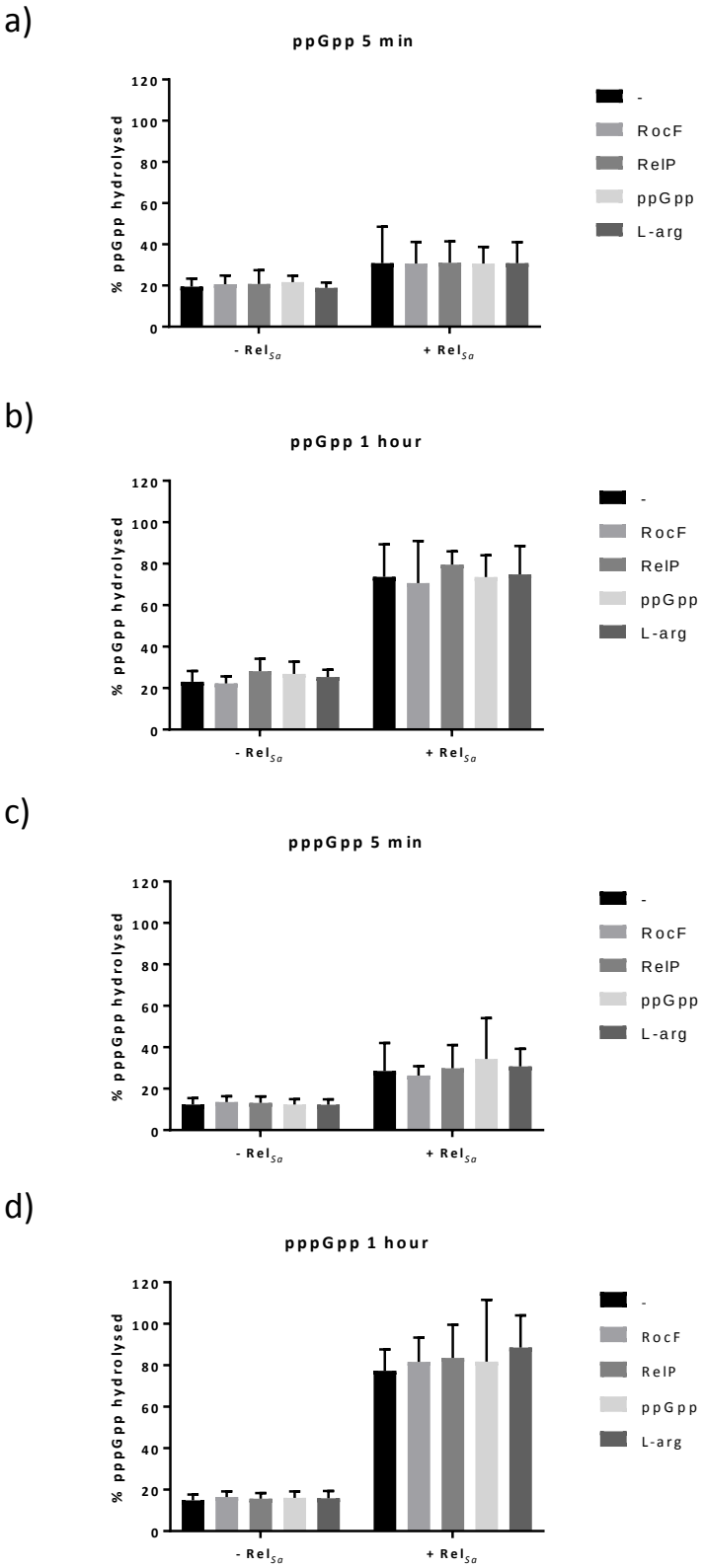

Figure 6.5.2 Assaying the effect of proteins and ligands on (p)ppGpp hydrolysis by Rel$_{Sa}$. Percentage of ppGpp hydrolysed with and without Rel$_{Sa}$ after 5 mins (a) and 1 h (b) at 37°C in the presence of RocF, RelP, ppGpp and L-arg or just storage buffer. Represents three repeats. Percentage of pppGpp hydrolysed with and without Rel$_{Sa}$ after 5 mins (c) and 1 h (c) at 37°C in the presence of RocF, RelP, ppGpp and L-arg or just storage buffer. All experiments were performed in triplicate, with means and standard deviations plotted.

6.6 Discussion

The results above aim to provide a purpose for the interaction between RocF-Rel$_{Sa}$ and a basis for further investigation. Firstly, RocF has been ruled out as a binding target of (p)ppGpp as it does not bind to the protein (Fig. 6.2). This also suggests that the increase in binding between RocF and Rel$_{Sa}$ seen in the presence of ppGpp is due to an effect on Rel$_{Sa}$, perhaps through a conformational change. The only known (p)ppGpp target protein to interact with a long-RSH protein is the GTPase Era as described in Chapter 4. RocF has not previously been pulled out in a screen of (p)ppGpp binding proteins in *S. aureus* (Corrigan *et al*., 2016) and so this negative result was expected.

In this study L-arg is shown to bind to Rel$_{Sa}$ which represents another step towards understanding how long-RSH proteins are regulated by their CTDs. Typically, ACT domains form a dimer to bind to their ligands and it could be that binding to L-arg forms a Rel$_{Sa}$ dimer (Grant, 2006). This could have an impact on Rel$_{Sa}$ activity because oligomerisation has been implicated in long-RSH protein regulation previously, with the dimer state being HYDROLASE-ON SYNTHETASE-OFF (Avarbock *et al*. 2005; Gropp *et al*. 2001; Yang and Ishiguro, 2001). We propose a model where during relaxed conditions Rel$_{Sa}$ is present in a dimer, coordinating L-arg or another amino acid, and during stringent conditions, when L-arg is limiting, the dimer dissociates. Whilst Gratani *et al.* 2018 state that the ACT domain has no effect on the correct stringent response in *S. aureus*, the mutant used in their study (669-DRNGLL-674 mutated to 669-ELQSNN-674) does not change the conserved asparagine (N687) shown to be important for BCAA binding in *R. capsulatus* (Fang and Bauer, 2018). This may explain the limited effect of the mutant on Rel$_{Sa}$ activity compared to other domains in the CTD (Gratani *et al*. 2018).

Future work on L-arg binding should focus on determining the kinetics of binding. This would allow comparison to physiological levels of L-arg in the cell to provide perspective on the relevance of the interaction. Rel$_{Sa}$ is a large protein (84,509 Da) and with the MBP-His tag used for purification, it has a weight of 136120.66 Da. This limits the concentration to which the protein can be prepared before aggregation or precipitation. If the Kd of arginine binding is as high as leucine binding (309 µM) then reaching saturation in a binding curve would prove difficult. In order to determine a Kd for arginine binding, a truncated version of Rel$_{Sa}$ would be used, either the CTD alone as in Fang and Bauer, 2018, or just the ACT domain to allow saturating concentrations to be reached. Using different truncations would also narrow down the domains responsible for L-arg binding. The binding constant can be experimentally derived using a DRaCALA (Roelofs *et al*., 2011), but isothermal calorimetry (ITC) would allow use of unlabelled amino acids, removing the potential impact of the fluorescent tag on binding. Using ITC, it would be interesting to look at Rel$_{Sa}$ binding to other amino acids and also how conserved L-arg binding is across long-RSH proteins from different species.

We have shown that, *in vivo*, under the conditions tested, that the activity of RocF is not regulated by Rel_{Sa}, $RelP_{Sa}$, ppGpp, L-arg, or Rel_{Sa} together with ppGpp. There is currently no known protein or ligand that modulates RocF activity and it is thought that its activity is predominately controlled on a transcriptional level, for example, through CcpA and regulatory RNA RsaE (Li *et al*., 2010; Rochat *et al*., 2018). The addition of L-arg to the assay did not affect RocF activity because L-arg is already present in the assay in excess. This study has shown that both RelP and ppGpp do not interact with RocF and so they were not expected to modulate RocF activity. Finally, there are no examples to date of a long-RSH protein binding to, and altering the activity of a protein.

The samples of RocF used for experiments in Fig. 5.3a and Fig. 5.3c were from different purifications, which may explain the difference in activity (U/L) seen. In future, the linear range should be determined for each purification. However, the activity measured in Fig. 5.3c is above the detection limit of the assay and the ratio between the sample and the blank is below 2 which is required by the assay. This suggests the results can be interpreted valid for this protein sample. The difference in activity between Fig. 5.3a and Fig. 5.3b is due to suboptimal buffers because the same protein sample was used.

Whilst Rel_{Sa} has both (p)ppGpp synthesis and hydrolysis activity only the hydrolysis activity is assayed here. This is due to the fact that full length Rel_{Sa} is in the HYDROLASE-ON SYNTHETASE-OFF confirmation *in vitro* (Gratani *et al*., 2018). In future work, truncated versions of Rel_{Sa} could be used to assess the effect of proteins and ligands on the synthetase activity of Rel_{Sa}. However, because the CTD is probably the domain responsible for most interactions with Rel_{Sa}, a truncated Rel_{Sa} may no longer interact with other molecules. If a ligand or protein binding partner increased Rel_{Sa} (p)ppGpp synthesis activity sufficiently, it may be possible to assay *in vitro* with full-length purified protein. Another possibility is to use radiolabelled ATP as the substrate of the assay and use the production of AMP as a proxy for (p)ppGpp production, which would avoid the problem of low levels of (p)ppGpp synthesis being obscured by high (p)ppGpp hydrolysis levels: AMP would remain in the reaction even if the (p)ppGpp produced is immediately hydrolysed. These approaches could be used to try to determine the impact of L-arg on synthetase activity of Rel_{Sa}. To look at the effect of L-arg on long-RSHs more generally, $RelA_{Ec}$ could be used. $RelA_{Ec}$ does not have any hydrolase activity and so after confirming it binds to L-arg, it could be used for synthetase assays.

During the stringent response the GTP pool within the cell drops leading to derepression of the CodY repressor and a reduction in transcription of rRNA (Geiger and Wolz, 2014; Kastle *et al*., 2015; Krasny and Gourse, 2004). This was hypothesised to be due to the consumption of GTP during the synthesis

of (p)ppGpp. Here we saw that GTP hydrolysis activity is low, however it may play some role in tipping the balance of nucleotides in the cell during the stringent response.

In conclusion, amino acid binding to Rel_{Sa} is an exciting avenue of research for the future. Particularly because a low amino acid level in the cell is a trigger for the stringent response. It is known that long-RSH enzymes can sense this stress indirectly through binding stalled ribosomes and uncharged tRNAs. L-arg is important in both carbon and nitrogen metabolism and may be used as a direct sensor for both by the stringent response.

Chapter 7 - Characterisation of (p)ppGpp synthetase mutants

7.1 Introduction

Following on from *in vitro* work of the biological function of the Rel_{Sa}-RocF interaction, we next looked to assess the role of the interaction in *S. aureus*. Although we were not able to show any change in RocF activity in the presence of Rel_{Sa} in the conditions tested *in vitro*, we hypothesised that in the host the Rel_{Sa}-RocF interaction does play a role in RocF activity, perhaps potentiated by other factors.

In *H. pylori,* RocF is required for acid stress survival (McGee *et al.*, 1999) and the stringent response is triggered by acid stress, perhaps indicting another link between RocF and the stringent response (Mouery *et al.*, 2006). In *S. aureus,* RocF is required for proline biosynthesis due to its role in the urea cycle (Li *et al.*, 2010; Halsey *et al.*, 2017). The urea cycle allows the interconversion of arginine and proline depending on the availability of both amino acids (Fig. 7.1). Although the expression of *rocF* is not altered during leu/val starvation in *S. aureus*, the expression of *proC* is upregulated due to CodY derepression (Geiger *et al.*, 2012), which occurs after a drop in GTP levels after activation of the stringent response. The *proC* gene encodes another enzyme in the arginine to proline conversion pathway that catalyses the formation of proline from P5C. The expression of *rocF* is repressed by CcpA, along with the expression of many other genes (Halsey *et al.,* 2017). CcpA is a carbon catabolite repressor that represses the expression of various genes involved in secondary carbon catabolism in the presence of glucose. It can also upregulate the expression of certain genes, such as the *ure* genes that encode the urease enzyme (Seidl *et al.,* 2009).

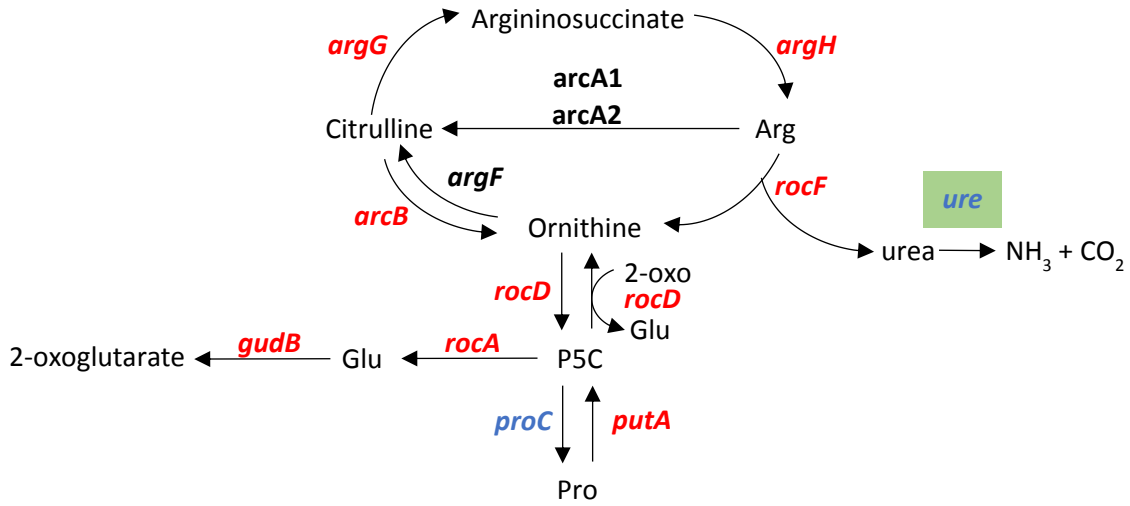

Fig. 7.1 Arginine and proline metabolism in *S. aureus*. Genes that are repressed by CcpA are shown in red, genes that are repressed by CodY are shown in blue, genes that are upregulated by CcpA are highlighted in green. Proline and arginine can be interconverted through the action of metabolic enzymes. An intermediate of this process, P5C, is converted to glutamate by RocA and then to 2-oxogluterate by GudB. 2-oxoglutarate then can feed into the citric acid cycle.

Given the connection of RocF to acid stress survival and proline catabolism, we sought to understand the role of the stringent response in these processes in *S. aureus.* Here we use mutants in the three (p)ppGpp synthetase mutants that were available in the laboratory to characterise their role of the stringent response. *The* rel_{syn} mutant has a single amino acid mutation in the synthetase region of the gene, meaning the protein is unable to synthesise (p)ppGpp but it has fully functional hydrolase activity. This is necessary because the hydrolase activity of Rel_{Sa} is essential due to the presence of (p)ppGpp produced by RelP and RelQ (Geiger *et al.*, 2010; Gentry *et al*., 2000). The *relP* mutant was made by phage transducing the Tn insertion from the NTML strain NE474 into the LAC* strain. The *relQ* mutation was constructed by replacing the native *relQ* gene with a tetracycline resistance cassette. Combinations of these mutants were made to give a full panel of (p)ppGpp synthetase single, double and triple mutants (rel_{syn}, *relP*, *relQ*, *relP* rel_{syn}, *relQ* rel_{syn}, *relP relQ*, and *relP relQ* rel_{syn}). The triple mutant is completely unable to synthesise (p)ppGpp and so is referred to as $(p)ppGpp^0$.

The ability of the panel of mutants to grow long term in various media was investigated, as well as growth in various chemically defined media (CDM). The use of CDMs allowed us to explore how the Rel_{Sa}-RocF interaction impacts growth in various stress conditions. This led us to measure the arginase and urease activity of the strains to understand if the stringent response had any regulatory impact on these enzymes, which are involved in survival of proline starvation and acid stress, respectively. We also investigated how the regulation of the (p)ppGpp synthetase enzymes in *S. aureus* are affected by different growth conditions. Using the bitLucopt system we investigated how Rel_{Sa} binding to CshA, RocF and itself changes in different conditions.

7.2 Arginase activity of (p)ppGpp synthetase mutants

In vitro experiments showed that RocF activity was not impacted by the presence of Rel_{Sa} in the conditions tested (Fig. 6.4). We hypothesised that, in the host, other factors may mediate regulation of RocF activity and so measured the arginase activity of *S. aureus* lysates was measured.

The expression of RocF should increase in a chemically defined medium without glucose compared to with glucose (CDM compared to CDMG) because of the derepression of CcpA. We wanted to see if the stringent response and the (p)ppGpp synthetase enzymes in *S. aureus* had any effect on the arginase activity of RocF in CDMG or CDM.

The arginase activity (U/g/L) was measured for each of the 8 (p)ppGpp synthetase mutant strains (LAC*, LAC* rel_{syn}, LAC* *relP*, LAC* *relQ*, LAC* *relP* rel_{syn}, LAC* *relQ* rel_{syn}, LAC* *relP relQ*, and $(p)ppGpp^0$) after growth in CDM with and without glucose (Fig. 7.2). Overnight cultures were washed in PBS and

normalised to an OD_{600} of 5 in TSM buffer with lysostaphin and PMSF. After lysis for 1 h the protein concentration of the lysates was measured, and the arginase activity was measured. The arginase activity was then calculated as arginase activity per g of protein per L of lysate (U/g/L) where one unit of arginase activity is the amount of enzyme that will convert 1.0 μmole of L-arginine to ornithine and urea per minute at pH 9.5 and 37°C.

As expected, when grown in CDMG the level of arginase activity was low due to the repression of *rocF* activity by CcpA (Fig. 7.2). For each strain there was a significant increase in arginase activity when grown without glucose compared to when grown with glucose (LAC*, p = 0.0005; LAC* *rel*$_{syn}$, p = 0.0069; LAC* *relP*, p = 0.0001; LAC* *relQ*, p < 0.0001; LAC* *relP rel*$_{syn}$, p = < 0.0001; LAC* *relQ rel*$_{syn}$, p = 0.0152; LAC* *relP relQ*, p = 0.0167; (p)ppGpp^0, p < 0.0001) (Fig. 7.2). This suggests that a functional stringent response is not essential for the increase in arginase activity upon glucose starvation. Whilst the LAC* *relP rel*$_{syn}$ strain did show a significantly higher arginase activity in CDM compared to CDMG, the activity in CDM was significantly lower than the WT LAC* strain (p = 0.0191) (Fig. 7.2). Interestingly, the triple mutant (p)ppGpp^0 does not show this small defect in arginase activity induction in CDM, perhaps implying that RelQ is having some negative effect on arginase activity in the absence on RelP and Rel$_{Sa}$. The impact of the *relP rel*$_{syn}$ double mutant was particularly interesting given the evidence that these two proteins interact (Fig. 5.2.1c). It is possible that both proteins are required to regulate RocF activity, which would explain why there were no changes in RocF activity seen *in vitro* because the three protein were not assayed together (Fig. 6.4).

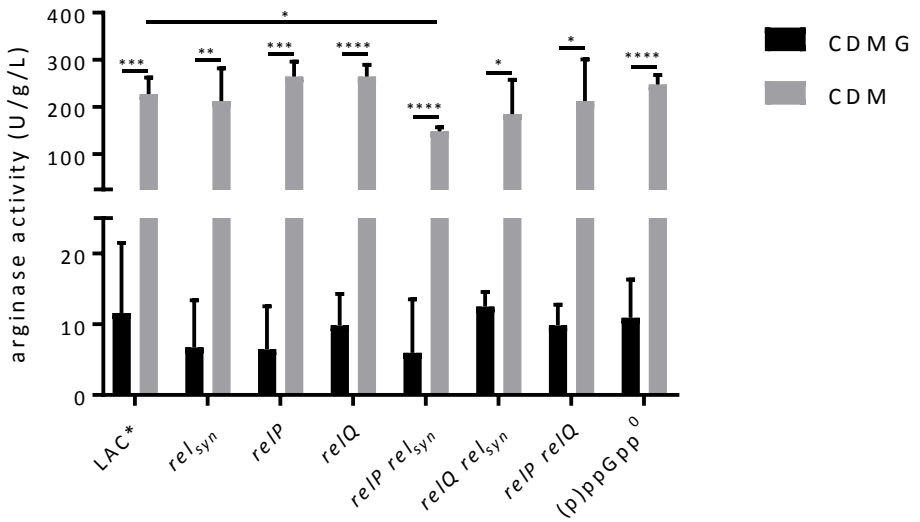

Figure 7.2 Arginase activity of (p)ppGpp synthetase mutant strains in CDMG and CDM. The arginase activity (U/g/L) was measured for each of the 8 strains (LAC*, LAC* *rel*$_{syn}$, LAC* *relP*, LAC* *relQ*, LAC* *relP rel*$_{syn}$, LAC* *relQ rel*$_{syn}$, LAC* *relP relQ*, and (p)ppGpp^0 after growth in CDM with (CDMG; black) and without glucose (CDM; grey). For each strain there was a significant increase in arginase activity when grown without glucose compared to when grown with glucose. LAC* *relP rel*$_{syn}$ had a significantly lower arginase activity when grown in CDM compared to the WT LAC* strain. This experiment was performed three times, with means and standard deviations plotted. * $p < 0.05$; ** $p < 0.01$; *** $p < 0.001$; **** $p < 0.0001$

7.3 Growth of (p)ppGpp synthetase mutants in chemically defined media

The difference in arginase activity of the *relP rel*$_{syn}$ double mutant in CDM compared to LAC* was only small. In order to assess if this would have an impact on arginine catabolism, we investigated the growth of the (p)ppGpp synthetase strains in various CDMs. During infection of the host, the level of glucose and other nutrients is limited and so *S. aureus* must be able to switch its metabolism to utilise alternative carbon sources (Kelly and O'Neill, 2015; Spahich *et al.*, 2016). *S. aureus* cannot utilise short chain fatty acids due to the lack of glyoxylate shunt and β-oxidation pathways, and so must rely on lactate and amino acids as carbon sources in the absence of glucose (Halsey *et al.*, 2018). In particular, the use of proline and arginine as carbon sources is important in the absence of glucose (Fig. 7.3.1).

Halsey *et al.* reported that the *S. aureus* WT strain JE2 grew in a chemically defined media lacking glucose and proline (CDM-P) but a *rocF* mutant could not grow. This suggests that, in the WT strain, proline synthesis is dependent on the presence of arginine in CDM-P. Arginine is hydrolysed by RocF into ornithine and then converted to P5C and ultimately proline by RocD and ProC respectively (Fig. 7.3.1). The authors also reported that the JE2 strain was not able to grow in CDM lacking glucose and arginine (CDM-R) showing that proline could not act as a precursor for arginine biosynthesis under these conditions, despite the metabolic pathway existing (Fig. 7.3.1), and therefore arginine is an essential amino acid in glucose starvation conditions. However, a *ccpA* mutant was able to grow in CDM-R. CcpA is a carbon catabolite repressor that represses gene expression in the presence of

glucose. When glucose is limited CcpA repression is released, resulting in an increase in the expression of various secondary carbon catabolism genes including RocF. CcpA represses genes that can produce arginine from proline, such as *putA*, hence why the *ccpA* mutant can grow on CDM-R but the WT strain could not. The reason the WT strain does not release CcpA repression in CDM-R despite the absence of glucose is unclear.

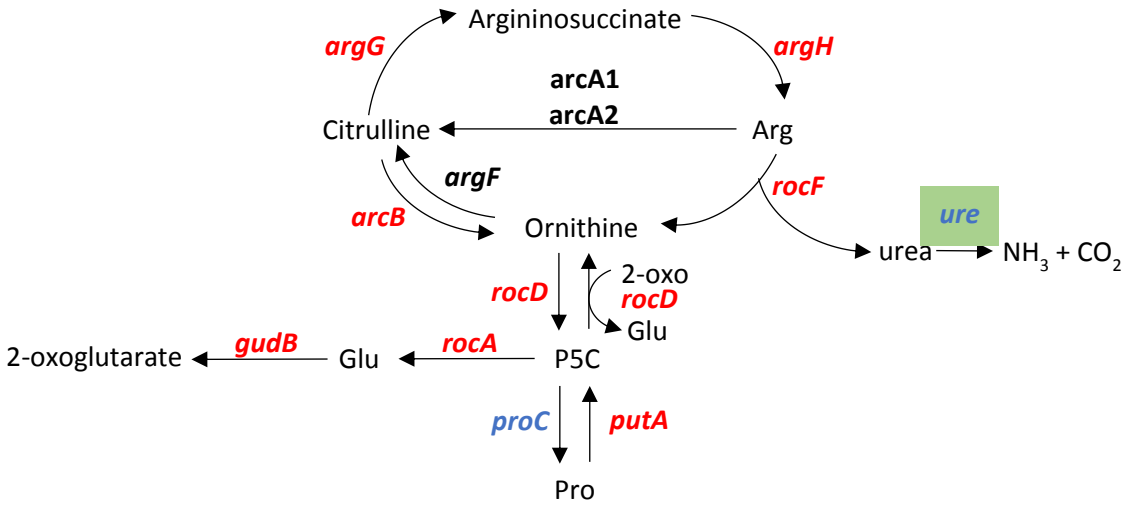

Fig. 7.3.1 Schematic diagram of proline and arginine metabolism in *S. aureus*. Genes that are repressed by CcpA are shown in red, genes that are repressed by CodY are shown in blue, genes that are upregulated by CcpA are highlighted in green. Proline and arginine can be interconverted through the action of metabolic enzymes. An intermediate of this process, P5C, is converted to glutamate by RocA and then to 2-oxogluterate by GudB. 2-oxoglutarate then can feed into the citric acid cycle. PutA converts proline to P5C which can then be converted to glutamic acid by RocA. Arginine is converted to ornithine by RocF. Ornithine can then be converted to P5C by RocD.

We tested the growth of the (p)ppGpp synthetase mutant strains in CDM, CDM-P and CDM-R in order to investigate if the stringent response plays any role in secondary carbon catabolism. A JE2 *rocF* mutant and the WT *S. aureus* strains LAC* and JE2 were also tested in these conditions. As reported by Halsey *et al.* the JE2 strain showed a growth defect in CDM-R (Fig. 7.3.2i – black line) (although some minimal growth was observed here) but grew well in CDM and CDM-P (Fig. 7.3.2g and Fig. 7.3.2h). The LAC* WT strain was included because the (p)ppGpp synthetase mutants are in a LAC* background. The LAC* strain showed a similar phenotype to the highly similar JE2 strain in that it grew well in CDM and CDM-P but had a growth defect when grown in CDM-R (Fig. 7.3.2g, Fig. 7.3.2h and Fig. 7.3.2i – green line). The growth defect of WT *S. aureus* strains in CDM-R is unexpected because, without a preferred carbon source, CcpA repression should be released allowing the expression of arginine biosynthesis genes such as *putA* (Nuxoll *et al.*, 2012). However, a *ccpA* mutation was required for JE2 growth in CDM-R (Halsey *et al.*, 2018). The JE2 *rocF* mutant also grew as expected based on work by Halsey *et al.* with normal growth in CDM, a growth defect in CDM-R and no growth in CDM-P (Fig. 7.3.2g, Fig. 7.3.2h and Fig. 7.3.2i – blue line). Without the activity of RocF, arginine cannot be

converted to proline and therefore the strain is auxotrophic for proline. JE2 *rocF* was the only strain to show a growth defect in CDM-P showing that the reduced arginase activity of the *relP* rel_{syn} lysate in CDM (Fig. 7.2) does not impact the ability of the strain to grow in CDM-P.

Growth in CDM was consistent in all synthetase mutant strains but the *relP* rel_{syn} strain (purple line), which reached a higher OD_{600} than the other strains (Fig. 7.3.2a). The reason for this is not clear, but it could be due to an increase in expression or activity of enzymes involved in secondary carbon catabolism.

In CDM-R, all the (p)ppGpp synthetase mutant strains grew differently from the WT. Strains with a *relQ* mutation did not grow at all in CDM-R (Fig. 7.3.2f – yellow, orange, green and brown lines), whereas *relP*, rel_{syn} and *relP* rel_{syn} strains all grew better than the WT (Fig. 7.3.2c – blue, pink and purple lines). RelQ is required for improved growth in CDM-R and so it seems that RelQ positively regulates arginine biosynthesis. However, an increase in arginine biosynthesis depends on *relP* or rel_{syn} mutations, suggesting RelP and Rel_{Sa} may negatively regulate arginine biosynthesis. The mechanism of stringent response regulation of arginine biosynthesis is unclear but may be mediated through CcpA. Previously, it was shown that a *ccpA* mutation is required to improve growth of JE2 in CDM-R (Halsey *et al*., 2017). Presumably, in a *ccpA* mutant the expression of enzymes that convert proline to arginine, such as *putA*, are more highly expressed.

The *relP* rel_{syn} double mutant did not show an additive effect compare to the *relP* and rel_{syn} single mutants, suggesting that both RelP and Rel_{Sa} play a connected role in suppression of proline to arginine conversion in CDM-R (Fig. 7.3.2c).

Taken together, these results show that the synthetase enzymes are not required for growth in CDM and are therefore not required for all aspects of alternative carbon catabolism. Furthermore, the conversion of arginine to proline in the absence of glucose depends on RocF but not Rel_{Sa}, RelP or RelQ. However, RelQ, Rel_{Sa} and RelP impact arginine biosynthesis, presumably from proline.

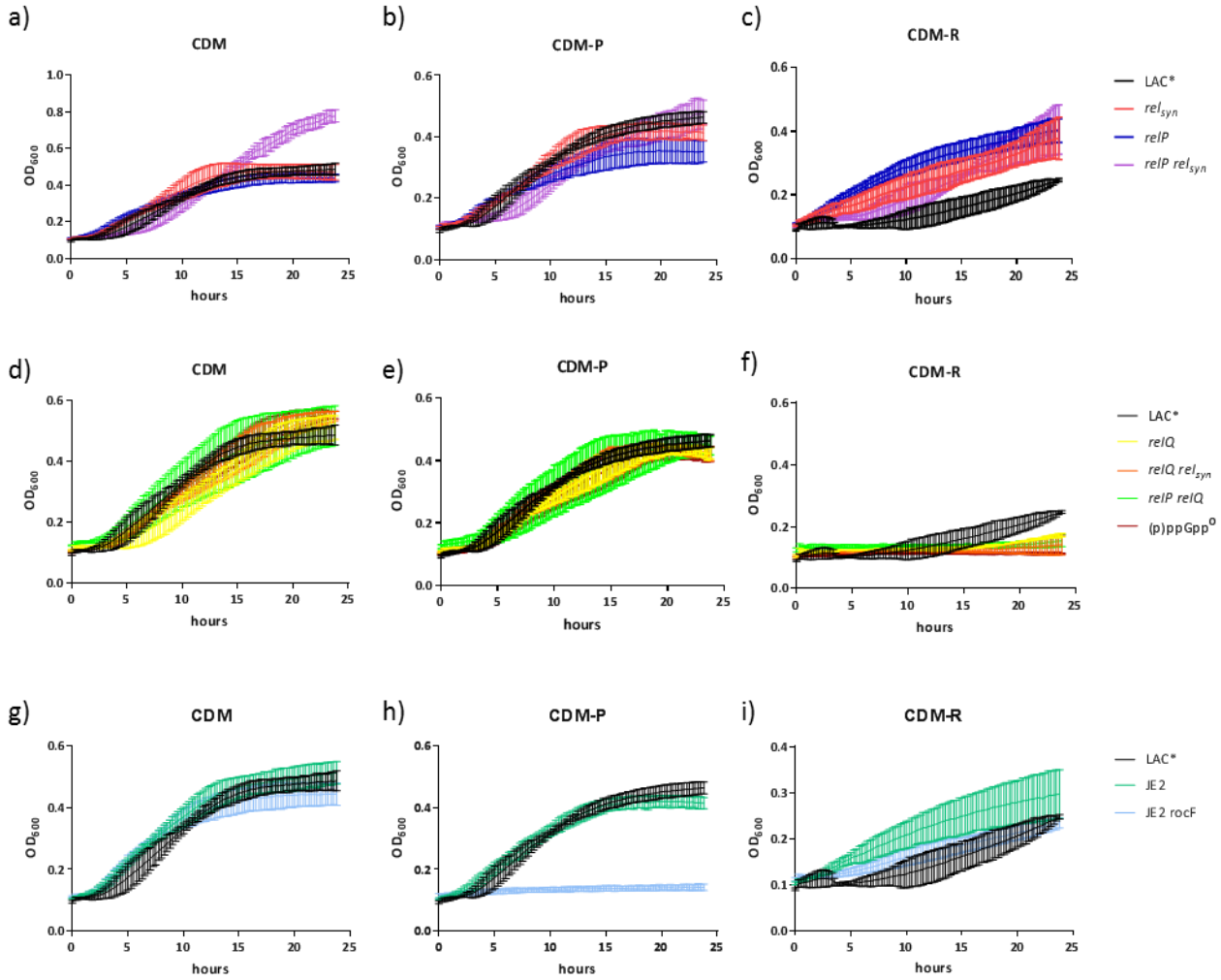

Fig. 7.3.2 Growth of (p)ppGpp synthetase mutant strains in CDM, CDM-P and CDM-R. The growth of LAC* (black), *rel*$_{syn}$ (pink), *relP* (blue), *relQ* (yellow), *relP rel*$_{syn}$ (purple), *relQ rel*$_{syn}$ (orange), *relP relQ* (green), (p)ppGpp^0 (brown), JE2 (teal) and JE2 *rocF* (light blue) in CDM (a,d,g), CDM-P (b,e,h) and CDM-R (c,f,i) was measured every 15 min over 24 h at 37°C. Experiments were repeated three times with means and standard deviations plotted.

7.4 Long term growth and survival of (p)ppGpp synthetase mutants under urea and acid stress

Next, we sought to investigate how the stringent response effected long-term survival in various media under acid and urea stress. Over time the nutrients in the media will be used up resulting in starvation conditions. After around 4-5 h all of the glucose in TSB is used up and so bacteria must switch to secondary carbon sources (Somerville *et al.*, 2003). We have already seen that *relQ* mutants have impaired growth in CDM-R, whereas *relP*, *rel*$_{syn}$ and *relP rel*$_{syn}$ mutants grew better than WT (Fig. 7.3.2). Therefore, we hypothesised that the (p)ppGpp synthetase mutants may have altered survival under long-term starvation conditions. In *Mycobacterium tuberculosis*, the stringent response is required for long term survival and persistence (Primm *et al.*, 2000; Dahl *et al.,* 2003). We decided to investigate whether this is true for *S. aureus* as well, by using the single, double and triple (p)ppGpp

synthetase mutants, as well as a *codY* mutant. The *codY* mutant was included because in *S. aureus* most of the transcriptional changes seen during the stringent response are due to the derepression of CodY, therefore a *codY* mutant should have broadly the same transcriptional profile as the WT strain during the stringent response (Geiger *et al.*, 2012). We also hypothesised that RocF activity would be more important for long-term survival in acidic conditions than the 24 h experiments at neutral pH (Fig. 7.3.2). This is because RocF hydrolyses arginine to urea that can be used by the urease enzyme to produce NH_3 (Fig. 7.4). NH_3 is basic and thus acts to increase the pH of the environment. Therefore, the reduced arginase activity of the *relP* rel_{syn} mutant in CDM compared to WT and the interaction between RocF and Rel_{Sa} (possibly with RelP) may have more of an impact on survival in acidic conditions over long-term growth.

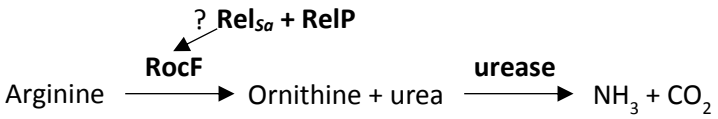

Fig. 7.4 Reaction scheme of RocF and urease catalysed reactions. Arginine is hydrolysed to citrulline and urea by RocF. Urease hydrolyses urea to NH_3 and CO_2 resulting in an increase in environmental pH. RelP interacts with Rel_{Sa} which can also bind to RocF but the impact on arginase activity is unclear.

The strains were grown in TSB, TSB acidified to pH 5.6 with HCl, human urine (HU) and synthetic human urine at pH 5.6 (SHU) for 72 h. These conditions were selected in order to investigate how low pH impacts on survival of the (p)ppGpp synthetase mutants. The stringent response is important for acid stress survival in *E. coli* and *H. pylori* (Kanjee *et al.*, 2011; Mourey *et al.*, 2006). Human urine was used because it is an environment in the human body with a low pH (usually around 5.6) with a high concentration of urea. Urea can protect against acid stress in *S. aureus* because the urease enzyme breaks urea down into ammonia which can neutralise excess protons in an acidic environment (Zhou *et al.*, 2019). SHU was used to reduce the variability seen with HU despite only using one donor, and because the composition of HU is unclear. The OD_{600} and CFU/ml were measured at 0, 8 24, 48 and 72 hours. An uninoculated culture (no cells) was included as a control for pH measurements to rule out effect the continued high temperature would have on the media pH.

7.4.1 Long term growth and survival in TSB

In TSB there was no significant difference between the CFU/ml recorded for each strain (Fig. 7.4.1a). Interestingly, there was no drop off in CFU/ml, even after 72 h. TSB is a nutrient rich broth and it could be that even after 72 h the nutrient levels had not depleted enough to impact survival. This could be tested by extending the experiment further to 96 h or beyond. As expected, the pH of the cultures dropped rapidly after 8 h growth as the glucose in the media was used up and acetate was produced

(Fig. 7.4.1b). The pH then rose steadily as the acetate in the media was used as a carbon source in the stationary phase. For clarity the pH changes of LAC*, *relP* rel_{syn} and (p)ppGpp^0 are presented separately in Fig. 7.4.1c. Although *relP* rel_{syn} and (p)ppGpp^0 showed the same pattern of acidification and de-acidification as the WT strain, the *relP* rel_{syn} culture had a significantly lower pH at 24 and 48 h compared to the WT (p = 0.0087 and p = 0.0092 respectively) and the (p)ppGpp^0 culture had a significantly higher pH at 24, 48 and 72 h (p = 0.0285; p < 0.0001 and p = 0.0019 respectively). However, ultimately, this pH difference did not affect the survival of either strain (Fig. 7.4.1a). After around 5 h growth the glucose in the TSB media will be depleted which should result in a release of CcpA repression and an increase in *rocF* expression. The arginase activity of *relP* rel_{syn} is lower than the WT in CDM (Fig. 7.2) which could explain the lower pH of this mutant after 8 hours.

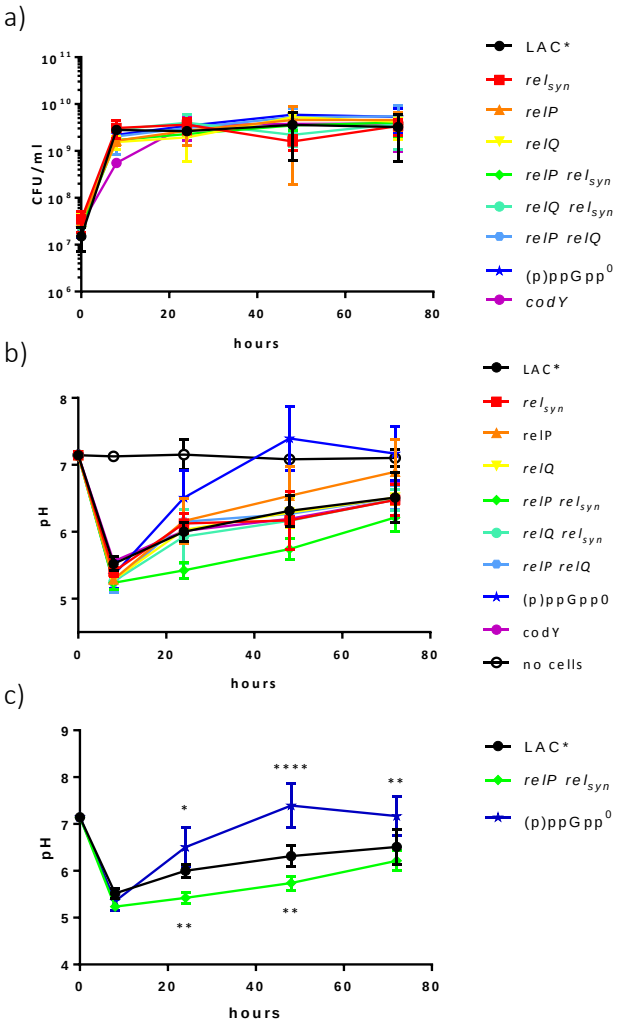

Fig. 7.4.1 Long term growth and survival in TSB. a) CFU/ml of LAC* (black), rel_{syn} (red), *relP* (orange), *relQ* (yellow), *relP* rel_{syn} (green), *relQ* rel_{syn} (turquoise), *relP relQ* (light blue), (p)ppGpp^0 (dark blue) and *codY* (purple). There was no significant difference between the strains. b) Culture pH of the strains listed in a), along with a control culture of no cells (empty black circle). c) Data from b) represented for clarity. The pH of the (p)ppGpp^0 (dark blue) culture was significantly higher than LAC* (black) after 24, 48 and 72 h. The pH of the *relP* rel_{syn} (green) culture was significantly lower than LAC* (black) after 24 and 48 h. Experiments performed three times, with means and standard deviations plotted. Two-way ANOVA was performed. * p < 0.05; ** p < 0.01; **** p < 0.0001

7.4.2 Long term growth and survival in TSB pH 5.6

In TSB pH 5.6 there was a significant difference in the CFU/ml of LAC* compared to *relP* rel_{syn} (Fig. 7.4.2a). The CFU/ml of the *relP* rel_{syn} culture was significantly lower after 48 and 72 h compared to the WT strain (p = 0.0123 and p = 0.0467 respectively) (Fig. 7.4.2b). There was also a significant difference in the culture pH of *relP* rel_{syn} and (p)ppGpp^0 cultures compared to the WT LAC* strain (Fig. 7.4.2c). A similar pH effect was seen as with TSB, in that the *relP* rel_{syn} culture had a significantly lower pH at 48 and 72 h compared to the WT (p = 0.0017 and p = 0.0003 respectively) and the (p)ppGpp^0 culture had a significantly higher pH at 48 (p = 0.0103) (Fig. 7.4.2d). The *relP* rel_{syn} strain is not able to increase the pH at all following the initial pH decrease following glucose consumption. This coincides with the decrease in CFU/ml at 24 and 48 h compared to LAC*. Only the *relP* rel_{syn} strain shows a survival defect in TSB pH 5.6, supporting our hypothesis that RocF activity has a greater impact on survival at low pH.

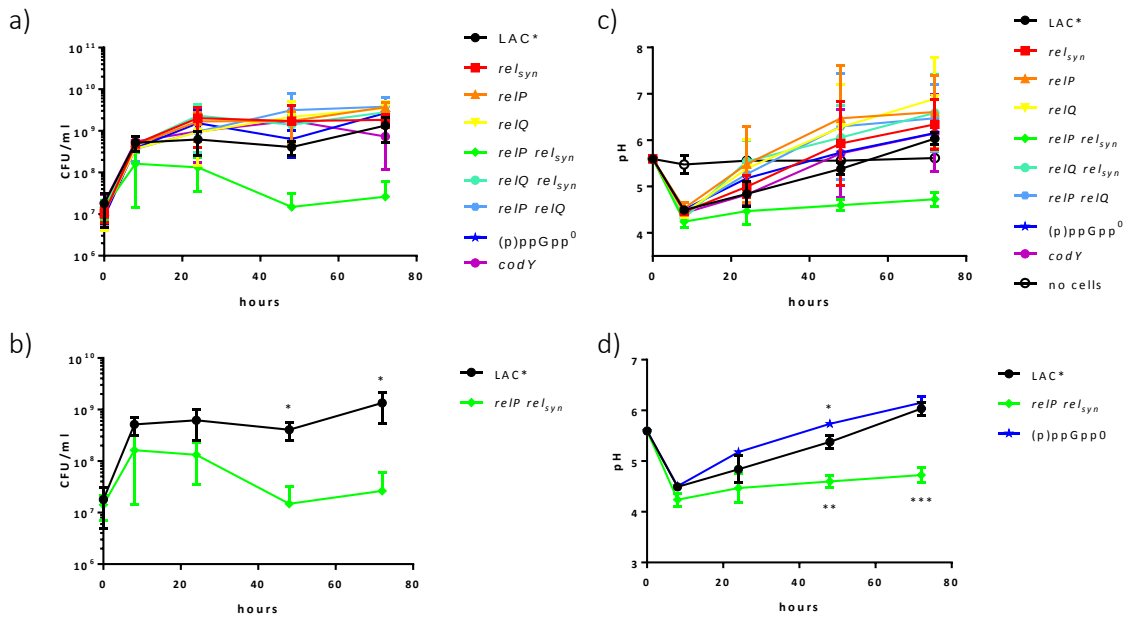

Fig. 7.4.2 Long term growth and survival in TSB pH 5.6. a) CFU/ml of LAC* (black), rel_{syn} (red), *relP* (orange), *relQ* (yellow), *relP* rel_{syn} (green), *relQ* rel_{syn} (turquoise), *relP relQ* (light blue), (p)ppGpp^0 (dark blue) and *codY* (purple). b) Culture pH of the strains listed in a), along with a control culture of no cells (empty black circle). c) Data from a) represented for clarity. The CFU/ml of the *relP* rel_{syn} (green) culture was significantly lower after 48 and 72 h. d) Data from b) represented for clarity. The pH of the (p)ppGpp^0 (dark blue) culture was significantly higher than LAC* (black) after 48 h. The pH of the *relP* rel_{syn} (green) culture was significantly lower than LAC* (black) after 48 and 72 h. Experiments were performed three times, with means and standard deviations plotted. Two-way ANOVA was performed. * $p < 0.05$; ** $p < 0.01$; *** $p < 0.001$

7.4.3 Long term growth and survival in HU

In HU only the *relP* rel_{syn} strain showed significantly different CFU/ml levels compared to LAC* (Fig. 7.4.3a). Interestingly, unlike with TSB and TSB pH 5.6, the CFU/ml counts declined for all strains after 24 h. This is most likely due to low nutrient levels in HU causing cell death. Equally, HU from a healthy

donor will have a low level of glucose and so the initial drop in pH seen with TSB and TSB pH 5.6 is not seen with HU (Fig. 7.4.3b). Instead the pH steadily increases from the starting point of around pH 6. Whilst the pH of the *relP* rel_{syn} culture was not significantly different to the WT, the CFU/ml was significantly lower at 24, 48 and 72 h ($p = 0.0377$; $p = 0.0002$ and $p = 0.0244$ respectively) (Fig. 6.6.3c). It seems that in HU the pH of the culture is not causing the cell death and perhaps it is due to an inability to scavenge nutrients from the depleted media. Although HU should theoretically have a high urea content and low glucose content this could vary from sample to sample and so we decided to use SHU to ensure consistency.

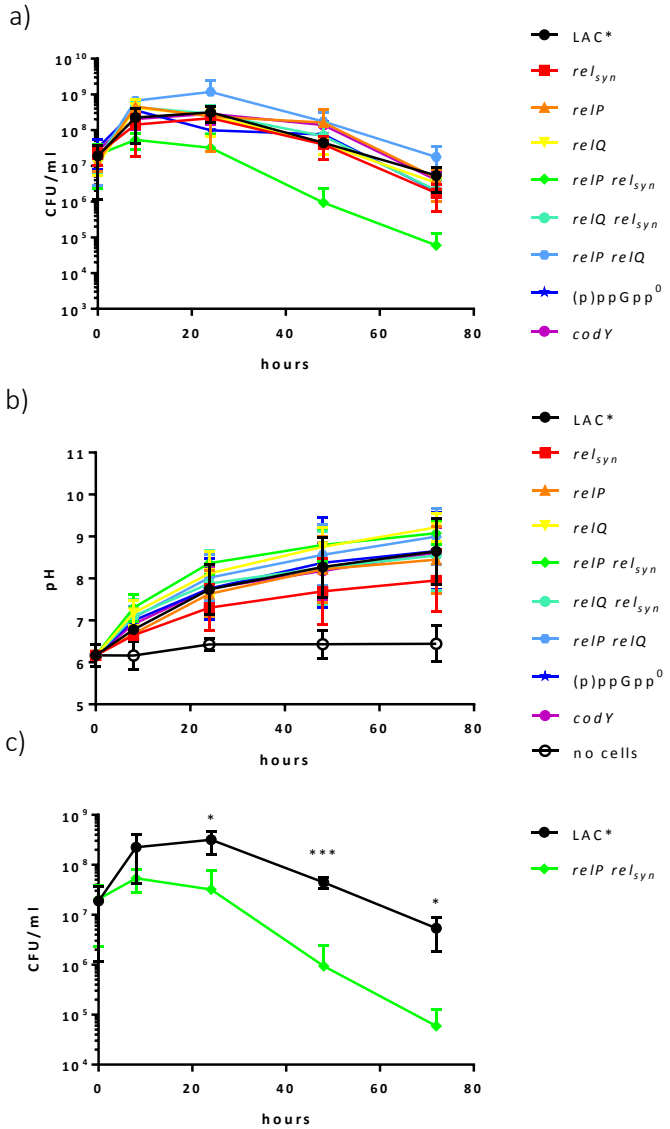

Fig. 7.4.3 Long term growth and survival in HU. a) CFU/ml of LAC* (black), rel_{syn} (red), *relP* (orange), *relQ* (yellow), *relP* rel_{syn} (green), *relQ* rel_{syn} (turquoise), *relP relQ* (light blue), (p)ppGpp^0 (dark blue) and *codY* (purple). b) Culture pH of the strains listed in a), along with a control culture of no cells (empty black circle). There was no significant difference between the strains. c) Data from a) represented for clarity. The CFU/ml of the *relP* rel_{syn} (green) culture was significantly lower after 24, 48 and 72 h. Experiments were performed four times, with means and standard deviations plotted. Two-way ANOVA was performed. * $p < 0.05$; *** $p < 0.001$

7.4.4 Long term growth and survival in SHU

The final medium used for the long term experiments was SHU, which is a chemically defined medium with 280 mM urea and no glucose (Ipe and Ulett, 2016). Again, only the *relP* rel_{syn} strain showed significantly different CFU/ml levels compared to LAC* (Fig. 7.4.4a). Just like with HU, the CFU/ml counts declined after 24 h due to low nutrient availability. SHU does not contain glucose and so the pH of the cultures did not decrease at 8 h and instead gradually rose (Fig. 7.4.4b). The CFU/ml of the *relP* rel_{syn} strain was significantly lower than the LAC* strain at 48 and 72 h ($p = 0.0395$ and $p = 0.0345$ respectively) (Fig. 7.4.4c). The pH of the *relP* rel_{syn} culture was higher than WT at 8, 24 and 48 h ($p = 0.0277$; $p = 0.0003$ and $p = 0.0005$ respectively) (Fig. 7.4.4d). There was no difference in pH with HU and it is unclear why there would be with SHU without knowing exactly how the two media differ in composition. It is interesting to note that although the *relP* rel_{syn} strain had a lower pH than WT in TSB and TSB pH 5.6, the opposite is true with SHU. This could be due to the high concentration of urea in the media, which could be more readily hydrolysed by the *relP* rel_{syn} strain.

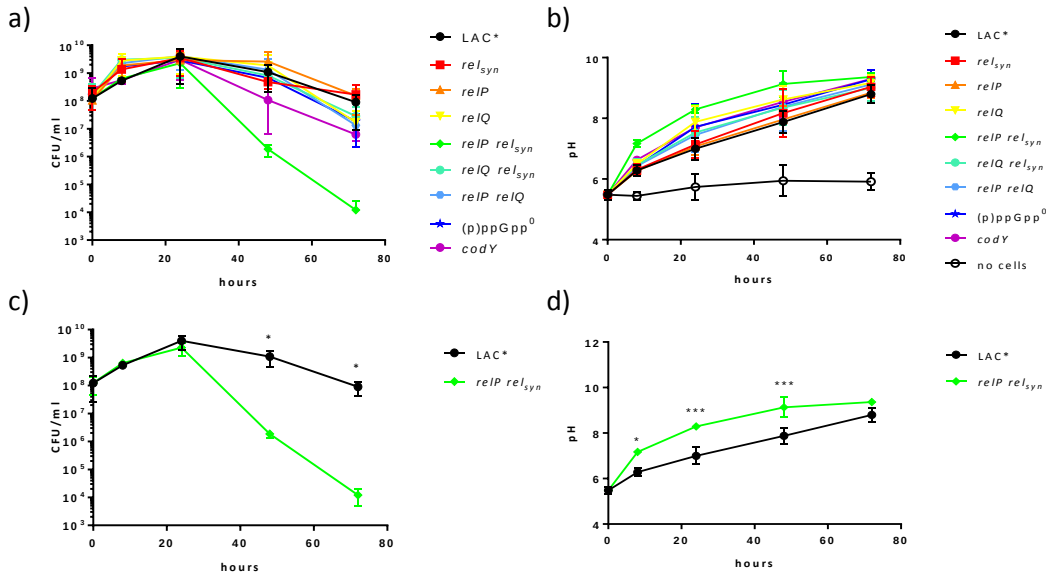

Fig. 7.4.4 Long term growth and survival in SHU. a) CFU/ml of LAC* (black), rel_{syn} (red), *relP* (orange), *relQ* (yellow), *relP* rel_{syn} (green), *relQ* rel_{syn} (turquoise), *relP relQ* (light blue), (p)ppGpp^0 (dark blue) and *codY* (purple). b) Culture pH of the strains listed in a), along with a control culture of no cells (empty black circle). c) Data from a) represented for clarity. The CFU/ml of the *relP* rel_{syn} (green) culture was significantly lower after 48 and 72 h. d) Data from b) represented for clarity. The pH of the *relP* rel_{syn} (green) culture was significantly higher than LAC* (black) after 8, 24 and 48 h. Experiments were performed three times, with means and standard deviations plotted. Two-way ANOVA was performed. * $p < 0.05$; *** $p < 0.001$

7.5 Using the bitLucopt system to investigate binding in different conditions

Next, we wanted to investigate whether the growth differences with the *relP* rel_{syn} double mutant seen in the various conditions reported in this chapter could be due to a change in the interactions of Rel_{Sa} and RocF. Using the bitLucopt system we focused on the novel Rel_{Sa} interactions outlined in

Chapter 5, along with the Rel_{Sa}-Rel_{Sa} interaction. The main advantage of the bitLucopt system is that it allows interactions to be investigated in the host organism. We hoped that this would allow us to investigate how interactions change during different conditions or stresses.

The luciferase activity of the bitLucopt strains was measured after growth in various chemically defined media (Fig. 7.5a). These media were CDMG (containing glucose), CDM (no glucose) and CDM-R (no glucose, no L-arg). There was no significant difference in LU/OD for any of the strains when grown in CDMG, CDM or CDM-R. This suggests that the availability of glucose and L-arg has no effect on the binding interactions between Rel_{Sa} and RocF, CshA and itself. The luciferase assay was also carried out using TSB, TSB acidified to pH 5.6, and SHU (Fig. 7.5b). The LU/OD for pAP118*relrel* was significantly higher in TSB than TSB pH 5.6 ($p = 0.0455$), however this was also the case for the positive control pAF259 ($p = 0.0395$) and so the change in LU/OD is probably not due to a change in Rel_{Sa}-Rel_{Sa} binding. The stress of the acidity could reduce transcription or translation resulting in a lower amount of luciferase tagged protein in the cell. The binding between RocF and Rel_{Sa} was not altered by low pH, high urea, glucose starvation or arginine starvation. However, it is still possible that the impact of the interaction is altered in different conditions based on binding of other ligands such as (p)ppGpp.

7.6 Urease activity of (p)ppGpp synthetase mutants

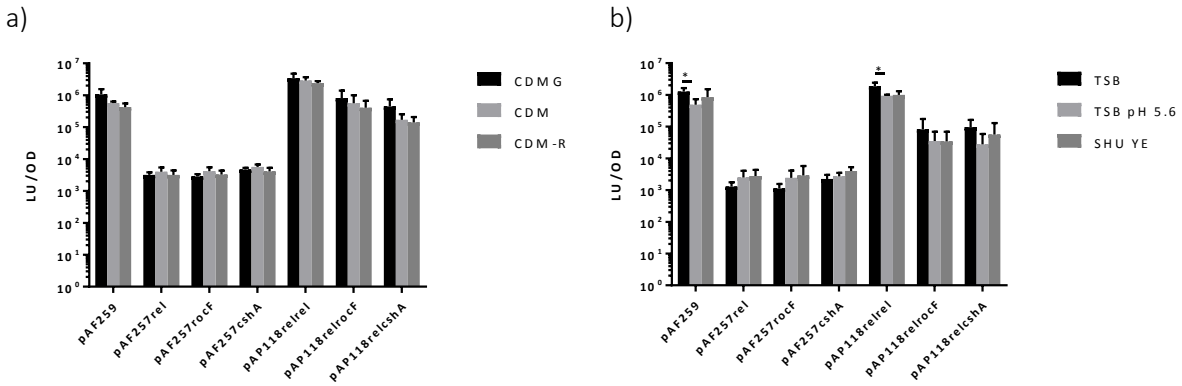

Fig. 7.5 The effect of different media on Rel_{Sa} binding to its partners. a) Luciferase activity per OD (LU/OD) of bitLucopt strains grown in CDMG (black), CDM (light grey) or CDM-R (dark grey). There is no significant difference in LU/OD in strains grown in CDMG, CDM or CDM-R. This experiment was performed three times, with means and standard deviations plotted. b) Luciferase activity per OD (LU/OD) of bitLucopt strains grown in TSB (black), TSB pH 5.6 (light grey) or SHU (dark grey). LU/OD is significantly lower when LAC* pAF259 and LAC* pAP118relrel are grown in TSB pH 5.6 compared to TSB. This experiment was performed three times, with means and standard deviations plotted. Statistical significance tested by unpaired T tests * $p < 0.05$

Following the observations of abnormal pH regulation in the *relP* rel_{syn} strain and that in SHU the *relP* rel_{syn} strain had a higher culture pH than LAC*, we next investigated the urease activity of the (p)ppGpp synthetase mutants. As discussed, urease activity is used as a mechanism to increase extracellular pH through the production of ammonia. In acidic conditions ammonia becomes protonated to

ammonium, reducing the pH of the environment. Urea can protect against weak acid stress due to the activity of urease (Zhou *et al.*, 2019).

Here we used Christensen's agar (1.5% agar, 0.2% KH_2PO_4, 0.1% peptone, 0.5% NaCl, 0.0012% phenol red and 2% urea) with and without 0.1% glucose to assess urease activity. Strains were grown overnight, normalised to the same OD_{600}, plated on to the agar and incubated for 16 h. If urea was hydrolysed into ammonia the pH indicator phenol red turned from yellow to pink. To ensure the change in pH was due to urea hydrolysis not, for example, due to glucose fermentation a control plate without urea was used. No colour change was seen on plates without urea, whether they contained glucose or not (data not shown), indicating that any colour changes on urea containing plates was indeed due to urea hydrolysis. *E. coli* was used as a negative control because it does not have the urease enzyme.

On agar containing urea and glucose, all *S. aureus* strains tested showed some level of urease activity (Fig. 7.6a). In order to attempt to compare the urease activity of the (p)ppGpp synthetase mutants, the area of the pink 'halo' was divided by the area of the inner culture spot meaning that a spot with no halo had a value of 1 (Fig. 7.6b). This quantification was only performed with the plates containing glucose because the urease activity on the plates without glucose was too low to produce 'halos'. The urease activity of *rel*$_{syn}$, *relQ*, *relP rel*$_{syn}$ and *relQ rel*$_{syn}$ was significantly lower that the WT strain (p = 0.0319; p = 0.0098; p = 0.0247 and p = 0.0467 respectively). Interestingly, there was no significant difference between the LAC* and (p)ppGpp^0 strains, suggesting that the stringent response is not essential for urease expression or activity.

Without glucose, only the *relP rel*$_{syn}$ strain showed any urease activity (Fig. 7.6c). This may explain the higher pH seen during long term growth in SHU for *relP rel*$_{syn}$ compared to LAC* (Fig. 7.4.4d). SHU contains urea but not glucose and based on the results presented here we would expect the WT strain to have no urease activity and the *relP rel*$_{syn}$ strain to have some urease activity in these conditions. As such, the *relP rel*$_{syn}$ would be able to increase the pH of the media more than the WT strain.

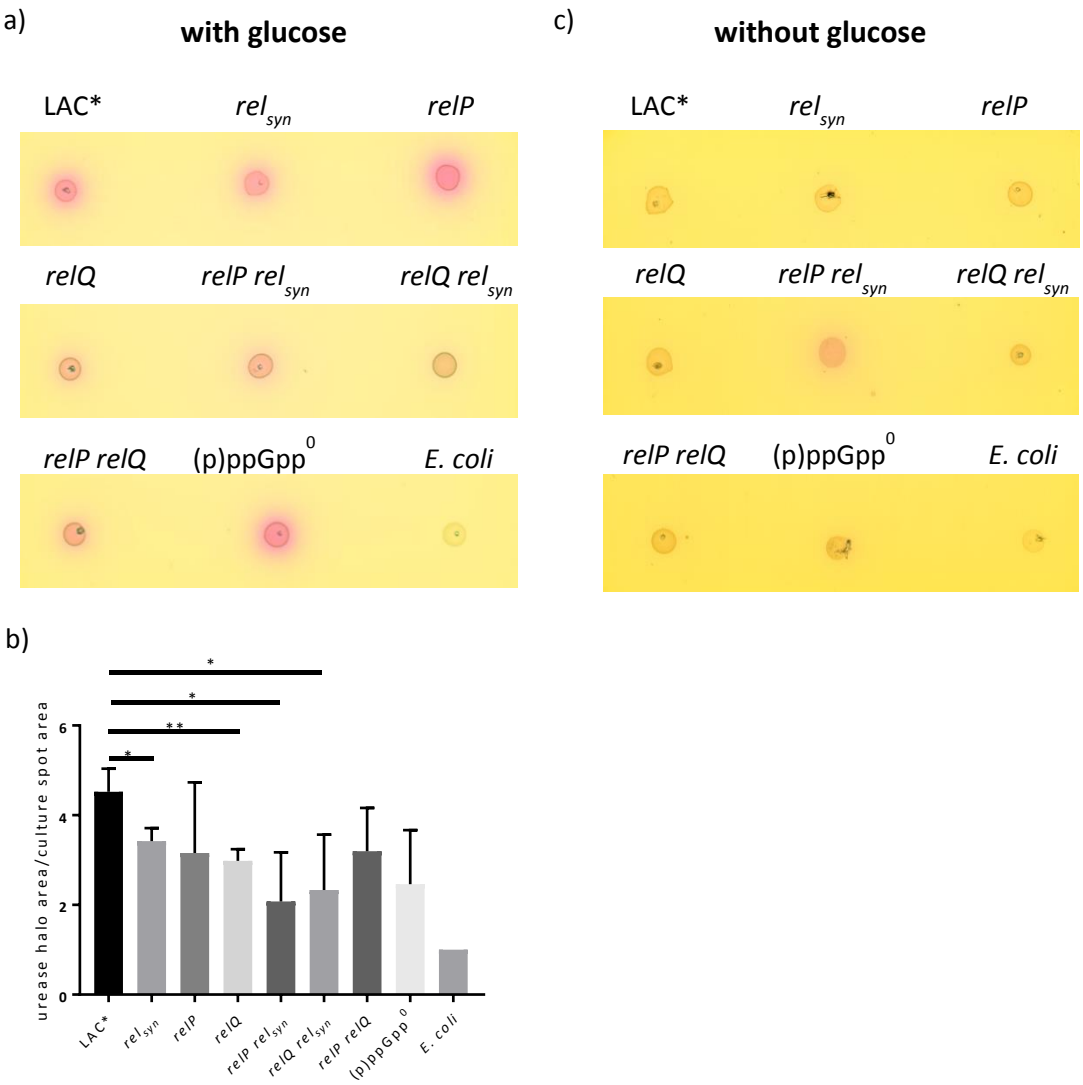

Fig. 7.6 Urease activity of (p)ppGpp synthetase mutants. Representative images of growth on Christensen's agar with 2% urea and a) with 0.1% glucose or b) without glucose. As urea is hydrolysed to ammonia the pH increases and the pH indicator phenol red changes colour from yellow to pink. a) all strains showed urease activity except the *E. coli* negative control. b) without glucose in the agar most strains did not show any urease activity. The *relP* rel_{syn} strain showed minor urease activity. c) quantification of urease activity with glucose. The urease activity of rel_{syn}, *relQ*, *relP* rel_{syn} and *relQ* rel_{syn} was significantly lower that the WT strain. Experiments were performed three times, with means and standard deviations plotted. Statistical significance tested by multiple T tests * $p < 0.05$; ** $p < 0.01$

7.7 Discussion

In this chapter we have shown that the stringent response plays a role in several aspects of the urea cycle, namely arginine biosynthesis, urease activity and arginase activity.

Arginine biosynthesis in CDM-R appears to be influenced by all three (p)ppGpp synthetases. The *relP* rel_{syn} double mutant, *relP* and rel_{syn} single mutants grew better in CDM-R than the WT strain, suggesting that both RelP and Rel_{Sa} are involved in repressing conversion of proline to arginine in the absence of glucose (Fig. 7.3.2c). Strains with a *relQ* mutation did not grow in CDM-R, probably because

repression of arginine biosynthesis enzymes by CcpA was not released (Fig. 7.3.2f). We proposed that RelQ acts to activate arginine biosynthesis, presumably through transcriptional regulation based on (p)pppGpp or GTP levels, whilst RelP and Rel_{Sa} act to inhibit this activation by RelQ (Fig. 7.7a). RocF was shown to bind to Rel_{Sa} in the presence and absence of L-arg and glucose and could act with RelP and Rel_{Sa} to regulate RelQ activation of arginine biosynthesis. As Rel_{Sa} binds to L-arg, it is possible that the Rel_{Sa}-RocF interaction acts as a sensor of arginine levels, with the biological role of the interaction changing depending on whether L-arg is bound.

The urease activity of the *relP* rel_{syn} mutant was higher than all the other strains tested in the absence of glucose (Fig. 7.6c). This phenotype required the presence of RelQ because the (p)ppGpp^0 strain has WT levels of urease activity in the absence of glucose (Fig. 7.6c). We suggest that RelQ positively regulates urease activity whilst RelP and Rel_{Sa} act independently to inhibit this positive regulation by RelQ (Fig. 7.7b). RelP and Rel_{Sa} must act independently because a single mutation does not alter the urease activity of the strain.

The arginase activity of *relP* rel_{syn} in CDM was significantly lower than WT however this did not seem to affect the growth of *relP* rel_{syn} in CDM-P which was the same as the WT strain (Fig. 7.2 and Fig. 7.3.2b). It seems that the level of arginase activity *relP* rel_{syn} has is sufficient to synthesise enough proline for growth in CDM-P. We hypothesise that RelQ negatively regulates RocF activity, most likely on a transcriptional level, either through altered (p)ppGpp or GTP levels. Furthermore, we hypothesise that RelP and Rel_{Sa} act independently to inhibit this negative regulation by RelQ (Fig. 7.7c). On the Biolog PM plates both the *hflX* and the (p)ppGpp^0 strains grew equally well with both L-arg and L-pro as a carbon source and it would be interesting to see if the same is true for a *relP* rel_{syn} double mutant.

The factor that links urease activity, arginase activity and arginine biosynthesis is CcpA. CcpA represses *rocF* expression in the presence of glucose and in the absence of glucose the repression is released. CcpA also represses the expression of *putA*, *rocD* and other arginine biosynthesis genes in the presence of glucose. However, this repression is not completely released in the absence of glucose because WT *S. aureus* strains do not grow well in CDM-R. CcpA positively regulates the expression of *ure* genes in the presence of glucose, presumably to help counteract the acidification of the environment during glucose metabolism. CcpA regulation of arginase, arginine biosynthesis and urease genes may be influenced by RelQ although the mechanism for this is not clear. In *Streptococcus suis,* RelA is required for full CcpA derepression of certain genes without glucose, including *arcABC*, and so there is precedent for CcpA regulation by the stringent response (Zhang *et al.*, 2016).

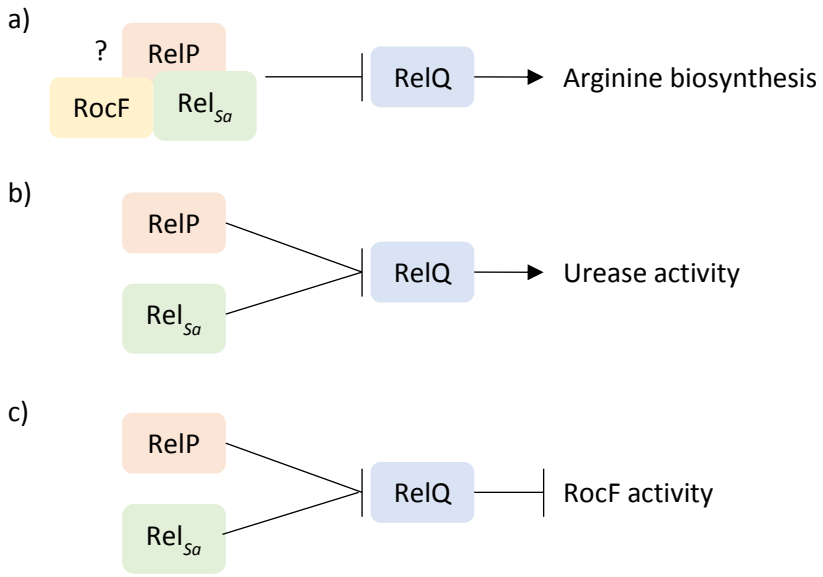

Fig. 7.7 Proposed regulation of arginine biosynthesis, urease activity and RocF activity by the stringent response in *S. aureus*. a) RelQ positively regulates arginine biosynthesis. RelP and Rel_{Sa} act together, perhaps in complex with RocF to inhibit this positive regulation by RelQ. b) RelQ positively regulates urease activity. RelP and Rel_{Sa} act independently to inhibit this positive regulation by RelQ. c) RelQ negatively regulates RocF activity. RelP and Rel_{Sa} act independently to inhibit this negative regulation by RelQ.

Long term growth survival was not affected by (p)ppGpp synthetase mutations unless the media was acidic, indicating that the stringent response may play a role in survival of acidic conditions. The *relP* rel_{syn} double mutant showed lower CFU/ml counts during long term growth in acidic media (TSB pH 5.6, HU and SHU) and abnormal pH readings in TSB, TSB pH 5.6 and SHU. In media which do not contain urea (TSB and TSB pH 5.6) the *relP* rel_{syn} cultures had a significantly lower pH that the WT cultures. However, in SHU which contains urea, the pH of the *relP* rel_{syn} cultures was significantly higher than the WT cultures. This could be due to the high level of urease activity *relP* rel_{syn} has without glucose (Fig. 7.6c).

Here, we use the bitLucopt system that was developed in *C. difficile* in *S. aureus* to investigate binding partners in the native host, where conditions for certain interactions may be preferential. We showed that this system can be used to assess the effect of different conditions and stresses on protein-protein interactions. However, some conditions also altered the luciferase activity of the control strains showing that not all conditions can be tested this way. The read out of luminescence is not a direct readout of the binding strength and therefore changes in transcription and translation levels could also impact it. This should be considered when using the bitLucopt system in this way and the appropriate controls should be included.

The experiments here have highlighted the complexity of the stringent response in *S. aureus* and how the three (p)ppGpp synthetases have nuanced roles in the regulation of certain aspects of metabolism. Particularly, the phenotypic difference between the *relP* rel_{syn} double mutant and the (p)ppGpp triple mutant suggests that there is some form of regulation between RelQ and RelP/Rel_{Sa} that would be interesting to investigate further.

S. aureus can colonise various acidic niches in the human host such as the vagina and the skin (Wagner and Ottesen, 1982; Ehlers *et al.*, 2001). The urinary tract is also acidic with a high concentration of urea (Spector *et al.*, 2007). Abscesses caused by *S. aureus* infection have a low pH, low glucose levels and are also predicted to have low arginine levels (Halsey *et al.*, 2017). Low arginine levels are predicted based on the activity of the host inducible nitric oxide synthetase, the action of host cell immunity and host arginase activity (Fang, 1997; Ochoa *et al*., 2001; Shi *et al.*, 2003). Therefore, in the abscess, arginine biosynthesis from proline is important for survival and so understanding the role of the stringent response in this process may help to tackle *S. aureus* infections.

Chapter 8 – Discussion

The stringent response in bacteria has been shown to play a role in a wide variety of bacterial processes including virulence, resistance, persistence and the survival of stress conditions. The stringent response in *S. aureus* is of particular interest because it is a Gram positive pathogen. The regulation of the stringent response in Gram positive bacteria is less well characterised than that of Gram negative bacteria. The stringent response has been linked to chronic infections as well as increased β-lactam resistance in MRSA strains (Gao *et al.*, 2003; Mwangi *et al*., 2013). As such, research into the stringent response in *S. aureus* could prove important in tackling this dangerous pathogen. The stringent response in *S. aureus* is mediated by three RSH-superfamily enzymes, Rel_{Sa}, RelP and RelQ. In this study, we focused on investigating how the activity of these enzymes is regulated on a transcriptional and post-transcriptional level, as well as the role the stringent response plays in growth and survival in various growth conditions.

Using promoter-*lacZ* fusions we have shown that the promoter activities of *relP* and *relQ* are differentially regulated during growth (Fig. 3.4). The promoter activity of *relP* peaked during late exponential phase, whereas *relQ* promoter activity peaked in exponential phase. These results corresponded well with experiments in *B. subtilis* (Nanamiya *et al.*, 2008). Any effect of the stringent response on the cell cycle in *S. aureus* is not mediated through transcriptional control of the *rel* gene as there was no change in *rel* promoter activity throughout growth. However, the effect of increased transcription of *relP* and *relQ* is unclear, given that *relP* and *relQ* single or double mutants showed no growth defect during growth over 8 h or abnormal transition from exponential phase to stationary phase.

The activity of the *rel* promoter was also unaffected by any of the stresses tested here, such as cell-wall active antibiotics or cerulenin (Fig. 3.5). This suggests that Rel_{Sa}-dependent (p)ppGpp accumulation following mupirocin treatment, for example, is not regulated transcriptionally but through direct regulation of the Rel_{Sa} protein. The transcription from *relP* and *relQ* promoters was induced by cell wall active antibiotics, in line with previous work on the transcriptional regulation of SAS genes in *S. aureus* (Geiger *et al.,* 2014). The activity of the *relP* promoter was also induced by human serum and it would be interesting to investigate which factors present in serum are required to trigger this response. The Biolog experiments indicated that the stringent response is required for optimum metabolism with various nutrient sources. In particular, the uses of various nitrogenous compounds as a nitrogen source depends on a complete stringent response (Fig. 4.2.2). This is probably mediated through a change in transcriptional profile, however it would be interesting to investigate how nitrogen starvation triggers the stringent response in *S. aureus.* In *E. coli*, the central

nitrogen starvation response regulator, NtrC, regulates the transcription of *relA* and *spoT* (Brown *et al.,* 2014). However, NtrC is not present in *S. aureus* and so during nitrogen starvation the stringent response may not be regulated through transcriptional regulation of *rel* (Amon *et al.,* 2010).

We have shown a novel interaction between the HD domain of Rel_{Sa} and RelP using a targeted BACTH approach (Fig. 5.2.2), however the biological function of this interaction is unclear. RelP reduced the GTP hydrolysis activity of Rel_{Sa} after 5 min but there was no significant difference in GTP hydrolysis after 1 h (Fig. 6.5.1). The interaction may impact the (p)ppGpp synthesis activity of either RelP or Rel_{Sa}, however this was not investigated here.

Other RelP interaction partners were identified, including a 30S ribosomal protein, S1 (Table 5.3.3b). Currently, there has not been any reported interaction between the ribosome and any SAS protein. Given that the ribosome is a key inducer of (p)ppGpp synthesis by RelA in *E. coli*, following up on this interaction could elucidate a mechanism for RelP regulation.

In addition, Rel_{Sa} binding partners CshA and RocF were identified and confirmed using targeted BACTH and the bitLucopt systems (Fig. 5.4.1.1 and Fig. 5.4.3). Of particular interest was the interaction between Rel_{Sa} and the arginase, RocF, and this interaction was confirmed using a pulldown experiment (Fig. 5.4.2). BACTH analysis of how RocF binds to Rel_{Sa} did not narrow down binding to a single domain. The interaction between RocF and Rel_{Sa} does not affect the arginase (Fig. 6.4) or hydrolysis (Fig. 6.5.1 and 6.5.2) activity of each protein respectively and so the biological function is unclear. However, the effect of RocF on Rel_{Sa} (p)ppGpp synthesis activity has not yet been tested. The interaction was stronger in the presence of ppGpp suggesting that it would also be stronger during the stringent response. If the interaction does affect (p)ppGpp synthesis it could be used as a signal to amplify or end the stringent response depending on how the activity is affected.

The genome fragment BACTH screen used here was not used exhaustively, and so we are hopeful that other (p)ppGpp synthetase interaction partners could be identified using this method. However, confirming the interactions already identified would also be interesting, such as the interaction between RelP and the small ribosomal protein S1. Whilst the BACTH method focuses on protein-protein interactions, RelP is mostly likely also allosterically regulated by a small ligand. The cleft formed by the RelQ tetramer, that is required for allosteric regulation by (p)ppGpp, is conserved in RelP. The small ligand binding partner of RelP is likely to be more positively charged than (p)ppGpp due to the charge of the cleft itself. We have shown that RelP does not bind to L-arg but it may interact with other positively charged amino acids.

We have shown that L-Arg can bind to Rel_{Sa} specifically and preferentially to other amino acids (Fig. 6.3). Although this binding had no impact on the hydrolysis activity of Rel_{Sa}, it would be interesting to see if it has any effect of (p)ppGpp synthesis activity. We hypothesise that L-Arg binding could cause dimerisation of Rel_{Sa} by bringing two ACT domains together (Fig. 8.1). This could potentially inhibit the (p)ppGpp synthesis activity of Rel_{Sa}, as seen in other organisms such as *M. tuberculosis* (Avarbock *et al.*, 2005). Alternatively, L-Arg binding could release intrinsic inhibition of the SYNTH domain by the CTD as seen in *S. equisimilis* (Mechold *et al.*, 2002). It is also possible that RocF 'presents' L-Arg to Rel_{Sa} as a mechanism for sensing L-Arg availability in the cell. This hypothesis could be investigated by examining how the interaction between Rel_{Sa} and RocF or L-Arg changes in the presence of the other ligand. Furthermore, ArgR DNA binding increases in the presence of arginine and so the ArgR repression of *rel* (Fig. 3.6) may be regulated by arginine concentration in the cell (Fig. 8.1).

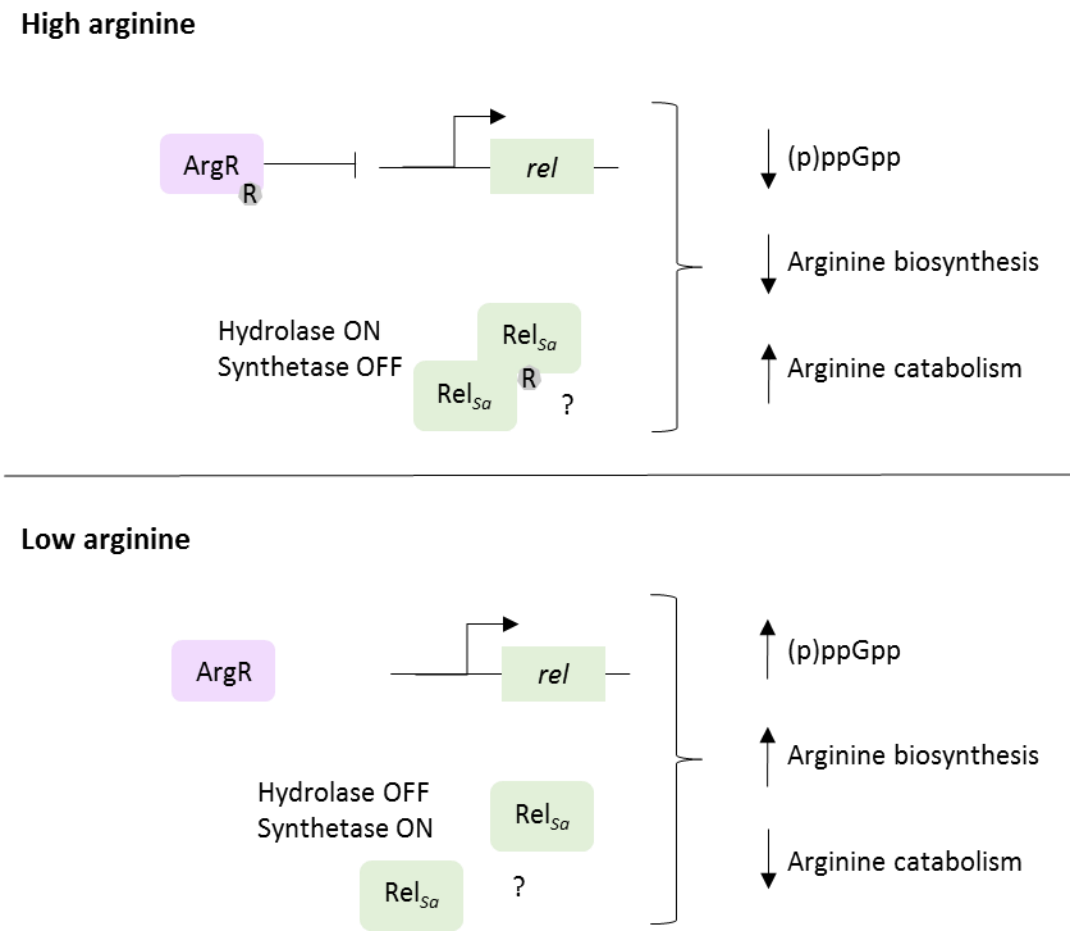

Fig. 8.1 Model for Rel_{Sa} regulation in the presence of high or low arginine levels. When the level of arginine (grey) is high it may bind to ArgR, preventing the transcription of *rel*. Arginine binds to Rel_{Sa} and may cause it to dimerise resulting in a hydrolase ON synthetase OFF state. This would result in a decrease in (p)ppGpp in the cell and may favour arginine catabolism over arginine biosynthesis. When arginine levels are low the stringent response could be induced through derepression of *rel* expression and release of the Rel_{Sa} dimer. This could switch arginine metabolism to favour biosynthesis over catabolism.

Whilst the activity of RocF was not altered by the presence of Rel_{Sa} under the conditions tested *in vitro*, the stringent response enzymes do influence the RocF activity of *S. aureus* lysates (Fig. 7.2). We have hypothesized that RelQ downregulates arginase activity on a transcriptional level through changes in (p)ppGpp or GTP levels, while RelP and Rel_{Sa} inhibit this regulation. In this way, we also have shown that urease (Fig. 7.6) and arginine biosynthesis (Fig. 7.3) activity is regulated by the stringent response. RelQ seems to upregulate urease and arginine biosynthesis activity, while RelP and Rel_{Sa} inhibit this regulation. Given the urease, arginase and arginine biosynthesis genes are regulated by the carbon catabolite repressor, CcpA, it seems likely that the stringent response is involved in regulating CcpA activity in the absence of glucose.

The phenotypic differences between the *relP* rel_{syn} double mutant and the WT and (p)ppGpp^0 suggests that the control of the stringent response is more complex than previously thought. The role of RelQ appears to be different depending if RelP and Rel_{Sa} are present, which could be due to regulation between the synthetases themselves. We have already shown an interaction between RelP and Rel_{Sa} and other direct or indirect interactions may also occur. It would also be interesting to compare the phenotype of the WT, *relP* rel_{syn} double mutant and (p)ppGpp mutant with a strain with a high level of (p)ppGpp (through overexpression of a synthetase).

In *S. aureus,* the stringent response does not appear to be involved in long term survival unless the medium is acidic. In acidic media the *relP* rel_{syn} double mutant shows reduced long term survival and dysfunctional pH homeostasis. This mutant also showed higher urease activity and lower arginase activity in the absence of glucose than the WT which may explain the difference seen between the culture pH of the *relP* rel_{syn} double mutant compared to the WT strain.

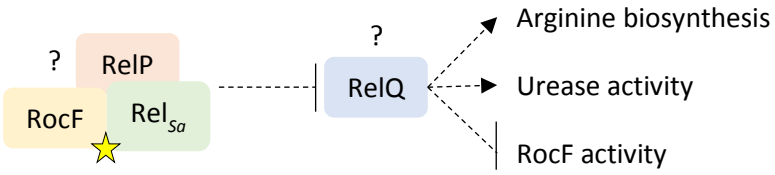

Fig. 8.2 Stringent response regulation of arginine biosynthesis, urease activity and RocF activity. RelQ (blue) could activate arginine biosynthesis and urease activity but inhibit RocF activity. This activity may be modulated by RocF (yellow), RelP (red) and Rel_{Sa} (green). RelP and Rel_{Sa} interact as do RocF and Rel_{Sa} with this binding increased by the presence of ppGpp (yellow star).

In conclusion, here we have provided new insights into the regulation of the stringent response in *S. aureus*. We have shown that the three synthetase genes are transcriptionally regulated by multiple factors and discovered several protein binding partners of Rel_{Sa} and RelP. The identification of the Rel_{Sa}-RocF interaction guided us to investigate the role of the stringent response in arginine

metabolism in *S. aureus*. We hope that the other (p)ppGpp synthetase interaction partners detailed in this study will also help to direct future research in the stringent response in *S. aureus*.

References

Abranches, J., Martinez, A.R., Kajfasz, J.K., Chavez, V., Garsin, D.A., and Lemos, J.A. (2009). The molecular alarmone (p)ppGpp mediates stress responses, vancomycin tolerance, and virulence in *Enterococcus faecalis*. J Bacteriol *191*, 2248-2256.

Ackermann, R.J., and Monroe, P.W. (1996). Bacteremic Urinary Tract Infection in Older People. J Am Geriatr Soc *44*, 8.

Amon, J., Titgemeyer, F., and Burkovski, A. (2010). Common patterns - unique features: nitrogen metabolism and regulation in Gram-positive bacteria. FEMS Microbiol Rev *34*, 588-605.

Anderson, K.L., Roberts, C., Disz, T., Vonstein, V., Hwang, K., Overbeek, R., Olson, P.D., Projan, S.J., and Dunman, P.M. (2006). Characterization of the *Staphylococcus aureus* Heat Shock, Cold Shock, Stringent, and SOS Responses and Their Effects on Log-Phase mRNA Turnover†. In J Bacteriol, pp. 6739-6756.

Anderson, K.L., Roux, C.M., Olson, M.W., Luong, T.T., Lee, C.Y., Olson, R., and Dunman, P.M. (2010). Characterizing the Effects of Inorganic Acid and Alkaline Shock on the *Staphylococcus aureus* Transcriptome and Messenger RNA Turnover. FEMS Immunol Med Microbiol *60*, 208-250.

Andresen, L., Tenson, T., and Hauryliuk, V. (2016a). Cationic bactericidal peptide 1018 does not specifically target the stringent response alarmone (p)ppGpp. Sci Rep *6*, 36549.

Andresen, L., Varik, V., Tozawa, Y., Jimmy, S., Lindberg, S., Tenson, T., and Hauryliuk, V. (2016b). Auxotrophy-based High Throughput Screening assay for the identification of *Bacillus subtilis* stringent response inhibitors. Sci Rep *6*, 35824.

Aravind, L., and Koonin, E.V. (1998). The HD domain defines a new superfamily of metal-dependent phosphohydrolases. Trends Biochem Sci *23*, 469-472.

Arenz, S., Abdelshahid, M., Sohmen, D., Payoe, R., Starosta, A.L., Berninghausen, O., Hauryliuk, V., Beckmann, R., and Wilson, D.N. (2016). The stringent factor RelA adopts an open conformation on the ribosome to stimulate ppGpp synthesis. Nucleic Acids Res *44*, 6471-6481.

Atkinson, G.C., Tenson, T., and Hauryliuk, V. (2011). The RelA/SpoT homolog (RSH) superfamily: distribution and functional evolution of ppGpp synthetases and hydrolases across the tree of life. PLoS One *6*, e23479.

Avarbock, A., Avarbock, D., Teh, J.S., Buckstein, M., Wang, Z.M., and Rubin, H. (2005). Functional regulation of the opposing (p)ppGpp synthetase/hydrolase activities of RelMtb from *Mycobacterium*

tuberculosis. Biochemistry *44*, 9913-9923.

Avarbock, D., Avarbock, A., and Rubin, H. (2000). Differential regulation of opposing RelMtb activities by the aminoacylation state of a tRNA.ribosome.mRNA.RelMtb complex. Biochemistry *39*, 11640-11648.

Baba, T., Bae, T., Schneewind, O., Takeuchi, F., and Hiramatsu, K. (2008). Genome sequence of *Staphylococcus aureus* strain Newman and comparative analysis of staphylococcal genomes: polymorphism and evolution of two major pathogenicity islands. J Bacteriol *190*, 300-310.

Bae, T., Glass, E.M., Schneewind, O., and Missiakas, D. (2008). Generating a collection of insertion mutations in the *Staphylococcus aureus* genome using bursa aurealis. Methods Mol Biol *416*, 103-116.

Basu, A., and Yap, M.N. (2017). Disassembly of the *Staphylococcus aureus* hibernating 100S ribosome by an evolutionarily conserved GTPase. Proc Natl Acad Sci U S A *114*, E8165-e8173.

Battesti, A., and Bouveret, E. (2006). Acyl carrier protein/SpoT interaction, the switch linking SpoT-dependent stress response to fatty acid metabolism. Mol Microbiol *62*, 1048-1063.

Battesti, A., and Bouveret, E. (2009). Bacteria possessing two RelA/SpoT-like proteins have evolved a specific stringent response involving the acyl carrier protein-SpoT interaction. J Bacteriol *191*, 616-624.

Beaman, T.C., Hitchins, A.D., Ochi, K., Vasantha, N., Endo, T., and Freese, E. (1983). Specificity and control of uptake of purines and other compounds in *Bacillus subtilis*. J Bacteriol *156*, 1107-1117.

Behr, S., Kristoficova, I., Witting, M., Breland, E.J., Eberly, A.R., Sachs, C., Schmitt-Kopplin, P., Hadjifrangiskou, M., and Jung, K. (2017). Identification of a High-Affinity Pyruvate Receptor in *Escherichia coli*. Sci Rep *7*, 1388.

Beljantseva, J., Kudrin, P., Andresen, L., Shingler, V., Atkinson, G.C., Tenson, T., and Hauryliuk, V. (2017). Negative allosteric regulation of *Enterococcus faecalis* small alarmone synthetase RelQ by single-stranded RNA. Proc Natl Acad Sci U S A *114*, 3726-3731.

Bhattacharya, M., Wozniak, D.J., Stoodley, P., and Hall-Stoodley, L. (2015). Prevention and treatment of *Staphylococcus aureus* biofilms. Expert Rev Anti Infect Ther *13*, 1499-1516.

Bischoff, M., Dunman, P., Kormanec, J., Macapagal, D., Murphy, E., Mounts, W., Berger-Bachi, B., and Projan, S. (2004). Microarray-based analysis of the *Staphylococcus aureus* sigmaB regulon. J Bacteriol *186*, 4085-4099.

Bischoff, M., Entenza, J.M., and Giachino, P. (2001). Influence of a functional sigB operon on the global

regulators sar and agr in *Staphylococcus aureus*. J Bacteriol *183*, 5171-5179.

Boisset, S., Geissmann, T., Huntzinger, E., Fechter, P., Bendridi, N., Possedko, M., Chevalier, C., Helfer, A.C., Benito, Y., Jacquier, A*., et al.* (2007). *Staphylococcus aureus* RNAIII coordinately represses the synthesis of virulence factors and the transcription regulator Rot by an antisense mechanism. Genes Dev *21*, 1353-1366.

Boles, B.R., Thoendel, M., Roth, A.J., and Horswill, A.R. (2010). Identification of genes involved in polysaccharide-independent *Staphylococcus aureus* biofilm formation. PLoS One *5*, e10146.

Boniecka, J., Prusińska, J., Dąbrowska, G.B., and Goc, A. (2017). Within and beyond the stringent response-RSH and (p)ppGpp in plants. In Planta, pp. 817-842.

Boutte, C.C., and Crosson, S. (2013). Bacterial lifestyle shapes stringent response activation. Trends Microbiol *21*, 174-180.

Bracher, S., Guerin, K., Polyhach, Y., Jeschke, G., Dittmer, S., Frey, S., Bohm, M., and Jung, H. (2016). Glu-311 in External Loop 4 of the Sodium/Proline Transporter PutP Is Crucial for External Gate Closure. J Biol Chem *291*, 4998-5008.

Bronner, S., Monteil, H., and Prevost, G. (2004). Regulation of virulence determinants in *Staphylococcus aureus*: complexity and applications. FEMS Microbiol Rev *28*, 183-200.

Brown, A., Fernandez, I.S., Gordiyenko, Y., and Ramakrishnan, V. (2016). Ribosome-dependent activation of stringent control. Nature *534*, 277-280.

Brown, D.R., Barton, G., Pan, Z., Buck, M., and Wigneshweraraj, S. (2014). Nitrogen stress response and stringent response are coupled in *Escherichia coli*. Nat Commun *5*, 4115.

Brunskill, E.W., and Bayles, K.W. (1996). Identification and molecular characterization of a putative regulatory locus that affects autolysis in *Staphylococcus aureus*. J Bacteriol *178*, 611-618.

Bugg, T.D., Wright, G.D., Dutka-Malen, S., Arthur, M., Courvalin, P., and Walsh, C.T. (1991). Molecular basis for vancomycin resistance in Enterococcus faecium BM4147: biosynthesis of a depsipeptide peptidoglycan precursor by vancomycin resistance proteins VanH and VanA. Biochemistry *30*, 10408-10415.

Burda, W.N., Miller, H.K., Krute, C.N., Leighton, S.L., Carroll, R.K., and Shaw, L.N. (2014). Investigating the genetic regulation of the ECF sigma factor sigmaS in *Staphylococcus aureus*. BMC Microbiol *14*, 280.

Butland, G., Peregrin-Alvarez, J.M., Li, J., Yang, W., Yang, X., Canadien, V., Starostine, A., Richards, D.,

Beattie, B., Krogan, N.*, et al.* (2005). Interaction network containing conserved and essential protein complexes in *Escherichia coli*. Nature *433*, 531-537.

Cao, H., Wei, D., Yang, Y., Shang, Y., Li, G., Zhou, Y., Ma, Q., and Xu, Y. (2017). Systems-level understanding of ethanol-induced stresses and adaptation in E. coli. Sci Rep *7*, 44150.

Cao, M., Kobel, P.A., Morshedi, M.M., Wu, M.F., Paddon, C., and Helmann, J.D. (2002). Defining the *Bacillus subtilis* sigma(W) regulon: a comparative analysis of promoter consensus search, run-off transcription/macroarray analysis (ROMA), and transcriptional profiling approaches. J Mol Biol *316*, 443-457.

Cashel, M. (1969). The control of ribonucleic acid synthesis in *Escherichia coli*. IV. Relevance of unusual phosphorylated compounds from amino acid-starved stringent strains. J Biol Chem *244*, 3133-3141.

Cashel, M. (1996). The Stringent Response. *Escherichia coli* and Salmonella Molecular and Cell Biology, 1458-1496.

Cavanagh, A.T., Chandrangsu, P., and Wassarman, K.M. (2010). 6S RNA regulation of relA alters ppGpp levels in early stationary phase. Microbiology *156*, 3791-3800.

Charity, J.C., Blalock, L.T., Costante-Hamm, M.M., Kasper, D.L., and Dove, S.L. (2009). Small molecule control of virulence gene expression in Francisella tularensis. PLoS Pathog *5*, e1000641.

Chastanet, A., Fert, J., and Msadek, T. (2003). Comparative genomics reveal novel heat shock regulatory mechanisms in *Staphylococcus aureus* and other Gram-positive bacteria. Mol Microbiol *47*, 1061-1073.

Cirz, R.T., Jones, M.B., Gingles, N.A., Minogue, T.D., Jarrahi, B., Peterson, S.N., and Romesberg, F.E. (2007). Complete and SOS-mediated response of *Staphylococcus aureus* to the antibiotic ciprofloxacin. J Bacteriol *189*, 531-539.

Clauditz, A., Resch, A., Wieland, K.P., Peschel, A., and Gotz, F. (2006). Staphyloxanthin plays a role in the fitness of *Staphylococcus aureus* and its ability to cope with oxidative stress. Infect Immun *74*, 4950-4953.

Claverys, J.P., Prudhomme, M., and Martin, B. (2006). Induction of competence regulons as a general response to stress in gram-positive bacteria. Annu Rev Microbiol *60*, 451-475.

Coates-Brown, R., Moran, J.C., Pongchaikul, P., Darby, A.C., and Horsburgh, M.J. (2018). Comparative Genomics of Staphylococcus Reveals Determinants of Speciation and Diversification of Antimicrobial Defense. Front Microbiol *9*, 2753.

Cole, A. (2013). MRSA and *C. difficile* deaths continue to fall in England and Wales. B M J *347*, f5278.

Corrigan, R.M., Bellows, L.E., Wood, A., and Grundling, A. (2016). ppGpp negatively impacts ribosome assembly affecting growth and antimicrobial tolerance in Gram-positive bacteria. Proc Natl Acad Sci U S A *113*, E1710-1719.

Corrigan, R.M., Bowman, L., Willis, A.R., Kaever, V., and Grundling, A. (2015). Cross-talk between two nucleotide-signaling pathways in *Staphylococcus aureus*. J Biol Chem *290*, 5826-5839.

Dahl, J.L., Kraus, C.N., Boshoff, H.I., Doan, B., Foley, K., Avarbock, D., Kaplan, G., Mizrahi, V., Rubin, H., and Barry, C.E., 3rd (2003). The role of RelMtb-mediated adaptation to stationary phase in long-term persistence of *Mycobacterium tuberculosis* in mice. Proc Natl Acad Sci U S A *100*, 10026-10031.

Dalebroux, Z.D., Edwards, R.L., and Swanson, M.S. (2009). SpoT governs Legionella pneumophila differentiation in host macrophages. Mol Microbiol *71*, 640-658.

Das, B., Pal, R.R., Bag, S., and Bhadra, R.K. (2009). Stringent response in *Vibrio cholerae*: genetic analysis of spoT gene function and identification of a novel (p)ppGpp synthetase gene. Mol Microbiol *72*, 380-398.

Daum, R.S., Ito, T., Hiramatsu, K., Hussain, F., Mongkolrattanothai, K., Jamklang, M., and Boyle-Vavra, S. (2002). A novel methicillin-resistance cassette in community-acquired methicillin-resistant *Staphylococcus aureus* isolates of diverse genetic backgrounds. J Infect Dis *186*, 1344-1347.

de la Fuente-Núñez, C., Reffuveille, F., Haney, E.F., Straus, S.K., and Hancock, R.E. (2014). Broad-spectrum anti-biofilm peptide that targets a cellular stress response. PLoS Pathog *10*, e1004152.

de la Fuente-Núñez, C., Reffuveille, F., Mansour, S.C., Reckseidler-Zenteno, S.L., Hernández, D., Brackman, G., Coenye, T., and Hancock, R.E. (2015). D-enantiomeric peptides that eradicate wild-type and multidrug-resistant biofilms and protect against lethal *Pseudomonas aeruginosa* infections. Chem Biol *22*, 196-205.

Deora, R., and Misra, T.K. (1996). Characterization of the primary sigma factor of *Staphylococcus aureus*. J Biol Chem *271*, 21828-21834.

Derre, I., Rapoport, G., and Msadek, T. (1999). CtsR, a novel regulator of stress and heat shock response, controls clp and molecular chaperone gene expression in gram-positive bacteria. Mol Microbiol *31*, 117-131.

Dotto, C., Lombarte Serrat, A., Cattelan, N., Barbagelata, M.S., Yantorno, O.M., Sordelli, D.O., Ehling-Schulz, M., Grunert, T., and Buzzola, F.R. (2017). The Active Component of Aspirin, Salicylic Acid,

Promotes *Staphylococcus aureus* Biofilm Formation in a PIA-dependent Manner. Front Microbiol *8*, 4.

Dunman, P.M., Murphy, E., Haney, S., Palacios, D., Tucker-Kellogg, G., Wu, S., Brown, E.L., Zagursky, R.J., Shlaes, D., and Projan, S.J. (2001). Transcription profiling-based identification of *Staphylococcus aureus* genes regulated by the agr and/or sarA loci. J Bacteriol *183*, 7341-7353.

Durfee, T., Hansen, A.M., Zhi, H., Blattner, F.R., and Jin, D.J. (2008). Transcription profiling of the stringent response in *Escherichia coli*. J Bacteriol *190*, 1084-1096.

Duval, M., Korepanov, A., Fuchsbauer, O., Fechter, P., Haller, A., Fabbretti, A., Choulier, L., Micura, R., Klaholz, B.P., Romby, P.*, et al.* (2013). *Escherichia coli* ribosomal protein S1 unfolds structured mRNAs onto the ribosome for active translation initiation. PLoS Biol *11*, e1001731.

Ehlers, C., Ivens, U.I., Moller, M.L., Senderovitz, T., and Serup, J. (2001). Females have lower skin surface pH than men. A study on the surface of gender, forearm site variation, right/left difference and time of the day on the skin surface pH. Skin Res Technol *7*, 90-94.

Eiamphungporn, W., and Helmann, J.D. (2008). The *Bacillus subtilis* sigma(M) regulon and its contribution to cell envelope stress responses. Mol Microbiol *67*, 830-848.

Public Health England (2018). Laboratory surveillance of *Staphylococcus aureus* bacteraemia in England, Wales and Northern Ireland: 2017 (Health Protection Report).

Fang, F.C. (1997). Perspectives series: host/pathogen interactions. Mechanisms of nitric oxide-related antimicrobial activity. J Clin Invest *99*, 2818-2825.

Fang, M., and Bauer, C.E. (2018). Regulation of stringent factor by branched-chain amino acids. Proc Natl Acad Sci U S A *115*, 6446-6451.

Fang, X., Ahmad, I., Blanka, A., Schottkowski, M., Cimdins, A., Galperin, M.Y., Römling, U., and Gomelsky, M. (2014). GIL, a new c-di-GMP binding protein domain involved in regulation of cellulose synthesis in enterobacteria. Mol Microbiol *93*, 439-452.

Fey, P.D., Endres, J.L., Yajjala, V.K., Widhelm, T.J., Boissy, R.J., Bose, J.L., and Bayles, K.W. (2013). A genetic resource for rapid and comprehensive phenotype screening of nonessential *Staphylococcus aureus* genes. MBio *4*, e00537-00512.

Fournier, B., Aras, R., and Hooper, D.C. (2000). Expression of the multidrug resistance transporter NorA from *Staphylococcus aureus* is modified by a two-component regulatory system. J Bacteriol *182*, 664-671.

Fournier, B., Klier, A., and Rapoport, G. (2001). The two-component system ArlS-ArlR is a regulator of

virulence gene expression in *Staphylococcus aureus*. Mol Microbiol *41*, 247-261.

Fowler, V.G., Jr., and Proctor, R.A. (2014). Where does a *Staphylococcus aureus* vaccine stand? Clin Microbiol Infect *20 Suppl 5*, 66-75.

Fridkin, S.K., Hageman, J.C., Morrison, M., Sanza, L.T., Como-Sabetti, K., Jernigan, J.A., Harriman, K., Harrison, L.H., Lynfield, R., and Farley, M.M. (2005). Methicillin-resistant *Staphylococcus aureus* disease in three communities. N Engl J Med *352*, 1436-1444.

Gaca, A.O., Abranches, J., Kajfasz, J.K., and Lemos, J.A. (2012). Global transcriptional analysis of the stringent response in *Enterococcus faecalis*. Microbiology *158*, 1994-2004.

Gaca, A.O., Kajfasz, J.K., Miller, J.H., Liu, K., Wang, J.D., Abranches, J., and Lemos, J.A. (2013). Basal levels of (p)ppGpp in *Enterococcus faecalis*: the magic beyond the stringent response. MBio *4*, e00646-00613.

Gaca, A.O., Kudrin, P., Colomer-Winter, C., Beljantseva, J., Liu, K., Anderson, B., Wang, J.D., Rejman, D., Potrykus, K., Cashel, M.*, et al.* (2015). From (p)ppGpp to (pp)pGpp: Characterization of Regulatory Effects of pGpp Synthesized by the Small Alarmone Synthetase of *Enterococcus faecalis*. J Bacteriol *197*, 2908-2919.

Gao, W., Chua, K., Davies, J.K., Newton, H.J., Seemann, T., Harrison, P.F., Holmes, N.E., Rhee, H.W., Hong, J.I., Hartland, E.L.*, et al.* (2010). Two novel point mutations in clinical *Staphylococcus aureus* reduce linezolid susceptibility and switch on the stringent response to promote persistent infection. PLoS Pathog *6*, e1000944.

Geiger, T., Francois, P., Liebeke, M., Fraunholz, M., Goerke, C., Krismer, B., Schrenzel, J., Lalk, M., and Wolz, C. (2012). The stringent response of *Staphylococcus aureus* and its impact on survival after phagocytosis through the induction of intracellular PSMs expression. PLoS Pathog *8*, e1003016.

Geiger, T., Goerke, C., Fritz, M., Schäfer, T., Ohlsen, K., Liebeke, M., Lalk, M., and Wolz, C. (2010). Role of the (p)ppGpp synthase RSH, a RelA/SpoT homolog, in stringent response and virulence of *Staphylococcus aureus*. Infect Immun *78*, 1873-1883.

Geiger, T., Kastle, B., Gratani, F.L., Goerke, C., and Wolz, C. (2014). Two small (p)ppGpp synthases in *Staphylococcus aureus* mediate tolerance against cell envelope stress conditions. J Bacteriol *196*, 894-902.

Geiger, T., and Wolz, C. (2014). Intersection of the stringent response and the CodY regulon in low GC Gram-positive bacteria. Int J Med Microbiol *304*, 150-155.

Gentry, D., Li, T., Rosenberg, M., and McDevitt, D. (2000). The rel gene is essential for in vitro growth of *Staphylococcus aureus*. J Bacteriol *182*, 4995-4997.

Giraudo, A.T., Cheung, A.L., and Nagel, R. (1997). The sae locus of *Staphylococcus aureus* controls exoprotein synthesis at the transcriptional level. Arch Microbiol *168*, 53-58.

Gkekas, S., Singh, R.K., Shkumatov, A.V., Messens, J., Fauvart, M., Verstraeten, N., Michiels, J., and Versees, W. (2017). Structural and biochemical analysis of *Escherichia coli* ObgE, a central regulator of bacterial persistence. J Biol Chem *292*, 5871-5883.

Gottesman, S. (1996). Proteases and their targets in *Escherichia coli*. Annu Rev Genet *30*, 465-506.

Graham, P.L., 3rd, Lin, S.X., and Larson, E.L. (2006). A U.S. population-based survey of *Staphylococcus aureus* colonization. Ann Intern Med *144*, 318-325.

Grant, G.A. (2006). The ACT domain: a small molecule binding domain and its role as a common regulatory element. J Biol Chem *281*, 33825-33829.

Gratani, F.L., Horvatek, P., Geiger, T., Borisova, M., Mayer, C., Grin, I., Wagner, S., Steinchen, W., Bange, G., Velic, A*., et al.* (2018). Regulation of the opposing (p)ppGpp synthetase and hydrolase activities in a bifunctional RelA/SpoT homologue from *Staphylococcus aureus*. PLoS Genet *14*, e1007514.

Greenwood, R.C., and Gentry, D.R. (2002). The effect of antibiotic treatment on the intracellular nucleotide pools of *Staphylococcus aureus*. FEMS Microbiol Lett *208*, 203-206.

Grice, E.A., and Segre, J.A. (2011). The skin microbiome. Nat Rev Microbiol *9*, 244-253.

Groicher, K.H., Firek, B.A., Fujimoto, D.F., and Bayles, K.W. (2000). The *Staphylococcus aureus* lrgAB operon modulates murein hydrolase activity and penicillin tolerance. J Bacteriol *182*, 1794-1801.

Gropp, M., Strausz, Y., Gross, M., and Glaser, G. (2001). Regulation of *Escherichia coli* RelA requires oligomerization of the C-terminal domain. J Bacteriol *183*, 570-579.

Grundling, A., and Schneewind, O. (2007). Genes required for glycolipid synthesis and lipoteichoic acid anchoring in *Staphylococcus aureus*. J Bacteriol *189*, 2521-2530.

Gully, D., Moinier, D., Loiseau, L., and Bouveret, E. (2003). New partners of acyl carrier protein detected in *Escherichia coli* by tandem affinity purification. FEBS Lett *548*, 90-96.

Hahn, J., Tanner, A.W., Carabetta, V.J., Cristea, I.M., and Dubnau, D. (2015). ComGA-RelA interaction and persistence in the *Bacillus subtilis* K-state. Mol Microbiol *97*, 454-471.

Halsey, C.R., Lei, S., Wax, J.K., Lehman, M.K., Nuxoll, A.S., Steinke, L., Sadykov, M., Powers, R., and Fey, P.D. (2017). Amino Acid Catabolism in *Staphylococcus aureus* and the Function of Carbon Catabolite Repression. MBio *8*.

Handford, J.I., Ize, B., Buchanan, G., Butland, G.P., Greenblatt, J., Emili, A., and Palmer, T. (2009). Conserved network of proteins essential for bacterial viability. J Bacteriol *191*, 4732-4749.

Hanifin, J.M., and Rogge, J.L. (1977). Staphylococcal infections in patients with atopic dermatitis. Arch Dermatol *113*, 1383-1386.

Hantke, K. (1981). Regulation of ferric iron transport in *Escherichia coli* K12: isolation of a constitutive mutant. Mol Gen Genet *182*, 288-292.

Haralalka, S., Nandi, S., and Bhadra, R.K. (2003). Mutation in the relA Gene of *Vibrio cholerae* Affects In Vitro and In Vivo Expression of Virulence Factors. In J Bacteriol, pp. 4672-4682.

Haseltine, W.A., and Block, R. (1973). Synthesis of guanosine tetra- and pentaphosphate requires the presence of a codon-specific, uncharged transfer ribonucleic acid in the acceptor site of ribosomes. Proc Natl Acad Sci U S A *70*, 1564-1568.

Haugen, S.P., Ross, W., Manrique, M., and Gourse, R.L. (2008). Fine structure of the promoter-sigma region 1.2 interaction. Proc Natl Acad Sci U S A *105*, 3292-3297.

Hauryliuk, V., Atkinson, G.C., Murakami, K.S., Tenson, T., and Gerdes, K. (2015). Recent functional insights into the role of (p)ppGpp in bacterial physiology. Nat Rev Microbiol *13*, 298-309.

Heath, R.J., Jackowski, S., and Rock, C.O. (1994). Guanosine tetraphosphate inhibition of fatty acid and phospholipid synthesis in *Escherichia coli* is relieved by overexpression of glycerol-3-phosphate acyltransferase (plsB). J Biol Chem *269*, 26584-26590.

Hiramatsu, K., Cui, L., Kuroda, M., and Ito, T. (2001). The emergence and evolution of methicillin-resistant *Staphylococcus aureus*. Trends Microbiol *9*, 486-493.

Hochstadt-Ozer, J., and Cashel, M. (1972). The regulation of purine utilization in bacteria. IV. Roles of membrane-localized and pericytoplasmic enzymes in the mechanism of purine nucleoside transport across isolated *Escherichia coli* membranes. J Biol Chem *247*, 2419-2426.

Hogg, T., Mechold, U., Malke, H., Cashel, M., and Hilgenfeld, R. (2004). Conformational antagonism between opposing active sites in a bifunctional RelA/SpoT homolog modulates (p)ppGpp metabolism during the stringent response [corrected]. Cell *117*, 57-68.

Holland, T.L., Arnold, C., and Fowler, V.G., Jr. (2014). Clinical management of *Staphylococcus aureus*

bacteremia: a review. J A M A *312*, 1330-1341.

Hood, R.D., Higgins, S.A., Flamholz, A., Nichols, R.J., and Savage, D.F. (2016). The stringent response regulates adaptation to darkness in the cyanobacterium *Synechococcus elongatus*. Proc Natl Acad Sci U S A *113*, E4867-4876.

Hooven, T.A., Catomeris, A.J., Bonakdar, M., Tallon, L.J., Santana-Cruz, I., Ott, S., Daugherty, S.C., Tettelin, H., and Ratner, A.J. (2018). The Streptococcus agalactiae Stringent Response Enhances Virulence and Persistence in Human Blood. Infect Immun *86*.

Houot, L., Fanni, A., de Bentzmann, S., and Bordi, C. (2012). A bacterial two-hybrid genome fragment library for deciphering regulatory networks of the opportunistic pathogen *Pseudomonas aeruginosa*. Microbiology *158*, 1964-1971.

Howden, B.P., Davies, J.K., Johnson, P.D., Stinear, T.P., and Grayson, M.L. (2010). Reduced vancomycin susceptibility in *Staphylococcus aureus*, including vancomycin-intermediate and heterogeneous vancomycin-intermediate strains: resistance mechanisms, laboratory detection, and clinical implications. Clin Microbiol Rev *23*, 99-139.

Howden, B.P., Ward, P.B., Charles, P.G., Korman, T.M., Fuller, A., du Cros, P., Grabsch, E.A., Roberts, S.A., Robson, J., Read, K.*, et al.* (2004). Treatment outcomes for serious infections caused by methicillin-resistant *Staphylococcus aureus* with reduced vancomycin susceptibility. Clin Infect Dis *38*, 521-528.

Hughes, J., and Mellows, G. (1978). On the mode of action of pseudomonic acid: inhibition of protein synthesis in *Staphylococcus aureus*. J Antibiot (Tokyo) *31*, 330-335.

Hughes, J., and Mellows, G. (1980). Interaction of pseudomonic acid A with *Escherichia coli* B isoleucyl-tRNA synthetase. Biochem J *191*, 209-219.

Hussain, M., Hastings, J.G., and White, P.J. (1991). A chemically defined medium for slime production by coagulase-negative staphylococci. J Med Microbiol *34*, 143-147.

Huycke, M.M., Moore, D., Joyce, W., Wise, P., Shepard, L., Kotake, Y., and Gilmore, M.S. (2001). Extracellular superoxide production by *Enterococcus faecalis* requires demethylmenaquinone and is attenuated by functional terminal quinol oxidases. Mol Microbiol *42*, 729-740.

Ipe, D.S., and Ulett, G.C. (2016). Evaluation of the in vitro growth of urinary tract infection-causing gram-negative and gram-positive bacteria in a proposed synthetic human urine (SHU) medium. J Microbiol Methods *127*, 164-171.

Iwase, T., Uehara, Y., Shinji, H., Tajima, A., Seo, H., Takada, K., Agata, T., and Mizunoe, Y. (2010). Esp inhibits *Staphylococcus aureus* biofilm formation and nasal colonization. Nature *465*, 346-349.

Ji, G., Beavis, R.C., and Novick, R.P. (1995). Cell density control of staphylococcal virulence mediated by an octapeptide pheromone. Proc Natl Acad Sci U S A *92*, 12055-12059.

Jiang, M., Sullivan, S.M., Wout, P.K., and Maddock, J.R. (2007). G-protein control of the ribosome-associated stress response protein SpoT. J Bacteriol *189*, 6140-6147.

Kahl, B.C., Becker, K., and Loffler, B. (2016). Clinical Significance and Pathogenesis of Staphylococcal Small Colony Variants in Persistent Infections. Clin Microbiol Rev *29*, 401-427.

Kajitani, M., and Ishihama, A. (1984). Promoter selectivity of *Escherichia coli* RNA polymerase. Differential stringent control of the multiple promoters from ribosomal RNA and protein operons. J Biol Chem *259*, 1951-1957.

Kanjee, U., Gutsche, I., Alexopoulos, E., Zhao, B., El Bakkouri, M., Thibault, G., Liu, K., Ramachandran, S., Snider, J., Pai, E.F*., et al.* (2011). Linkage between the bacterial acid stress and stringent responses: the structure of the inducible lysine decarboxylase. Embo j *30*, 931-944.

Karimova, G., Dautin, N., and Ladant, D. (2005). Interaction network among *Escherichia coli* membrane proteins involved in cell division as revealed by bacterial two-hybrid analysis. J Bacteriol *187*, 2233-2243.

Karimova, G., Pidoux, J., Ullmann, A., and Ladant, D. (1998). A bacterial two-hybrid system based on a reconstituted signal transduction pathway. Proc Natl Acad Sci U S A *95*, 5752-5756.

Karimova, G., Ullmann, A., and Ladant, D. (2001). Protein-protein interaction between Bacillus stearothermophilus tyrosyl-tRNA synthetase subdomains revealed by a bacterial two-hybrid system. J Mol Microbiol Biotechnol *3*, 73-82.

Katayama, Y., Sekine, M., Hishinuma, T., Aiba, Y., and Hiramatsu, K. (2016). Complete Reconstitution of the Vancomycin-Intermediate *Staphylococcus aureus* Phenotype of Strain Mu50 in Vancomycin-Susceptible S. aureus. Antimicrob Agents Chemother *60*, 3730-3742.

Keasling, J.D., Bertsch, L., and Kornberg, A. (1993). Guanosine pentaphosphate phosphohydrolase of *Escherichia coli* is a long-chain exopolyphosphatase. Proc Natl Acad Sci U S A *90*, 7029-7033.

Kelly, B., and O'Neill, L.A. (2015). Metabolic reprogramming in macrophages and dendritic cells in innate immunity. Cell Res *25*, 771-784.

Kessler, J.R., Cobe, B.L., and Richards, G.R. (2017). Stringent Response Regulators Contribute to the

Recovery from Glucose-Phosphate Stress in *Escherichia coli*. Appl Environ Microbiol.

Kim, S., Corvaglia, A.R., Leo, S., Cheung, A., and Francois, P. (2016). Characterization of RNA Helicase CshA and Its Role in Protecting mRNAs and Small RNAs of *Staphylococcus aureus* Strain Newman. Infect Immun *84*, 833-844.

Klinkenberg, L.G., Lee, J.H., Bishai, W.R., and Karakousis, P.C. (2010). The stringent response is required for full virulence of *Mycobacterium tuberculosis* in guinea pigs. J Infect Dis *202*, 1397-1404.

Korch, S.B., Henderson, T.A., and Hill, T.M. (2003). Characterization of the hipA7 allele of *Escherichia coli* and evidence that high persistence is governed by (p)ppGpp synthesis. Mol Microbiol *50*, 1199-1213.

Kriel, A., Bittner, A.N., Kim, S.H., Liu, K., Tehranchi, A.K., Zou, W.Y., Rendon, S., Chen, R., Tu, B.P., and Wang, J.D. (2012). Direct regulation of GTP homeostasis by (p)ppGpp: a critical component of viability and stress resistance. Mol Cell *48*, 231-241.

Krishnan, S., Petchiappan, A., Singh, A., Bhatt, A., and Chatterji, D. (2016). R-loop induced stress response by second (p)ppGpp synthetase in *Mycobacterium smegmatis*: functional and domain interdependence. Mol Microbiol *102*, 168-182.

Krásný, L., and Gourse, R.L. (2004). An alternative strategy for bacterial ribosome synthesis: *Bacillus subtilis* rRNA transcription regulation. EMBO J *23*, 4473-4483.

Kästle, B., Geiger, T., Gratani, F.L., Reisinger, R., Goerke, C., Borisova, M., Mayer, C., and Wolz, C. (2015). rRNA regulation during growth and under stringent conditions in *Staphylococcus aureus*. Environ Microbiol *17*, 4394-4405.

Lacey, K.A., Geoghegan, J.A., and McLoughlin, R.M. (2016). The Role of *Staphylococcus aureus* Virulence Factors in Skin Infection and Their Potential as Vaccine Antigens. Pathogens *5*.

Lee, S.M., Ender, M., Adhikari, R., Smith, J.M., Berger-Bachi, B., and Cook, G.M. (2007a). Fitness cost of staphylococcal cassette chromosome mec in methicillin-resistant *Staphylococcus aureus* by way of continuous culture. Antimicrob Agents Chemother *51*, 1497-1499.

Lee, V.T., Matewish, J.M., Kessler, J.L., Hyodo, M., Hayakawa, Y., and Lory, S. (2007b). A cyclic-di-GMP receptor required for bacterial exopolysaccharide production. Mol Microbiol *65*, 1474-1484.

Legault, L., Jeantet, C., and Gros, F. (1972). Inhibition of in vitro protein synthesis by ppGpp. FEBS Lett *27*, 71-75.

Lemos, J.A., Brown, T.A., Jr., and Burne, R.A. (2004). Effects of RelA on key virulence properties of

planktonic and biofilm populations of Streptococcus mutans. Infect Immun *72*, 1431-1440.

Lemos, J.A., Lin, V.K., Nascimento, M.M., Abranches, J., and Burne, R.A. (2007). Three gene products govern (p)ppGpp production by Streptococcus mutans. Mol Microbiol *65*, 1568-1581.

Leyden, J.J., Marples, R.R., and Kligman, A.M. (1974). *Staphylococcus aureus* in the lesions of atopic dermatitis. Br J Dermatol *90*, 525-530.

Li, C., Sun, F., Cho, H., Yelavarthi, V., Sohn, C., He, C., Schneewind, O., and Bae, T. (2010). CcpA mediates proline auxotrophy and is required for *Staphylococcus aureus* pathogenesis. J Bacteriol *192*, 3883-3892.

Liang, X., Zheng, L., Landwehr, C., Lunsford, D., Holmes, D., and Ji, Y. (2005). Global regulation of gene expression by ArlRS, a two-component signal transduction regulatory system of *Staphylococcus aureus*. J Bacteriol *187*, 5486-5492.

Lin, C.Y., Awano, N., Masuda, H., Park, J.H., and Inouye, M. (2013). Transcriptional repressor HipB regulates the multiple promoters in *Escherichia coli*. J Mol Microbiol Biotechnol *23*, 440-447.

Lina, G., Jarraud, S., Ji, G., Greenland, T., Pedraza, A., Etienne, J., Novick, R.P., and Vandenesch, F. (1998). Transmembrane topology and histidine protein kinase activity of AgrC, the agr signal receptor in *Staphylococcus aureus*. Mol Microbiol *28*, 655-662.

Little, J.W., Edmiston, S.H., Pacelli, L.Z., and Mount, D.W. (1980). Cleavage of the *Escherichia coli* lexA protein by the recA protease. Proc Natl Acad Sci U S A *77*, 3225-3229.

Loeb, L. (1903). The Influence of certain Bacteria on the Coagulation of the Blood 1. J Med Res *10*, 407-419.

Lopez, J.M., Dromerick, A., and Freese, E. (1981). Response of guanosine 5'-triphosphate concentration to nutritional changes and its significance for *Bacillus subtilis* sporulation. J Bacteriol *146*, 605-613.

Loveland, A.B., Bah, E., Madireddy, R., Zhang, Y., Brilot, A.F., Grigorieff, N., and Korostelev, A.A. (2016). Ribosome*RelA structures reveal the mechanism of stringent response activation. Elife *5*.

Maciag, M., Kochanowska, M., Lyzen, R., Wegrzyn, G., and Szalewska-Palasz, A. (2010). ppGpp inhibits the activity of *Escherichia coli* DnaG primase. Plasmid *63*, 61-67.

Madsen, S.M., Beck, H.C., Ravn, P., Vrang, A., Hansen, A.M., and Israelsen, H. (2002). Cloning and inactivation of a branched-chain-amino-acid aminotransferase gene from Staphylococcus carnosus and characterization of the enzyme. Appl Environ Microbiol *68*, 4007-4014.

Majerczyk, C.D., Dunman, P.M., Luong, T.T., Lee, C.Y., Sadykov, M.R., Somerville, G.A., Bodi, K., and Sonenshein, A.L. (2010). Direct targets of CodY in *Staphylococcus aureus*. J Bacteriol *192*, 2861-2877.

Manav, M.C., Beljantseva, J., Bojer, M.S., Tenson, T., Ingmer, H., Hauryliuk, V., and Brodersen, D.E. (2018). Structural basis for (p)ppGpp synthesis by the *Staphylococcus aureus* small alarmone synthetase RelP. J Biol Chem *293*, 3254-3264.

Marshall, J.H., and Wilmoth, G.J. (1981). Proposed pathway of triterpenoid carotenoid biosynthesis in *Staphylococcus aureus*: evidence from a study of mutants. J Bacteriol *147*, 914-919.

Matthews, K.R., Roberson, J., Gillespie, B.E., Luther, D.A., and Oliver, S.P. (1997). Identification and Differentiation of Coagulase-Negative *Staphylococcus aureus* by Polymerase Chain Reaction. Journal of Food Protection. *6.*

McGee, D.J., Radcliff, F.J., Mendz, G.L., Ferrero, R.L., and Mobley, H.L. (1999). Helicobacter pylori rocF is required for arginase activity and acid protection in vitro but is not essential for colonization of mice or for urease activity. J Bacteriol *181*, 7314-7322.

McGee, D.J., Zabaleta, J., Viator, R.J., Testerman, T.L., Ochoa, A.C., and Mendz, G.L. (2004). Purification and characterization of Helicobacter pylori arginase, RocF: unique features among the arginase superfamily. Eur J Biochem *271*, 1952-1962.

Mechold, U., Murphy, H., Brown, L., and Cashel, M. (2002). Intramolecular regulation of the opposing (p)ppGpp catalytic activities of Rel(Seq), the Rel/Spo enzyme from Streptococcus equisimilis. J Bacteriol *184*, 2878-2888.

Mechold, U., Potrykus, K., Murphy, H., Murakami, K.S., and Cashel, M. (2013). Differential regulation by ppGpp versus pppGpp in *Escherichia coli*. Nucleic Acids Res *41*, 6175-6189.

Meganathan, R. (2001). Biosynthesis of menaquinone (vitamin K2) and ubiquinone (coenzyme Q): a perspective on enzymatic mechanisms. Vitam Horm *61*, 173-218.

Merlie, J.P., and Pizer, L.I. (1973). Regulation of Phospholipid Synthesis in *Escherichia coli* by Guanosine Tetraphosphate. J Bacteriol *116*, 355-366.

Metzger, S., Dror, I.B., Aizenman, E., Schreiber, G., Toone, M., Friesen, J.D., Cashel, M., and Glaser, G. (1988). The nucleotide sequence and characterization of the relA gene of *Escherichia coli*. J Biol Chem *263*, 15699-15704.

Michel, A., Agerer, F., Hauck, C.R., Herrmann, M., Ullrich, J., Hacker, J., and Ohlsen, K. (2006). Global regulatory impact of ClpP protease of *Staphylococcus aureus* on regulons involved in virulence,

oxidative stress response, autolysis, and DNA repair. J Bacteriol *188*, 5783-5796.

Michel, B. (2005). After 30 Years of Study, the Bacterial SOS Response Still Surprises Us. PLoS Biol *3*.

Miller, D.L., Cashel, M., and Weissbach, H. (1973). The interaction of guanosine 5'-diphosphate, 2' (3')-diphosphate with the bacterial elongation factor Tu. Arch Biochem Biophys *154*, 675-682.

Miller, H.K., Carroll, R.K., Burda, W.N., Krute, C.N., Davenport, J.E., and Shaw, L.N. (2012). The extracytoplasmic function sigma factor sigmaS protects against both intracellular and extracytoplasmic stresses in *Staphylococcus aureus*. J Bacteriol *194*, 4342-4354.

Morfeldt, E., Taylor, D., von Gabain, A., and Arvidson, S. (1995). Activation of alpha-toxin translation in *Staphylococcus aureus* by the trans-encoded antisense RNA, RNAIII. EMBO J *14*, 4569-4577.

Mouery, K., Rader, B.A., Gaynor, E.C., and Guillemin, K. (2006). The stringent response is required for Helicobacter pylori survival of stationary phase, exposure to acid, and aerobic shock. J Bacteriol *188*, 5494-5500.

Murdeshwar, M.S., and Chatterji, D. (2012). MS_RHII-RSD, a dual-function RNase HII-(p)ppGpp synthetase from *Mycobacterium smegmatis*. J Bacteriol *194*, 4003-4014.

Mwangi, M.M., Kim, C., Chung, M., Tsai, J., Vijayadamodar, G., Benitez, M., Jarvie, T.P., Du, L., and Tomasz, A. (2013). Whole-genome sequencing reveals a link between beta-lactam resistance and synthetases of the alarmone (p)ppGpp in *Staphylococcus aureus*. Microb Drug Resist *19*, 153-159.

Nakagawa, A., Oshima, T., and Mori, H. (2006). Identification and characterization of a second, inducible promoter of relA in *Escherichia coli*. Genes Genet Syst *81*, 299-310.

Nanamiya, H., Kasai, K., Nozawa, A., Yun, C.S., Narisawa, T., Murakami, K., Natori, Y., Kawamura, F., and Tozawa, Y. (2008). Identification and functional analysis of novel (p)ppGpp synthetase genes in *Bacillus subtilis*. Mol Microbiol *67*, 291-304.

Neusser, T., Polen, T., Geissen, R., and Wagner, R. (2010). Depletion of the non-coding regulatory 6S RNA in E. coli causes a surprising reduction in the expression of the translation machinery. BMC Genomics *11*, 165.

Nuxoll, A.S., Halouska, S.M., Sadykov, M.R., Hanke, M.L., Bayles, K.W., Kielian, T., Powers, R., and Fey, P.D. (2012). CcpA regulates arginine biosynthesis in *Staphylococcus aureus* through repression of proline catabolism. PLoS Pathog *8*, e1003033.

Ochoa, J.B., Strange, J., Kearney, P., Gellin, G., Endean, E., and Fitzpatrick, E. (2001). Effects of L-arginine on the proliferation of T lymphocyte subpopulations. JPEN J Parenter Enteral Nutr *25*, 23-29.

Oliveira Paiva, A.M., Friggen, A.H., Qin, L., Douwes, R., Dame, R.T., and Smits, W.K. (2019). The Bacterial Chromatin Protein HupA Can Remodel DNA and Associates with the Nucleoid in *Clostridium difficile*. J Mol Biol.

Painter, K.L., Strange, E., Parkhill, J., Bamford, K.B., Armstrong-James, D., and Edwards, A.M. (2015). *Staphylococcus aureus* adapts to oxidative stress by producing H2O2-resistant small-colony variants via the SOS response. Infect Immun *83*, 1830-1844.

Pando, J.M., Pfeltz, R.F., Cuaron, J.A., Nagarajan, V., Mishra, M.N., Torres, N.J., Elasri, M.O., Wilkinson, B.J., and Gustafson, J.E. (2017). Ethanol-induced stress response of *Staphylococcus aureus*. Can J Microbiol *63*, 745-757.

Paul, B.J., Barker, M.M., Ross, W., Schneider, D.A., Webb, C., Foster, J.W., and Gourse, R.L. (2004). DksA: a critical component of the transcription initiation machinery that potentiates the regulation of rRNA promoters by ppGpp and the initiating NTP. Cell *118*, 311-322.

Paul, B.J., Berkmen, M.B., and Gourse, R.L. (2005). DksA potentiates direct activation of amino acid promoters by ppGpp. Proc Natl Acad Sci U S A *102*, 7823-7828.

Peng, H.L., Novick, R.P., Kreiswirth, B., Kornblum, J., and Schlievert, P. (1988). Cloning, characterization, and sequencing of an accessory gene regulator (agr) in *Staphylococcus aureus*. J Bacteriol *170*, 4365-4372.

Perl, T.M., Cullen, J.J., Wenzel, R.P., Zimmerman, M.B., Pfaller, M.A., Sheppard, D., Twombley, J., French, P.P., and Herwaldt, L.A. (2002). Intranasal mupirocin to prevent postoperative *Staphylococcus aureus* infections. N Engl J Med *346*, 1871-1877.

Persky, N.S., Ferullo, D.J., Cooper, D.L., Moore, H.R., and Lovett, S.T. (2009). The ObgE/CgtA GTPase influences the stringent response to amino acid starvation in *Escherichia coli*. Mol Microbiol *73*, 253-266.

Pier, G.B. (2013). Will there ever be a universal *Staphylococcus aureus* vaccine? Hum Vaccin Immunother *9*, 1865-1876.

Pietiainen, M., Gardemeister, M., Mecklin, M., Leskela, S., Sarvas, M., and Kontinen, V.P. (2005). Cationic antimicrobial peptides elicit a complex stress response in *Bacillus subtilis* that involves ECF-type sigma factors and two-component signal transduction systems. Microbiology *151*, 1577-1592.

Pizarro-Cerda, J., and Tedin, K. (2004). The bacterial signal molecule, ppGpp, regulates Salmonella virulence gene expression. Mol Microbiol *52*, 1827-1844.

Pletzer, D., Wolfmeier, H., Bains, M., and Hancock, R.E.W. (2017). Synthetic Peptides to Target Stringent Response-Controlled Virulence in a. Front Microbiol *8*, 1867.

Pohl, K., Francois, P., Stenz, L., Schlink, F., Geiger, T., Herbert, S., Goerke, C., Schrenzel, J., and Wolz, C. (2009). CodY in *Staphylococcus aureus*: a regulatory link between metabolism and virulence gene expression. J Bacteriol *191*, 2953-2963.

Potrykus, K., and Cashel, M. (2008). (p)ppGpp: still magical? Annu Rev Microbiol *62*, 35-51.

Potrykus, K., Murphy, H., Philippe, N., and Cashel, M. (2011). ppGpp is the major source of growth rate control in E. coli. Environ Microbiol *13*, 563-575.

Primm, T.P., Andersen, S.J., Mizrahi, V., Avarbock, D., Rubin, H., and Barry, C.E., 3rd (2000). The stringent response of *Mycobacterium tuberculosis* is required for long-term survival. J Bacteriol *182*, 4889-4898.

Pulschen, A.A., Sastre, D.E., Machinandiarena, F., Crotta Asis, A., Albanesi, D., de Mendoza, D., and Gueiros-Filho, F.J. (2017). The stringent response plays a key role in *Bacillus subtilis* survival of fatty acid starvation. Mol Microbiol *103*, 698-712.

Puszynska, A.M., and O'Shea, E.K. (2017). ppGpp Controls Global Gene Expression in Light and in Darkness in S. elongatus. Cell Rep *21*, 3155-3165.

Ravcheev, D.A., Best, A.A., Tintle, N., DeJongh, M., Osterman, A.L., Novichkov, P.S., and Rodionov, D.A. (2011). Inference of the Transcriptional Regulatory Network in *Staphylococcus aureus* by Integration of Experimental and Genomics-Based Evidence▽ †. In J Bacteriol, pp. 3228-3240.

Recsei, P., Kreiswirth, B., O'Reilly, M., Schlievert, P., Gruss, A., and Novick, R.P. (1986). Regulation of exoprotein gene expression in *Staphylococcus aureus* by agar. Mol Gen Genet *202*, 58-61.

Reiss, S., Pane-Farre, J., Fuchs, S., Francois, P., Liebeke, M., Schrenzel, J., Lindequist, U., Lalk, M., Wolz, C., Hecker, M.*, et al.* (2012). Global analysis of the *Staphylococcus aureus* response to mupirocin. Antimicrob Agents Chemother *56*, 787-804.

Reynolds, P.E. (1961). Studies on the mode of action of vancomycin. Biochim Biophys Acta *52*, 403-405.

Rochat, T., Bohn, C., Morvan, C., Le Lam, T.N., Razvi, F., Pain, A., Toffano-Nioche, C., Ponien, P., Jacq, A., Jacquet, E.*, et al.* (2018). The conserved regulatory RNA RsaE down-regulates the arginine degradation pathway in *Staphylococcus aureus*. Nucleic Acids Res *46*, 8803-8816.

Roelofs, K.G., Wang, J., Sintim, H.O., and Lee, V.T. (2011). Differential radial capillary action of ligand

assay for high-throughput detection of protein-metabolite interactions. Proc Natl Acad Sci U S A *108*, 15528-15533.

Rojas, A.M., Ehrenberg, M., Andersson, S.G., and Kurland, C.G. (1984). ppGpp inhibition of elongation factors Tu, G and Ts during polypeptide synthesis. Mol Gen Genet *197*, 36-45.

Rudin, L., Sjöström, J.E., Lindberg, M., and Philipson, L. (1974). Factors Affecting Competence for Transformation in *Staphylococcus aureus*. J Bacteriol *118*, 155-164.

Rymer, R.U., Solorio, F.A., Tehranchi, A.K., Chu, C., Corn, J.E., Keck, J.L., Wang, J.D., and Berger, J.M. (2012). Binding mechanism of metalNTP substrates and stringent-response alarmones to bacterial DnaG-type primases. Structure *20*, 1478-1489.

Sajish, M., Tiwari, D., Rananaware, D., Nandicoori, V.K., and Prakash, B. (2007). A charge reversal differentiates (p)ppGpp synthesis by monofunctional and bifunctional Rel proteins. J Biol Chem *282*, 34977-34983.

Samarrai, W., Liu, D.X., White, A.M., Studamire, B., Edelstein, J., Srivastava, A., Widom, R.L., and Rudner, R. (2011). Differential responses of *Bacillus subtilis* rRNA promoters to nutritional stress. J Bacteriol *193*, 723-733.

Schwan, W.R., Wetzel, K.J., Gomez, T.S., Stiles, M.A., Beitlich, B.D., and Grunwald, S. (2004). Low-proline environments impair growth, proline transport and in vivo survival of *Staphylococcus aureus* strain-specific putP mutants. Microbiology *150*, 1055-1061.

Seidl, K., Müller, S., François, P., Kriebitzsch, C., Schrenzel, J., Engelmann, S., Bischoff, M., and Berger-Bächi, B. (2009). Effect of a glucose impulse on the CcpA regulon in *Staphylococcus aureus*. In BMC Microbiol, p. 95.

Senn, M.M., Giachino, P., Homerova, D., Steinhuber, A., Strassner, J., Kormanec, J., Fluckiger, U., Berger-Bachi, B., and Bischoff, M. (2005). Molecular analysis and organization of the sigmaB operon in *Staphylococcus aureus*. J Bacteriol *187*, 8006-8019.

Seyfzadeh, M., Keener, J., and Nomura, M. (1993). spoT-dependent accumulation of guanosine tetraphosphate in response to fatty acid starvation in *Escherichia coli*. Proc Natl Acad Sci U S A *90*, 11004-11008.

Shaw, L.N., Lindholm, C., Prajsnar, T.K., Miller, H.K., Brown, M.C., Golonka, E., Stewart, G.C., Tarkowski, A., and Potempa, J. (2008). Identification and characterization of sigma, a novel component of the *Staphylococcus aureus* stress and virulence responses. PLoS One *3*, e3844.

Shi, H.P., Most, D., Efron, D.T., Witte, M.B., and Barbul, A. (2003). Supplemental L-arginine enhances wound healing in diabetic rats. Wound Repair Regen *11*, 198-203.

Shyp, V., Tankov, S., Ermakov, A., Kudrin, P., English, B.P., Ehrenberg, M., Tenson, T., Elf, J., and Hauryliuk, V. (2012). Positive allosteric feedback regulation of the stringent response enzyme RelA by its product. EMBO Rep *13*, 835-839.

Siboo, I.R., Chambers, H.F., and Sullam, P.M. (2005). Role of SraP, a Serine-Rich Surface Protein of *Staphylococcus aureus*, in binding to human platelets. Infect Immun *73*, 2273-2280.

Singh, R., Singh, M., Arora, G., Kumar, S., Tiwari, P., and Kidwai, S. (2013). Polyphosphate deficiency in *Mycobacterium tuberculosis* is associated with enhanced drug susceptibility and impaired growth in guinea pigs. J Bacteriol *195*, 2839-2851.

Somerville, G.A., Said-Salim, B., Wickman, J.M., Raffel, S.J., Kreiswirth, B.N., and Musser, J.M. (2003). Correlation of acetate catabolism and growth yield in *Staphylococcus aureus*: implications for host-pathogen interactions. Infect Immun *71*, 4724-4732.

Sonenshein, A.L. (2007). Control of key metabolic intersections in *Bacillus subtilis*. Nat Rev Microbiol *5*, 917-927.

Sorensen, M.A., Fricke, J., and Pedersen, S. (1998). Ribosomal protein S1 is required for translation of most, if not all, natural mRNAs in *Escherichia coli* in vivo. J Mol Biol *280*, 561-569.

Soutourina, O., Poupel, O., Coppee, J.Y., Danchin, A., Msadek, T., and Martin-Verstraete, I. (2009). CymR, the master regulator of cysteine metabolism in *Staphylococcus aureus*, controls host sulphur source utilization and plays a role in biofilm formation. Mol Microbiol *73*, 194-211.

Spahich, N.A., Vitko, N.P., Thurlow, L.R., Temple, B., and Richardson, A.R. (2016). *Staphylococcus aureus* lactate- and malate-quinone oxidoreductases contribute to nitric oxide resistance and virulence. Mol Microbiol *100*, 759-773.

Spector, D.A., Yang, Q., and Wade, J.B. (2007). High urea and creatinine concentrations and urea transporter B in mammalian urinary tract tissues. Am J Physiol Renal Physiol *292*, F467-474.

Stayton, M.M., and Fromm, H.J. (1979). Guanosine 5'-diphosphate-3'-diphosphate inhibition of adenylosuccinate synthetase. J Biol Chem *254*, 2579-2581.

Steinchen, W., Schuhmacher, J.S., Altegoer, F., Fage, C.D., Srinivasan, V., Linne, U., Marahiel, M.A., and Bange, G. (2015). Catalytic mechanism and allosteric regulation of an oligomeric (p)ppGpp synthetase by an alarmone. Proc Natl Acad Sci U S A *112*, 13348-13353.

Sun, F., Li, C., Jeong, D., Sohn, C., He, C., and Bae, T. (2010). In the *Staphylococcus aureus* two-component system sae, the response regulator SaeR binds to a direct repeat sequence and DNA binding requires phosphorylation by the sensor kinase SaeS. J Bacteriol *192*, 2111-2127.

Sun, W., Roland, K.L., Branger, C.G., Kuang, X., and Curtiss, R., 3rd (2009). The role of relA and spoT in Yersinia pestis KIM5 pathogenicity. PLoS One *4*, e6720.

Sureka, K., Dey, S., Datta, P., Singh, A.K., Dasgupta, A., Rodrigue, S., Basu, J., and Kundu, M. (2007). Polyphosphate kinase is involved in stress-induced mprAB-sigE-rel signalling in mycobacteria. Mol Microbiol *65*, 261-276.

Tagami, K., Nanamiya, H., Kazo, Y., Maehashi, M., Suzuki, S., Namba, E., Hoshiya, M., Hanai, R., Tozawa, Y., Morimoto, T.*, et al.* (2012). Expression of a small (p)ppGpp synthetase, YwaC, in the (p)ppGpp(0) mutant of *Bacillus subtilis* triggers YvyD-dependent dimerization of ribosome. MicrobiologyOpen *1*, 115-134.

Takahashi, K., Kasai, K., and Ochi, K. (2004). Identification of the bacterial alarmone guanosine 5'-diphosphate 3'-diphosphate (ppGpp) in plants. Proc Natl Acad Sci U S A *101*, 4320-4324.

Takahashi, T., Satoh, I., and Kikuchi, N. (1999). Phylogenetic relationships of 38 taxa of the genus Staphylococcus based on 16S rRNA gene sequence analysis. Int J Syst Bacteriol *49 Pt 2*, 725-728.

Tan, L., Li, S.R., Jiang, B., Hu, X.M., and Li, S. (2018). Therapeutic Targeting of the *Staphylococcus aureus* Accessory Gene Regulator (agr) System. Front Microbiol *9*.

Tarusawa, T., Ito, S., Goto, S., Ushida, C., Muto, A., and Himeno, H. (2016). (p)ppGpp-dependent and -independent pathways for salt tolerance in *Escherichia coli*. J Biochem *160*, 19-26.

Thackray, P.D., and Moir, A. (2003). SigM, an extracytoplasmic function sigma factor of *Bacillus subtilis*, is activated in response to cell wall antibiotics, ethanol, heat, acid, and superoxide stress. J Bacteriol *185*, 3491-3498.

Tornero, E., Garcia-Oltra, E., Garcia-Ramiro, S., Martinez-Pastor, J.C., Bosch, J., Climent, C., Morata, L., Camacho, P., Mensa, J., and Soriano, A. (2012). Prosthetic joint infections due to *Staphylococcus aureus* and coagulase-negative staphylococci. Int J Artif Organs *35*, 884-892.

Traxler, M.F., Zacharia, V.M., Marquardt, S., Summers, S.M., Nguyen, H.T., Stark, S.E., and Conway, T. (2011). Discretely calibrated regulatory loops controlled by ppGpp partition gene induction across the 'feast to famine' gradient in *Escherichia coli*. Mol Microbiol *79*, 830-845.

Ubeda, C., Maiques, E., Knecht, E., Lasa, I., Novick, R.P., and Penades, J.R. (2005). Antibiotic-induced

SOS response promotes horizontal dissemination of pathogenicity island-encoded virulence factors in staphylococci. Mol Microbiol *56*, 836-844.

Vagner, V., Dervyn, E., and Ehrlich, S.D. (1998). A vector for systematic gene inactivation in *Bacillus subtilis*. Microbiology *144 (Pt 11)*, 3097-3104.

van der Biezen, E.A., Sun, J., Coleman, M.J., Bibb, M.J., and Jones, J.D. (2000). Arabidopsis RelA/SpoT homologs implicate (p)ppGpp in plant signaling. Proc Natl Acad Sci U S A *97*, 3747-3752.

van Hal, S.J., Jensen, S.O., Vaska, V.L., Espedido, B.A., Paterson, D.L., and Gosbell, I.B. (2012). Predictors of mortality in *Staphylococcus aureus* Bacteremia. Clin Microbiol Rev *25*, 362-386.

van Wamel, W.J.B. (2017). *Staphylococcus aureus* infections, some second thoughts. Curr Opin Infect Dis *30*, 303-308.

Vandenesch, F., Naimi, T., Enright, M.C., Lina, G., Nimmo, G.R., Heffernan, H., Liassine, N., Bes, M., Greenland, T., Reverdy, M.E*., et al.* (2003). Community-acquired methicillin-resistant *Staphylococcus aureus* carrying Panton-Valentine leukocidin genes: worldwide emergence. Emerg Infect Dis *9*, 978-984.

Vanderpool, C.K., and Gottesman, S. (2004). Involvement of a novel transcriptional activator and small RNA in post-transcriptional regulation of the glucose phosphoenolpyruvate phosphotransferase system. Mol Microbiol *54*, 1076-1089.

Vasina, J.A., and Baneyx, F. (1996). Recombinant protein expression at low temperatures under the transcriptional control of the major *Escherichia coli* cold shock promoter cspA. Appl Environ Microbiol *62*, 1444-1447.

Vestergaard, M., Paulander, W., and Ingmer, H. (2015). Activation of the SOS response increases the frequency of small colony variants. In BMC Res Notes.

Viator, R.J., Rest, R.F., Hildebrandt, E., and McGee, D.J. (2008). Characterization of Bacillus anthracis arginase: effects of pH, temperature, and cell viability on metal preference. BMC Biochem *9*, 15.

Villadsen, I.S., and Michelsen, O. (1977). Regulation of PRPP and nucleoside tri and tetraphosphate pools in *Escherichia coli* under conditions of nitrogen starvation. J Bacteriol *130*, 136-143.

von Eiff, C., Becker, K., Machka, K., Stammer, H., and Peters, G. (2001). Nasal carriage as a source of *Staphylococcus aureus* bacteremia. Study Group. N Engl J Med *344*, 11-16.

Wagner, G., and Ottesen, B. (1982). Vaginal physiology during menstruation. Ann Intern Med *96*, 921-923.

Walters, M.S., Eggers, P., Albrecht, V., Travis, T., Lonsway, D., Hovan, G., Taylor, D., Rasheed, K., Limbago, B., and Kallen, A. (2015). Vancomycin-Resistant *Staphylococcus aureus* - Delaware, 2015. MMWR Morb Mortal Wkly Rep *64*, 1056.

Wang, B., Dai, P., Ding, D., Del Rosario, A., Grant, R.A., Pentelute, B.L., and Laub, M.T. (2019). Affinity-based capture and identification of protein effectors of the growth regulator ppGpp. Nat Chem Biol *15*, 141-150.

Wang, J.D., Sanders, G.M., and Grossman, A.D. (2007). Nutritional control of elongation of DNA replication by (p)ppGpp. Cell *128*, 865-875.

Weber, M.H., and Marahiel, M.A. (2003). Bacterial cold shock responses. Sci Prog *86*, 9-75.

Wexselblatt, E., Kaspy, I., Glaser, G., Katzhendler, J., and Yavin, E. (2013). Design, synthesis and structure-activity relationship of novel Relacin analogs as inhibitors of Rel proteins. Eur J Med Chem *70*, 497-504.

Wexselblatt, E., Oppenheimer-Shaanan, Y., Kaspy, I., London, N., Schueler-Furman, O., Yavin, E., Glaser, G., Katzhendler, J., and Ben-Yehuda, S. (2012). Relacin, a novel antibacterial agent targeting the Stringent Response. PLoS Pathog *8*, e1002925.

Wiegert, T., Homuth, G., Versteeg, S., and Schumann, W. (2001). Alkaline shock induces the *Bacillus subtilis* sigma(W) regulon. Mol Microbiol *41*, 59-71.

Wilson, D., Charoensawan, V., Kummerfeld, S.K., and Teichmann, S.A. (2008). DBD—taxonomically broad transcription factor predictions: new content and functionality. Nucleic Acids Res *36*, D88-92.

Wolz, C., Pohlmann-Dietze, P., Steinhuber, A., Chien, Y.T., Manna, A., van Wamel, W., and Cheung, A. (2000). Agr-independent regulation of fibronectin-binding protein(s) by the regulatory locus sar in *Staphylococcus aureus*. Mol Microbiol *36*, 230-243.

Wood, A., Irving, S.E., Bennison, D.J., and Corrigan, R.M. (2018). Stringent response-mediated control of rRNA processing via the ribosomal assembly GTPase Era.

Wout, P., Pu, K., Sullivan, S.M., Reese, V., Zhou, S., Lin, B., and Maddock, J.R. (2004). The *Escherichia coli* GTPase CgtAE cofractionates with the 50S ribosomal subunit and interacts with SpoT, a ppGpp synthetase/hydrolase. J Bacteriol *186*, 5249-5257.

Xiong, A., Singh, V.K., Cabrera, G., and Jayaswal, R.K. (2000). Molecular characterization of the ferric-uptake regulator, fur, from *Staphylococcus aureus*. Microbiology *146 (Pt 3)*, 659-668.

Yang, X., and Ishiguro, E.E. (2001). Dimerization of the RelA protein of *Escherichia coli*. Biochem Cell

Biol *79*, 729-736.

Zhang, T., Zhu, J., Wei, S., Luo, Q., Li, L., Li, S., Tucker, A., Shao, H., and Zhou, R. (2016). The roles of RelA/(p)ppGpp in glucose-starvation induced adaptive response in the zoonotic *Streptococcus suis*. Sci Rep *6*.

Zhou, C., Bhinderwala, F., Lehman, M.K., Thomas, V.C., Chaudhari, S.S., Yamada, K.J., Foster, K.W., Powers, R., Kielian, T., and Fey, P.D. (2019). Urease is an essential component of the acid response network of *Staphylococcus aureus* and is required for a persistent murine kidney infection. PLoS Pathog *15*, e1007538.

Zhu, W., Murray, P.R., Huskins, W.C., Jernigan, J.A., McDonald, L.C., Clark, N.C., Anderson, K.F., McDougal, L.K., Hageman, J.C., Olsen-Rasmussen, M*., et al.* (2010). Dissemination of an Enterococcus Inc18-Like vanA plasmid associated with vancomycin-resistant *Staphylococcus aureus*. Antimicrob Agents Chemother *54*, 4314-4320.

Zuo, Y., Wang, Y., and Steitz, T.A. (2013). The mechanism of E. coli RNA polymerase regulation by ppGpp is suggested by the structure of their complex. Mol Cell *50*, 430-436.